On the Mechanics of Disc-Soil-Planter Interaction

A Thesis Submitted to the College of

Graduate Studies and Research

In Partial Fulfillment of the Requirements

For the Degree of Master of Science

In the Department of Mechanical Engineering

University of Saskatchewan

Saskatoon

By

Yun Zhang

Permission to Use

In presenting this thesis/dissertation in partial fulfillment of the requirements for a Postgraduate degree from the University of Saskatchewan, I agree that the Libraries of this University may make it freely available for inspection. I further agree that permission for copying of this thesis/dissertation in any manner, in whole or in part, for scholarly purposes may be granted by the professor or professors who supervised my thesis/dissertation work or, in their absence, by the Head of the Department or the Dean of the College in which my thesis work was done. It is understood that any copying or publication or use of this thesis/dissertation or parts thereof for financial gain shall not be allowed without my written permission. It is also understood that due recognition shall be given to me and to the University of Saskatchewan in any scholarly use which may be made of any material in my thesis/dissertation.

Requests for permission to copy or to make other uses of materials in this thesis/dissertation in whole or part should be addressed to:

Head of the Department of Mechanical Engineering

University of Saskatchewan, College of Engineering

3B48 Engineering Building, 57 Campus Drive

Saskatoon, Saskatchewan, S7N 5A9, Canada

Abstract

The main objective of this research project was to understand the disc-soil-planter interaction in order to provide the lowest draft force for robotic planters. For that purpose, an analytical investigation was conducted and the mathematical model of the interaction was developed. Then a series of experimental tests were completed and reported. This constitutes the thesis' contribution to research in this area. Finally, optimization of parameters was investigated to minimize the drag force.

With the analytical model, the global coordinate system was defined. A local transformation for the disc coordinate system was developed for ease of analysis. The forces coming from the soil were separated from the forces pulling the disc by using a transformation of coordinates. Equations for cutting and normal forces were developed. The soil forces can be estimated from the measured planter forces. That is one of the benefits of the analysis since they are difficult to measure experimentally. This also avoids extremely complex FEA analysis involving soil mechanics for determining the forces in soil.

The experiments for both disc coulter and planter were designed and performed in the Soil Bin in the College of Engineering at University of Saskatchewan. The experimental procedure was established. Then a series of tests were conducted to investigate the forces required to pull the disc or the planter in a controlled simulated field condition. During the disc tests, the draft, vertical, and side forces were measured in three orthogonal directions using six load cells that were attached to the carriage with a combination of disc angles and tilt angles. The soil was properly prepared according to a four-step preparation procedure to ensure the consistency of test conditions. Before each test the soil moisture content and hardness (cone index), which are the main factors affecting the experiment results were measured. The results

obtained in these experiments were further used in developing the mathematical model of the disc-soil-planter interaction.

An optimized model was proposed based on an analytical model. The relationships were built between the draft forces and disc parameters with a constrained cutting width. The optimization problem was solved by an one-dimensional graphical optimization procedure establishing the minimum draft force F_z in terms of the disc parameters ($\alpha,\ \beta$), while the cutting width and depth was constrained.

Acknowledgment

I want to thank my supervisors Prof. Reza Fotouhi and Prof. Walerian Szyszkowski whose guidance, support and patience during all stages of this research. I am also grateful for the help of my graduate advisory committee, Prof. Scott Noble, Prof. Fangxiang Wu, and Prof. Moh Boulfiza, for their valuable suggestions. I am thankful to the Department of Mechanical Engineering for providing a comfortable research environment.

I also want to thank my colleagues, Mr. Ahad Armin and Mr. Reza Adminzadeh, and Mr. Mobin Moshiri, who helped me with my experiments. Also department assistants, Mr. Douglas Bitner and Mr. Louis Ruth are greatly appreciated for helping me to setup the experiment setups.

Dedication

This thesis is dedicated to my mother Zeping Wei and my father Yong Zhang,

who support me to make my dream come true.

Table of Contents

List of Figures

List of Tables

Nomenclature

Listed below are the symbols and abbreviations used most frequently in the text. Occasionally, the same symbol may have a different meaning defined in the text.

a horizontal axes of the ellipsis (Figure 5-2)

$A(.)$ function of soil force in term of measured force

b vertical axes of the ellipsis (Figure 5-2)

C center point at the depth that the disc is under the soil

d depth for the disc part that is under the soil

dA arbitrary area

dF_r friction force for the arbitrary area

$\%\ diff\ between\ trails$ percent difference between trail a and trail b

$\%\ diff\ with\ ori.$ percent difference between the retest data and the original data

e represent part of the equation (5.8) solving for x1, x2

f represent part of the equation (5.8) solving for x1, x2

F_c cutting force

FFT Fast Fourier Transform

F_r friction force

F_x side force in global coordinate system

F_y vertical force in global coordinate system

F_z draft force in global coordinate system

$F_{x"}$ side force in local coordinate system

$F_{y"}$ vertical force in local coordinate system

$F_{z"}$ draft force in local coordinate system

g represent part of the equation (5.8) solving for x1, x2

$\%\, moisture\ content$ percent of the moisture content

m_{wet} mass of the wet soil (g)

m_{dry} mass of the dry soil (g)

M_x side moment in global coordinate system

M_y vertical moment in global coordinate system

M_z draft moment in global coordinate system

$M_{x"}$ side moment in local coordinate system

$M_{y"}$ vertical moment in local coordinate system

$M_{z"}$ draft moment in local coordinate system

N normal force

P point that acts in opposite direction of Q (Figure 2-6)

$P1$ starting point of the line that horizontally crossed ellipse

$P2$ ending point of the line that horizontally crossed ellipse

Q point that acts in opposite direction of P (Figure 2-6)

r_c distance from center to the friction force

T transformation matrix

T_i period

$1/T_i$ frequency

$trail\ a$ first trail of the experimental test

$trail\ b$ second trail of the experimental test

$trail\ Re_a$ first re-test trail of the experimental test

$trail\ Re_b$ second re-test trail of the experimental test

V velocity disc travel

w furrow width

xp time interval from the frequency test, second

yp voltage measured from the frequency test, volt

x coordinate system for furrow width calculation (Figure 5-2)

y coordinate system for furrow width calculation (Figure 5-2)

$x1$ horizontal point 1 on the coordinate system for furrow width calculation (Figure 5-2)

$y1$ vertical point 1 on the coordinate system for furrow width calculation (Figure 5-2)

$x2$ horizontal point 2 on the coordinate system for furrow width calculation (Figure 5-2)

$y2$ vertical point 2 on the coordinate system for furrow width calculation (Figure 5-2)

X horizontal axis of the global coordinate system

Y vertical axis of the global coordinate system

Z side axis of the global coordinate system

X' horizontal axis after applied disc angle, α

Y' vertical axis after applied disc angle, α

Z' side axis after applied disc angle, α

$X"$ horizontal axis of the local coordinate system

$Y"$ vertical axis of the local coordinate system

$Z"$ side axis of the local coordinate system

α disc angle

β tilt angle

γ angle from center to the cutting point

δ angle for the cutting force

μ coefficient of friction

ρ radius

Chapter 1 – Introduction

1.1 Background

Agricultural crop production in the world is increasing driven by a growing demand for food. Increasing crop production with limited land, water, labour resources and minimum energy consumption will be required to provide food in future years. The use of highly efficient robotic farming tools is one important method to meet the goal of increased food production. Robotic technology can help to improve efficiency of day-to-day repetitive work in the field that requires an extensive effort such as planting, weeding, spraying and harvesting. A robotic farming system can provide a more accurate method to follow and plant seeds along a predefined path when compared to a human operator. These robotic systems will be able to greatly increase agricultural productivity while using less energy. For this reason, robotic farming will play a significant role in the next few decades.

This research project is part of a larger project, called “Developing robotics assisted technology for farming”. In the overall project, new robotic technology will be developed to help farmers in weed control and planting for certain types of crops. The overall project can be broken down into a few sub-projects. One of the sub-projects is to optimize the design of a seeding mechanism that requires a minimum pulling force from a mobile robot.

The furrow forming disc coulter was chosen to attach to this mobile robot. Of the many types of soil engagement components, discs are considered one of the most energy-efficient tillage tools for cutting and moving soil [1]. They are used in many tillage operations, in particular in planting and seeding where more precise furrows are required. The mechanics of

such tools, which can be attached to many agricultural types of equipment, appears to be relatively unknown. The forces associated with discs in operation are difficult to determine, and therefore are evaluated most often experimentally for each specific situation. This project is to advance the state of understanding of mechanics of discs used for tillage by developing analytical methods and validating by experiments.

To understand the disc-soil-planter interaction and to find the best combination of tilt angle and disc angle that result in the lowest draft forces for robotic farming, an analytical model of the disc was developed by using a two-coordinate systems approach. A global system is attached to the planter and a local system is attached to the disc. During the analytical investigation, the forces coming from the soil were separated from the forces pulling the disc through a transformation of coordinates. The draft force, F_z, the vertical force, F_y, and the side force, F_x , were obtained from the test data. Then the disc model was used to determine the soil-disc interaction forces which are both cutting force and normal force.

The force required to pull the robotic planter through the soil is of key importance to this effort. The reduction of the pulling force becomes quite crucial especially for small robotized devices with a limited power supply. The subject of this research is to minimize the pulling force or the draft force.

In order to get lowest draft or pulling forces, a series of experiments were conducted with a disc operating in the soil with a uniform speed and specified depth. All of the test experiments were based on the combination different tilt angles and different disc angles.

In this research project, the planter forces were determined experimentally, and then an analytical investigation model was developed to obtain the soil-disc interaction forces which are difficult to be measured experimentally.

The majority of previous work in this area was done experimentally mostly by agriculture manufacturers and as such the data is confidential and are unfortunately not available to the public, the test is important for this project. Since it is hard to measure the soil-disc interaction forces directly the analytical model presented is critical important for research in this area.

The analytical model and independent experimental study presented here are major advacements on research in this area. There are two main benefits. One, is to provide the lowest draft force for robotic planters. The other is to obtain the forces in the soil without complex FEA analysis involving soil mechanics.

The optimization section investigates how the draft force F_z is influenced by the normal and cutting forces that change with the disc parameters of tilt angle. Namely, increasing tilt angle brings about increasing F_c and decreasing N.

At the end of this research, an optimization model is proposed for the draft forces and disc parameters with a constrained cutting width. The optimization model was established by a one-dimensional graphical optimization procedure to get the minimum draft force F_z in terms of the disc parameters ($\alpha,\ \beta$), while the cutting width and depth was constrained.

1.2 Motivation

The larger project *"Developing robotics assisted technology for farming"* is carried out by other students in our research group in the University of Saskatchewan. Fatemeh Heydari (Ph.D. student) worked on the navigation of the mobile robot, Ahad Armin (Ph.D. student) was

involved in mechanics of soil-tool interaction in robotic assisted farming research, and Reza Aminzadeh (M.Sc. student) designed a seeding mechanism by using the existing CNH planter. The contribution of this research project is to understand the disc-soil interaction in order to provide the lowest draft force for robotic planters using a disc.

1.3 Objectives and Methodology

The objectives of this project are to understand the disc mechanics, and to provide geometry that ensures minimum draft force when pulled by a mobile robot. These objectives can be broken down into several tasks and each of them is discussed in detail below.

Analytical Investigation:

The main goal is to define the disc-soil-planter interactions in terms of the system's geometry which is discussed in Chapter 2. A model is introduced that separates the soil forces acting on the disc (the soil-disc interaction) from the force generated by the planter to pull the disc (the disc-planter interaction). The soil forces are the forces representing the resistance of the soil, and they are difficult to define and to measure.

Experiments with disc and tilt angle combination resulting in lowest draft force:

A series of experiments were designed and performed for both a single disc coulter in the soil bin to study the effect of disc angle and tilt angle on the forces applied to disc, as discussed in Chapter 3 and 4. The results led to a better understanding of the disc force dependence on the disc angle and tilt angle. The relationships between the draft force and the disc parameters as well as cutting width and disc parameters are established.

Optimization problem:

The key issue is to minimize the draft force by optimization of the disc parameters, while the cutting width is constrained (Chapter 5). The prepared model of the disc is used for that task.

1.4 Outline of the thesis

This thesis consists of 6 chapters and 10 appendices.

Chapter 1 is the overview of the research project and an introduction to the field of design of soil engagement tools. A review of literature research is also provided in this field.

Chapter 2 describes how the analytical model was built.

Chapter 3 walks through the experiments for the disc and planter. It explains how the tests were designed and performed. The setup of the key test parameters for both single disc and planter are also included.

Chapter 4 presents an analysis of the experimental data and the effect of disc and tilt angle on soil-disc interaction.

Chapter 5 covers the optimization of the relationships between the draft force and disc parameters, while the cutting width is constrained.

Chapter 6 brings a summary and conclusion of this research. Also the suggestions for improvements and future work are discussed.

At the end of the thesis a list of the references that were used in this thesis is provided. Appendices include the Matlab code used for data filtering, plotted disc experimental data,

retested disc experimental data, cutting force, normal force, cutting width data, and optimization with different depths and speeds.

1.5 Literature review

Many researchers have published on the development of seeders and planters. The paper [1] conducted a field experiment to measure and to compare the draft and energy inputs for tillage implements in a clay loam soil. This study showed that the disc is the most energy-efficient tillage implement. The large difference in energy data obtained in this study showed that substantial energy saving can be realized by selecting energy-efficient tillage systems.

The paper [2] explained soil-tool interaction by using a non-linear three-dimensional finite element model. In this paper, the finite element method was used to analyze the soil force and displacement, which are dependent on soil properties, tool geometry, and cutting speed. A similar finite element method can be used to evaluate the disc and compare with the experimental value. However, this finite element modeling method is very complex and may be difficult to validate.

Another paper [3] from Ohio State University, explained both clay and sandy loam soil forces caused by a disc plow. It concludes that forces can be predicted by using both tilt angle and plowing speed. The soil forces including draft, vertical and side forces, were compared by having different plowing speeds combined with different tilt angles. Information contained in this paper can be used to compare to some of the experimental data obtained in the research of this thesis.

Another paper [4] explains how the calculation of forces were performed using the combination of disc and tilt angles. There are three different kinds of forces, draft, vertical and

side forces. Some parts of experimental data of this thesis can be compared with this paper. However, the test data in this paper are very limited because it only compared the soil forces (draft, vertical and side forces) with 2 different plowing speeds combined with 3 different tilt angles.

The paper [5] provided an equation of how to evaluate the draft force. Draft force can be modeled by a function including soil properties, working depth, tool geometry, speed, and width of the implement. Those are the most important parameters to consider in order to evaluate the performance of the energy demanded while using the tillage tool. Soil properties can be determined by the soil moisture content, bulk density, cone index, soil texture, and soil strength. Such method can also be considered while evaluating the research experimental data in this thesis. The model accuracy depends on the quality of the experimental data, which means input data verification is important.

The paper [6] developed a methodology to predict the draft requirements of combination tillage implements in any soil and operating conditions. Laboratory experiments were conducted to measure the draft requirements of the tillage implements. It was found that the draft force of all the tillage implements increased with increase in soil compaction, depth and speed of operation. The similar prediction can be used with the experimental data from this thesis.

The paper [7] illustrated the application of these models by means of a detailed worked example which sets out a systematic calculation procedure for estimating soil reaction generated by a Mohr-Coulomb soil on a concave spherical agricultural disc of specified curvature and size. These investigations were carried out under carefully controlled laboratory conditions with the disc working loam soils.

The paper [8] conducted field tests with a view to determine the effects of speed and depth on the draft of tillage implements in sandy loam soils. A significant increase in draft was observed for all the tillage implements with an increase in forward speed and tillage depth. Similar results should be observed in this thesis.

The paper [9] investigated the effect of speed and depth on draft of many tillage implements. Draft was found to be a linear function of speed for a disc plow and was directly proportional to depth for all implements. This result could be compared to some of the experimental data in the research of this thesis.

The paper [10] studied the influence of soil parameters involved with moisture content and cone index on draught force and soil disturbance of model tillage tools. Draught force increased quadratically with a decreasing rate with moisture content; draught force increased quadratically at an increasing rate with cone index.

The paper [11] developed empirical equations to enable the draught prediction of tillage implements in different soil conditions. The draught prediction equation for tillage implements was developed using the concept of the draught requirements of a reference tillage tool in a reference soil condition and the scale factors related to soil properties and implement width.

The paper [12] studied the force relations on large harrow discs, which showed optimum harrow design and operating conditions were influenced by disc blade geometry. Increases in draft caused by increases in forward velocity were linear. Similar experimental results should be observed in this research thesis.

The paper [13] determined the effect of various soil, implement and operating parameters on the depth of penetration of a disc harrow. By conducting the experiments in the field, a linear

relation between depth and different factors, including diameter of the disc, angle of the harrow, weight of the harrow per disc, speed of operation, cone index of soil and acceleration due to gravity, were found.

The paper [14] conducted a field experiment to compare draft and energy inputs for different primary tillage implements in a clay loam soil. The large range in implement draft, fuel consumption, and tractor efficiency indicate that substantial energy saving can be readily obtained by selecting energy-efficient tillage implements.

The paper [15] developed a mathematical model to predict the energy requirement for the combined effect of a disc plow and a rotary blade in clay soil. The developed equations were checked with experiments conducted in an indoor soil tank. Similar method can be used in this thesis to predict the energy requirement.

The paper [16] showed that the width and depth of disc cuts are variables, which can be used to influence of forces on discs. The increases in draft cared by increases in depth of cut are accompanied by increases in soil disturbance.

The paper [17] developed and installed an instrumentation system on a custom made tool carrier to measure the effect of seeding depth on the draft and vertical force acting on a double disc seeder. The results from the field trials suggested that depth control varied considerable from the theoretical setting.

The paper [18] predicted draft and fuel consumption rate magnitude by the models. The disc harrow is the most energy efficient implement in terms of fuel consumption and energy saving.

The paper [19] studied soil stress around a simple vertical tillage tool and pressure distribution on the tool surface using computational fluid dynamics (CFD). Higher tool speed is accompanied by an increase in soil stress as well as increase soil pressure.

The paper [20] introduced the fuzzy model as one of the methods for predicting soil fragmentation for seedbed preparation during the tillage operation. Field experiments were conducted with inputs including soil moisture content, tractor forward speed and soil sampling depth.

The paper [21] developed a 5-9-1 artificial neural network (ANN) model to predict draught requirements of different tillage implements in a sandy clay loam soil under vary operating and soil conditions. The width of cut, depth of operation, speed of operation, soil moisture content and soil bulk density are the input parameters of the network.

The paper [22] presented a rapid method for calculating the draught force generated by a concave disc tool when cutting a Mohr-Coulomb soil. The equivalent stress, derived by distributing the draught force uniformly over the furrow cross-section, is calculated using a set of non-dimensional factors.

The paper [23] derived a functional relationship between the minimum disc angle, disc diameter, and the depth. The small disc is preferred to have the minimum draft and maximum penetration ability (minimum vertical reaction). This conclusion can be used in the verification of the experimental data in this thesis.

The paper [24] studied tillage drafts and fuel measurements for 12 soil series with major implements used. Disc was the most fuel-efficient implement among those studies, which was measured by an instrumented tractor that was developed to measure ground speed, fuel

consumption and implement draft. This is one of the reasons that the disc coulter is used in this thesis.

The paper [25] predicted the recommended engine power and fuel consumption for tractor-disc harrows system that is valid for undisturbed loamy soil. A measurement of draught could be used to estimate fuel consumption, to demonstrate correct tractor-implement set-up and to select the crop production system.

The paper [26] developed a soil mechanical resistance sensor with a large-diameter disc coulter to delineate areas of differing soil strength acrossing agricultural field. In this research, an instrumented disc coulter capable of measuring and recording the geo-referenced depth of operation was developed and evaluated.

The paper [27] explained that the vertical and draft force increased with the increase in depth of penetration and size of coulter. The paper concludes that seed placement under the crop residue is the basic problem associated with no-till and minimum tillage planting.

The paper [28] performed disc plow experiments in two different soil types as a function of disc angle, tilt angle, forward speed and plowing depth in terms of soil physical properties and draft force. Yet, the conditions for testing the optimum region (disc angle between 45° to 50°) in this paper is not suitable for the conditions in this thesis (disc angle between 0° to 28°).

The paper [29] showed the effects of moldboard plow components and adjustments on its performance when used in a clay soil. Effects were analyzed using both modeling and experimental results. Due to the complexity of modeling, current formulations of FEM cannot predict for this behavior. Field experiments are necessary, yet they may not allow a clear resolution of changing a single part due to compounding effects.

The paper [30] explained how the calculation of forces are performed using the combination of disc and tilt angle. There are three different key forces, draft, vertical, and side forces. Conclusions of the paper included the increased depth of operation results in increased draft and vertical force and decreased side force.

The paper [31] explained that as tillage operations are not required, no-till producers do not need to purchase tillage implements. No-till farming can reduce soil erosion, conserve soil moisture and minimize labor and fuel consumption, however, the result of no-till will cause seeding problems.

The paper [32] was concerned with the mechanics of agricultural soil as a simple tillage tool was forced through it. The paper obtains an understanding of the soil-failure process and thereby finds an analytical solution that would predict the main aspect of a flat tool moving through the soil, yet, the formula is only applied for a blade.

The paper [33] designed a theoretical soil working tool. The draft force and soil failure geometry of narrow cutting blades were provided. In this way many variations of tool design could be tried theoretically in order to find a configuration which is best suited for a particular application.

The paper [34] developed a generalized mathematical model to examine its validity for predicting the tillage tool performance in soils. The mathematical model for predicting the behavior of a narrow tillage tool in soil was based on a limit equilibrium analysis, however, it might not provide accurate result if the tillage tool is in the shape of a disc.

The paper [35] predicted draft force of a simple implement in cohesionless granular material. This study was capable of predicting draft force correctly and allowed the model to extend to more complex tool geometries, such as a disc.

The paper [36] provided an understanding of the relationship between tool forces and speed, which is important in evolving management strategies for optimum performance. The experimental observation for the blade showed that the tool force was a function of speed and square of the speed. For the situation of a disc, a similar relationship might exist.

The paper [37] provided the effect of the comboplow (disc plow combined with rotary blades), which is used for soil preparation for planting. This paper explained that the soil texture can be varied with different rotational velocity of the blade that is used for soil preparation. With different soil texture, the forces reacted on the soil would be different.

The paper [38] used a model that was developed to predict the horizontal force acting upon mouldboard ploughs based on Mohr-coulomb soil properties and inertia effect. In this paper, given the parameters of working width, depth, forward speed for the model, the experimental results for the soil force can be analyzed, which maybe similar to the research of this thesis.

The thesis [39] analyzed the interaction between machine elements and soil seeks. It provided calculation procesure for estimating soil reactions, identified the boundaries of soil disturbance, and evalued the deformation imposed on soil.

Most of the works reported in this literature review were involved with the modeling mechanics of disc-soil interaction with the disc shape as in this research. Some papers may not be closely related to this thesis. However, they are listed for completeness. The thesis [39] seems

the closest to my project. However, the article is using a concave disc, which is a different type of disc this thesis is used, so it cannot be fully evaluated.

Chapter 2 - Analytical Investigation

2.1 Introduction

This chapter presents a simplified analytical model of the disc. Two coordinate systems are used, one attached to the planter (global) and the second attached to the disc (local). A transformation of coordinates is developed that permits the analysis of the forces exerted on the disc-soil-planter system. The chapter closes with a review of available research literature.

The main goal is to define the disc-soil-planter interactions in terms of the system's geometry. The model introduced here separates the soil forces acting on the disc (the soil-disc interaction) from the force generated by the planter to pull the disc (the disc-planter interaction). The first step of this approach is to define the coordinate systems.

Figure 2-1 shows the orientation of the disc in the global coordinate system XYZ (the planter is moving in the Z-direction). This orientation is specified by the disc angle α, the tilt angle β, and the depth d. The planter forces are the forces generated by the planter to move the disc forward (Figure 2-2), and are specified by the draft force, F_z, the vertical force, F_y, and the side force, F_x. The moments required to maintain the disc configuration are denoted as M_x, M_y, and M_z. The forces moving the disc and the moments would be measured by instrumenting the disc frame with strain gages and calibrating for forces or torque.

The soil forces are the forces representing the resistance of the soil and are difficult to measure experimentally. They are identified by the normal force, N, the friction force, F_r,the cutting force, F_c (Figure 2-2 and Figure 2-3). In addition, the angles, δ, of the cutting force and the angle, γ, from the disc center to the cutting point define the direction and part of application

of F_c. It is assumed that the soil is pushed forward and sideways by the normal to the disc and tangential components of the resultant forces, while the soil cutting force is the resultant of forces applied at the edge in the disc plane. At a constant depth, the disc configuration is expected to affect only the point of application of F_c, but not its magnitude.

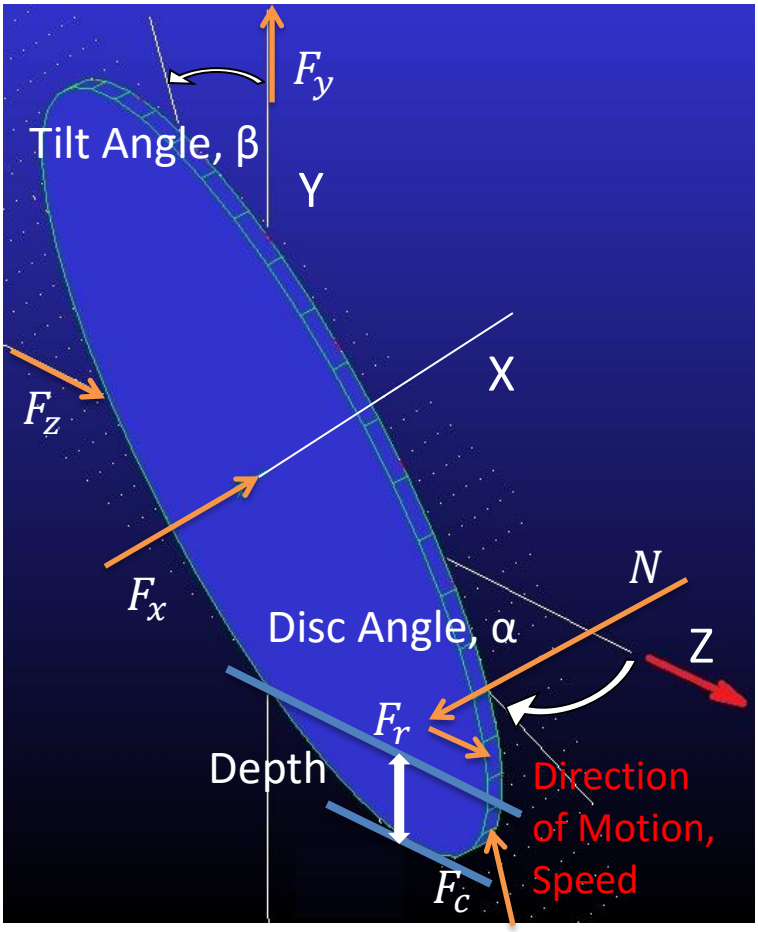

Figure 2- 1: Orientation of the disc

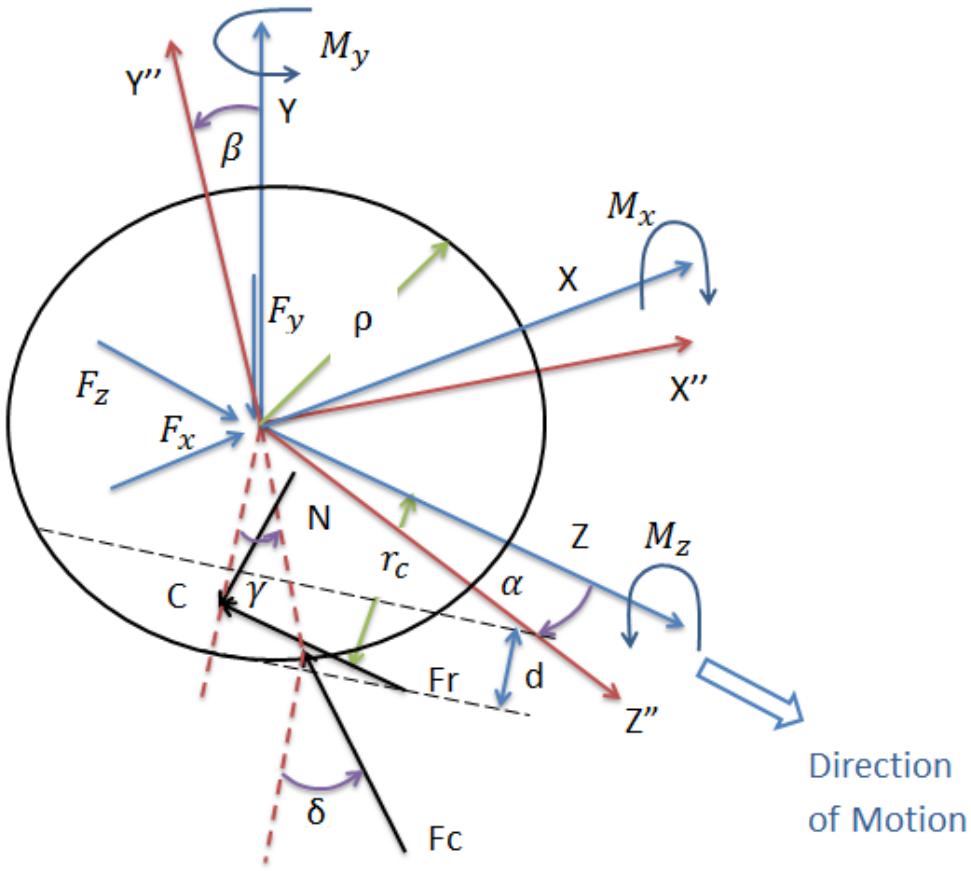

Figure 2- 2: Disc parameters

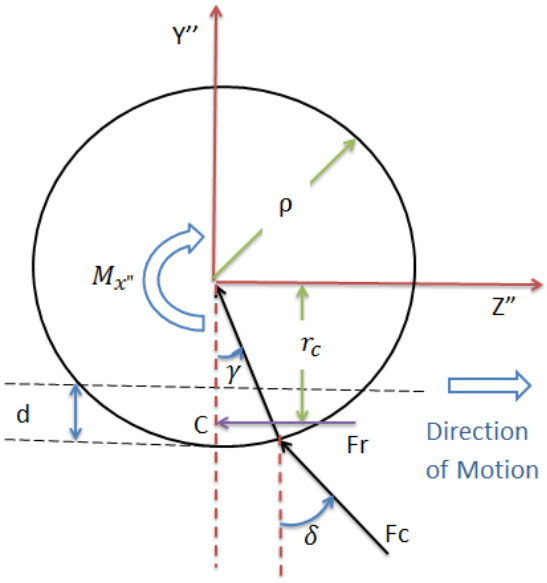

Figure 2- 3: Disc parameters in Y''-Z'' plane

The soil forces mainly depend on the internal friction of the soil, cohesion, and disc-soil friction. They also depended on the soil volume being pushed forward and sideways, which is related to the furrow's geometry. In this thesis the soil forces will be determined from the experimentally measured planter forces for each particular dimension/configuration (i.e. α, β).

2.2 The Global-Local Coordinates Transformation

A transformation from the global coordinate system to the local coordinate system was developed in order to understand the relationship between the planter forces and the soil forces.

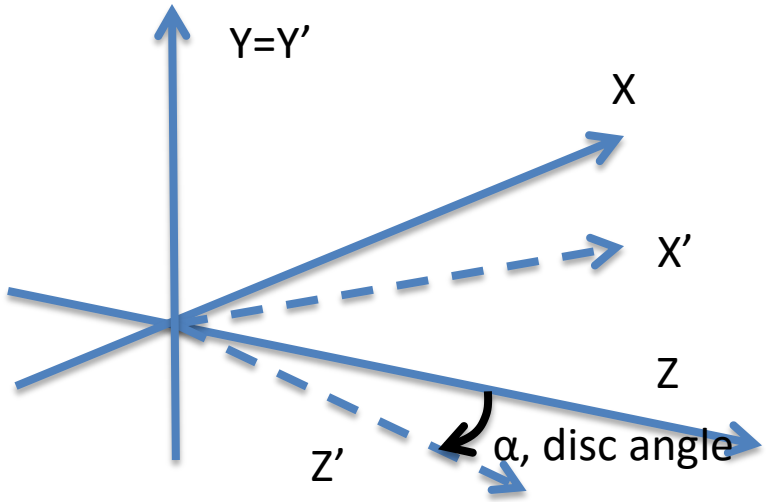

Figure 2- 4: Disc angle transformation

First the Y-axis of the global coordinate system shown in Figure 2.1 is rotated by the disc angle, α. The coordinates X, Y, Z can be transferred into *X'*, *Y'*, *Z'* as follows (in the formula such X, Y, Z are used).

$$\begin{aligned} X' &= X\cos\alpha + Z\sin\alpha \\ Z' &= -X\sin\alpha + Z\cos\alpha \\ Y' &= Y \end{aligned} \qquad (2.1)$$

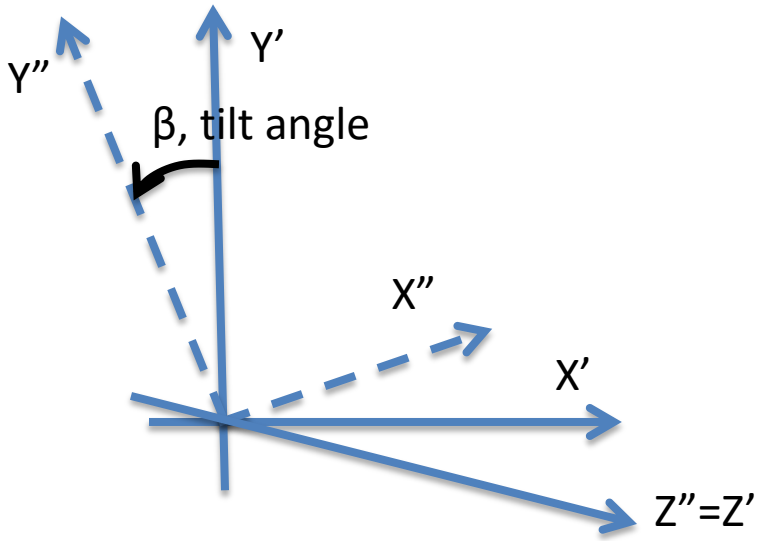

Figure 2- 5: Tilt angle transformation

Then the Z'-axis is rotated by the tilt angle, β, with the coordinates X', Y', Z' transferred into X'', Y'', Z'' as follows.

$$\begin{aligned} X'' &= X'\cos\beta + Y'\sin\beta \\ Y'' &= -X'\sin\beta + Y'\cos\beta \\ Z'' &= Z' \end{aligned} \tag{2.2}$$

The coordinates X'', Y'', Z'' are attached to the disc, therefore they align with the local coordinate system. Then, combining equation (2.1) and equation (2.2), the global coordinate system can be transferred into local coordinate system as

$$\begin{aligned} X'' &= (X\cos\alpha + Z\sin\alpha)\cos\beta + Y\sin\beta \\ Y'' &= -(X\cos\alpha + Z\sin\alpha)\sin\beta + Y\cos\beta \\ Z'' &= -X\sin\alpha + Z\cos\alpha \end{aligned} \tag{2.3}$$

or, in the matrix form

$$\begin{bmatrix} X'' \\ Y'' \\ Z'' \end{bmatrix} = T \begin{bmatrix} X \\ Y \\ Z \end{bmatrix} \tag{2.4}$$

where $T = \begin{bmatrix} cos\alpha cos\beta & sin\beta & sin\alpha cos\beta \\ -cos\alpha sin\beta & cos\beta & -sin\alpha sin\beta \\ -sin\alpha & 0 & cos\alpha \end{bmatrix}$

2.3 Forces Transformation

The transformation formula (2.4) is applicable to any vector and can be used to which the components of the force and moment vectors. The force component transformation is as follows:

$$\begin{bmatrix} F_{x"} \\ F_{y"} \\ F_{z"} \end{bmatrix} = \begin{bmatrix} cos\alpha cos\beta & sin\beta & sin\alpha cos\beta \\ -cos\alpha sin\beta & cos\beta & -sin\alpha sin\beta \\ -sin\alpha & 0 & cos\alpha \end{bmatrix} \begin{bmatrix} F_x \\ F_y \\ F_z \end{bmatrix} = T \begin{bmatrix} F_x \\ F_y \\ F_z \end{bmatrix} \quad (2.5)$$

Where, as defined before, the planter forces in the global coordinate system are F_x (the side force), F_y (the vertical force), and F_z (the draft force). While the forces $F_{x"}$, $F_{y"}$, $F_{z"}$ in the local coordinate system are related to the soil forces N (the resultant normal force acting on the disc), F_r (the resultant friction force in the plane on the disc), and F_c (the resultant cutting force applied to the edge of the disc).

From Figure 2-3 results that:

$$\begin{aligned} F_{x"} &= N \\ F_{y"} &= -F_c cos\delta \\ F_{z"} &= F_r + F_c sin\delta \end{aligned} \quad (2.6)$$

The forces of the local coordinate system can be checked that for $\alpha = \beta = 0$ equation (2.5) yields

$$\begin{bmatrix} N \\ -F_c cos\delta \\ F_r + F_c sin\delta \end{bmatrix} = \begin{bmatrix} 1 & 0 & 0 \\ 0 & 1 & 0 \\ 0 & 0 & 1 \end{bmatrix} \begin{bmatrix} F_x \\ F_y \\ F_z \end{bmatrix} \quad (2.7)$$

The draft force, F_z, vertical force, F_y, and side forces, F_x, can be determined from equation (2.5) as

$$\begin{bmatrix} F_x \\ F_y \\ F_z \end{bmatrix} = T^{-1} \begin{bmatrix} N \\ -F_c cos\delta \\ F_r + F_c sin\delta \end{bmatrix} = \begin{bmatrix} cos\alpha cos\beta & sin\beta & sin\alpha cos\beta \\ -cos\alpha sin\beta & cos\beta & -sin\alpha sin\beta \\ -sin\alpha & 0 & cos\alpha \end{bmatrix}^{-1} \begin{bmatrix} N \\ -F_c cos\delta \\ F_r + F_c sin\delta \end{bmatrix} \quad (2.8)$$

Or from the following equation

$$\begin{bmatrix} F_x \\ F_y \\ F_z \end{bmatrix} = \begin{bmatrix} cos\alpha cos\beta & -sin\alpha & -sin\alpha sin\delta + cos\alpha sin\beta cos\delta \\ sin\beta & 0 & -cos\beta cos\delta \\ cos\beta sin\alpha & cos\alpha & cos\alpha sin\delta + sin\alpha sin\beta cos\delta \end{bmatrix} \begin{bmatrix} N \\ F_r \\ F_c \end{bmatrix}$$

$$= A(\alpha, \beta, \delta) \begin{bmatrix} N \\ F_r \\ F_c \end{bmatrix} \quad (2.9)$$

For checking the forces of the global coordinate system, assume that $\alpha = \beta = 0$, then the equation (2.9) becomes

$$\begin{bmatrix} F_x \\ F_y \\ F_z \end{bmatrix} = \begin{bmatrix} 1 & 0 & 0 \\ 0 & 0 & -cos\delta \\ 0 & 1 & sin\delta \end{bmatrix} \begin{bmatrix} N \\ F_r \\ F_c \end{bmatrix} \quad (2.10)$$

which is identical as equation (2.7).

As mentioned, for a given α and β, the planter forces (F_x, F_y, F_z) can be measured, and then the soil force (N, F_r, F_c) can be calculated. Equation (2.9) can be inverted to obtain

$$\begin{bmatrix} N \\ F_r \\ F_c \end{bmatrix} = A(\alpha, \beta, \delta)^{-1} \begin{bmatrix} F_x \\ F_y \\ F_z \end{bmatrix}$$

$$= \begin{bmatrix} (cos\beta cos\alpha) & (sin\beta) & (cos\beta sin\alpha) \\ \left(\frac{-cos\alpha sin\beta sin\delta - cos\delta sin\alpha}{cos\delta}\right) & \left(\frac{cos\beta sin\delta}{cos\delta}\right) & \left(\frac{-sin\alpha sin\beta sin\delta + cos\alpha cos\delta}{cos\delta}\right) \\ \left(\frac{cos\alpha sin\beta}{cos\delta}\right) & \left(\frac{-cos\beta}{cos\delta}\right) & \left(\frac{sin\alpha sin\beta}{cos\delta}\right) \end{bmatrix} \begin{bmatrix} F_x \\ F_y \\ F_z \end{bmatrix}$$

(2.11)

This is a key equation used later in the analysis of Chapter 4.

The soil forces (N, F_r, F_c,) will be determined from the experimentally measured planter forces (F_x, F_y, F_z) for a given sets of the disc angles, α, and tilt angle, β. Note that the angle δ in this equation is also unknown. This issue is dealt with the following way.

Because the disc is allowed to rotate around the *X"* axis ($M_{x"} = 0$), the relation between friction force, F_r, and cutting force, F_c, is as follow (see Figure 2-2)

$$\sum M_x" = F_r r_c - F_c \rho cos\delta sin\gamma + F_c \rho sin\delta cos\gamma = 0 \qquad (2.12)$$

Then, from this equation one obtains

$$F_r = \frac{1}{r_c} F_c \rho sin(\gamma - \delta) \qquad (2.13)$$

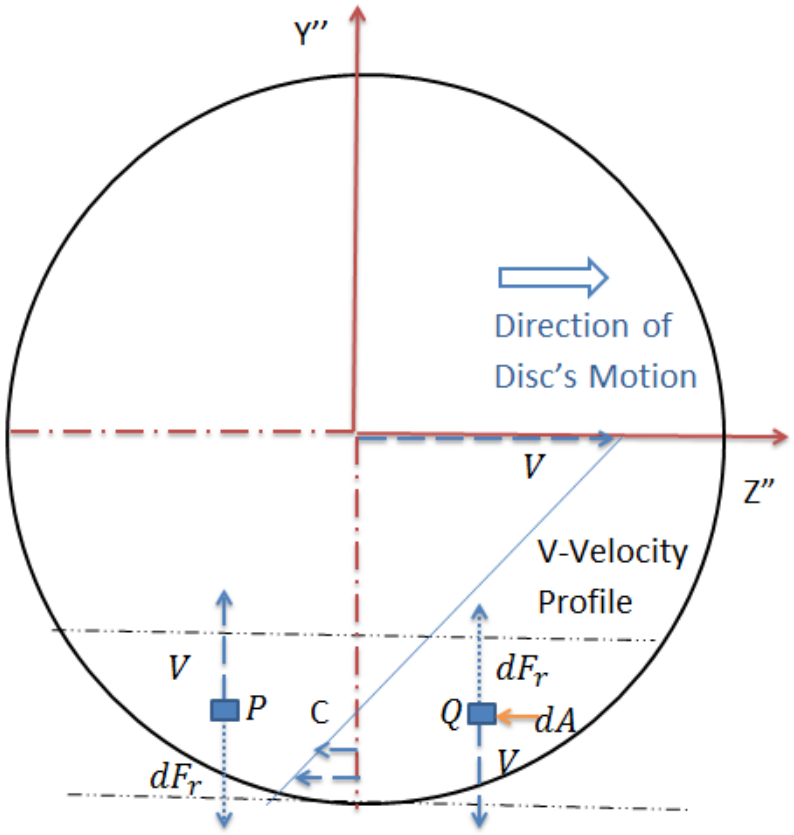

Figure 2- 6: Friction force

However, it should be noticed that if the disc is free to rotate, then the friction force, F_r, is near zero. The reasoning behind this is that the instantaneous rotation center of the rotating disc, while moving forward, is approximately located at point C, therefore the relative velocity of soil at C is close to zero. Clearly, around C, any friction force, dF_r (Figure 2-6), acting on an arbitrary area dA of the disc is opposing the relative velocity, V (of disc with respect to soil). For example, the friction forces, dF_r, for points P and Q will be acting in opposite directions and will be practically balancing one another. Therefore, the resultant friction force related to normal force, N, is close to zero, or equivalently the corresponding friction coefficient, define as $\mu = F_r/N$ is also close to zero. Note that the coefficient of friction, μ, is not the same as it would be for a plow that is moving forward but not rotating.

Because $F_r \approx 0$, then we can assume that $\gamma \approx \delta$ (Equation(2.7)), and (see Figure 2-7) equation (2.7) gives

$$\begin{bmatrix} N \\ -F_c cos\delta \\ F_c sin\delta \end{bmatrix} = \begin{bmatrix} 1 & 0 & 0 \\ 0 & 1 & 0 \\ 0 & 0 & 1 \end{bmatrix} \begin{bmatrix} F_x \\ F_y \\ F_z \end{bmatrix} \tag{2.14}$$

Or for $\alpha = \beta = 0$ (recall that F_x, F_y, F_z can be measured)

$$F_x = N \tag{2.15}$$

$$F_y = -F_c cos\delta \tag{2.16}$$

$$F_z = F_c sin\delta \tag{2.17}$$

Equations (2.16) and (2.17) gives

$$\frac{F_z}{F_y} = \frac{sin\delta}{-cos\delta} = -tan\delta \tag{2.18}$$

So, the cutting angle, δ, can be obtained from experiment as

$$\delta = tan^{-1}\left(-\frac{F_z}{F_y}\right) \tag{2.19}$$

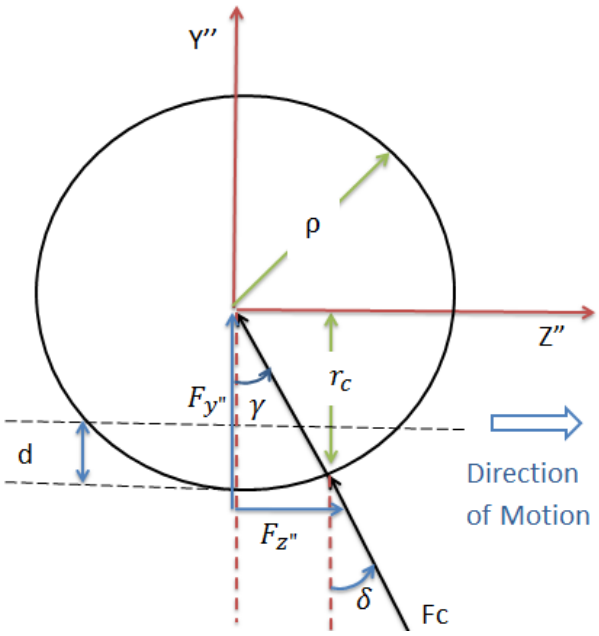

Figure 2- 7: The cutting force for $F_r \approx 0$

In the case, where $\delta \neq \gamma$, then $F_r \neq 0$ and $\mu = F_r/N$ can be substituted into (2.9), to obtain

$$\begin{bmatrix} F_x \\ F_y \\ F_z \end{bmatrix} = \begin{bmatrix} cos\alpha cos\beta - \mu sin\alpha & -sin\alpha sin\delta + cos\alpha sin\beta cos\delta \\ sin\beta & -cos\beta cos\delta \\ cos\beta sin\alpha + \mu cos\alpha & cos\alpha sin\delta + sin\alpha sin\beta cos\delta \end{bmatrix} \begin{bmatrix} N \\ F_c \end{bmatrix}$$

$$= B(\alpha, \beta, \delta, \mu) \begin{bmatrix} N \\ F_c \end{bmatrix} \quad (2.20)$$

Also, substituting $F_r = \mu N$ in equation (2.9) gives

$$F_r = \frac{1}{r_c} F_c \rho sin(\gamma - \delta) = \mu N \quad (2.21)$$

Then, from equation (2.21), F_c can be determined as

$$F_c = \frac{\mu r_c}{\rho \sin(\gamma - \delta)} N \quad (2.22)$$

Substituting equations (2.22) into equation (2.7), gives

$$\begin{bmatrix} F_x \\ F_y \\ F_z \end{bmatrix} = \begin{bmatrix} cos\alpha cos\beta - sin\alpha \left[\dfrac{\mu r_c sin\delta}{\rho \sin(\delta-\gamma)} + \mu\right] + \dfrac{\mu r_c cos\alpha sin\beta cos\delta}{\rho \sin(\delta-\gamma)} \\ sin\beta - \dfrac{\mu r_c cos\beta cos\delta}{\rho \sin(\gamma-\delta)} \\ cos\beta sin\alpha + cos\alpha \left[\mu + \dfrac{\mu r_c sin\delta}{\rho \sin(\delta-\gamma)}\right] + \dfrac{\mu r_c sin\alpha sin\beta cos\delta}{\rho \sin(\delta-\gamma)} \end{bmatrix} N$$

$$= C(\alpha, \beta, \delta, \gamma, \mu, r_c, \rho)N \tag{2.23}$$

The moment vector can be transformed similarly as the force vector. Namely, using equation (2.4), the moments in the global and local coordinate system are related via the equation:

$$\begin{bmatrix} M_{x''} \\ M_{y''} \\ M_{z''} \end{bmatrix} = \begin{bmatrix} cos\alpha cos\beta & sin\beta & sin\alpha cos\beta \\ -cos\alpha sin\beta & cos\beta & -sin\alpha sin\beta \\ -sin\alpha & 0 & cos\alpha \end{bmatrix} \begin{bmatrix} M_x \\ M_y \\ M_z \end{bmatrix} = T \begin{bmatrix} M_x \\ M_y \\ M_z \end{bmatrix} \tag{2.24}$$

Note that $M_{x''} = 0$ for a free rotating disc.

2.4 Forces Verification

The force equation (2.5) is verified by assuming $\alpha = \beta = 0$ to obtain

$$\begin{bmatrix} F_x \\ F_y \\ F_z \end{bmatrix} = \begin{bmatrix} 1 & 0 & 0 \\ 0 & 0 & -cos\delta \\ 0 & 1 & sin\delta \end{bmatrix} \begin{bmatrix} N \\ F_r \\ F_c \end{bmatrix} = \begin{bmatrix} N \\ -F_c cos\delta \\ F_r + F_c sin\delta \end{bmatrix} = \begin{bmatrix} 1 & 0 & 0 \\ 0 & 1 & 0 \\ 0 & 0 & 1 \end{bmatrix} \begin{bmatrix} F_x \\ F_y \\ F_z \end{bmatrix} \tag{2.25}$$

Then the three equations are

$$F_x = N \;\rightarrow\; N = F_x \tag{2.26}$$

$$F_y = -F_c cos\delta \;\rightarrow\; F_c = \frac{-F_y}{cos\delta} \tag{2.27}$$

$$F_z = F_r + F_c sin\delta \rightarrow\; F_r = F_z - F_c sin\delta \tag{2.28}$$

Experimental data are required when using equation (2.19) to evaluate angle δ for different depths with different speeds are shown in Table 2-1. These data were obtained for $\alpha = \beta = 0$ and for different depths and different widths of furrows. Eight experimental trials are outlined in the table below.

Table 2- 1: The estimation of δ angle

Trial	Parameters	Fx	Fy	Fz	tanδ	δ	μ'
1	depth=2in,speed=3mph	122	-242	91	0.377	21	0.134
2		146	-253	109	0.430	23	0.0263
3	depth=3in,speed=3mph	199	-269	124	0.460	25	0.0196
4		166	-246	121	0.493	26	0.0706
5	depth=2in,speed=5mph	241	-325	137	0.420	23	0.0340
6		236	-318	143	0.449	24	0.0049
7	depth=3in,speed=5mph	218	-286	142	0.498	26	0.0698
8		196	-299	141	0.471	25	0.0390
	average δ					24	

These δ are plotted in Figure 2-8. From the plot, one can conclude that δ does not vary much, though increasing the speed or/and increasing the depth would slightly increase this angle.

The average of those 8 different trails are used in further hand calculations; this means the δ angle ($\delta_{avg} = 24°$) is assumed constant for the rest of the experimental data. The consequences of this assumption is briefly discussed next.

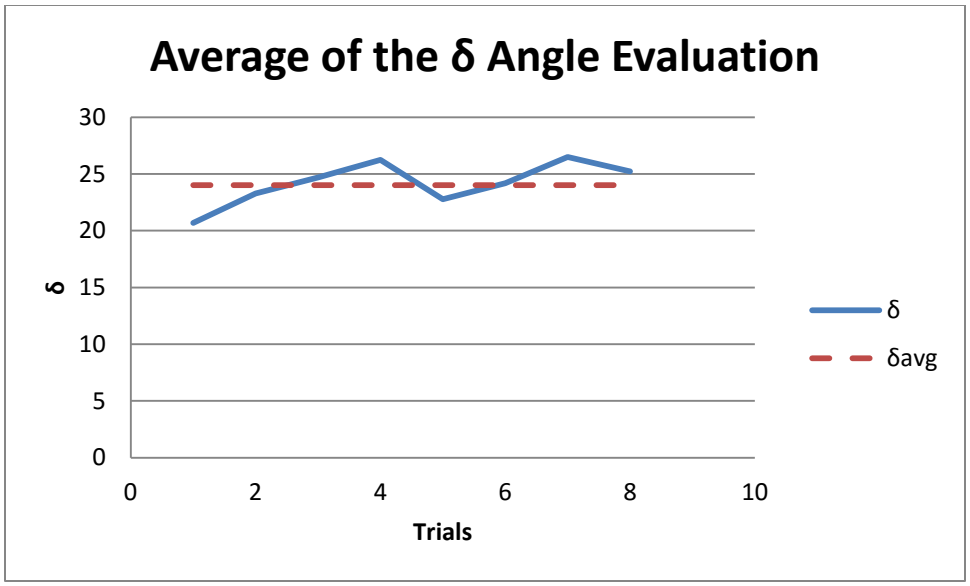

Figure 2- 8: Measurement of δ (from Table 2-1)

For example, trial 6 provided the experimental test data (depth at 2in and speed at 5mph) in which $\delta_6 = 24°$ (the same as the average δ)

$$N = F_x = 237N \tag{2.29}$$

$$F_c = \frac{-F_y}{cos\delta} = \frac{-(-317.7)}{cos24} = 348N \tag{2.30}$$

$$F_r = F_z - F_c sin\delta = 142.6 - 347.8 sin24 = 1.15N \tag{2.31}$$

$$\mu' = \frac{|F_r|}{N} = \frac{|1.151|}{236.4} = 0.0049 \tag{2.32}$$

However, if trial 1 is analyzed and $\delta_{avg} = 24°$ is used instead of $\delta_1 = 21°$ from the experiment, then

$$N = F_x = 122N \tag{2.33}$$

$$F_c = \frac{-F_y}{cos\delta} = \frac{-(-242.2)}{cos24} = 265N \tag{2.34}$$

$$F_r = F_z - F_c sin\delta = 91.40 - 265.1 sin24 = -16.4N \quad (2.35)$$

$$\mu' = \frac{|F_r|}{N} = \frac{|-16.43|}{122.2} = 0.134 \quad (2.36)$$

Similarly, for trial 2 ($\delta_2 = 23°$) the experimental test data generates

$$N = F_x = 146N \quad (2.37)$$

$$F_c = \frac{-F_y}{cos\delta} = \frac{-(-253.4)}{cos24} = 277N \quad (2.38)$$

$$F_r = F_z - F_c sin\delta = 109.0 - 277.4 sin24 = -3.82N \quad (2.39)$$

$$\mu' = \frac{|F_r|}{N} = \frac{|-3.821|}{145.5} = 0.0263 \quad (2.40)$$

For trial 4, however, in which $\delta_4 = 26°$ we obtain

$$N = F_x = 166N \quad (2.41)$$

$$F_c = \frac{-F_y}{cos\delta} = \frac{-(-246.3)}{cos24} = 270.N \quad (2.42)$$

$$F_r = F_z - F_c sin\delta = 121.4 - 269.6 sin24 = 11.7N \quad (2.43)$$

$$\mu' = \frac{F_r}{N} = \frac{11.74}{166.3} = 0.0706 \quad (2.44)$$

Similarly, calculated coefficients of friction μ' for the other cases are shown in the last column of Table 2.1.

It should be noted that $F_r > 0$ for $\delta_i > \delta_{avg}$ (the friction force is opposing the travel direction), while $F_r < 0$ for $\delta_i < \delta_{avg}$ (the friction force acts in the direction of travel). One can conclude that (see Equation 2.13): for $\delta_i < \delta_{avg}$, it should be assumed that $\gamma < \delta_{avg}$, while for

$\delta_i > \delta_{avg}$ it should be assumed that $\gamma > \delta_{avg}$ in order to obtain $F_r \approx 0$ again. It should be also noted that μ' in Table 2-1 can be considered small in comparison to $\mu \approx 0.6$ that is typically used in plowing operation with non-rotation tools [40].

This section developed an analytical model. From this model, the soil forces, (N, F_c, F_r) can be calculated from the measured forces (F_x, F_y, F_z). The next step of process is to investigate available literature for similar types of parameters and functions as used in this research project.

2.5 Review and Compare with Literatures

Most of the published research reviewed focused on obtaining experimentally the forces (drag, lift and side forces) exerted on the disc when cutting the soil. For example, the dependence of these forces on the disc's diameter and angles, and its velocity were investigated in [12]. The relationships between the disc forces and the cutting depth/speed were presented in [16]. It was concluded that the tillage efficiency including the fuel consumption is mainly affected by the drag force controlled by orientation of the disc, represented by the tilt and disc angles. Identical cutting parameters of the furrow (i.e. width and depth) can be achieved by different combinations of these angles. Obviously, a combination that would provide the minimum disc force is most desired. Much of the research effort was directed at experimentally establishing the optimal combination of the angles that minimized the drag forces in the disc operation. Drag forces for tilt angles in a range of 15° to 25° and for a range of disc angles 5° to 25° were reported in [3].

The spherical, double concavity, and conical discs were investigated in [23] with the disc angles of 15°, 30°, and 45°. It should be emphasized that all these works were experimental, none of the above papers had any analytical models to represent the disc mechanics. The main

purpose of the research in this thesis is to develop just such an analytical model and to validate it by soil tests.

In the published literature, the disc forces were obtained using mainly experimental methods. The results presented by various authors are not particularly consistent, most likely due to inconsistency of the soil properties in the experiments. There were some attempts in the literatures to derive analytical models that relate the forces to the basic disc geometry, and to the cutting conditions. Mathematical models were developed in [7, 39]. The forces acting on the soil were considered in terms of the geometry of the contact surfaces of the discs and the soil reactions which act on them. The most difficult task in this approach was to correctly characterize the soil properties. The disc forces could also be analyzed by using finite element numerical models [2, 3]. These models concentrated mostly on simulating the complex behavior of the soil and would be rather cumbersome in design applications.

2.6 Summary

In this chapter a number of key steps for building an analytical model were presented. The global coordinate system was defined. A local transformation for the disc coordinate system was developed for ease of analysis. Equation (2.20) for cutting and normal forces was developed. The reason for developing analytical model is to determine forces in soil without running complex analysis involving soil mechanics. The conclusion drawn here is that soil forces can be determined from the measured planter forces. The next chapter describes the testing procedure to measure experimentally the planter forces in the lab for each particular dimensions/configuration of the disc (i.e. α, β) and the resulting depth and width of the groove.

Chapter 3 – Description of Experiments

3.1 Introduction

This chapter explains the experimental settings for both the disc and the modified planter tests. First, a single disc alone was tested. Then the modified planter was tested using the information from the single disc tests. The definitions of the disc set up, the planter set up, the soil preparation, and the test procedures for the disc and the planter will be described in the following sections.

The performance of the disc, due to soil interactions, is influenced by many parameters, including disc diameter, disc thickness, edge angle, disc angle, tilt angle, and depth of the cut. The sharpness created by both disc angle and tilt angle can change the forces acting on the disc when cutting through the soil. In order for the disc to open a furrow wide enough for a seed to fit in, the disc angle should be greater than zero. The main advantage of having a non-zero tilt angle is to reduce the draft force. Ideally, the reaction forces should be zero for a disc with zero disc angle and tilt angle. The results measured are small and they are non-zero for these conditions because other parameters affect the reaction forces on the disc. These other contributing factors may be from part manufacturing tolerance, assembly tolerance and soil variation. They will not be investigated here.

Two sets of experiments (disc and planter) were designed and performed in the soil bin facility of the College of Engineering at the University of Saskatchewan. The soil was properly prepared before performing the experiments using the developed procedure. The goal of the disc experimental tests was to find the best combination of disc and tilt angle that results in a

minimum draft force. Once key parameters were selected from a single disc, tests were then run on the planter in order to study the performance for a few selected working conditions.

3.2 Disc Test Parameters

All tests were performed at constant disc forward speed. The diameter of the disc was 18.1in (460mm), the depth of cut was set to be 2in (50.8mm) or 3in (76.2mm), and the speed was set to be 3mph (4.83km/h) or 5mph (8.05km/h). This is because the developed planter used in this research has the same diameter of 18.1in (460mm); the planter experimental tests can be comparable to the disc experimental tests due to the same disc diameter, depth, and speed. A series experimental tests were conducted on a disc with various tilt and disc angles in different combination. In other words, the tilt angles and different disc angles were selected to produce a desired cutting width with a given depth and speed, in order to reach the goal of finding the best combination of disc angle and tilt angle which led to minimum draft force.

Tests were also performed on a modified planter to study the same effects. The planter has a compound angle of 7° disc angle and 25° tilt angle, and same disc diameter of 460mm. Such experimental tests allowed understanding of the planter's performance focused on different working conditions.

In the following section, a single disc set up and disc in planter test set up are described. The details for planter parts are described in the section 3.2.2.

3.2.1 Single Disc Test Set Up

The orientation of the tilt and disc angles are shown in Figure 3-1. Tilt angle, β, is between disc plane and Y-axis (vertical). Disc angle, α, is between disc plane and Z-axis (horizontal). The disc angle is what generates the furrow width.

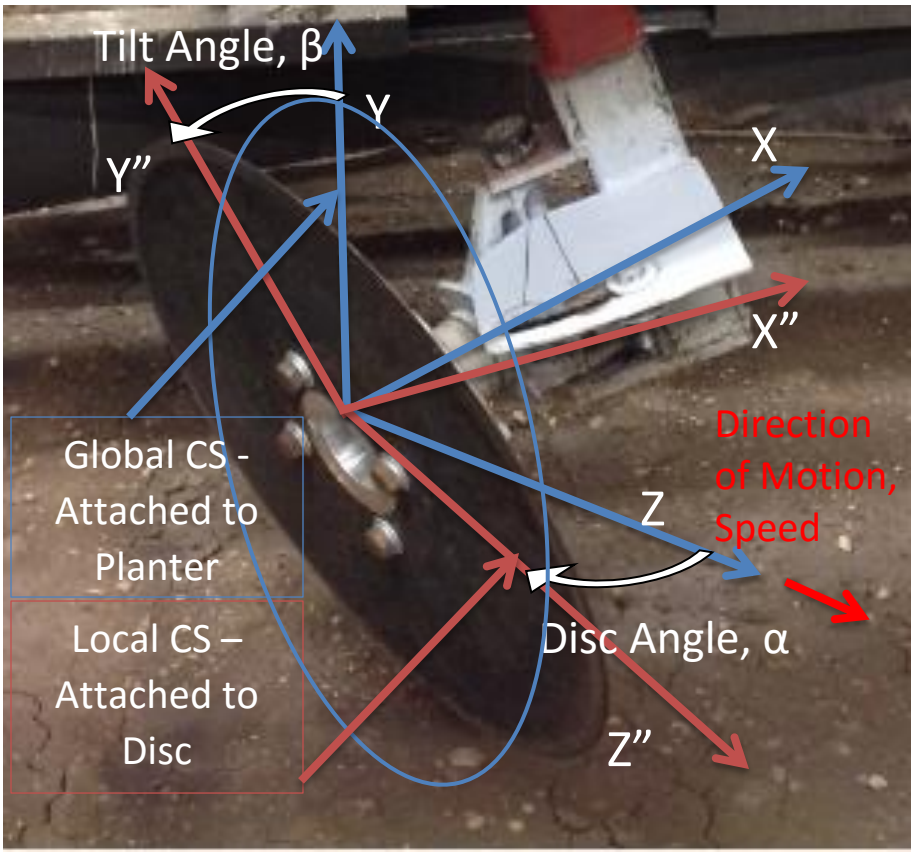

Figure 3- 1: Disc and tilt angle orientation

The experimental study of the soil-disc interaction was performed capturing the effects of disc forward speed, depth of cut, and width of cut. A design of experiments (DOE) was defined for the disc coulter, which covered test parameters such as different depths with different speeds as shown in the Table 3-1:

Table 3- 1: Test parameters for the disc/planter

Group #	Depth, in (mm)	Speed, mph (km/h)
1	2 (50.8)	3 (4.83)
2	2 (50.8)	5 (8.05)
3	3 (76.2)	3 (4.83)
4	3 (76.2)	5 (8.05)

Usually following completion of the soil preparation, the disc coulter was attached to the carriage with selected disc angle and tilt angle to conduct the experiments. The depth zero point was set by lowering the disc until it touched the surface of the soil. The cutting depth was then measured below this zero point. The start button was pressed for the carriage forward motion. The data were recorded when the first trigger switch was activated until the end switch was reached. The stop button shown in Figure 3-8 was pressed to stop the carriage before it reached the end of the soil bin. This procedure was also applied to the planter test.

The draft forces, vertical forces and side forces acting on the tool were measured using six load cells in three orthogonal directions (horizontal, vertical and lateral). The details of this are discussed in the next section. The adjustable tilt angles (0°, 15°, 20°, 25°) and disc angles (0°, 7°, 14°, 21°, 28°) were selected to produce a desired cut width for a given design of experiment (DOE). The test method consists of a fully factored DOE.

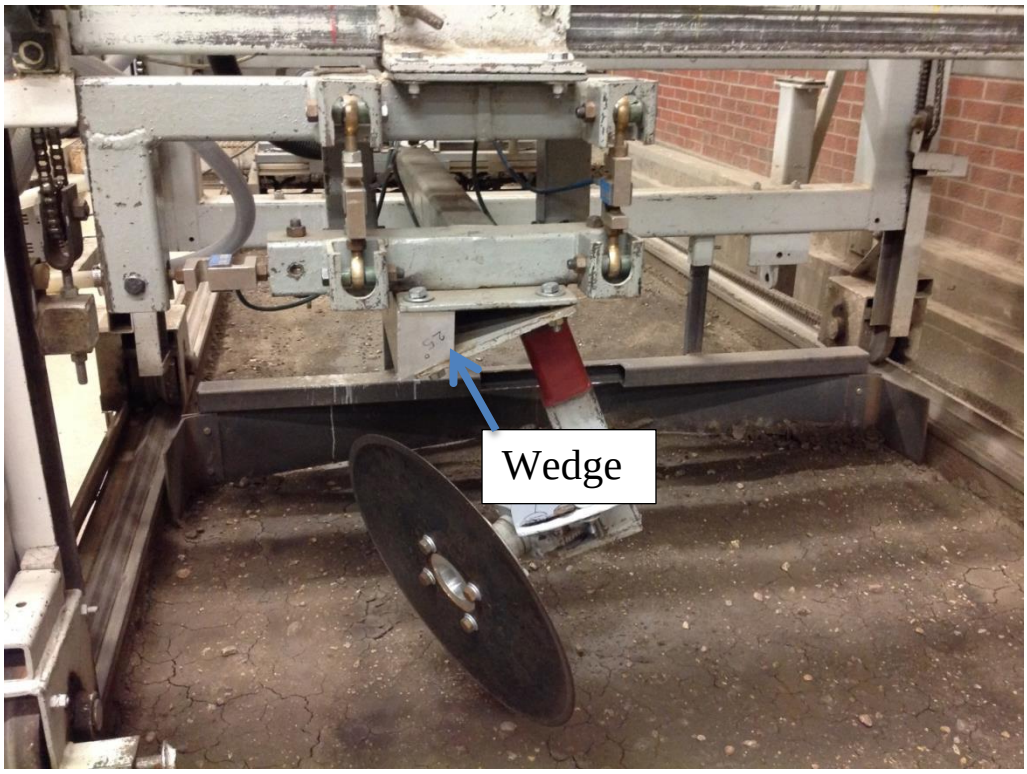

Figure 3- 2: Using wedge to set tilt angle

The disc was attached to the carriage with an adjustable connection link to set the disc angle, as shown in Figure 3-2. Wedges with different angles were used in between the bolting plates to set the tilt angle. Figure 3-2 shows a condition that the adjustable connection link was set at disc angle of 0° while tilt angle was at 25°.

3.2.2 Disc in Planter Test Set Up

The previous section explained the parameter settings of the disc coulter only. This section introduces the settings when the disc coulter was integrated into a sub-section of a planter. The test subject planter is capable of seed planting. The draft, vertical and side forces can be measured and compared with the results of other available commercial planters. A connection mechanism was designed so the planter could be directly connected to the carriage of the soil bin.

Using this method, all the forces on the planter, including draft, vertical, and side force were measured. This planter (see Figure 3-3) was developed in the robotic lab [41].

Experimental tests were arranged for the developed planter in order to study the operating performance for different working conditions. A DOE was run on the planter. It covered test parameters such as depth and speed (Table 3-1). The values of test parameters in planter tests were chosen to be the same as the ones in Table 3-1 for the disc test.

Figure 3- 3: Developed planter

In order to understand disc-soil interaction and design a ground engagement tool for a planter mechanism, an investigation of forces using the developed planter in the soil bin was necessary. Investigations were based on the model (Figure 3-3) introduced here which separated

the forces coming from the soil (the soil forces) and from the forces pulling the disc (the disc forces). Similar with single disc tests, the disc forces were measured during a series of tilt and disc angle experiments performed in the soil bin. The measured force data was then used to determine parameters to reduce the drag force. This process was used to find the best combination of tilt and disc angle to deliver the minimum draft force. Further development of the planter can continue after the optimization of the disc orientation.

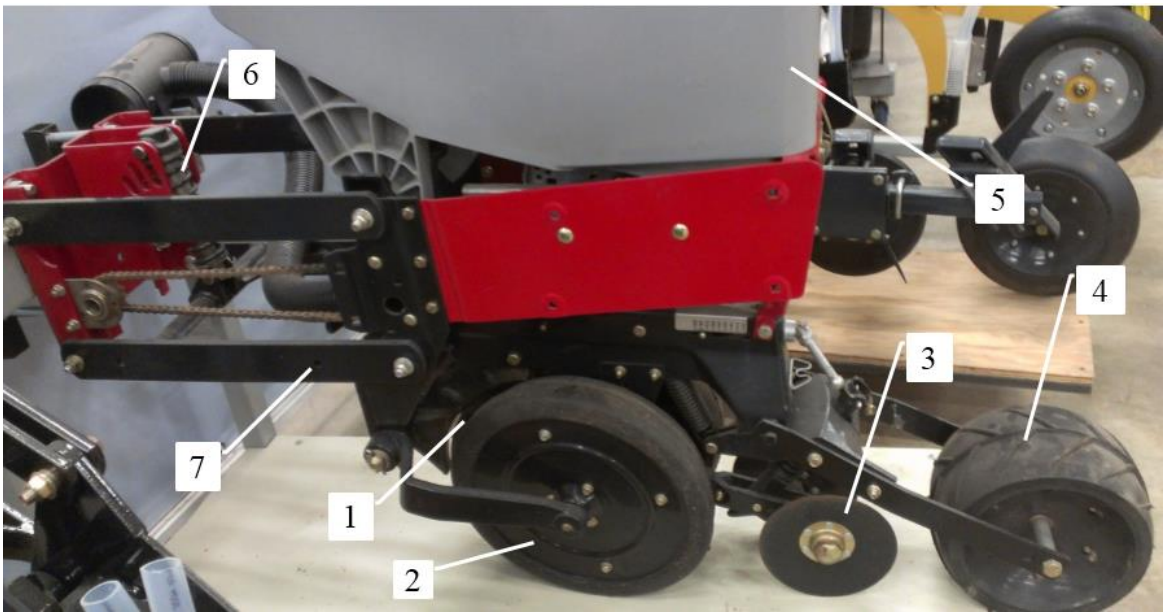

Figure 3- 4: The single planter parts: 1-Disc coulter, 2-Gauge wheel, 3-Soil covering disc, 4-Press wheel, 5-Seed hopper, 6-Shock absorber spring, 7-Parallelogram linkage [41]

CNH in Saskatoon donated two planters to be used for development of the prototype. The modified CNH planter was designed and built previously by a colleague with an improvement in its efficiency [41]. Further improvements of the planter are required, including redesign of several mechanisms and calculations supporting the changes. The planter tested was formed from two planters with disc and tilt angles which were mirrored with respect to each other. Two planters with mirrored angles will cancel out the lateral force on the connection and allow a

mobile robot to pull them straight and with more ease. Each planter was connected by seven main parts as shown in Figure 3-4.

The functions of the parts in Figure3-4 are as follows [41]:

1. A disc coulter is a soil engaging component, which opens a furrow by cutting and pushing the soil to the side. A disc is more accurate and more effective in the fields with large amount of residue than other furrow openers, such as a blade; also it needs less draft force and makes fewer disturbances in the soil. However, the disc has shorter life due to its small thickness and its axial rotation compared to other furrow openers.
2. Gauge wheel is mainly used to utilize a disc opener in seeding mechanisms by its accuracy in depth. It is usually installed on the side of the disc. The height can be changed and set to get the proper depth.
3. The soil covering disc covers the soil after seeding.
4. The process of putting soil back into the furrow after the seed is placed in the soil is called packing. Seed should be properly packed in complete contact with the soil to grow and not be blown away by the wind. The soil covering disc covers the seed after seeding, while the press wheel is the soil packing components.
5. Seed hopper is where the seeds are located.
6. Shock absorber spring should be designed for the seeding mechanism to avoid shock loads applied to the soil engagement tool, such as rocks in the soil that causes heavy loads. This spring system gives the ability to the seeding mechanism to go up and down as it goes through the field.
7. Parallelogram system and trial arm system are the two types of mechanisms to control the depth of furrow. A trialing arm system is simpler, cheaper, and lighter than parallelogram

system, but it does not provide enough accuracy in depth control and down force control. A parallelogram system is mainly used to control the depth of furrow due to its accuracy, ease of control, and more rigidness with higher strength. However, the system is more complex and expensive than other systems. It also needs more space and is heavier than the other systems.

Many experimental tests were carried out in order to study the modified CNH planter's performance under different working conditions. The planter was attached to the carriage with the designed attachment part shown in Figure 3-5. The design of experiments covered planter performance with different depths and speeds as given in Table 3-2.

Figure 3- 5: Developed planter attached to the carriage

3.3 Soil Preparation for Experiments

The forces acting on different soil engagement tools were measured in the soil bin at the lab in the College of Engineering, University of Saskatchewan. The soil used in the soil bin is silt clay loam, 47% sand, 24% silt, and 29% clay and of a depth of about 0.3m. The dimensions of the soil bin are 1.8m wide and 9m long (Figure 3-6).

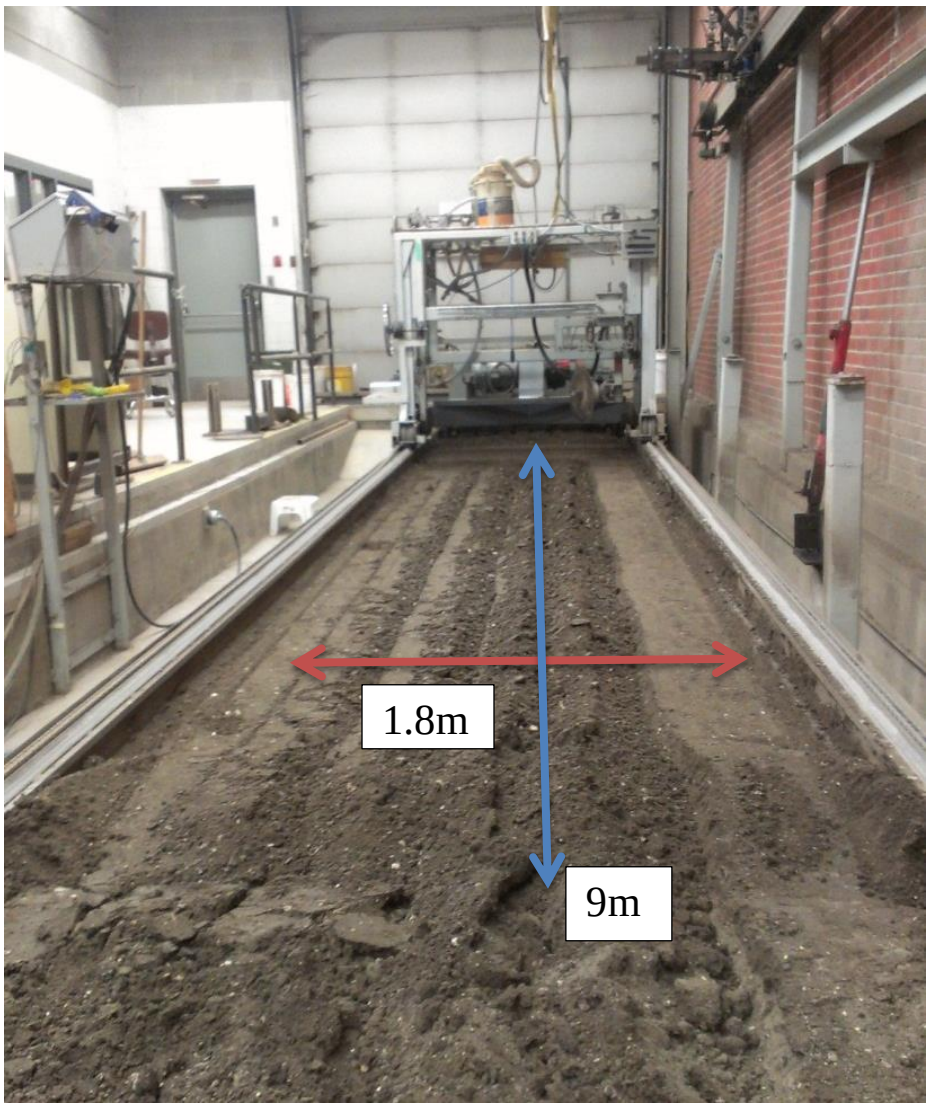

Figure 3- 6: Soil Bin, College of Engineering, University of Saskatchewan

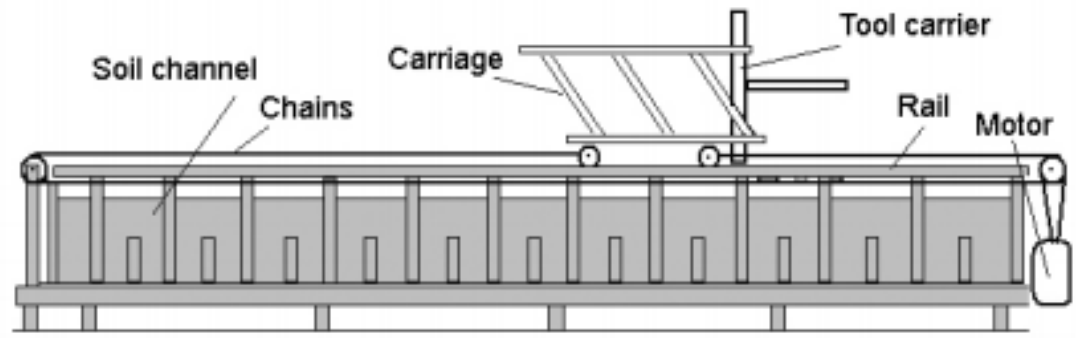

Figure 3- 7: Schematic diagram of soil bin facility [42]

An electric drive system is used to pull the carriage by two chains; the carriage has a capacity of testing prototypes of tools at each run. The testing tools on the moving carriage are pulled or pushed in the soil channel through a chain drive system [42]. A constant speed is desired for the evaluation of the forces. Due to the changing speed while the equipment accelerates up to the desired speed, this acceleration section of the travelling time is not used for data acquisition. The middle section of the soil bin, approximately 5.7m, where the carriage travels at a constant speed, is used for force measurements.

The soil engagement tools are attached to a carriage. The carriage (shown in Figure 3-7) is able to move along the soil bin on four steel wheels on two rails, one on each side of the soil bin. It is powered by an electric motor with an electromagnetic clutch providing the mechanical force to move the carriage in the chain. It is used to carry tools to prepare the soil and pull the attachment tool for measuring forces.

A procedure for the preparation of the soil was developed and used for each run of the test rig. The tillage tool is connected to the carriage that spans the width of the soil bin. The carriage speed, start, stop, and direction of the motion of the carriage are controlled by a control panel (shown in Figure 3-8).

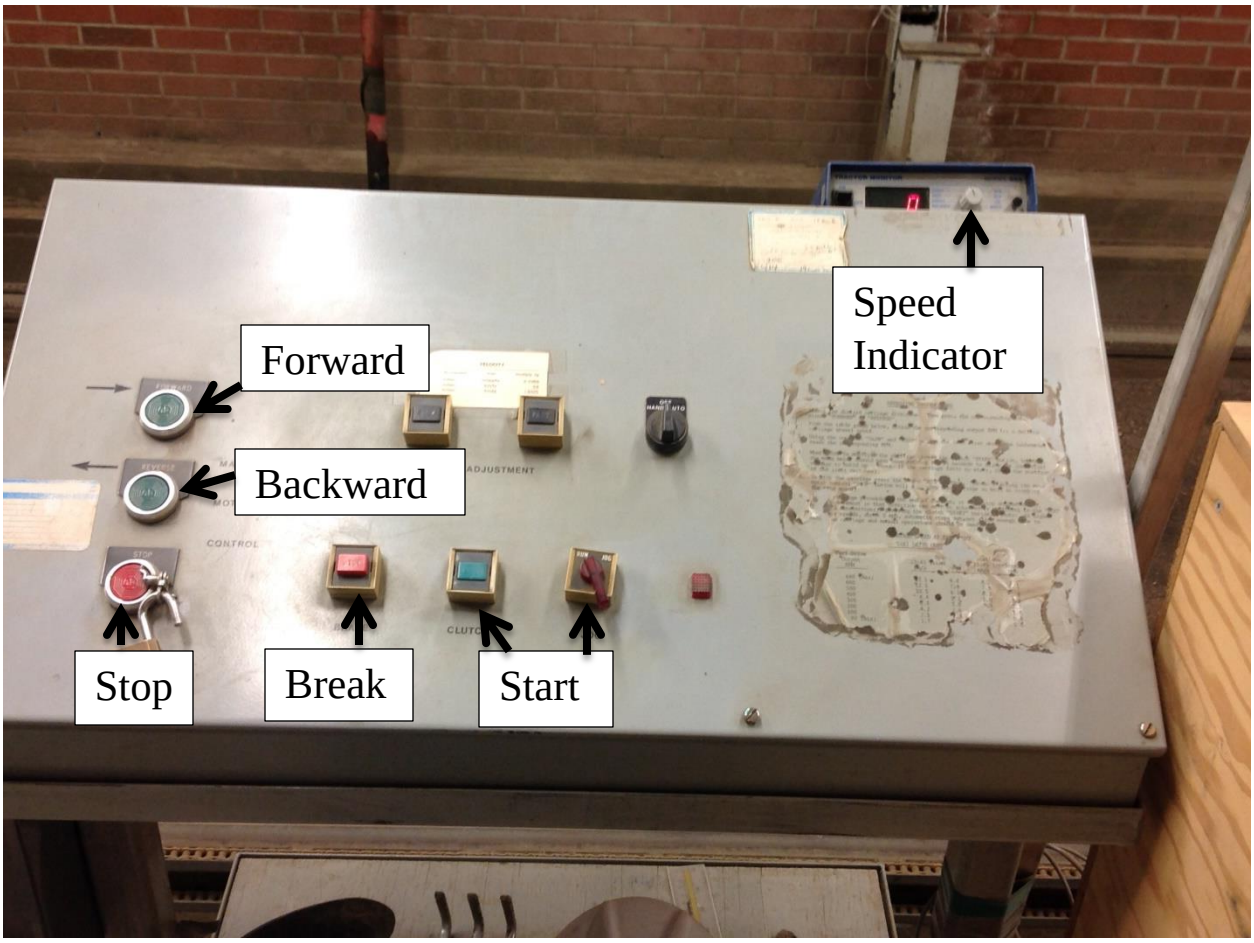

Figure 3- 8: Control panel for soil bin

The first step of the soil preparation is to spray water on the soil in order to increase the water content to a desired level for the soil. The water moisture content should remain consistent for the experiments. The second step of the soil preparation is to attach a roto-tiller to the carriage (See Figure 3-9). It is used to prepare the soil after spraying the water. During the soil preparation, two passes of the roto-tiller (Figure 3-10) are used to loosen and mix the soil. While the soil is loosened, the leveler (Figure 3-11) attached to the carriage is used to flatten the soil.

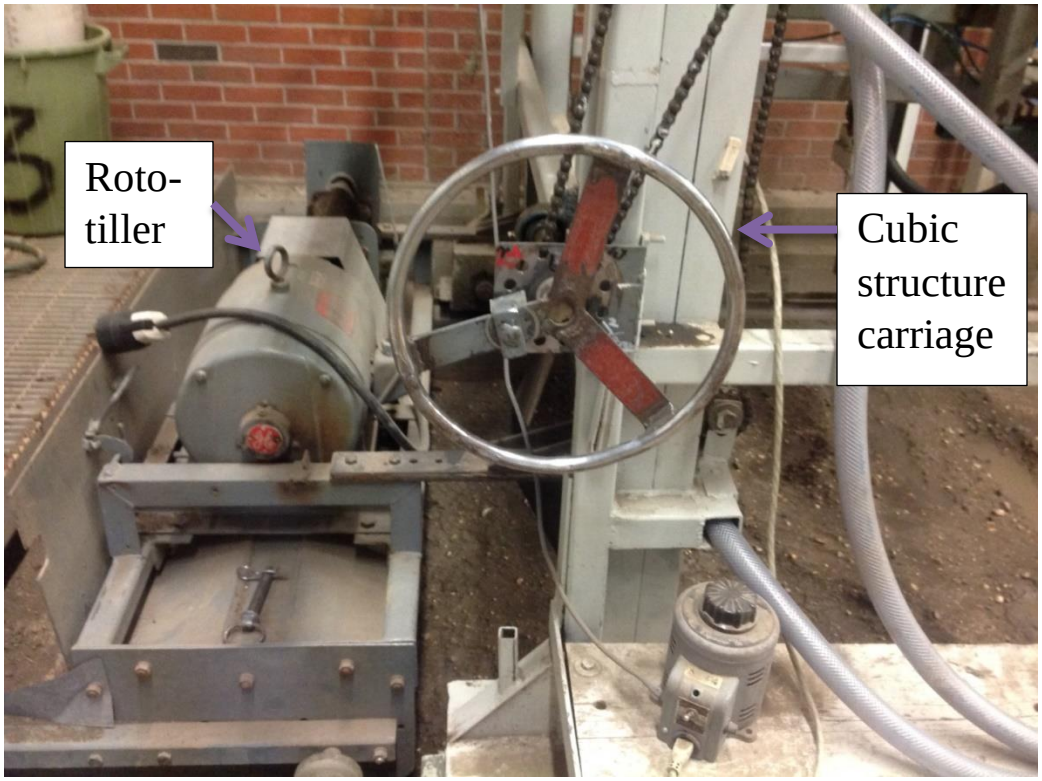

Figure 3- 9: 1. Roto-tiller attached to the cubic structure carriage

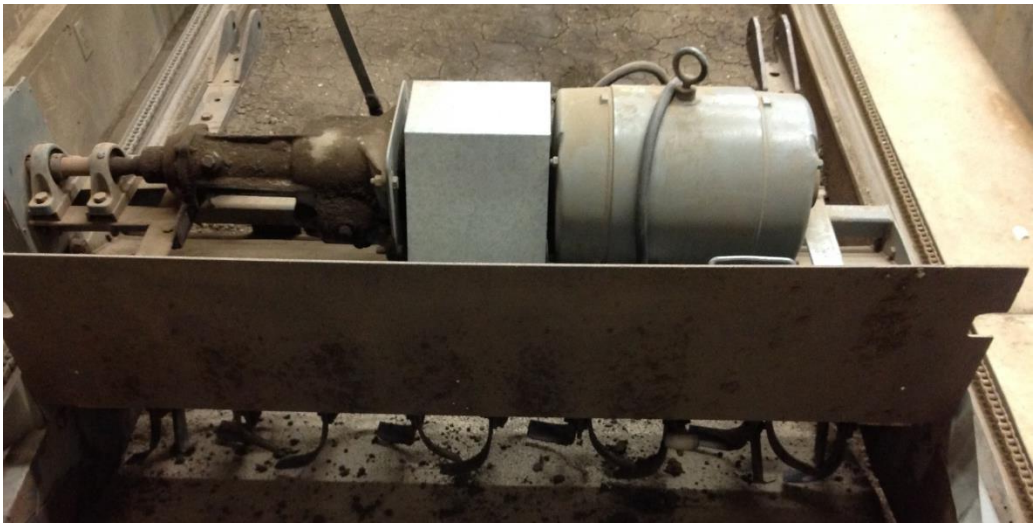

Figure 3- 10: Roto-tiller

Figure 3- 11: The leveller, to flatten the soil

The third step of the soil preparation is to use the sheep foot. The sheep foot (part 1 in Figure 3-12) and smooth roller (part 2 in Figure 3-12), are used to pack the soil. The sub-surface soil is packed by using four passes of the sheep foot. Then, the leveler (Figure 3-11) attached to the carriage is again used to flatten the soil.

The fourth step of the soil preparation is to use the smooth roller. The smooth roller is used for the final packing of the soil. After the leveler is used to flatten the soil, four passes of the roller (part 2 in Figure 3-12) was used to do the final flatten and packing of the soil. This soil preparation method was used for all of the experiments carried out here.

Figure 3- 12: Pictures of 1-Sheep foot on top 2-smooth roller on bottom

In both disc and planter experimental tests, the soil was properly prepared before doing the experiments as defined in the previous procedure. Forces acting on the tool were measured using load cells in horizontal (draft), vertical, and lateral directions (see Figure 3-13 and Figure 3-14). Load cells can be categorized by the device that generates the output signal (Pneumatic, hydraulic, electric) or by the way they detect force (bending, shear, compression, tension, torsion); force applied on the device creates an electrical signal (voltage) proportional to the stress generated on the structure itself, which is translated into an electrical signal through the use of strain gauges [43].

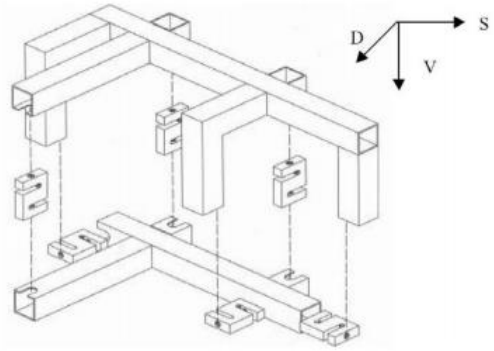

Figure 3- 13: Six s-shape load cell arrangement [43]

The forces applied to the tillage tool in the vertical, horizontal, and lateral directions were measured by using six load cells. The position and orientation of the load cells are identified in Figure 3-13. The vertical force was measured by three load cells, marked as 3. Two of the load cells were located in front and one load cell in back (not shown in Figure 3-14). The draft force (horizontal force) was measured by two load cells, marked as 2. The side force (lateral force) was measured by one load cell, marked as 1.

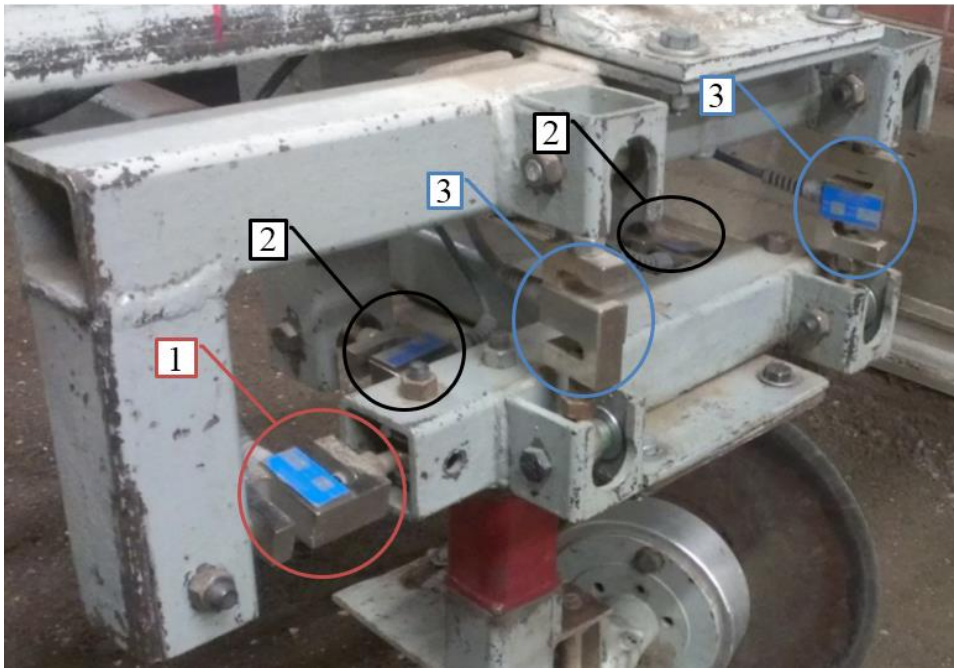

Figure 3- 14: Load cells, position and orientation: 1-Side force, 2-Draft force, 3-Vertical force [43]

The test data were acquired using a data logger and LabView 2013 version 13.0, which was made by National Instruments. The two sensors were placed on each end of the middle section of the soil bin's length in order to gather the data from the experimental tests. The first sensor started the data recording and the other ended the data recording. Then, the LabView 2013 program, which was developed for the soil bin experimental tests, measured signals in real time, displayed on the monitor screen and recorded them into a computer. LabView2013

program was used to transform all the recorded data during the soil bin experiments into draft, vertical, and side forces.

3.4 Measurement of Soil Parameters

One of the main components that affect the soil bin experimental tests is the moisture content. Moisture content is the amount of water contained in soil. Water content is used in a wide range of agriculture areas, and is expressed as a ratio, which can range from completely dry to saturate. Two samples of the prepared soil were collected and the soil moisture content was measured by placing them in an oven for 24 hours in 100℃ to dry. The soil moisture content was calculated using the American Society for Testing and Materials Standards guidelines with the following formula. The wet soil was initially measured on the weight measurement machine in grams, and the dry soil was measured the next day. The soil moisture content is

$$\%\, moisture\ content = \frac{\left|m_{wet} - m_{dry}\right|}{m_{dry}}$$

Where m_{wet} is the mass of the wet soil (g) and m_{dry} is the mass of the dry soil (g).

Soil hardness, which is defined by using the cone index, is another main component that affects the experimental measurements. Cone index was used to measure soil hardness after soil preparation and before each test. A diagnostic tool to measure the extent and depth of subsurface compaction is a penetrometer, or soil compaction tester; this tool can help producers determine if subsoil might be beneficial and at what depth the subsoil should be set [44]. The penetrometer rod (shown in Figure 3-15) should be driven into the soil vertically down at a rate of approximately 1 inch per second until it reaches a depth of 5 inch. The data on the dial-indicator would increase while pushed down on the penetrometer; it should be recorded for every inch the

penetrometer is pushed into the soil. The readings from dial-indicator can be analyzed and called the cone index. Due to the variation of the cone index values, readings from different locations of the soil bin are required for the same preparation of the soil. The average of those cone indexes is then calculated as the final cone index for the particular prepared soil.

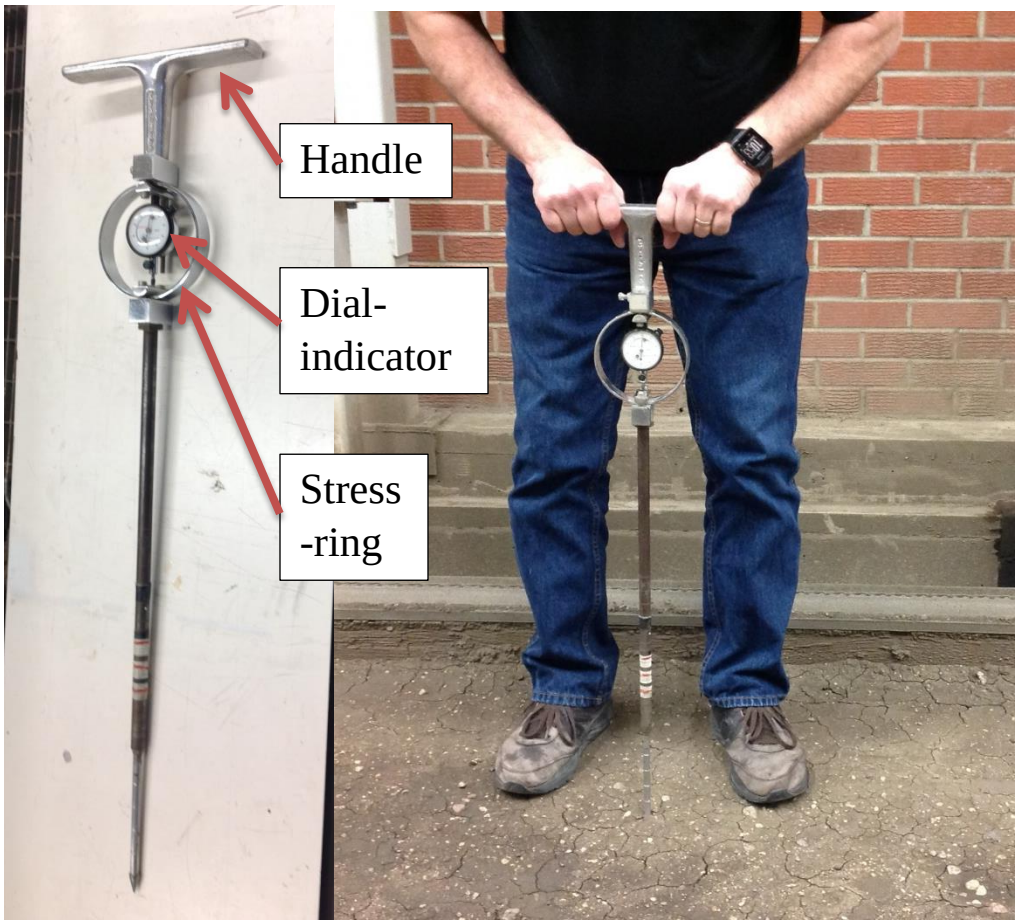

Figure 3- 15: Penetrometer for measuring cone index

3.5 Test Parameters for the single disc test

Many tests were conducted on a disc with a diameter of 460mm and thickness of 4mm. The combination of tilt angles (0°, 15°, 20°, 25°) and disc angles (0°, 7°, 14°, 21°, 28°) produced a desired cutting width with a given depth and speed. The results of the tests, especially

the draft force**,** were compared with the analytical calculations. Table 3-2 show the parameters used for experiments. The parameters were held consistent during all the experiments. The variable parameters are values of input conditions used in the experiments and their range of change.

Table 3- 2: Parameters of the experiments

Constant parameter name	Value	Unit
Soil moisture(water content)	9-12%	NA
Disc size	460 (18.1)	mm (in)
Disc Thickness	4 (0.157)	mm (in)

The forces acting on the tool in horizontal, vertical and lateral directions were measured by load cells. A combination of the tilt and disc angle was selected to produce a desired cut width at a given depth. A full matrix of tests were completed, for each tilt angle (0°, 15°, 20°, 25°) and disc angles (0°, 7°, 14°, 21°, 28°). All of the test~~s,~~ results were recorded.

Disc Angle, α, (degree): 0°, 7°, 14°, 21°, 28°

Tilt Angle, β, (degree): 0°, 15°, 20°, 25°

Carriage Speed, mph (km/h): 3(4.84), 5(8.05)

Cutting Depth, in (mm): 2(50.4), 3(76.2)

For the single disc experimental tests, at least two tests were performed for the same tilt and disc angles with the same depth and speed. This ensured a level of repeatability in the test results. If the results of two tests were not similar, the test condition was repeated until

acceptable results were obtained; i.e. test results would not differ more than 20%. In Ahad Armin's thesis, he compared these forced frequencies with the natural frequencies of the machinery and concluded that 1.5 Hz was the force frequency of the system that should be filtered out; therefore this signal was filtered to exclude all frequencies above 2 Hz [43]. Moreover, in Reza Aminzadeh's thesis, he mentioned that the cut off frequency of the low pass filter was set to 2Hz [41]. Two closest tests were selected and analyzed in the Matlab program using a filter of 2Hz to make the data easier to interpret. This was to exclude noise and any vibration effects of the disc. For each combined tilt and disc angle test, the initial 25% of the run was ignored due to speed variation while the unit achieving its constant speed. A detailed example of how to use the filter in the Matlab program with further interpretation for the particular case of 7° disc angle and 25° tilt angle is shown in Appendix A. Similarly, the rest of data were generated as the average force of the disc.

3.6 Test procedure for planter

The planter with the combination of disc angle ($\alpha = 7°$) and tilt angle ($\beta = 25°$) was attached to the carriage after the soil was prepared in the soil bin. Due to limitations of space, the tests for the planter were started from the opposite direction as were the disc experimental tests. The test procedure for the planter was similar to the test procedure for the disc. The depth zero point was defined as the lowest point of the disc coulter in the planter when it touched the surface of the soil. The cutting depth (2in or 3in) was measured below this point, which was set by the gauge wheel of the planter. Data recording began when the planter passed the first trigger switch until it touched the end switch.

3.7 Summary

This chapter discussed a series of experiments that were designed and conducted to find the disc angle and tilt angle that could result in a minimum draft force. The experimental procedure was established. First, the experiment settings were defined, then a series of tests were conducted to investigate the forces required to pull the disc or the planter in a controlled simulated field condition. The draft, vertical and side force were measured. The soil was properly prepared according to a four-step preparation procedure to ensure the consistency of test conditions. Soil moisture content and hardness (cone index), which are the main factors affecting the experiment results, were measured.

In chapter 4, the effect on various disc and tilt angles on the forces applied on the disc or planter from the soil is studied and analyzed based on the detailed test results.

Chapter 4 – Review of Test Data and Discussion

4.1 Introduction

In this chapter the experimental testing results are discussed. The test procedure was outlined in the previous chapter and the analysis results from the data will be used in the next chapter. Test set up validation is presented first. The next sections cover the discussion of single disc test data followed by the planter tests. In every experimental test there is some variation from one test to another due to uncontrolled variables. The experiments were always repeated to confirm the repeatability and reliability of the test data. The data presented here shows that the controlled variables account for the majority of the response.

Test data from a series of experiments performed in the soil bin were grouped into two sets based on equipment type. One was for the single disc and the other was for the planter. For simplicity most of test data was extracted from the single disc test in the analytical investigation. In each test, the width of the furrow must be greater than zero due to seeding requirements, which means both disc and tilt angle cannot be zero. The draft, vertical, and side forces for zero disc and tilt angle show that there are other parameters that influence the disc performance while the disc moves in the soil. These factors, such as the variation due to manufacturing and assemble tolerances were ignored in the tests.

At the end of this chapter, the cutting force and normal force were calculated from an analytical model based on the draft force, the vertical force, and the side force that were measured with the compound angle of 7° disc angle and 25° tilt angle.

4.2 Setup Validation

The collected data was filtered to reduce the noise. However, filtering causes loss of data. By selecting the filter appropriately the data loss can be minimized and the effect on the findings can be neglected. The vibrations of the disc added undesirable noise to the recorded signal. A filter was added to reduce this noise. The following was completed to help identify the cut off frequency of the filter.

Figure 4- 1: Accelerometer for the natural frequency test

The natural frequency test was performed using two sensors on top and on the side as shown in Figure 4-1. An Accelerometer (shown in Figure 4-1) was used to measure the frequencies of the disc while one end is in the air or in the soil. The sensors were selected to insure ensure the frequency response was correct for this application. From these experiments, the natural frequencies of the disc with two different boundary conditions were determined. The natural frequencies were calculated in two different ways, one is to use the code developed by Matlab program, the other is plotting data using a Matlab program which measured peak to peak

response in order to double check the natural frequency calculation. Appendix I gives details of the two methods.

Table 4-1 shows the natural frequencies of the disc. The natural frequencies from the analyzer were approximately 195Hz to 234Hz with the disc in the air and approximately 78Hz to 98Hz when its end was in the soil. The nature frequencies calculated by Matlab code method were 218Hz to 270Hz in the air and approximately 77Hz to 79Hz in the soil. The difference between the values calculated by the two methods is within 20% of each other, which means they were measured reasonably well. With a Natural frequency above 75Hz it is safe to assume that all unwanted effects of the disc vibration can be excluded from the data if the low pass filter is set to 2Hz. My fellow graduated PhD student Ahad Armin in his thesis (Page 93-98), Mechanics of soil-blade interaction, has proved that 2Hz filter is the most reasonable amount for soil-blade interaction [43]. With a similar analogy it can be shown that for the disc coulter, a 2Hz filter is reasonable to exclude the noisy signals for soil-disc interactions.

Table 4- 1: Results for natural frequency test

		Matlab						Accelerometer	% diff
Top	Disc Constraint	Peak 1		Peak 2		Period	Freq	Freq	
Scope		xp	yp	xp	yp	Ti(s)	1/Ti(Hz)	FFT (MatLab)	
		Second	Volt	Second	Volt				
0	air	0.008	0.135	0.012	0.160	0.004	270	234	14%
1	air	0.000	0.155	0.005	0.180	0.005	218	195	11%
2	air	0.008	0.193	0.013	0.180	0.004	233	234	-1%
3	air	0.005	0.993	0.009	1.087	0.004	237	195	19%
4	soil	0.028	1.212	0.041	0.556	0.013	79	78	1%
5	soil	0.002	0.637	0.015	0.497	0.013	77	98	-23%

4.3 Disc test data and discussion

Many tests were conducted on the single disc with various disc angles between 0 to 28 degrees where the tilt angles varied between 0 to 25 degrees. The different combination of tilt and disc angle were selected to produce a desired cutting width with a given depth and speed.

Each test was repeated at least twice in order to have consistent and repeatable results with the same test settings, and same soil conditions. Those two similar test results were analyzed in the Matlab program using a 2Hz filter. Due to the acceleration of the disc, the initial 22% of the data were ignored in each test. Only the steady state data was used for generating the modified average draft, vertical, and side forces for the disc coulter.

As the experiment setting in Chapter 3, the horizontal (draft) force was calculated by summing the two load cells in horizontal (or global Z) direction. The vertical force was the summation of the three load cells in vertical (or global Y) direction. The side force was measured by only one load cell in the global X direction. The draft force is the most important variable measured during the motion of disc, because it leads to the minimum energy consumption for the planter as used in real field conditions. The results of the tests, especially the draft force, were compared with the analytical calculations.

4.3.1 Modified Average Force Method and Examples

This section shows the detail test data of the draft force, F_z, the vertical force, F_y, and the side force, F_x presented in graphical form. The examples given in this section demonstrate the method used to obtain the modified average forces. The examples show only one combination of tilt and disc angles of 25° and 7°. The modified average forces were generated for use in the next section.

Example of the analyzed draft force data with depth of 2in, speed of 3mph, and the combined tilt and disc angles of 25° and 7° is shown in Figure 4-2. The Matlab code is given in Appendix A.

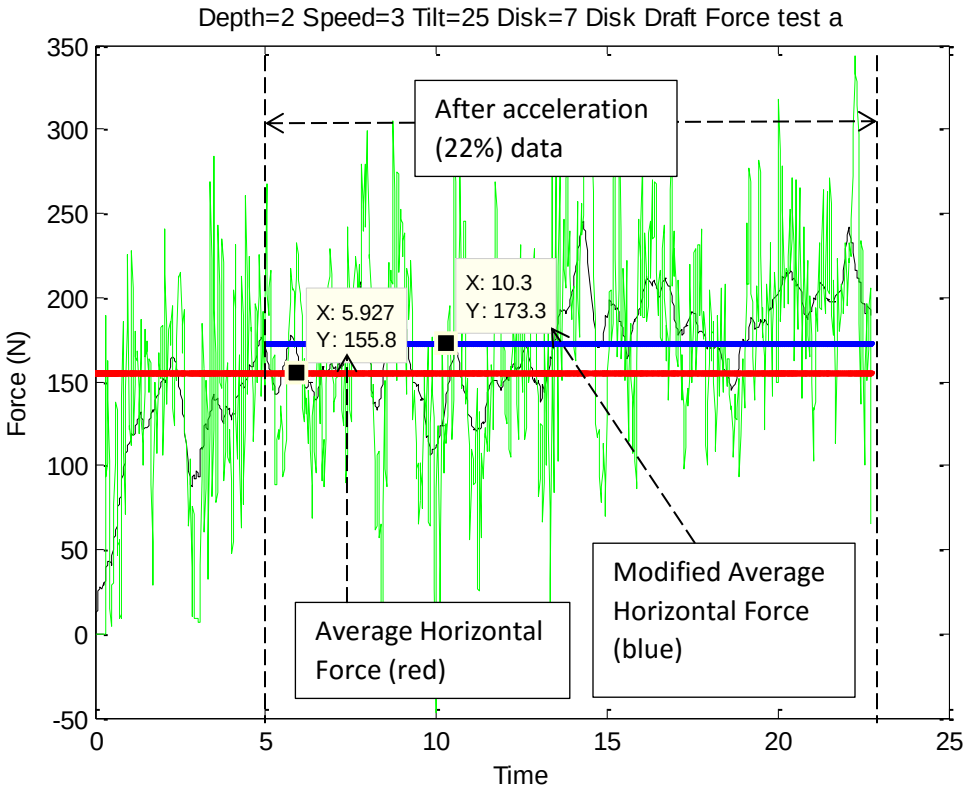

Figure 4- 2: The measure disc draft force, noise below 2Hz are filtered out

The first trial was compared with the second trial for the repeated experimental tests with the same tilt and disc angles, same depth, and same speed. The two tests would be accepted if the trials were within 20% of each other. Otherwise, a third trial was performed and was compared with the previous two trials and combined with the trial which had the closest match, or within 20% difference. In Figure 4-2, the raw data of this particular trial is represented in green. The chosen test result from each trial was then filtered using a 2Hz filter to make the data easier to

interpret (solid black line in Figure 4-2). Then, the average of the draft force, 156N, was calculated (shown in red in Figure 4-2). The experimental tests began with zero force and obtained a constant force, this implies that some acceleration occurs before constant velocity was reached. It is reasonable to assume that during the experimental tests, the constant velocity was obtained after 22% of each distance set of the experiment. In order to contain more reliable force values, the initial data (assumed to be about 22% of the data) was ignored. The data without acceleration is called the modified average force. The rest of the data, the modified average draft force, 173N, is more reasonable to be interpreted (shown in blue in Figure 4-2).

Similarly, Figure 4-3 is the plot of the vertical force with depth of 2in, speed of 3mph, and the combined tilt and disc angles of 25° and 7°. The modified vertical force, which was used for further calculations (the equations from in Chapter 2) was 389N. Figure 4-4 shows the modified side force, which was 251N, for this particular example.

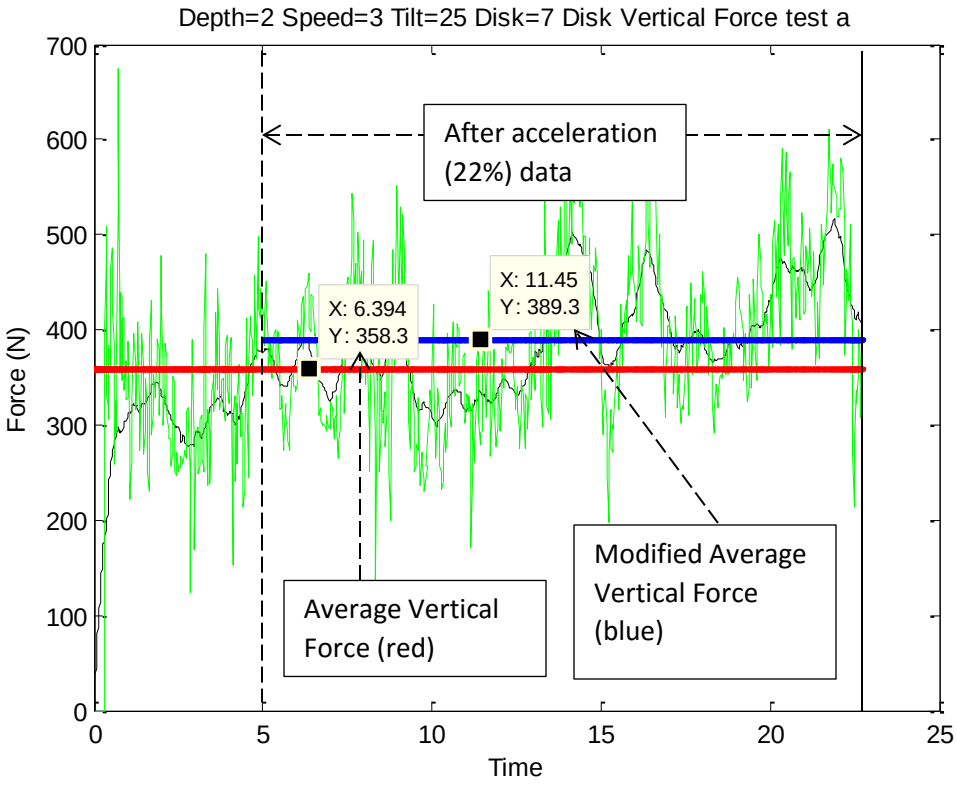

Figure 4- 3: The measured disc vertical force, noise below 2Hz are filtered out

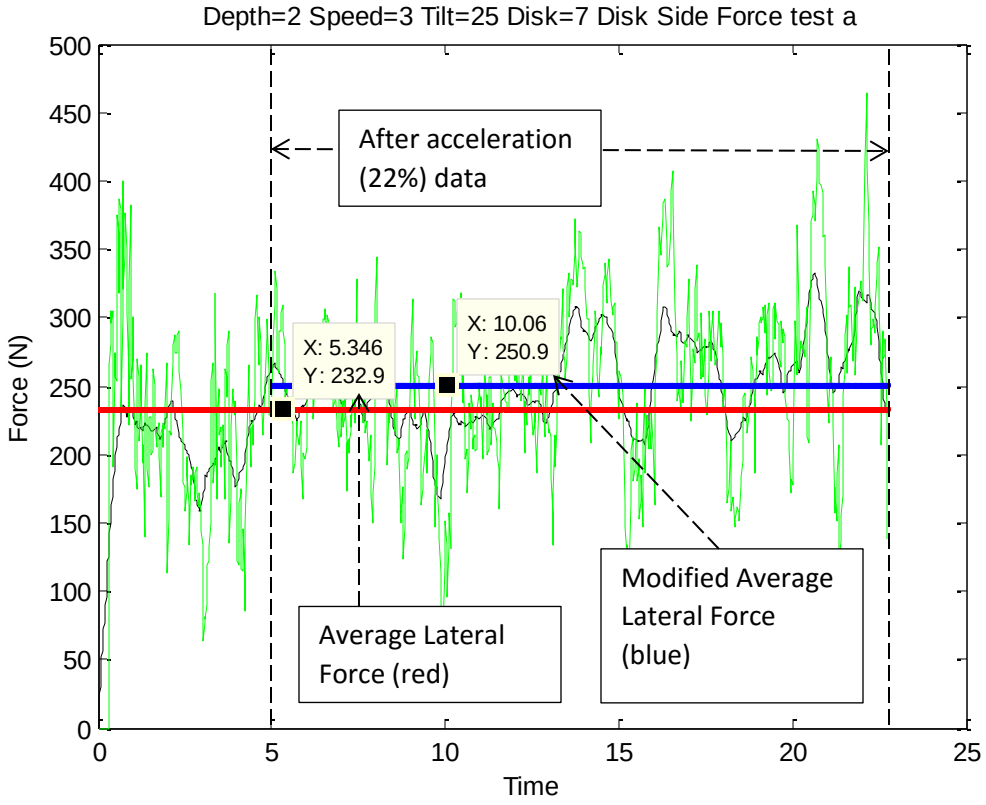

Figure 4- 4: The measured disc side force, noise below 2Hz are filtered out

The above examples demonstrate the modified average force method. In the next section only the modified data is used for further analytical work.

4.3.2 Test results for 2in depth and 3mph speed

There were 4 groups of disc test. Each group had a different depth and different disc speed (Table 3-1). The series of tests with all combinations of various tilt and disc angles were performed for each group. This section shows the results for group one which had depth of 2in and speed of 3mph. The experimental data from the other 3 groups are shown in Appendix B.

The vertical, draft, and side forces of the two trials with the application of 2Hz filter are analyzed here. Data of the two similar runs would be analyzed by using the Matlab program, and then the two chosen data sets were evaluated and compared. The average of the filtered forces for the disc is much easier to use than the average of the raw force data. The modified average of the vertical, draft, and side forces can be plotted, as shown in the following figures.

Figure 4-5 and Figure 4-6 show effects of disc and tilt angles on the draft force. When tilt angle is zero, draft force increases with the increasing of disc angle. The reason for this phenomenon is that when the disc angle increases, the disc pushes soil aside to open the furrow, which increases the drag force. When the tilt angle is not zero, the combination of disc and tilt angles lifts up the soil and displaces it to the side which increases side and vertical forces. The tilt angle can help to keep the draft force from increasing rapidly while increasing the disc angle for the same cutting width. Figure 4-5 shows the draft force, F_z, increases with increasing disc angle for the disc with depth of 2in and speed of 3mph. The relationship between draft force and disc angle appears to be almost linear. The slope of the curve increases with tilt angle increasing. Figure 4-6 shows the draft force, F_z,, increases slowly, nearly constant, with increasing tilt angle. The two repeated experimental trials are called “low” and “high” in the figures. The low is the lower value of the two trials, and the high is the higher values of the two trails.

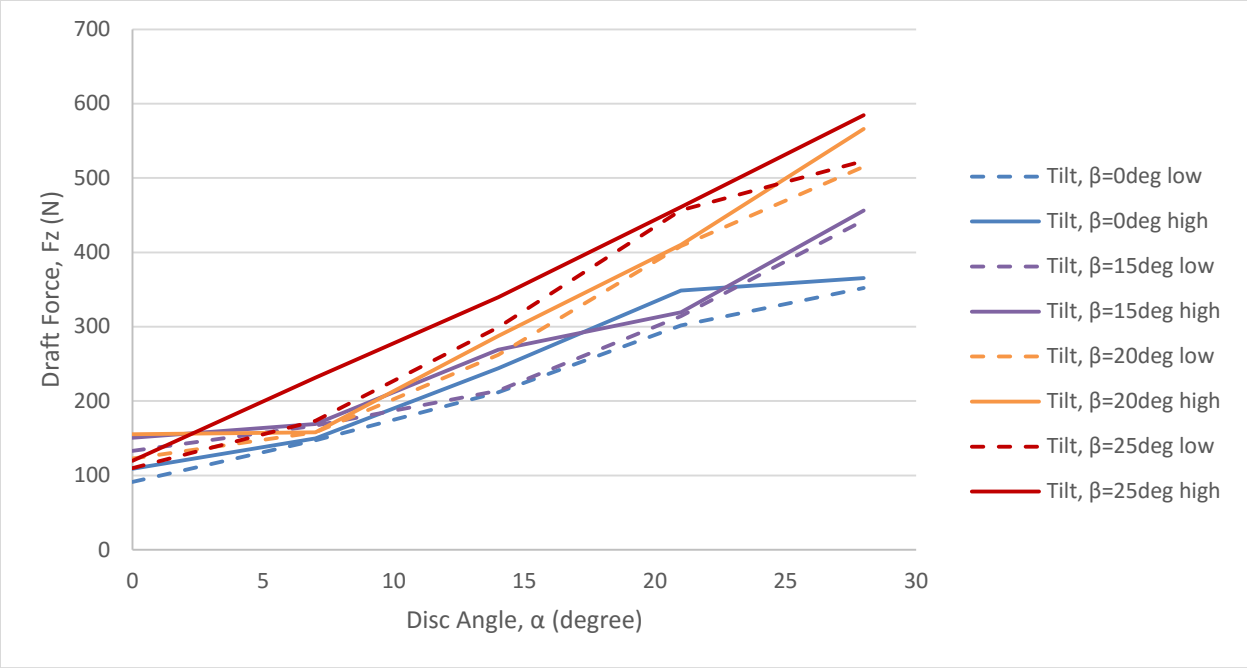

Figure 4- 5: Draft force, Fz, for the disc (disc angle, α) with depth=2in speed=3mph

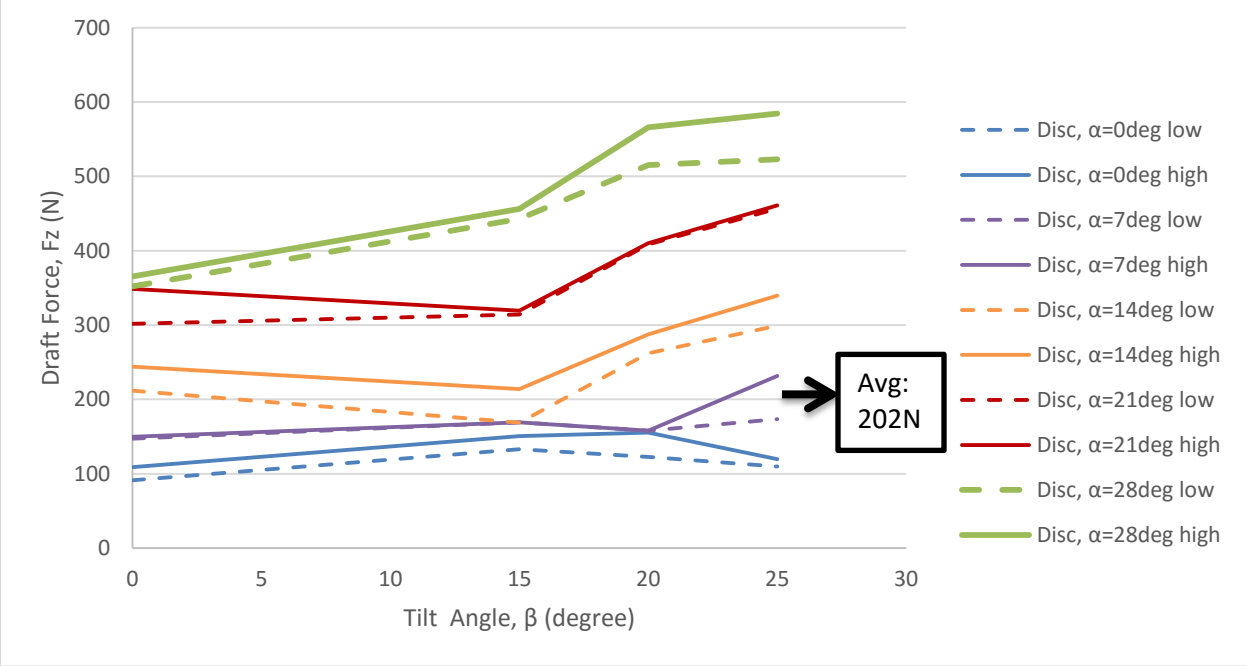

Figure 4- 6: Draft force, Fz, for the disc (tilt angle, β) with depth=2in speed=3mph

The relationship between draft force and tilt angle is not completely linear but will be treated as nearly linear here. Curve fits are shown in Chapter 5. Draft force for the zero disc angle test shows no increase as the tilt angle is increased. This effect is as to be expected. The slope of the draft force curves increases as the disc angle increases. With zero tilt angle, disc angle is a significant driver of the draft force. Overall, the tilt angle and disc angle are important in driving the force up.

A larger disc angle results in larger draft force. In order to keep the draft force as low as possible, a smaller disc angle should be chosen. However, disc angle cannot be zero, because it determines the width of the furrow. With the depth of 2in and speed of 3mph, the most reasonable compound angle (non-zero disc angle) for the lowest draft force is 7° disc angle and 25° tilt angle. Both Figure 4-5 and Figure 4-6 show that the average of the minimum draft force is 202N.

The amount of the force needed to keep the disc in the soil when pulling the disc forward is called the vertical force. The weight of the disc does not affect the vertical load, since the zero of the load cells was set when the disc was attached to the carriage and not in contact with the soil.

Figure 4-7 and Figure 4-8 show the vertical force for different disc angles (0°, 7°, 14°, 21°, 28°) combined with different tilt angles (0°, 15°, 20°, 25°). Figure 4-7 shows the absolute value of the vertical force, Fy, increases with the increasing of the disc angle. However, in Figure 4-8, for the disc with depth of 2in and speed of 3mph, the absolute value of the vertical force, Fy, stays almost constant with increasing tilt angle, when the disc angle is small. The most suitable disc and tilt compound angle is mainly chosen by the lowest draft force. The vertical force is not so critical as draft force for further study and analysis of the experimental tests. As the experimental

results showed, the corresponding average vertical force for the minimum draft force with a compound angle of 7° disc angle and 25° tilt angle is -358N shown in Figure 4-7 and Figure 4-8.

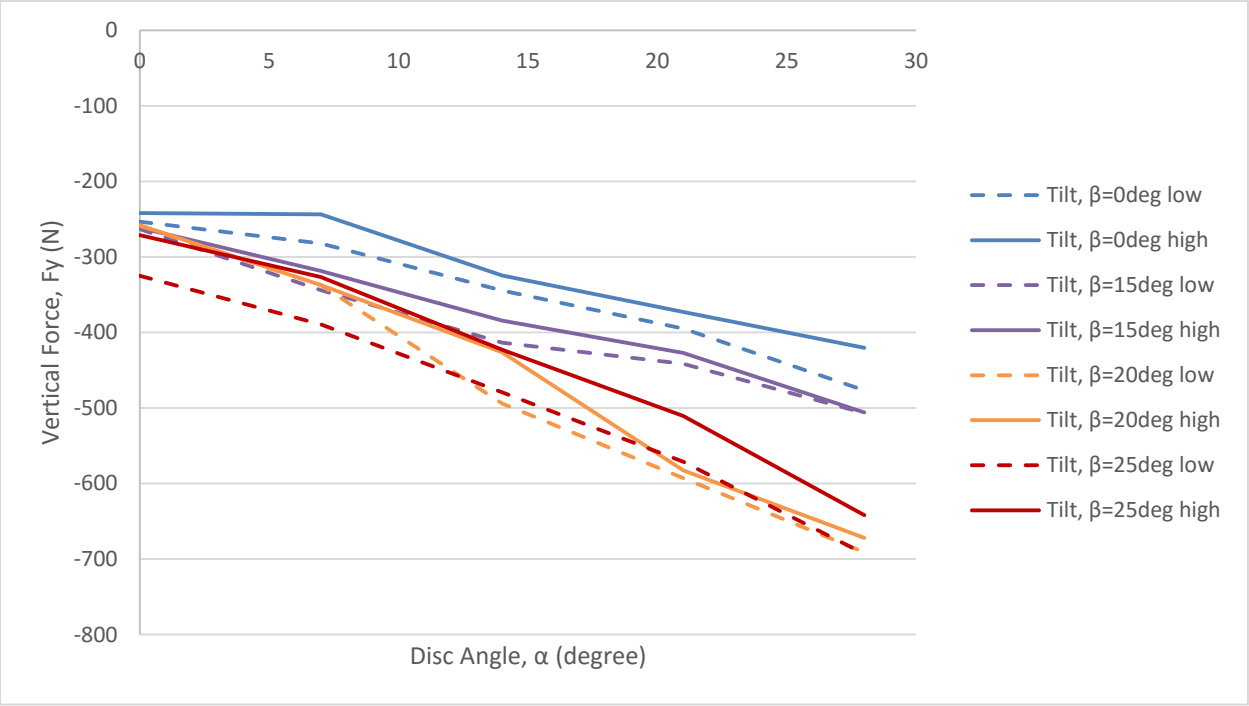

Figure 4- 7: Vertical force, Fy, for the disc (disc angle, α) with depth=2in speed=3mph

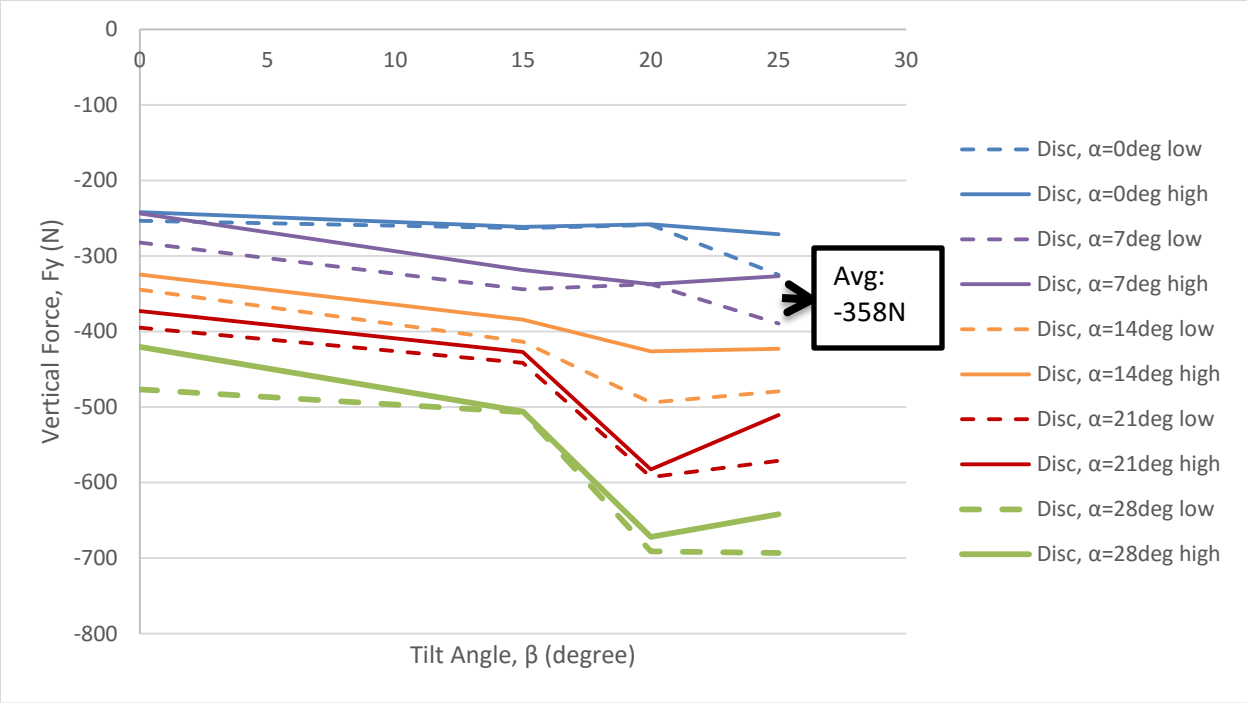

Figure 4- 8: Vertical force, Fy, for the disc (tilt angle, β) with depth=2in speed=3mph

From the results of the side (lateral) forces, due to the non-zero disc angle and non-symmetrical system, the higher the disc angle the higher the side force. However, the combination of disc and tilt angle reduced the side force. The compound angle disc lifts up the soil and displaces it to the side instead of pushing and pressing the soil to the side. Figure 4-9 shows the side force F_x, increases with increasing disc angle for the disc with depth of 2in and speed of 3mph. Figure 4-10 shows the side force, F_x, stays almost constant with the increasing of tilt angle for the disc especially when the disc angle is small. The chosen disc and tilt angle for the lowest draft force yields the average side force of 244N as shown in Figure 4-9 and Figure 4-10.

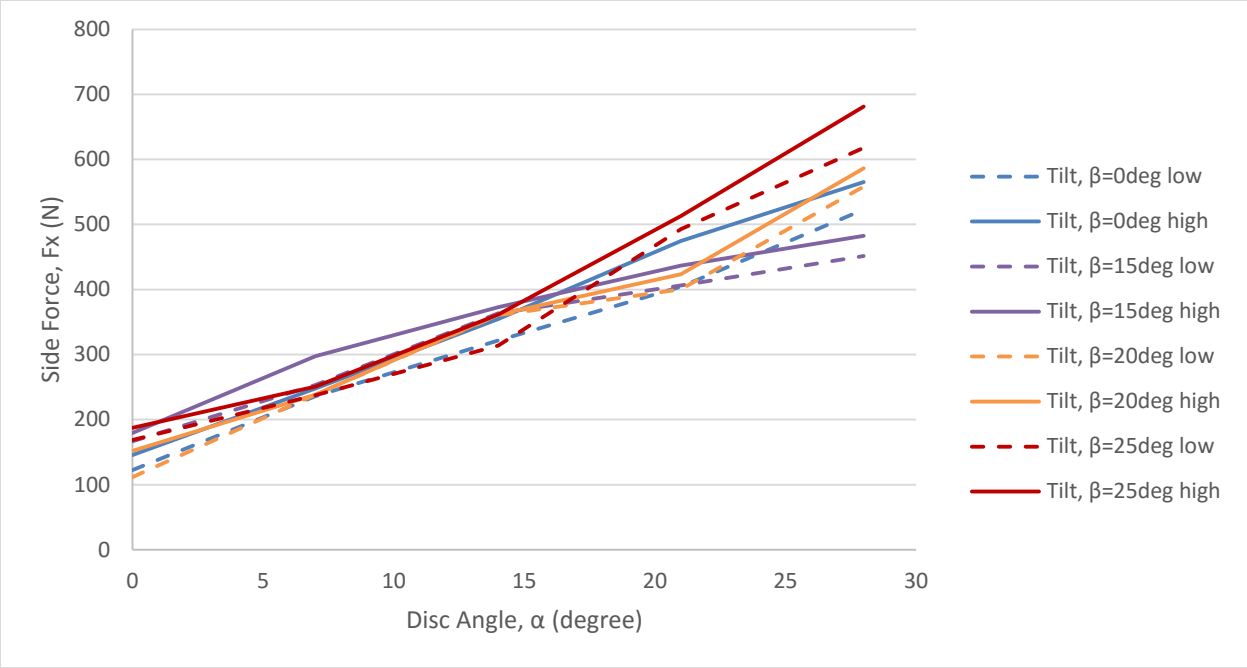

Figure 4- 9: Side force, Fx, for the disc (disc angle, α) with depth=2in speed=3mph

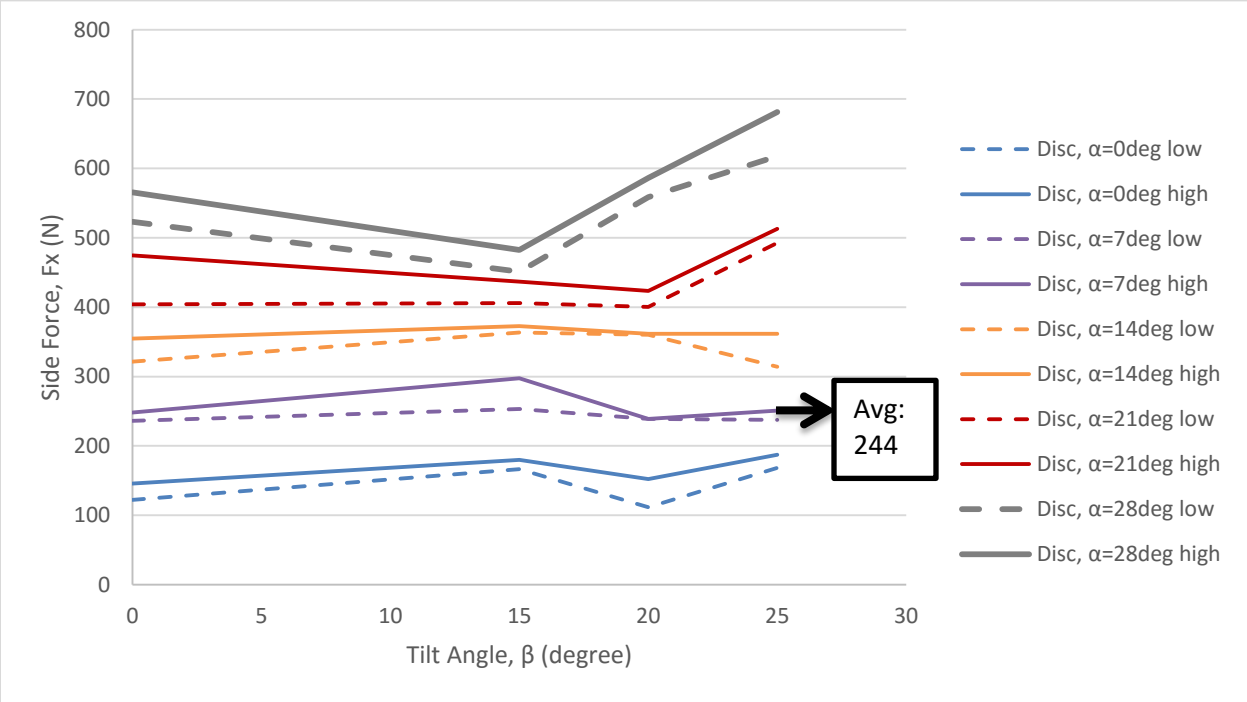

Figure 4- 10: Side force, Fx, for the disc (tilt angle, β) with depth=2in speed=3mph

The goal of the single disc tests was to find the best combination of disc angle and tilt angle which leads to a minimum draft force. From the above figures, the results of the disc coulter experimental tests show that the compound angle of 7° disc angle and 25° tilt angle gives the lowest draft force for a depth of 2in and a speed of 3mph.

In Appendix B, a detailed analysis of all the other three major groups with different depth and disc speed is presented. The conclusion for the each group in Appendix B also showed that the combination of 7° disc angle and 25° tilt angle gives the lowest draft force for different depths with different speeds (Table 3-1). The comparison of the combined 7° disc angle and 25° tilt angle with different depth and speed is summarized and shown in Table 4-2 for all four major group tests. An increase of the depth of cut will bring more friction and more interaction between soil and disc on the sides of the disc. Therefore, the reaction forces increased with increased depth of cut. We can conclude that by increasing the depth of disc in the soil, it increased forces in all three directions (draft, vertical and side). Increased disc speed also increased draft, vertical and side force.

Table 4- 2: Results of draft, vertical, and side forces with 7° disc angle and 25° tilt angle

Group #	1	2	3	4
	Depth =2in Speed =3mph	Depth =3in Speed =3mph	Depth =2in Speed =5mph	Depth =3in Speed =5mph
Draft	202N	299N	334N	343N
Vertical	-358N	-503N	-502N	-525N
Side	244N	366N	424N	430N

4.4 Comparison with Retest

It is necessary to confirm the repeatability and reliability of the test data, because there are many uncontrolled factors when dealing with soil conditions. The retests involved a choice of certain combined disc and tilt angles with different depths and different speeds (Table 3-1). The compound disc and tilt angle for retested experiments are as follow:

Table 4- 3: Retest experimental tests

Disc Angle, α, (Degree)	Tilt Angle, β, (Degree)
0	0
14	0
28	0
0	25
14	25
28	25

Table 4-3 is the retest for disc angle at zero degree and tilt angle at zero degree with different depths and different speeds. The rest of the retest data can be viewed in Appendix C. During the retests, the moisture content was measured at 7% and cone index was measured at 1.24Mpa (refer to Chapter 3 section 3.4 for explanation). Then, the average of the two retested trials (trial Re_a, trial Re_b) were compared with the average of the two original trials (trial a, trial b) in order to verify the original experimental test data. The retests (Table 4-4) were repeated until the percent difference was within 20% for most cases, which is considered a reasonable range with all the variables involved. Sometimes retest results showed more than 20% difference with the original test data or with the retested data on another day. Since there are so many

parameters involved in preparation of soil before tests, these differences may not be explained every time.

Both original data difference and the retest data difference has been calculated using the following formula

$$\%\ diff\ between\ trials = \frac{trial\ a - trial\ b}{(trial\ a + trial\ b)/2} \quad (4.1)$$

The difference between the retest data and the original data is calculated as follow

$$\%\ diff\ with\ ori. = \frac{(trial\ a + trial\ b)/2 - (trial\ Re_a + trial\ Re_b)/2}{((trial\ a + trial\ b)/2 + (trial\ Re_a + trial\ Re_b)/2)/2} \quad (4.2)$$

Table 4- 4: Disc, α=0 and tilt, β =0 comparison

				Moisture	7%		**Cone index**		1.24Mpa
Original Trials and Retest							after	22%	
	Trials	Tilt	Disc	Vertical	Draft	Side	Vertical	Draft	Side
Depth=2 in Speed=5 mph	a	0	0	-283	163	179	-325	143	241
	b	0	0	-268	150	158	-318	141	236
Original difference				-6%	-9%	-13%	-2%	-1%	-2%
Depth=2 in Speed=5 mph	Re a	0	0	-260	133	158	-295	118	205
	Re b	0	0	-277	152	184	-327	125	240
Re-test difference				6%	14%	15%	10%	6%	16%
Difference with original				-2%	-10%	1%	-3%	-15%	-7%
Depth=3 in Speed=5 mph	a	0	0	-261	122	268	-286	137	218
	b	0	0	-267	144	247	-299	143	196
Original difference				2%	17%	-8%	4%	4%	-10%
Depth=3 in	Re a	0	0	-255	112	230	-299	124	235

Speed=5 mph	Re b	0	0	-264	125	226	-283	132	266
Re-test difference				4%	11%	-2%	-5%	6%	12%
Difference with original				-2%	-12%	-12%	0%	-10%	19%
Depth=2 in Speed=3 mph	a	0	0	-280	119	164	-242	91	122
	b	0	0	-279	129	148	-253	109	146
Original difference				1%	-7%	10%	-5%	-18%	-17%
Depth=2 in Speed=3 mph	Re a	0	0	-286	120	139	-222	124	159
	Re b	0	0	-266	113	151	-259	115	135
Re-test difference				7%	5%	-8%	-15%	7%	16%
Difference with original				-1%	-6%	-7%	-3%	18%	9%
Depth=3 in Speed=3 mph	a	0	0	-346	135	177	-269	124	199
	b	0	0	-331	128	174	-246	121	166
Original difference				4%	6%	2%	9%	2%	18%
Depth=3 in Speed=3 mph	Re a	0	0	-381	163	175	-317	128	158
	Re b	0	0	-357	145	195	-292	121	162
Re-test difference				6%	12%	-11%	8%	6%	-2%
Difference with original				9%	16%	5%	17%	1%	-13%

Considering the variability of soil, the data can be used with a 20% difference. In Table 4-4, the highest difference for disc angle of zero and tilt angle of zero is about 19% for side force. This means that data are within the reasonable range.

4.5 Planter Test Data and discussion

The test data for the planter was analyzed in the same manner as the single disc data. There are also four major groups in the planter experimental tests. The goal is the same, which is to find the planter parameters for minimum draft force for different depths and different speeds (Table 3-2). Two tests were performed for the same depth, speed, tilt and disc angles. To make the data easier to interpret, the two similar test results were analyzed in the Matlab program using a filter of 2Hz.

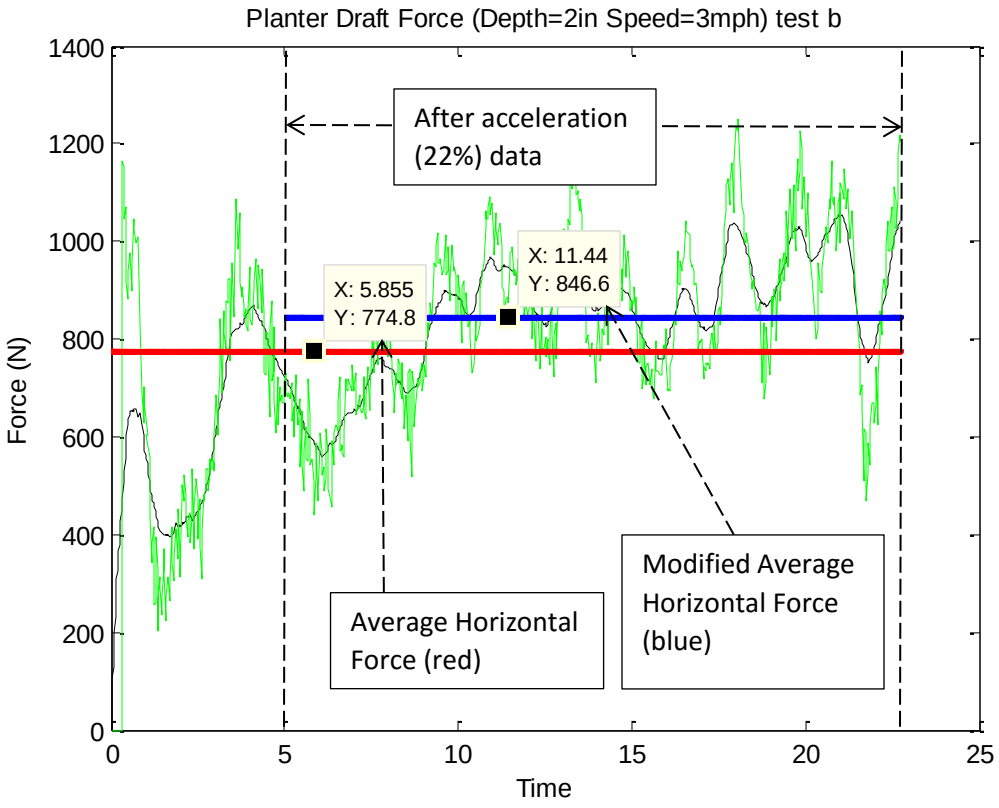

Figure 4- 11: The measured planter draft force, noise below 2Hz are filtered out

An example of the data analysis for the measured draft force of planter is shown in Figure 4-11. The raw data for planter with depth of 2in and speed of 3mph is shown in green. Data is then evaluated by using a 2Hz filter as shown in black. The average of the draft forces in full range is 775N as shown in red while the modified average forces is 847N as shown in blue. The modified average vertical, draft, and side forces are then used for further analyzing.

Similarly, Figure 4-12 shows the vertical force of the planter with depth of 2in, speed of 3mph. The modified vertical force is 256N. Figure 4-13 shows the modified side force (88.2N) for this particular example. The modified forces were used to plot in next Figures.

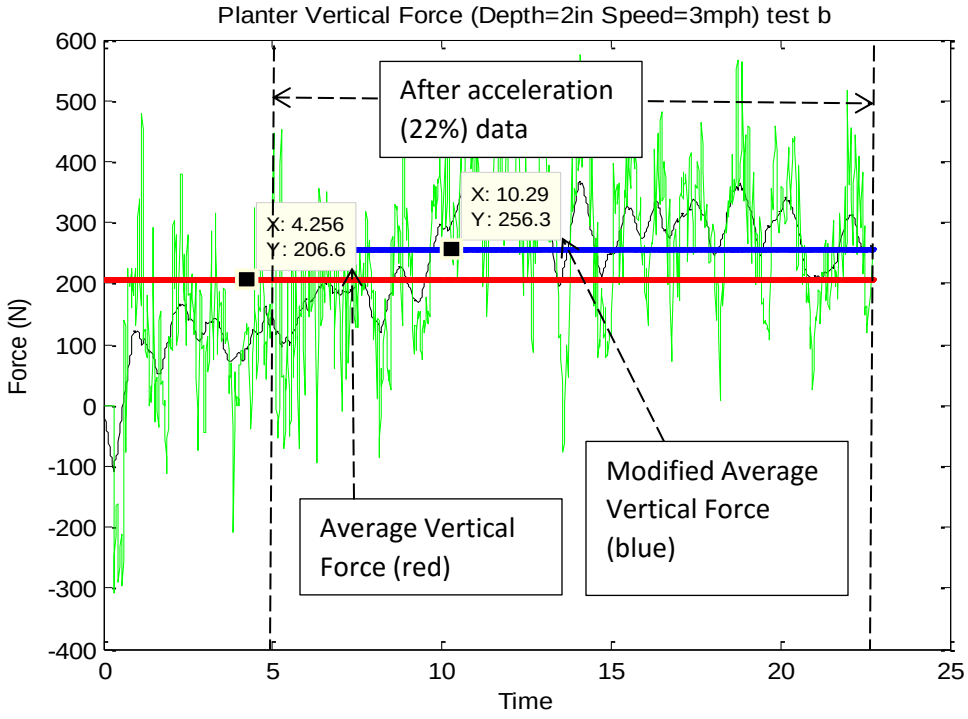

Figure 4- 12: The measured planter vertical force, noise below 2Hz are filtered out

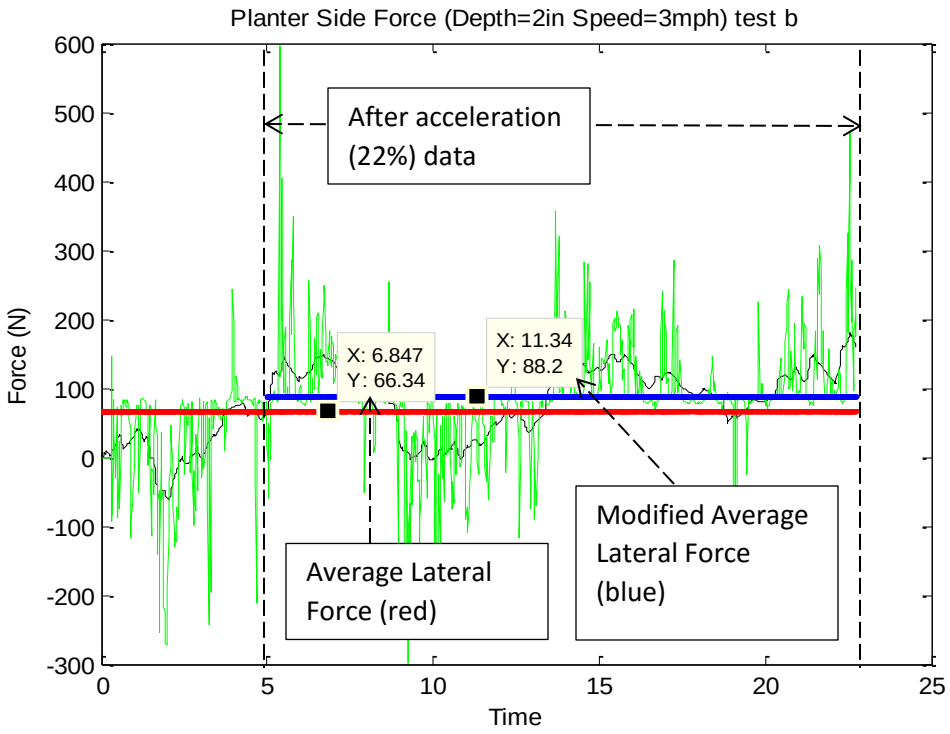

Figure 4- 13: The measured planter side force, noise below 2 Hz are filtered out

Again, draft, vertical and side forces from two tests with the same depth and speed were accepted when the error difference was 20% or less. A third test was performed to compare and to verify with the previews two tests. The priority is to consider the draft force, then the vertical force. The value for the side force is relatively small compared with draft force and vertical force; also, it is not as important as the other forces. The two closest planter experimental test data were recorded in Table 4-5.

Table 4- 5: Planter experimental test data

		Original			After 22%		
Depth	Speed	Vertical	Draft	Side	Vertical	Draft	Side
(in)	(mph)	(N)	(N)	(N)	(N)	(N)	(N)
2	3	207	775	16	256	847	18
	3	179	760	13	217	790	15
	ave	193	768	15	237	818	16
	% diff	14%	2%	22%	17%	7%	22%
	5	613	1055	25	627	985	32
	5	606	1066	26	670	1139	26
	ave	609	1061	25	648	1062	29
	% diff	1%	-1%	-2%	-7%	-15%	20%
3	3	256	923	31	278	937	31
	3	232	988	24	249	980	21
	ave	244	955	28	264	958	26
	% diff	10%	-7%	24%	11%	-4%	38%
	5	647	1273	67	675	1236	77
	5	640	1303	65	665	1324	67
	ave	643	1288	66	670	1280	72
	% diff	1%	-2%	2%	1%	-7%	15%

The planter draft force is the main concern of this set of experiments. It directly influences planter efficiency and energy consumption. The high and low values from the two same trials were within 20% of each other. The modified average draft force for different depths and different speeds (Table 3-1) are plotted in Figure 4-14. The draft force is assumed to be linear with speed when this is plotted. For depth at 2in, the average draft force for speed of 3mph is 818N and for speed of 5mph is1062N. For depth at 3in, the average draft force for speed at 3mph is 958N and for speed of 5mph is 1280N. As a result, Figure 4-14 shows that increasing speed will increase the draft force; also, by increasing the cutting depth the draft force is also

increased. The slope of curves for cutting depth of 2in and 3in are very similar. The variation is less at higher speed, this may be an important issue for further study.

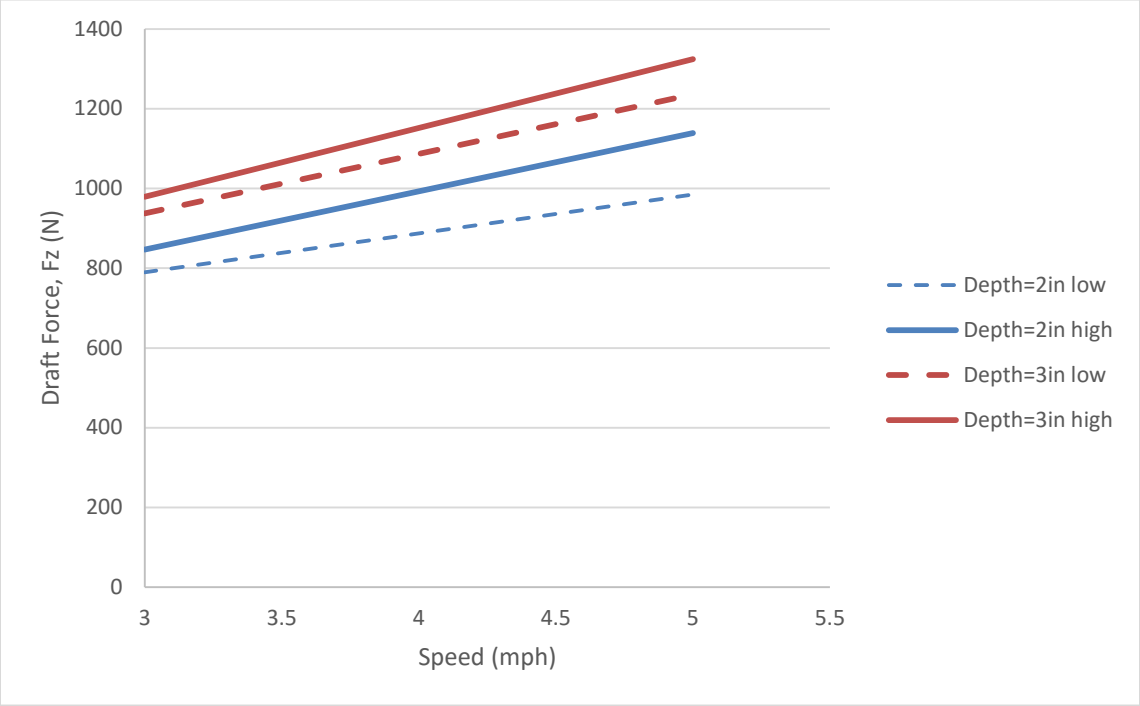

Figure 4- 14: Modified average draft force for the planter

The planter vertical force is the amount of the force on the planter upward from the soil when it is being pulled forward. Figure 4-15 shows the plot for modified average vertical force in different depths and different speeds (Table 3-1). The average vertical force with speed of 3mph is 237N and for speed of 5mph is 648N for depth of 2in. The average vertical force with speed of 3mph is 264N and speed of 5mph is 670N for depth of 3in. This shows that increasing the speed will increase the vertical force. While with the increasing of cutting depth, the vertical force increase slightly.

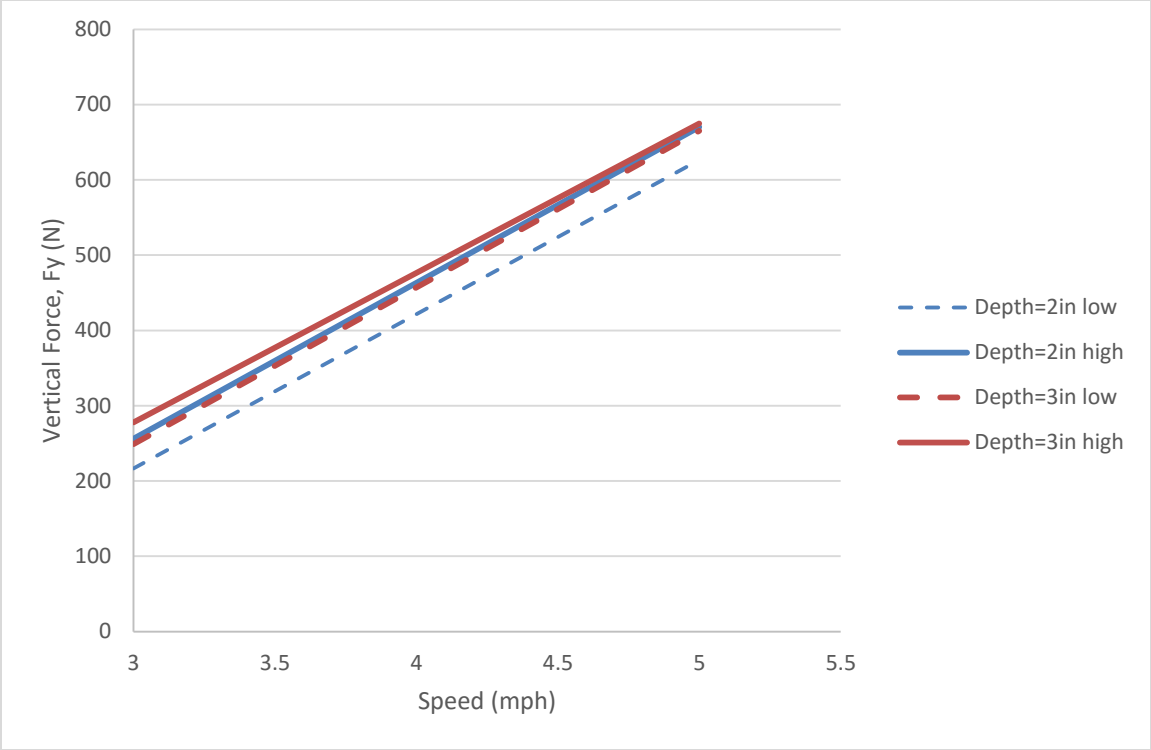

Figure 4- 15: Modified vertical force for the planter

Due to the symmetrical design of the planter, the two discs were placed with opposite tilt and disc angles to each other, thus the side forces should cancel each other's out, ideally. However, side forces do exist in these experiments due to the imperfection of the planter and soil. In Figure 4-16, the modified average side force for different depths and different speeds (Table 3-2) are plotted. For cutting depth of 2in, the average side force for speed of 3mph is 16N and for speed of 5mph is 29N. For cutting depth of 3in, the average side force for speed of 3mph is 26N and for speed of 5mph is 72N. As a result, the figure shows that increased speed will increase side forces; also, by increasing the cutting depth the side force is also increased. With a full size planter there will be many more discs to help balance the side forces. Due to the limitation of the soil bin equipment, the side force measured is the overall planter side force. Perhaps for future

experiments, the two separated actual side force data can be provided and the side to side variation in force can be shown.

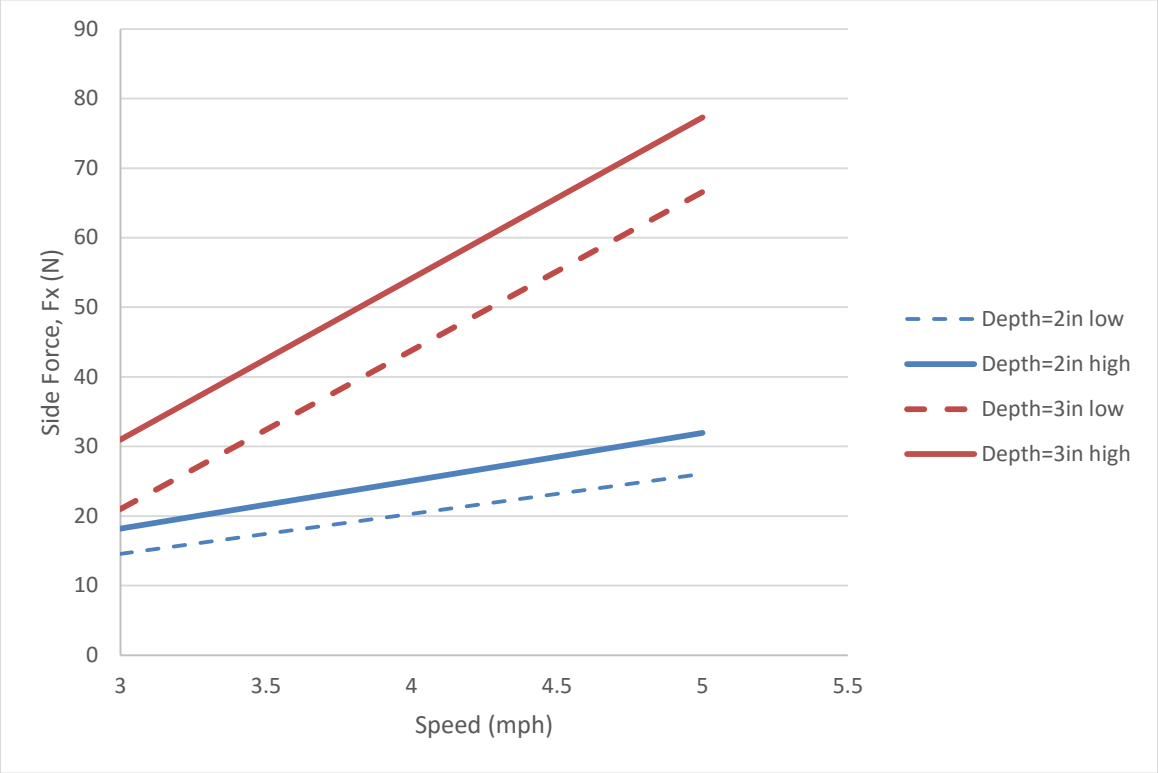

Figure 4- 16: Modified average side force for the planter

4.6 Cutting Force

Cutting force is the amount of the force that the disc coulter encounters while cutting soil. The cutting force acts at a certain point on the edge of the disc coulter where it contacts the soil. Cutting force cannot be measured directly. The cutting force can be evaluated by equation(2.11). Cutting forces are a combination of the draft, vertical, and side forces. For identical discs, soil conditions, depth, and a range of disc angle and tilt angle, the soil forces are calculated from the measured planter forces for each experimental setup in order to determine how cutting force depends on the disc configuration. Each dependency found is to be justified on the principles of

soil mechanics, or at least attempted to do so. This justification can be performed after experimental data are analyzed. The cutting force determines how much force is required for the disc coulter to cut through the soil.

With experimental data of depth of 2in and speed of 3mph (test a)

Given:

Angles: $\alpha = 7°, \beta = 25°$

Forces: $F_x = 250.9N, F_y = -389.3N, F_z = 173.3N$

Recall equation (2.11) showing as follow

$$\begin{bmatrix} N \\ F_r \\ F_c \end{bmatrix} = A(\alpha, \beta, \delta)^{-1} \begin{bmatrix} F_x \\ F_y \\ F_z \end{bmatrix}$$

$$= \begin{bmatrix} (cos\beta cos\alpha) & (sin\beta) & (cos\beta sin\alpha) \\ \left(\frac{-cos\alpha sin\beta sin\delta - cos\delta sin\alpha}{cos\delta}\right) & \left(\frac{cos\beta sin\delta}{cos\delta}\right) & \left(\frac{-sin\alpha sin\beta sin\delta + cos\alpha cos\delta}{cos\delta}\right) \\ \left(\frac{cos\alpha sin\beta}{cos\delta}\right) & \left(\frac{-cos\beta}{cos\delta}\right) & \left(\frac{sin\alpha sin\beta}{cos\delta}\right) \end{bmatrix} \begin{bmatrix} F_x \\ F_y \\ F_z \end{bmatrix}$$

Assumption: $\delta = \delta_{avg} = 24°$

Solution:

With equation (2.11) we get

$$F_c = -\frac{F_x cos\alpha sin\beta + F_z sin\alpha sin\beta - F_y cos\beta}{cos\delta} \tag{4.3}$$

$$F_c = -\frac{250.9cos7sin25 + 173.3sin7sin25 - (-389.3)cos25}{cos24} = 511.2N \tag{4.4}$$

Figure 4-17 shows the cutting force for depth of 2in and speed of 3mph. The most reasonable compound angle (non-zero disc angle) for the lowest draft force is 7° disc angle and 25° tilt angle. The average of the minimum cutting force is 511N. The cutting force,F_c, of the disc with tilt angles (0°, 15°, 20°, 25°) is shown in Figure 4-17. This figure shows that the cutting force, Fc, increases with the increase of disc angle for the disc with depth of 2in and speed of 3mph.

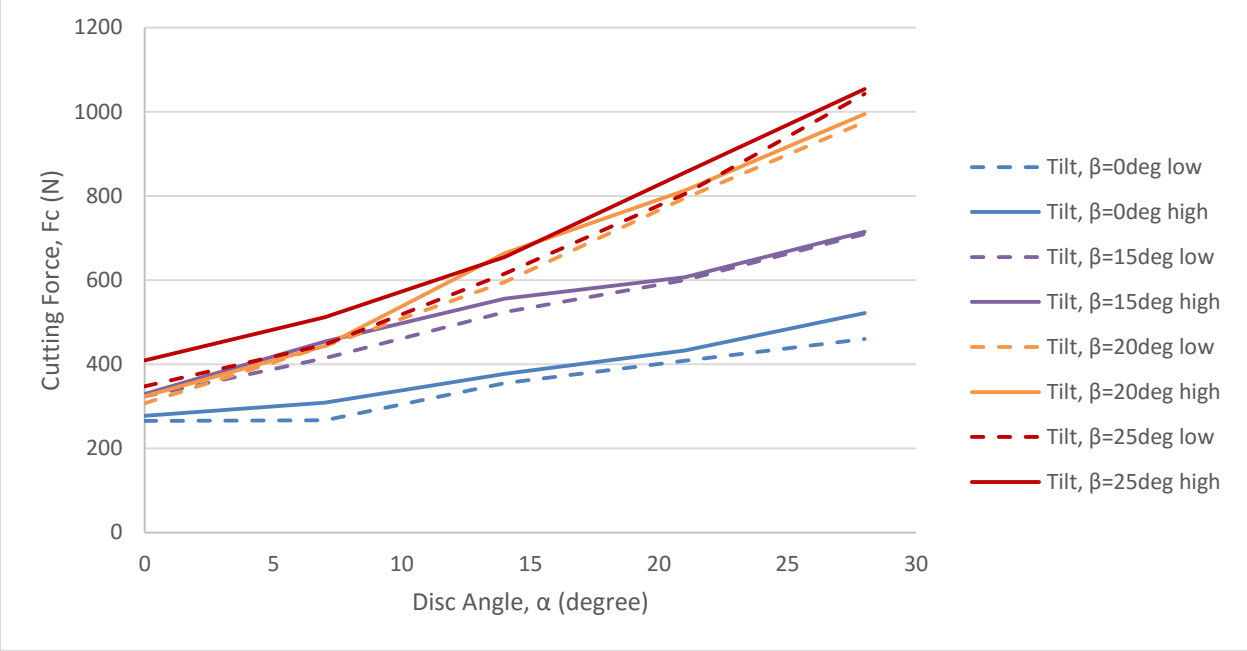

Figure 4- 17: Cutting Force, Fc, for the Disc (Disc Angle, α) with Depth=2in Speed=3mph

The cutting force,F_c, of the disc with disc angles (0°, 7°, 14°, 21°, 28°) at depth of 2in and speed of 3mph is shown in Figure 4-18. This figure shows the cutting force, Fc, increases slightly with the increase of the tilt angle, especially for lower disc angle.

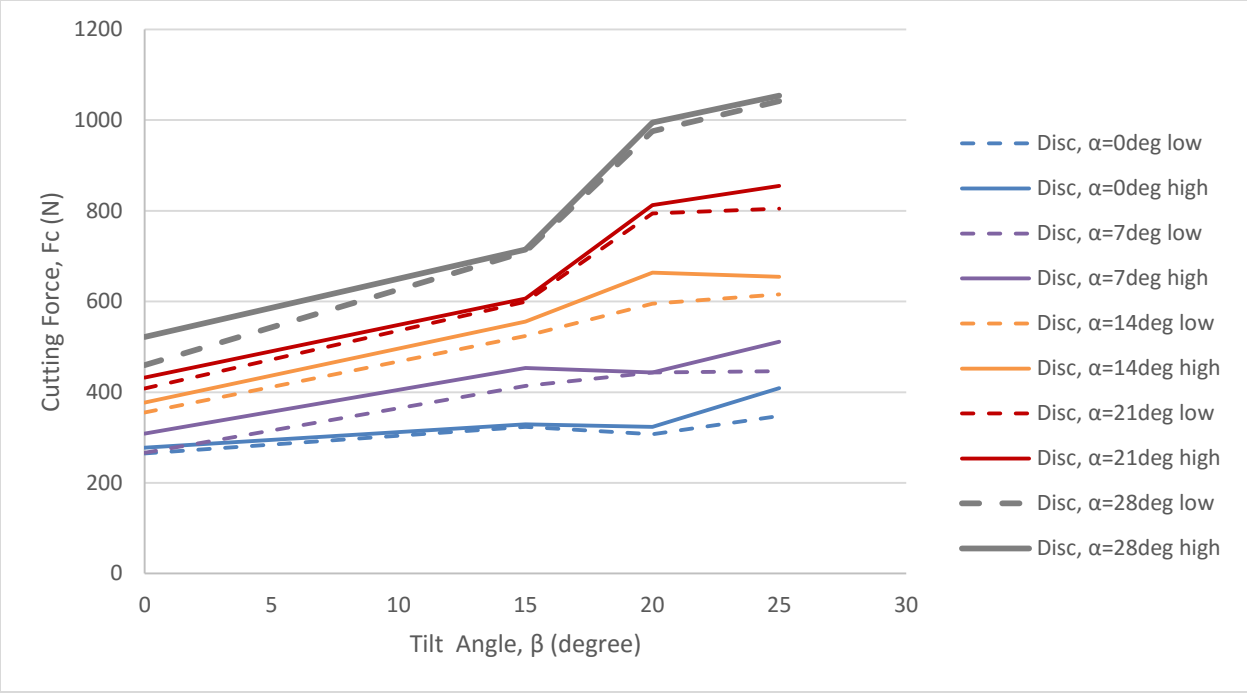

Figure 4- 18: Cutting Force, Fc, for the Disc (Tilt Angle, β) with Depth=2in Speed=3mph

More figures for different depths (2in and 3in) with different speeds (3mph and 5mph) are included in Appendix D. They indicate that increasing the depth of cut increases the cutting force; increase of the speed also increases the cutting force.

4.7 Normal Force

Normal force is the force from the soil that acts perpendicularly on the surface of the disc coulter contacting with soil. Normal force is also assumed to act at a certain point on the surface of the disc coulter where it contacts the soil. The normal force also cannot be measured easily. The normal force can be evaluated by equation(2.11). Similarly, the normal forces are calculated from the measured disc forces for each experimental setup in order to determine how normal force varies with disc configuration. The following figures only show the cutting force for depth of 2in and speed of 3mph.

With experimental data of depth of 2in and speed of 3mph (test a)

Given:

Angles: $\alpha = 7°, \beta = 25°$

Forces: $F_x = 250.9N, F_y = -389.3N, F_z = 173.3N$

Recall equation (2.11) showing as follow

$$\begin{bmatrix} N \\ F_r \\ F_c \end{bmatrix} = A(\alpha, \beta, \delta)^{-1} \begin{bmatrix} F_x \\ F_y \\ F_z \end{bmatrix}$$

$$= \begin{bmatrix} (cos\beta cos\alpha) & (sin\beta) & (cos\beta sin\alpha) \\ \left(\frac{-cos\alpha sin\beta sin\delta - cos\delta sin\alpha}{cos\delta}\right) & \left(\frac{cos\beta sin\delta}{cos\delta}\right) & \left(\frac{-sin\alpha sin\beta sin\delta + cos\alpha cos\delta}{cos\delta}\right) \\ \left(\frac{cos\alpha sin\beta}{cos\delta}\right) & \left(\frac{-cos\beta}{cos\delta}\right) & \left(\frac{sin\alpha sin\beta}{cos\delta}\right) \end{bmatrix} \begin{bmatrix} F_x \\ F_y \\ F_z \end{bmatrix}$$

Assumption: $\delta = \delta_{avg} = 24°$

Solution:

With equation (2.11) we get

$$N = F_x cos\beta cos\alpha + F_z cos\beta sin\alpha + F_y sin\beta \quad (4.5)$$

$$N = 250.9 cos25 cos7 + 173.3 cos25 sin7 + (-389.3) sin25 = 80.31N \quad (4.6)$$

For depth of 2in and speed of 3mph, the compound angle 7° disc angle and 25° tilt angle has the lowest draft force (non-zero disc angle). The average of the minimum normal force with 7° disc angle and 25° tilt angle is 80.3N. The Normal force,N, of the disc with tilt angles (0°, 15°, 20°, 25°) at depth of 2in and speed of 3mph is shown in Figure 4-19. This figure shows the normal force, N, increases with the increasing of disc angle.

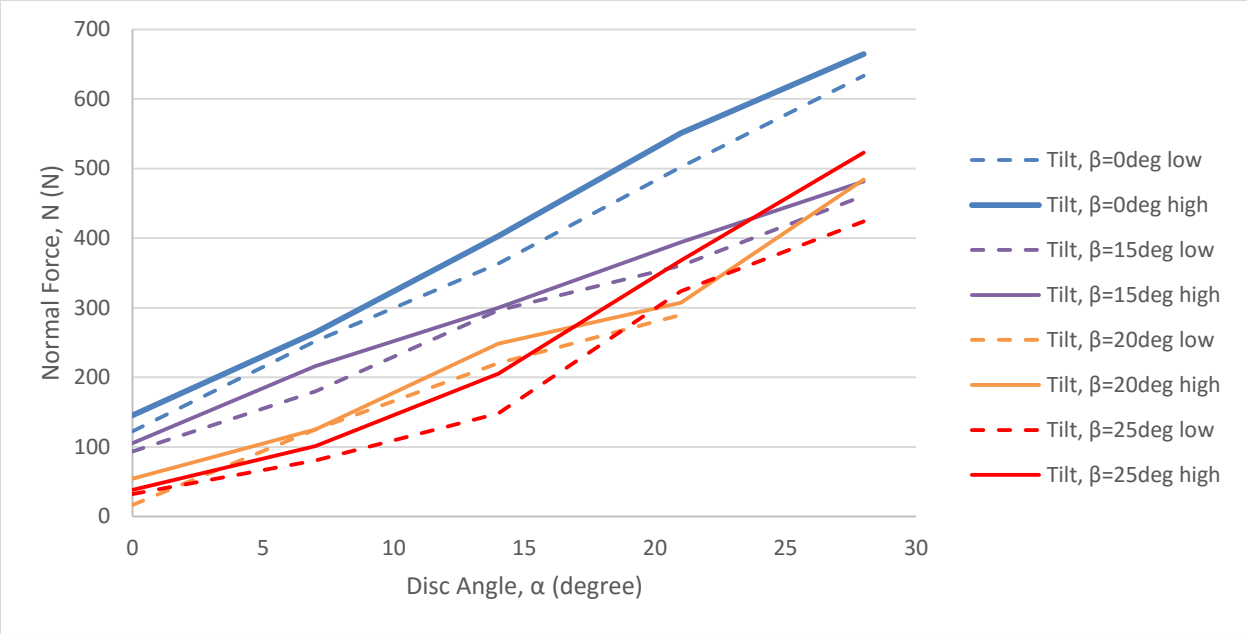

Figure 4- 19: Normal Force, N, for the Disc (Disc Angle, α) with Depth=2in Speed=3mph

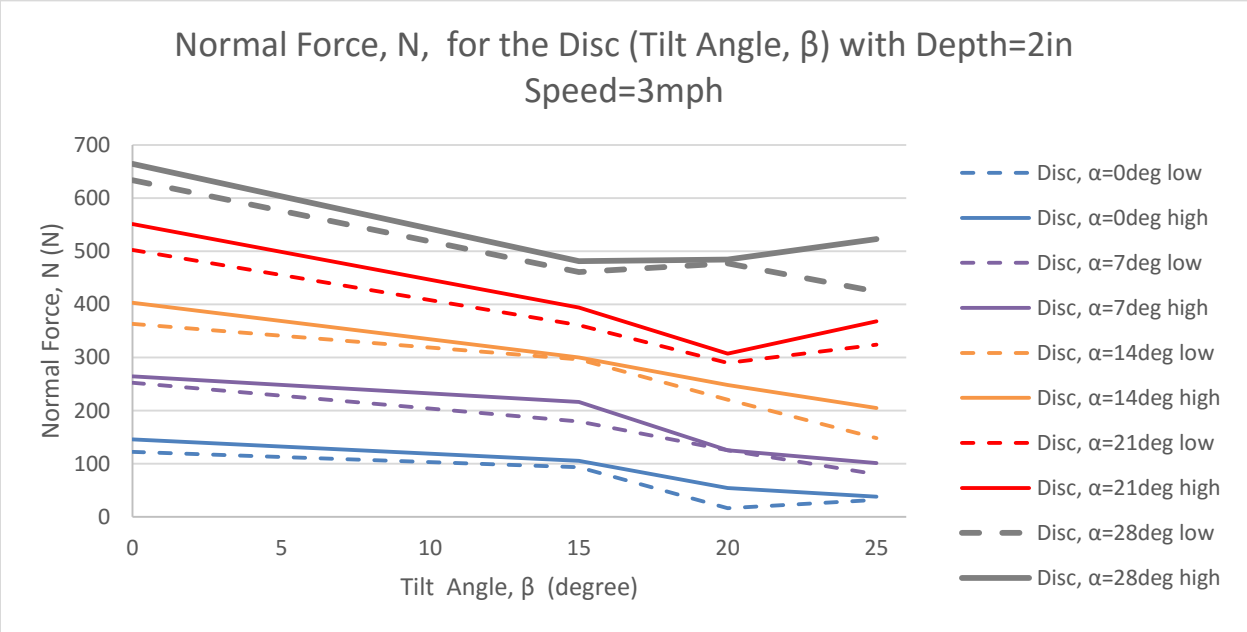

Figure 4- 20: Normal Force, N, for the Disc (Tilt Angle, β) with Depth=2in Speed=3mph

The normal force,*N*, vs the tilt angles (10°, 15°, 20°, 25°) at depth of 2in and speed of 3mph is shown in Figure 4-20. This figure shows the normal force, N, slightly decreases with

increased tilt angle. This may be from the variation of the soil property (cone index, soil moisture).

More figures for different depths (2in and 3in) with different speeds (3mph and 5mph) are included in Appendix E. They show that increased cutting depth increases the normal force in addition increases of the speed also increase the normal force.

4.8 Summary

This chapter starts out with a discussion of how the frequency testing was conducted on the disc coulter. A 2Hz low pass filter was applied to the original data in order to eliminate this unwanted low frequency vibration signals.

Next only the steady state data was used in the calculations. The reason and method of eliminating data of rig acceleration were explained. In addition, the methodology for averaging two test signals and checking for the reliability of the data was discussed. The data was then organized into four groups for simplicity.

Then the effect of various disc and tilt angles on the forces applied to the disc from the soil was studied and analyzed with data from a series of experiments for both a single disc and planter tests. In addition, some tests were repeated to confirm the repeatability of the test data. At the end-this chapter the cutting force and normal force calculation were conducted with analytical model from the measured data.

Overall, test results from one of the four data groups, the single disc test with 2in and 3mph speed was discussed in detail. The experimental data is shown graphically, which showed the trend of the draft forces. The conclusion is that the compound angle of 7° disc angle and 25°

tilt angle provided the minimum draft force. The results of other test groups are shown in the Appendix.

Chapter 5 - Optimization

5.1 Defining the Problem

In farming operations the desired width and depth of the furrow are typically known. Therefore, to maximize power efficiency the operator should select the disc's geometry securing the minimum draft force. The optimization of the draft force for disc parameters, while constraining the cutting furrow width and furrow depth, is discussed in this section. The problem is analyzed using the proposed model. The width w (see Figure 5-1) for a given furrow's depth d is defined in term of the disc's configuration(α, β). The draft force, F_z, (see Chapter 2) depends directly on α and β, but also on the soil force N and the cutting force F_c (F_f is assumed negligible due to free rotations of the disc). According to equation (2.9) this relation is:

$$F_z = N cos\beta sin\alpha + F_c(cos\alpha sin\delta + sin\alpha sin\beta cos\delta) \quad (5.1)$$

Where the N and F_c in terms of α and β were discussed in Chapter 4.

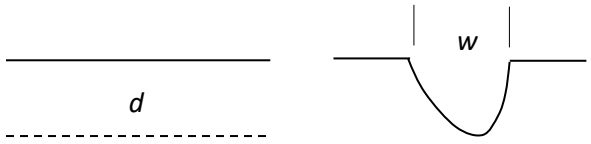

Figure 5- 1: Furrow's depth and width

So, the analytical model of the optimization problem is as follows

$$F_z[\alpha, \beta, N(\alpha, \beta), F_c(\alpha, \beta), \delta(\alpha, \beta), \gamma(\alpha, \beta)] \rightarrow min \quad (5.2)$$

$$subject\ to\ w(\alpha, \beta) = const\ (given\ width) \quad (5.3)$$

The analysis covers the range of:

$$0 \leq \alpha \leq 28° \tag{5.4}$$

$$0 \leq \beta \leq 25° \tag{5.5}$$

This is a problem with two independent optimization variables α, β. In objective (5.2), the relations $N(\alpha, \beta)$ and $F_c(\alpha, \beta)$ are obtained experimentally. Based on our experiments, the variables $\delta(\alpha, \beta)$ and $\gamma(\alpha, \beta)$ are initially assumed as independent of α, β. The geometrical relations between w and α, β in the constraint (5.3) will be obtained using geometrical analysis presented in the next section.

5.2 Defining Furrow Width (or Cutting Width)

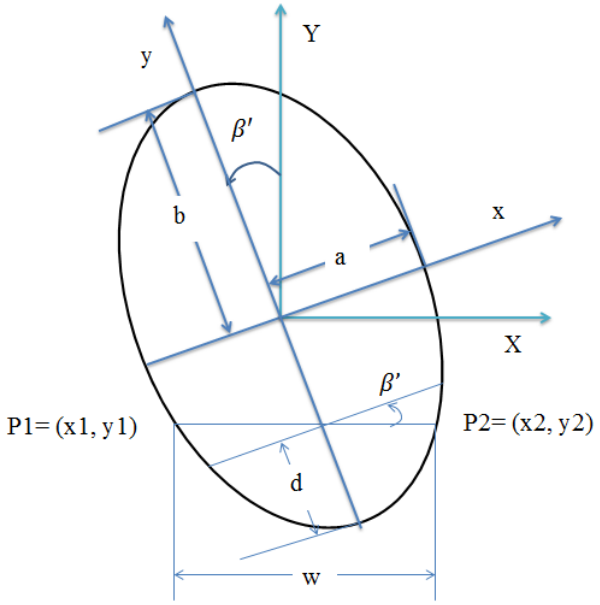

Figure 5- 2: Disc parameters

In the global coordinate system X-Y (see Figure 2-1), the furrow's width is represented by a line of the length P1-P2 as shown in Figure 5-2. This Figure also shows the disc in the configuration specified by the angles α and β as seen from the direction Z. In such a configuration the disc is represented by the ellipsis of axes a and b where $a = \rho sin\alpha$, $b =$

$\rho cos\beta''$ ($\rho = 0.23m$) rotated by the angle β' where $sin\beta' = sin\beta cos\alpha$ and $sin\beta'' = sin\beta sin\alpha$. For the range of α and β considered one can assume that $cos\beta'' \approx 1$ and $\beta' \approx \beta$.

By combining the equation of an ellipse and the equation of a line, the location of P1 and P2 is found. Then the distance between P1 and P2, which is the cutting width, is determined. The following equations showed how the coordinates x1, y1 and x2, y2 are calculated.

$$\frac{x^2}{a^2} + \frac{y^2}{b^2} = 1 \tag{5.6}$$

$$y = -(tan\beta)x - (b - d) \tag{5.7}$$

Substitute (5.6) into (5.7)

$$x1, x2 = \frac{-f \pm \sqrt{f^2 - 4eg}}{2e} \qquad where \begin{cases} e = \dfrac{1}{a^2} + \dfrac{(tan\beta)^2}{b^2} \\ f = \dfrac{2(tan\beta)(b-d)}{b^2} \\ g = \dfrac{(b-d)^2}{b^2} - 1 \end{cases} \tag{5.8}$$

$$y = -(tan\beta)x - (b - d) \tag{5.9}$$

Then, the cutting width will be

$$w(\alpha, \beta, d) = \sqrt{(x1 - x2)^2 + (y1 - y2)^2} \tag{5.10}$$

By using the given parameters, such as the disc diameter, disc angle and tilt angle, the cutting widths were calculated and reported in Appendix F.

The furrow width with variation of disc angle, α (0°, 7°, 14°, 21°, 28°) for the depth of 2in is shown in Figure 5-3. The results indicated that while increasing the disc angle, α, from 0° to 28°, the cutting width increases significantly.

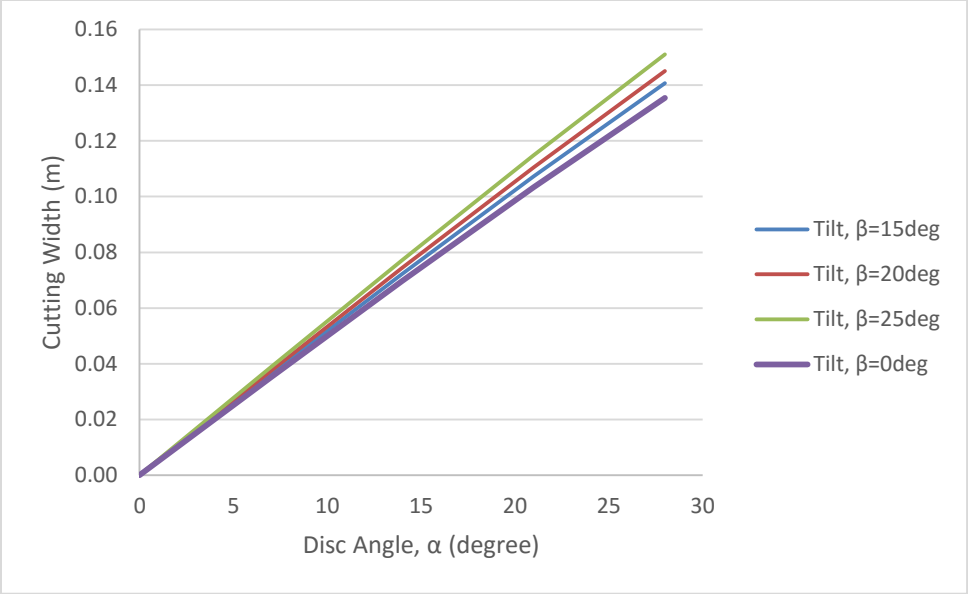

Figure 5- 3: Cutting width (disc angle, *α*) for depth of 2in (0.0508m)

Figure 5-4 shows the cutting widths for a 2in (0.0508m) depth of cut for various disc parameters. When disc angle is small, change of the tilt angle (0°, 15°, 20°, 25°) has only a slight effect on the cutting width.

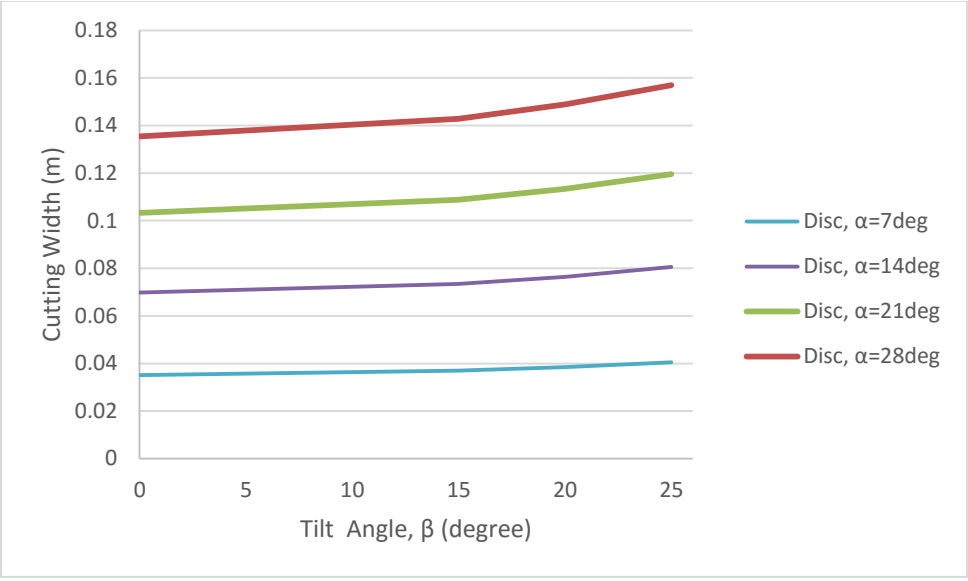

Figure 5- 4: Cutting width (tilt angle, β) for depth of 2in (0.0508m)

Figure 5-5 shows the cutting width for 3in (0.0762m) depth of cut with the change of the disc angle, α (0°, 7°, 14°, 21°, 28°). The cutting width increases with an increase of disc angle from 0° to 28° similarly as before.

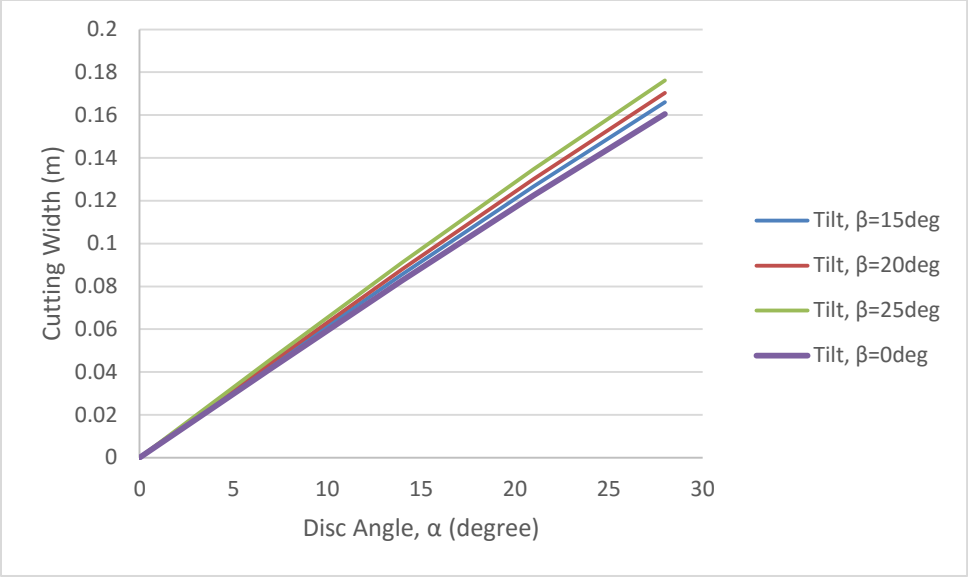

Figure 5- 5: Cutting width (disc angle, α) for depth of 3in (0.0762m)

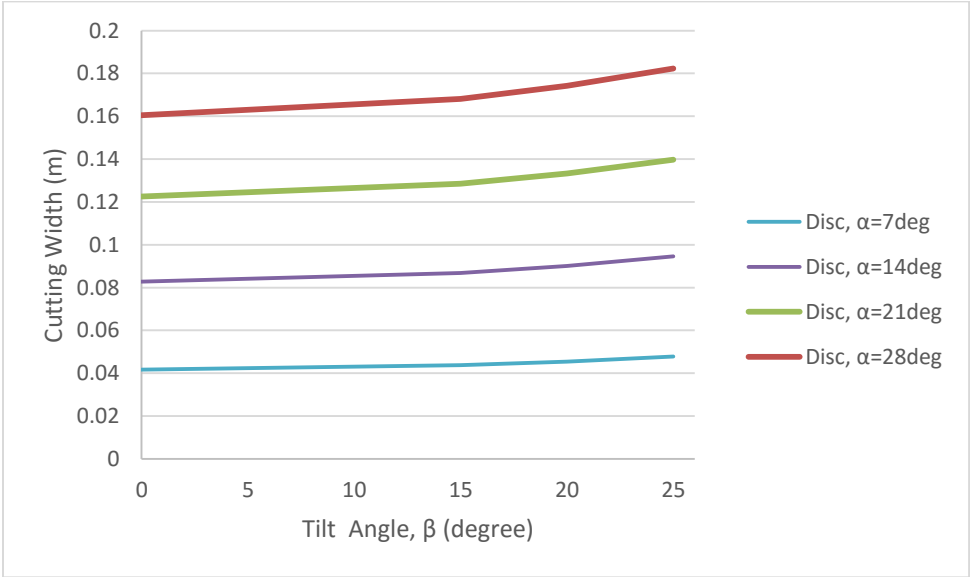

Figure 5- 6: Cutting width (tilt angle, β) for depth of 3in (0.0762m)

Cutting width verses the tilt angles of β for a cutting depth of 3in (0.0762m) is shown in Figure 5-6. The plot shows that increasing the tilt angle from $0°$ to $25°$ increases the cutting width.

Overall, the results show that increasing the disc angle increases the cutting width significantly and increasing the tilt angle also increased the cutting width but it has a much smaller impact.

As shown in Appendix F, the relation (5.10) for $0 \leq \alpha \leq 28°$ and $0 \leq \beta \leq 25°$ can be simplified to the form (where d is in meters):

$$w(\alpha, \beta, d) = \left(0.00573 + 0.000560\left(\frac{\beta}{25}\right)^2\right)\alpha\left(\frac{0.100 + 0.995d}{0.176}\right) \tag{5.11}$$

From which the disc angle is defined as follows

$$\alpha = \frac{w}{\left(0.00573 + 0.000560\left(\frac{\beta}{25}\right)^2\right)\left(\frac{0.100 + 0.995d}{0.176}\right)} \tag{5.12}$$

Equation (5.11) is verified by substituting $\alpha = 28°$, $\beta = 25°$ and $d = 3in = 0.0762m$

Then,

$$w(\alpha, \beta, d) = \left(0.00573 + 0.000560\left(\frac{25}{25}\right)^2\right)(28)\left(\frac{0.100 + 0.995(0.0762)}{0.176}\right)$$

$$= 0.176m \tag{5.13}$$

Substituting the value α, β, d into (5.10) one obtains 0.176m also (within 3 digits accuracy). The value 0.176m matches the measured the width of soil bin at the lab. This value was used to validate the analytical model.

5.3 Defining Cutting Force

The force of the disc cutting the soil was defined as the cutting force. This force with a given combination of disc and tilt angles was analyzed in Chapter 4.

In particular, Figure 5-7 shows the cutting force, F_c, with the variation of the disc angle α (0°, 7°, 14°, 21°, 28°) for depth of 2in and speed of 3mph. It shows that the cutting force increases with the increase of the disc angle. By using this data (shown in Chapter 4), a second degree formula for the cutting force is generated. More results are shown in Appendix G. The cutting force in terms of disc angle can be approximated by

$$F_c(\alpha) = 330 + 9.38\alpha + 0.217\alpha^2 \qquad (5.14)$$

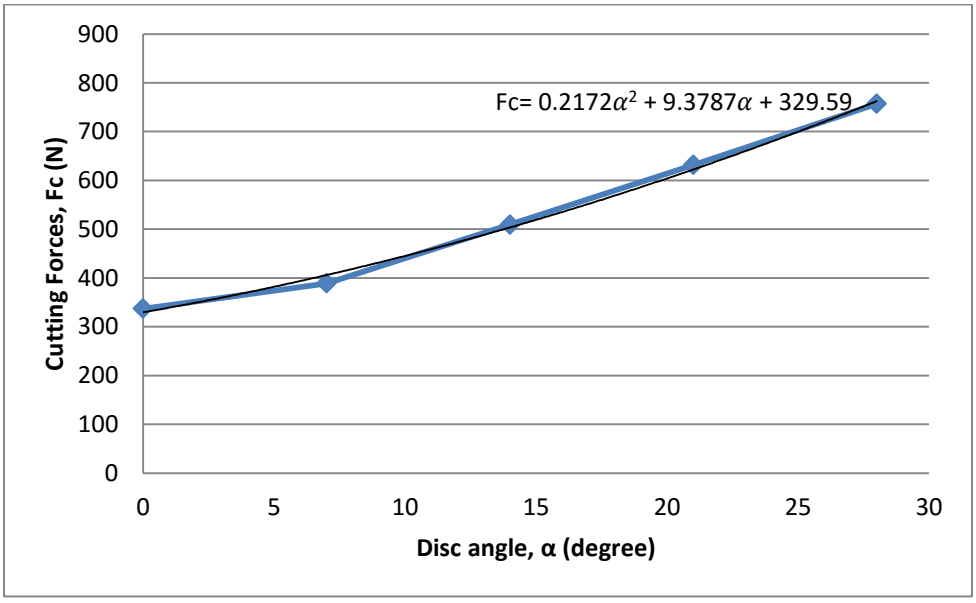

Figure 5- 7: Cutting force, Fc, for the disc (disc angle, α) with depth=2in speed=3mph

Figure 5-8 shows the cutting force, F_c, with the variation of the tilt angle β (0°, 15°, 20°, 25°) for a depth of 2in and speed of 3mph. It shows that the cutting force increases with

increased tilt angle. The second degree formula (5.15) for cutting force in terms of tilt angle can also be generated in the form

$$F_c(\beta) = 0.295\beta^2 + 5.51\beta + 391 \qquad (5.15)$$

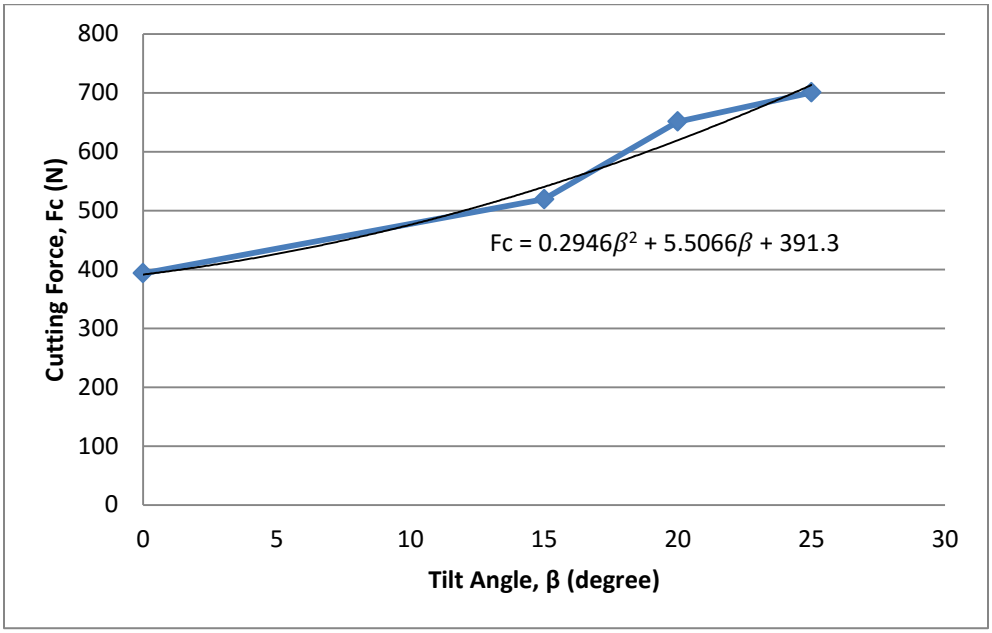

Figure 5- 8: Cutting force, Fc, for the disc (tilt angle, β) with depth=2in speed=3mph

In order to analyze the combination of angles in defining the cutting force, both Figure 5-7 and Figure 4-17 are used. The approximated formula is chosen as follows

$$F_c(\alpha,\beta) = \left(A + B\beta + C\beta^2\right) + \left(D + E\beta + F\beta^2\right)\left(\frac{\alpha}{28}\right) + \left(G + H\beta + I\beta^2\right)\left(\frac{\alpha}{28}\right)^2 \qquad (5.16)$$

The calculation for the depths of 2in and 3in and speed of 3mph is giving the following approximation (details in Appendix G)

$$F_c(\alpha,\beta,d) = \left(\left(282 - 2.29\beta + 0.549\beta^2\right) + \left(-80.2 + 80.6\beta - 2.32\beta^2\right)\left(\frac{\alpha}{28}\right) + \left(201 - 59.5\beta + 2.39\beta^2\right)\left(\frac{\alpha}{28}\right)^2 \right)\left(\frac{626 + 8340d}{1260}\right) \quad (5.17)$$

Equation (5.17) is verified by substituting $\alpha = 28°$, $\beta = 25°$ and $d = 3in = 0.0762m$

To obtain

$$F_c(\alpha,\beta,d) = \left(\left(282 - 2.29(25) + 0.549(25)^2\right) + \left(-80.2 + 80.6(25) - 2.32(25)^2\right)\left(\frac{28}{28}\right) + \left(201 - 59.5(25) + 2.39(25)^2\right)\left(\frac{28}{28}\right)^2 \right)\left(\frac{626 + 8340(0.0762)}{1260}\right)$$

$$= 1260N \quad (5.18)$$

The same result can be seen in Appendix D Figure D-1.

Similar formula can be obtained for a speed of 5mph (detail in Appendix G)

$$F_c(\alpha,\beta,d) = \left(\left(320 + 5.02\beta + 0.0476\beta^2\right) + \left(370 + 20.1\beta - 0.114\beta^2\right)\left(\frac{\alpha}{28}\right) + \left(58.5 - 23.0\beta + 1.23\beta^2\right)\left(\frac{\alpha}{28}\right)^2 \right)\left(\frac{1200 + 4310d}{1530}\right) \quad (5.19)$$

This section showed that the cutting force increased with increased disc and tilt angle. More results are shown in Appendix G.

5.4 Defining Normal Force

To form the furrow the disc pushes the soil which generates the normal force N. This force for a given combination of disc and tilt angles was determined in Chapter 4.

Figure 5-9 shows N varing with the disc angles for depth of 2in and speed of 3mph. More results are shown in Appendix H. It shows the normal force increases with an increase of disc angle. Similarly, the second degree formula for normal force can also be generated to approximate this force in the form of

$$N(\alpha) = 0.156\alpha^2 + 12.4\alpha + 79.1 \qquad (5.20)$$

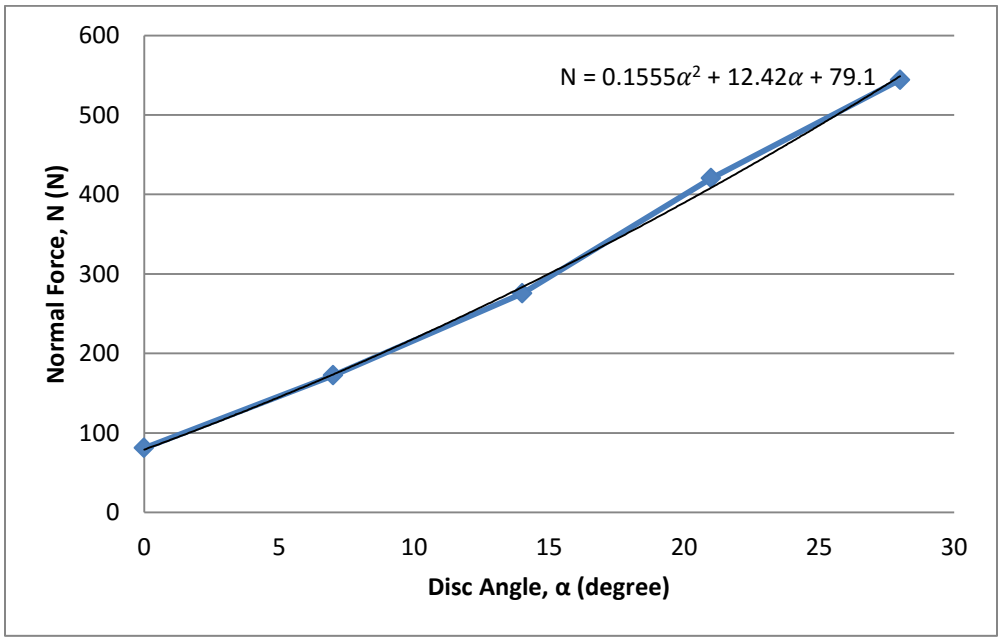

Figure 5- 9: Normal force, N, for the disc (disc angle, α) with depth=2in speed=3mph

Figure 5-10 shows the normal force, N, with the variation of the tilt angle β (0°, 15°, 20°, 25°) for depth of 2in and speed of 3mph. The second degree formula to approximated this force is

$$N(\beta) = 0.292\beta^2 - 12.2\beta + 394 \qquad (5.21)$$

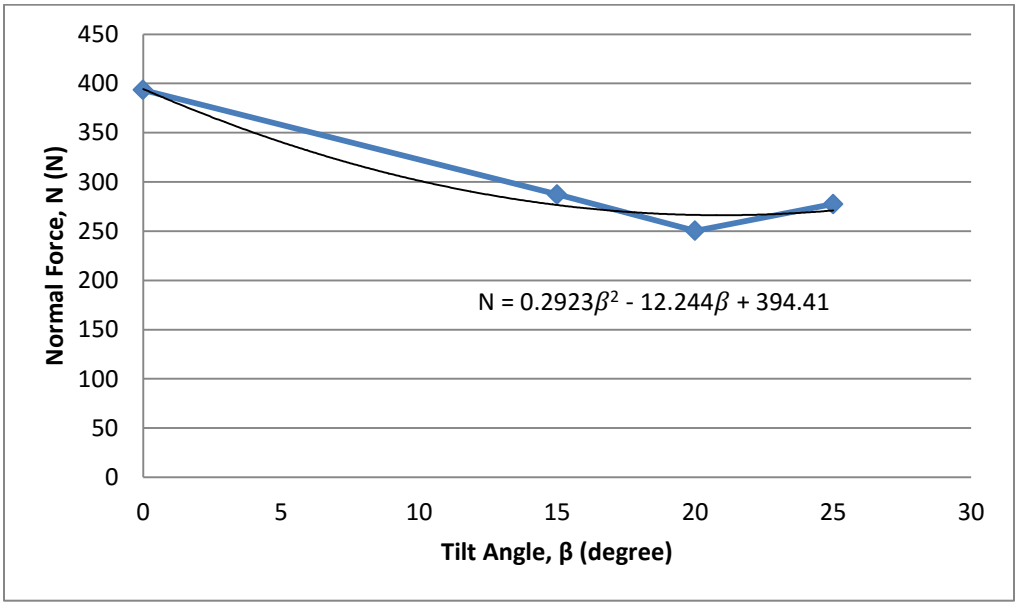

Figure 5- 10: Normal force, N, for the disc (tilt angle, β) with depth=2in speed=3mph

In order to analyze the combination of disc and tilt angle the following approximation can be generated

$$N(\alpha,\beta) = \left(A + B\beta + C\beta^2\right) + \left(D + E\beta + F\beta^2\right)\left(\frac{\alpha}{28}\right) + \left(G + H\beta + I\beta^2\right)\left(\frac{\alpha}{28}\right)^2 \qquad (5.22)$$

For the depth of 2in and 3in and speed of 3mph this formula is (details in Appendix H)

$$N(\alpha,\beta,d) = \left(\left(182 + 15.2\beta - 0.738\beta^2\right) + \left(365 + 7.76\beta - 1.32\beta^2\right)\left(\frac{\alpha}{28}\right) + \left(49.5 - 32.5\beta + 2.30\beta^2\right)\left(\frac{\alpha}{28}\right)^2\right)\left(\frac{398 + 1480d}{511}\right) \qquad (5.23)$$

Equation (5.23) is verified by substituting $\alpha = 28°$, $\beta = 25°$ and $d = 3in = 0.0762m$

Substituting into equation (5.23) one obtains

$$N(\alpha,\beta,d) = \left(\left(182 + 15.2(25) - 0.738(25)^2\right) + \left(365 + 7.76(25) - 1.32(25)^2\right)\left(\frac{28}{28}\right) \right.$$

$$\left. + \left(49.5 - 32.5(25) + 2.30(25)^2\right)\left(\frac{28}{28}\right)^2 \right)\left(\frac{398 + 1480(0.0762)}{511}\right)$$

$$= 509N \tag{5.24}$$

The result from the plot is 511N shown in Appendix E, so the error is

$$\%error = \frac{511 - 509}{511} \times 100\% = 0.391\% \tag{5.25}$$

Similar equation is obtained for speed of 5mph in the form (Appendix H)

$$N(\alpha,\beta,d) = \left(\left(207 + 4.31\beta - 0.444\beta^2\right) + \left(262 + 13.7\beta - 0.567\beta^2\right)\left(\frac{\alpha}{28}\right) \right.$$

$$\left. + \left(243 - 21.2\beta + 1.16\beta^2\right)\left(\frac{\alpha}{28}\right)^2 \right)\left(\frac{164 + 7410d}{728}\right) \tag{5.26}$$

5.5 1-D Optimization

The simplest method to optimize the combination of disc and tilt angle for a particular width w is to use the 1-D graphical optimization approach. The draft force F_z is defined by equation (5.1) which is repeated here in the form

$$F_z(\alpha,\beta) = N cos\beta sin\alpha + F_c(cos\alpha sin\delta + sin\alpha sin\beta cos\delta) \tag{5.27}$$

However, from equation (5.12), the disc angle α can be defined in terms of tilt angle β and furrow width w as

$$\alpha(\beta, w) = \frac{w}{\left(0.00573 + 0.000560\left(\frac{\beta}{25}\right)^2\right)\left(\frac{0.100 + 0.995d}{0.176}\right)} \tag{5.28}$$

So, for a given width w, and an assumed value of β the corresponding value of α can be calculated from (5.28), then the value of N and F_c from (5.22) and (5.17) respectively, and finally the value of F_z from (5.27). The results of such calculations are presented in the next section.

5.5.1 Result for Width=0.12m (Speed=3mph)

Table 5-1 shows the disc angle α, cutting force F_c, normal force N, and the draft force F_z in term of the tilt angle β for the furrow width $w = 0.12m$ and the depth 0.0508m (2in)

Table 5- 1: Combination of disc and tilt angle for depth=2in (0.0508m)

β	α	Fc	N	Fz
(deg)	(deg)	(N)	(N)	(N)
0	24	305	499	320
5	24	406	482	362
10	24	520	457	411
15	24	645	423	465
20	23	775	371	521
25	22	904	293	574
25	7	585	71	271

The corresponding plots are presented in Figure 5-11 and Figure 5-12.

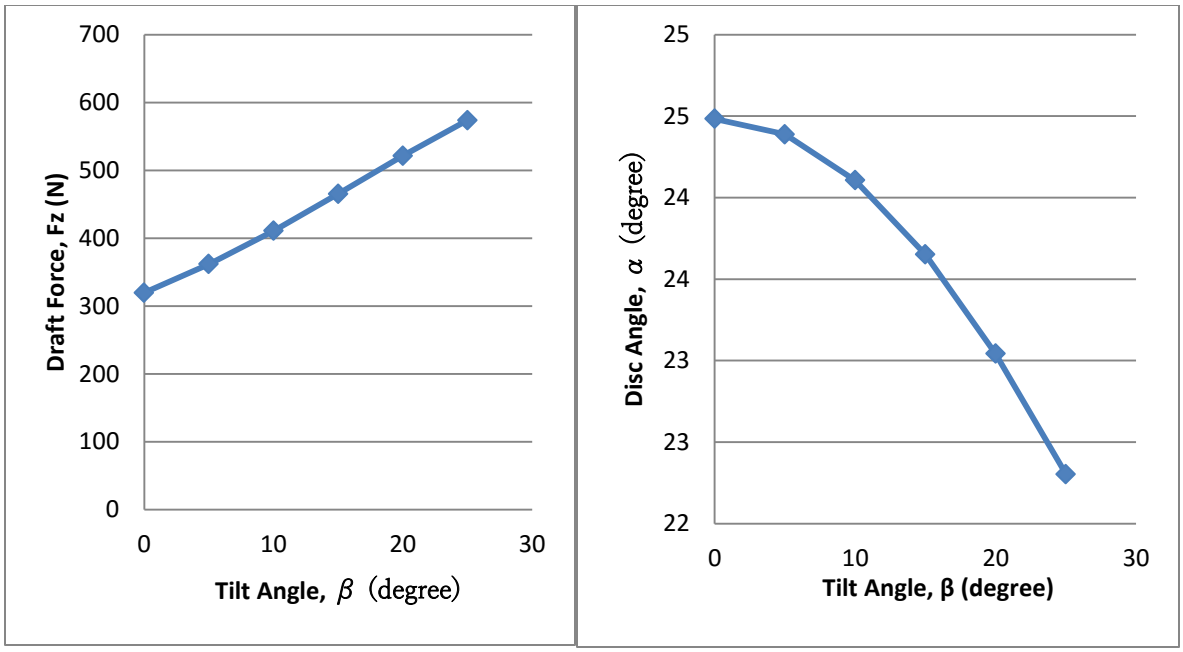

Figure 5- 11: Draft force, Fz, and disc angle, α, with depth=2in (0.0508m) speed=3mph

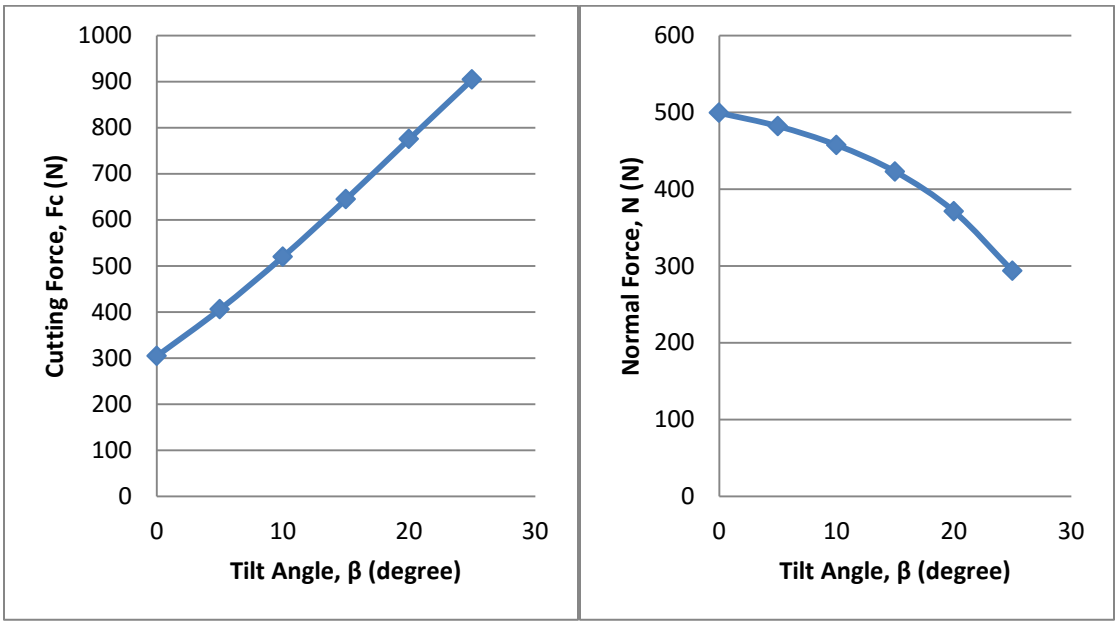

Figure 5- 12: Cutting force, Fc, and normal force, N, with depth=2in (0.0508m) speed=3mph

For the same furrow width of 0.12 m but for the depth of 3in (0.0762m) the calculations are shown in Table 5-2 and presented in Figure 5-13 and Figure 5-14.

Table 5- 2: Combination of disc and tilt angle for depth=3in (0.0762m)

β	α	Fc	N	Fz
(deg)	(deg)	(N)	(N)	(N)
0	21	335	483	300
5	21	462	485	361
10	21	594	464	421
15	20	730	419	479
20	20	866	344	532
25	19	996	233	578
25	7	703	76	325

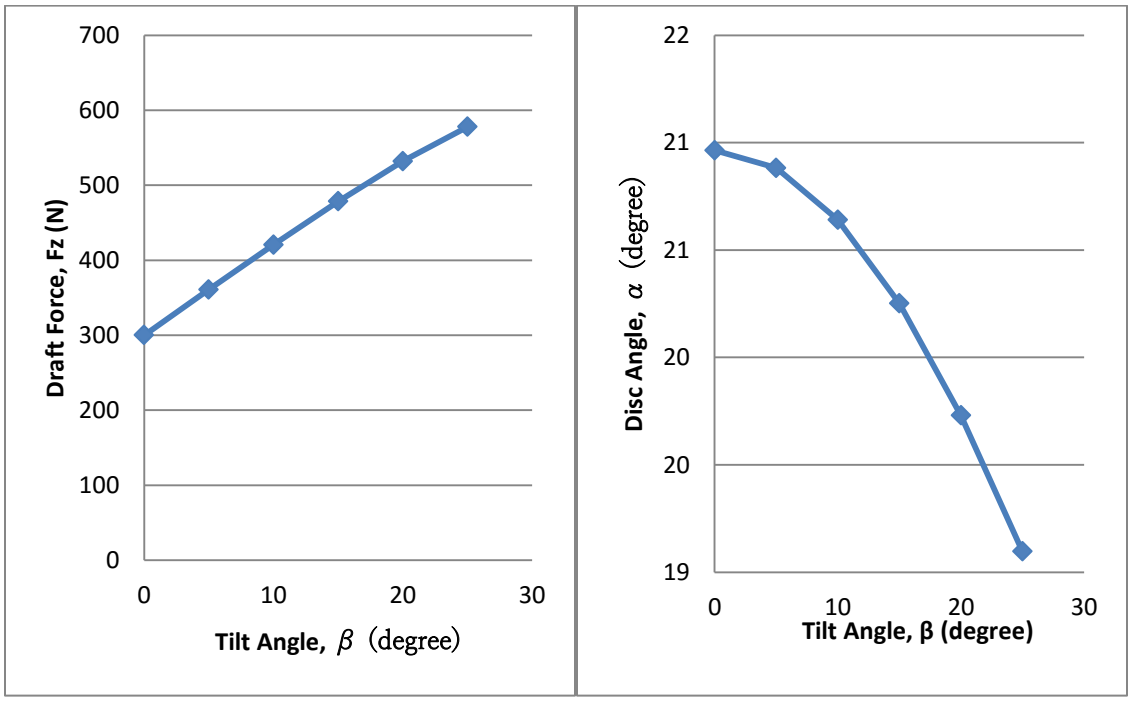

Figure 5- 13: Draft force, Fz, and disc angle, α, with depth=3in (0.0762m) speed=3mph

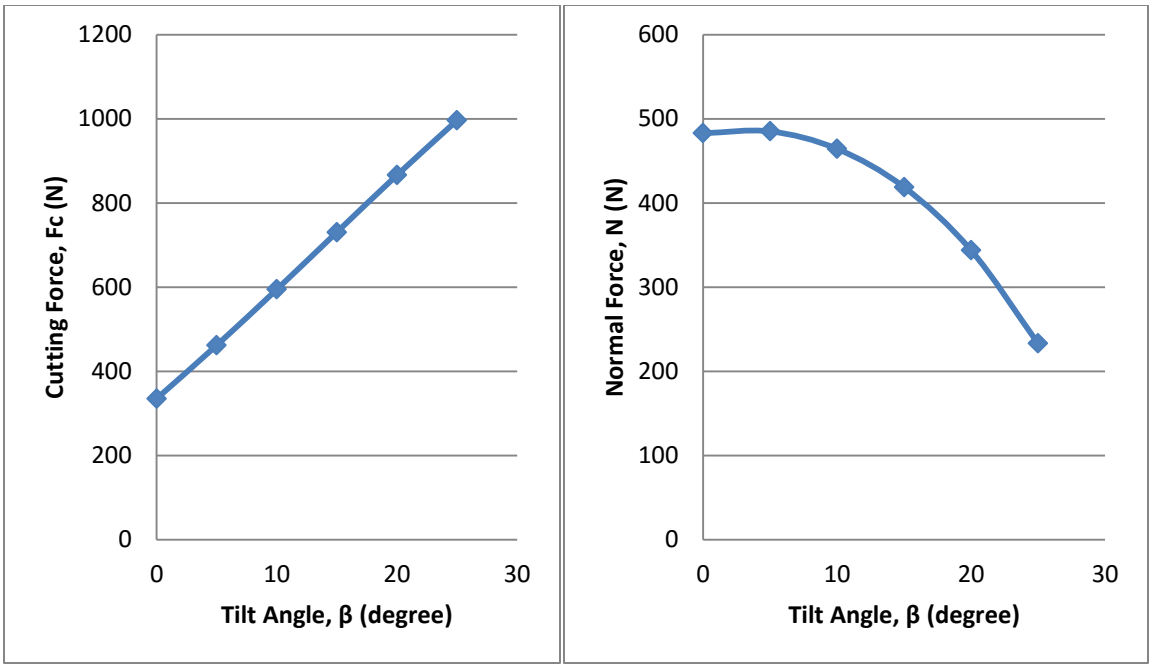

Figure 5- 14: Cutting force, Fc, and normal force, N, with depth=3in (0.0762m) speed=3mph

5.6 Summary

The plots presented in the previous section indicate how the draft force F_z is influenced by the normal and cutting forces that are changing with the tilt angle β. Namely, increasing β brings about increasing F_c and decreasing N. The combined effect of these two forces gives the value of F_z which for the case considered is minimal at $\beta = 0$. However, for different soil conditions the effects of the tilt angle on the cutting and normal forces may be different and the minimal draft force may have different corresponding values of β. Also, the furrow may be required to be asymmetric for other reasons necessitating a positive tilt angle.

Similarly, for speed of 5mph the disc angle α, cutting force F_c, normal force N, and the draft force F_z in term of tilt angle β are plotted in Appendix J.

Chapter 6 – Conclusion and Future Work

The goal of this research project was to understand the disc-soil-planter interaction in order to find the best combination of tilt angle and disc angle that delivers the lowest draft forces. The planter forces were determined experimentally, and then an analytical investigation was necessary to obtain the soil-disc interaction forces which are difficult to measure experimentally. The majority of any previous work in this area was done experimentally mostly by agriculture manufacturers. Such data are generally confidential and are not available to the public. The analytical model and independent experimental study reported here are major contributions to research in this area. All the experiments were done in the soil bin, facility of College of Engineering, University of Saskatchewan.

6.1 Conclusion

The contributions of this thesis can be summarized as follows:

Analytical Investigation

In Chapter 2, a static model of the disc was developed. A two-coordinate systems approach was used to build the model, a global system attached to the planter and a local system attached to the disc. During the analytical investigation, the forces coming from the soil were separated from the forces pulling the disc through a transformation of coordinates. The draft force, F_z, the vertical force, F_y, and the side force, F_x , were obtained from the test data. Then the model was used to determine the soil-disc interaction forces which are made up of cutting force and normal force. The analytical hand calculation was also used to compare and verify the results for particular soil properties in Chapter 4 and Chapter 5.

Independent Experiments and Results

A series of experiments were performed with a disc operating through the soil with a uniform speed and specified depth. All of the test experiments were based on the combination tilt angles (0°, 15°, 20°, 25°) and disc angles (0°, 7°, 14°, 21°, 28°). Before each test, a four-step soil preparation procedure was completed to ensure consistency of test conditions. Draft forces, vertical forces and side forces were measured in three orthogonal directions using six load cells that were attached to the carriage as explained in Chapter 3. In addition, some tests were repeated to confirm the repeatability and reliability of the test data as shown in Chapter 4.

The test data was filtered to eliminate the effects of disc vibration. A 2Hz low pass filter was used on the original data in order to eliminate unwanted low frequency. This produced less noisy signals for soil-disc interactions without loss of information. All of the force results obtained from experiments are available in Chapter 4. The experimental data is shown graphically, which showed the trend of the draft forces.

From the experimental study of the disc properties and of soil-disc interaction, it was concluded that the compound angle of 7° disc angle and 25° tilt angle provided the lowest draft force.

Optimization

In Chapter 5, an optimized model was proposed based on the analytical models. The relationships were built between the draft forces and disc parameters with a constrained cutting width. The optimization problem was solved by the simplification: 1-D graphical optimization method. The minimum draft force F_z could be found in terms of the disc parameter (α, β), while the cutting width and depth were constrained.

6.2 Future Work

In the future more works can be done on the three main aspects of this project.

Analytical Investigation

Rather than assuming the angle for cutting force δ and the angle from the disc center to cutting point γ are constant for calculations of normal force and cutting force, develop a formula for both angle δ and γ, which may make calculated results more accurate.

Experiments

Experiments with disc and tilt angle combination can be further conducted in different types of the soil properties. Different hardness of soil and moisture content can be considered during experimental tests along with different percent of sand, silt and clay. There are likely different minimum values of draft forces for different types of soil properties and possibly different configurations of angles. With more testing the impact of these different types of the soil conditions can be better understood.

Optimization problem

For future consideration the Lagrange Multiplier Method can be used to analyze the 2-D Optimization problem as specified by Equation 5.2 -5.5.

References

1. Askari, M., & Khalifahamzehghasem, S. (2013). Draft force inputs for primary and secondary tillage implements in a clay loam soil. *World Applied Sciences Journal*, Vol.21, No.12, 1789-1794.

2. Chi, L., & Kushwaha, R. (1991). Three-dimensional, finite element interaction between soil and simple tillage tool. *Transactions of the ASAE*, Vol.34(2), 0361-0366.

3. Abu-Hamdeh, N. H., & Reeder, R. C. (2003). A nonlinear 3D finite element analysis of the soil forces acting on a disk plow. *Soil & Tillage Research*, Vol.74, No.2, 115-124.

4. Afify, M., Kushwaha, R., & Gerein, M. (2001). Effect of combined disc angle on soil force of coulter discs. *ASAE Meeting Paper*, No.01-1059, 1-14.

5. Coates, W. (2002, July). *Agricultural Machinery Management*. Retrieved from College of Agriculture and Life Science: http://ag.arizona.edu/crop/equipment/agmachinerymgt.html

6. Sahu, R., & Raheman, H. (2006). An approach for draft prediction of combination tillage implements in sandy clay loam soil. *Soil & Tillage Research*, Vol.90(1), 145-155.

7. Hettiaratchi, D., & Alam, M. (1997). Calculation, validation and simulation of soil reactions on concave agricultural disc. *Journal of Agriculture Engineering Research*, Vol.68, No.1, 63-75.

8. Al-Janobi, A., & Al-Suhaibani, S. (1998). Draft of primary tillage implements in sandy loam soil. *Applied Engineering in Agriculture*, Vol.14, N0. 4, 343-349.

9. Summers, J., Khalilian, A., & Batchelder, D. (1986). Draft relationship for primary tillage in Oklahoma soils. *Transactions of the ASAE,* Vol.29(1), 37-39.

10. Manuwa, S., & Ademosun, O. (2007). Draught and soil disturbance of model tillage tines under varing soil parameters. *Agricultural Engineering International: the CIGR Ejournal*, Vol.9,1-18.

11. Sahu, R., & Raheman, H. (2006). Draught prediction of agricultural implements using reference tillage tools in sandy clay loam soil. *Biosystems Engineering*, Vol.94(2), 275-284.

12. Gill, W., Reaves, C., & Bailey, A. (1980). The effect of geometric parameter on disk forces. *Transaction of the ASAE*, Vol.23(2), 266-269.

13. Singh, J., Ganguly, P., & Singh, K. (1978). Effect of soil and implement parameter on depth of penetration of a disc harrow. *Transactions of the ASAE*, Vol.21(4), 620-622.

14. Mclaughlin, N., Drury, C., Reynolds, W., Yang, X., Li, Y., Welacky, T., & Stewart, G. (2008). Energy inputs for conservation and conventional primary tillage implements in a clay loam soil. *Transactions of the ASABE*, Vol.51(4), 1153-1163.

15. Ahmad, D., & Amran, F. (2004). Energy prediction model for disk plow combined with a rotary blade in wet clay soil. *International Journal of Engineering and Technology*, Vol. 1, No. 2, 102-114.

16. Reaves, C., Gill, W., & Bailey, A. (1981). Influence of width and eepth of cut on disc forces. *Transactions of the ASAE*, Vol.24(3), 572-578.

17. Gerber, W., Misener, G., & Campbell, A. (1994). An instrumentation system for the measurement of performance parameters of a no-till seeder. *Canadian Agricultural Engineering*, Vol.36, No.2, 79-84.

18. Kheiralla, A., Yahya, A., Zohadie, M., & Ishak, W. (2004). Modelling of power and energy requirements for tillage implements operating in Serdang sandy clay loam, Malaysia. *Soil & Tillage Research*, Vol. 78, 21-34.

19. Karmakar, S., Kushwaha, R., & Laugue, C. (2007). Numerical modelling of soil stress and pressure distribution on a flat tillage tool using computational fluid dynamics. *Biosystems engineering*, Vol. 97, 407-414.

20. Abbaspour-Gilandeh, Y., & Sedghi, R. (2015). Predicting soil fragmentation during tillage operation using fuzzy logic approach. *Journal of Terramechanics*, Vol. 57, 61-69.

21. Roul, A., Raheman, H., Pansare, M., & Machavaram, R. (2009). Predicting the draught requirement of tillage implements in sandy clay loam soil using an artificial neural network. *Biosystems Engineering*, Vol. 104, 476-485.

22. Hettiaratchi, D. (1997). Predicting the draught requirements of concave agricultural disc. *Terramechanics*, Vol.34, No.3, 209-224.

23. Harrison, H., & Thivavarnvongs, T. (1976). Soil reacting forces from laboratory measuremetns with disks. *Canadian Agricultural Engineering*, Vol.18, No.1, 49-53.

24. Bowers, C. (1989). Tillage draft and energy measurements for twelve southeastern soil series. *Transactions of the ASAE*, Vol.32(5), 1492-1502.

25. Serrano, J., Peca, J., da Silva, M., Oinheiro, A., & Carvalho, M. (2007). Tractor energy requirements in disc harrow systems. *Biosystems Engineering*, Vol. 98, 286-296.

26. Hemmat, A., Adamchuk, V., & Jasa, P. (2008). Use of an instrumented disc coulter for mapping soil mechanical resistance. *Soil & Tillage Research*, Vol. 98, 150-163.

27. Kushwaha, R., Vaishnav, A., & Zoerb, G. (1986). Soil bin evalution of disc coulters under no-till crop residue conditions. *Canadian Agricultural Engineering*, Vol.28, No.2, 85-90.

28. El-Shazly, M., Morad, M., Ali, M., & Wasfy, K. (2008). Optimization of disk plow performance under egyptian condition. *Misr Journal Agricuture Engineering*, 25(1): 15-37.

29. Plouffe, C., Lague, C., Tessier, S., Richard, M., & Mclaughlin, N. (1999). Moldboard plow performance in a clay soil: simulations and experiment. *Transactions of the ASAE*, Vol. 42(6): 1531-1540.

30. Afify, M., Kushwaha, R., & Gerein, M. (2001). Effect of combined disc angle on soil force of coulter discs. *ASAE Meeting Paper*, No.01-1059, 1-14.

31. Chen, Y., Tessier, S., & Irvine, B. (2004). Drill and crop performances as affected by different drill ocnfigurations for no-till seeding. *Soil & Tillage Research*, Vol.77, No.2, 147-155.

32. Siemens, J., Weber, J., & Thornburn, T. (1965). Mechanics of soil as influenced by model tillage tools. *Transaction of the ASAE*, Vol.8(1), 1-7.

33. McKyes, E. (1978). The calculation of draft forces and soil failure boundaries of narrow cutting blades. *Transaction of the ASAE,* Vol.21(1),20-24.

34. Perumpral, J., Grisso, R., & Desai, C. (1983). A soil-tool model based on limit equilibrium analysis. *Transaction of ASAE,* Vol.26(4), 991-995.

35. Obermayr, M., Dressler, K., Vrettos, C., & Eberhard, P. (2011). Prediction of draft forces in cohesionless soil with the Discrete Element Method. *Journal of Terramechanics*, Vol.48, No.5, 347-358.

36. Onwualu, A., & Watts, K. (1998). Draught and vertical forces obtained from dynamic soil cutting by plane tillage tools. *Soil & Tillage Research*, Vol.48(4), 239-253.

37. Hashemi, A., Ahmad, D., Othman, J., & Sulaiman, S. (2012). Design, development and performance of a disk plow combined with rotary blades. *Materials Science and Engineering*, Vol.36, 1-8.

38. Saunders, C., Godwin, R., & O'Dogherty, M. (2000). Prediction of soil forces acting on mouldboard ploughs. *Fourth International Conference on Soil Dynamics, Adelaide*.

39. Alam, M. (1989). *Soil reaction forces on agricultural disc implements.* PhD Thesis. The University of Newcastle.

40. GEOL615. (2015). Retrieved from Some useful numbers on the engineering properties of materials (geologic and otherwise): http://www.jsg.utexas.edu/tyzhu/files/Some-Useful-Numbers.pdf

41. Aminzadeh, R. (2014). *Modified design of precision planter for a robotic assistant farmer*. MsC Thesis. University of Saskatchewan.

42. Mardani, A., Shahidi, K., Rahmani, A., Mashoofi, B., & Karimmaslak, H. (2010). Studies on a long soil bin for soil-tool interaction. *A Long Soil Bin For Soil-Tool Interaction,* Vol.13, No.2, 5-10.

43. Armin, A. (2014). *Mechanics of soil-blade interaction.* PhD Thesis. University of Saskatchewan.

44. Sjoerd, W. (2002). *Diagnosing soil compaction using a penetrometer*. Retrieved from PennState Extension: http://extension.psu.edu/plants/crops/soil-management/soil-compaction/diagnosing-soil-compaction-using-a-penetrometer

45. Nave, R. (2016). *Fast Fourier Transform*. (Geogia State University) Retrieved from http://hyperphysics.phy-astr.gsu.edu/hbase/math/fft.html

Appendix A – Experimental Data Analysis by Matlab

For the experimental tests using the disc, at least two tests were performed for the same trial (same depths, speeds, tilt angles and disc angles). Two similar test results from each trial were picked and analyzed in the Matlab program using a filter of 2Hz (to reduce unwanted noise). For each combined tilt and disc angle, the initial 22% of the data is ignored for each trial. Only the steady state data is used to generate the modified average forces for the disc.

The method of analyzing the experimental test data (the combined tilt angle at 25° and disc angle at 7° with depth of 2in and speed of 3mph) is explained here. The code in Figure A-1 is used in Matlab first to restore the experimental test data for a particular trial run in Matlab. The Simulink program in Matlab is run next. See Figure A-2 for block diagram. This program modifies the experimental test data with a 2Hz filter. Then, the code in Figure A-3 is used in Matlab in order to provide the plot shown in Figure A-4.

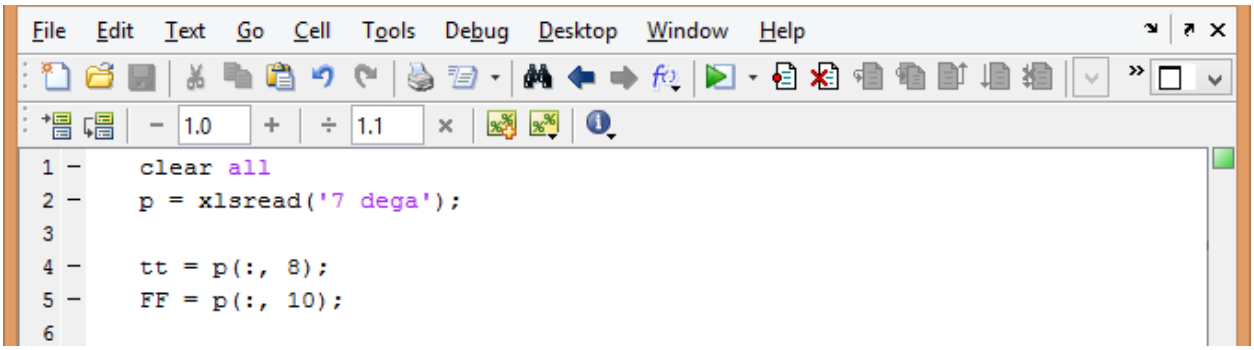

Figure A- 1: An example of the Matlab code with filter of 2Hz

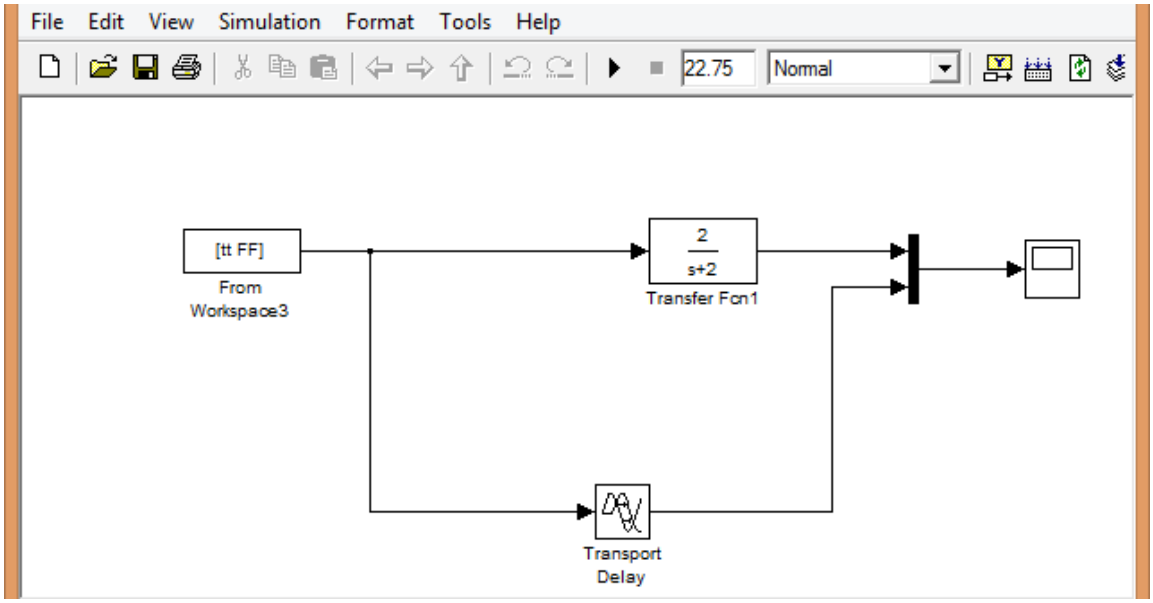

Figure A- 2: An example of Matlab Simulink with filter of 2Hz

```
% test after 2Hz filter (black)
plot(st_1_f(:,1), st_1_f(:,2),'k')
hold on

% original test data (green)
plot(st_1_f(:,1), st_1_f(:,3),'g')
hold on

% average data after 2Hz filter (red)
plot(st_1_f(:,1), mean(st_1_f(:,2)),'r')
hold on

% matlab = excel - 4

% Vertical
% plot(st_1_f((291:1019),1), mean(st_1_f((291:1019),2)),'b')
% plot(st_1_f((262:1022),1), mean(st_1_f((262:1022),2)),'b')

% Draft
 plot(st_1_f((352:1260),1), mean(st_1_f((352:1260),2)),'b')
% plot(st_1_f((317:1299),1), mean(st_1_f((317:1299),2)),'b')

% Side
% plot(st_1_f((265:960),1), mean(st_1_f((265:960),2)),'b')
% plot(st_1_f((236:934),1), mean(st_1_f((236:934),2)),'b')

title('Depth=2 Speed=3 Tilt=25 Disk=7 Disk Draft Force test a');
xlabel('Time');
ylabel('Force (N)');
```

Figure A- 3: An example of the Matlab code with filter of 2Hz

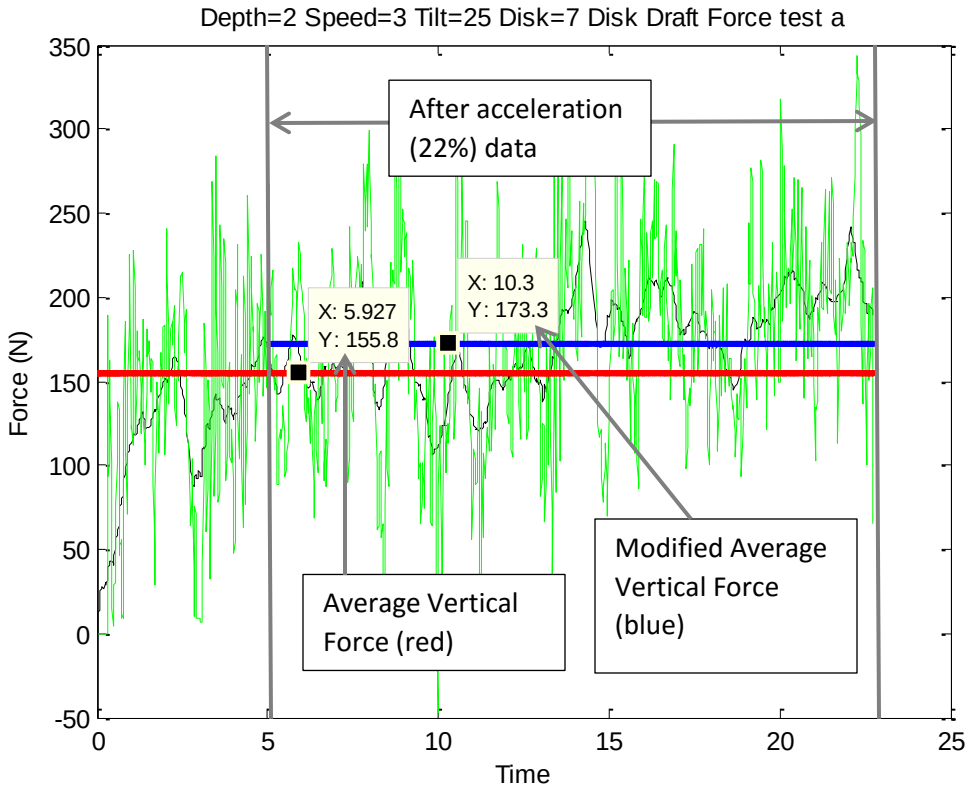

Figure A- 4: An example of the analyzed data by using Matlab program with filter of 2Hz

For the chosen experimental test data is then evaluated by using filter of 2Hz in Matlab program to make the value easier to interpret, which is shown in Figure A-4 in black. Then, the average of the vertical, draft, and side forces can be analyzed, which is shown in Figure A-4, in red. For the beginning of the test, since the initial force values are starting from 0N, 22% of the initial data should be ignored due to the ignoring of the acceleration. The rest as the average of the modified average forces is more reasonable to interpret, which is shown in Figure A-4 in blue. The modified average vertical, draft, and side force for the disc coulter is the average vertical, draft, and side force without the acceleration of the disc speed.

Appendix B – Disc Experimental Data Results

The rest experimental test data are shown in Appendix B. Including depth of 3in and speed of 3mph after using the filter of 2Hz, depth of 2in and speed of 5mph after using the filter of 2Hz, and depth of 3in and speed of 5mph after using the filter of 2Hz.

B.1 - Depth=3in and Speed=3mph

One of the set of experimental test has depth of 3in and speed of 3mph. The average of the vertical, draft, and side forces of the two data after using the filter of 2Hz for the disc experimental tests is analyzed. The modified average of the vertical, draft, and side forces can be plotted, which were shown in the following figures.

Figure B-1 and Figure B-2 showed the effect of disc and tilt angles on the draft force. Figure B-1 showed the draft force, Fz, increased with increased disc angle for the disc with depth of 3in and speed of 3mph. When tilt angle is zero, draft force increased when increased the disc angle. The reason for this phenomenon is because as disc angle increased, the direction of motion increased, which will increased the drag force. When tilt angle is not zero, the combination of disc and tilt angle lifted up the soil and displaced it to the sides to open the furrow. The tilt angle can help to keep the draft force from increasing intensively while increasing the disc angle. When disc angle is zero, draft force increased when increased the tilt angle. Figure B-2 showed the draft force, Fz, increased with increased tilt angle for the disc with depth of 3in and speed of 3mph.

The larger the disc angle resulted larger draft force. However, disc angle cannot be zero, because it is responsible for the width of the furrow. In order to keep the draft as low as possible, the smaller disc angle should be chosen. With the depth of 3in and speed of 3mph, the most

reasonable compound angle (non-zero disc angle) for the lowest draft force is 7° disc angle and 25° tilt angle. The average of the minimum draft force is 299N.

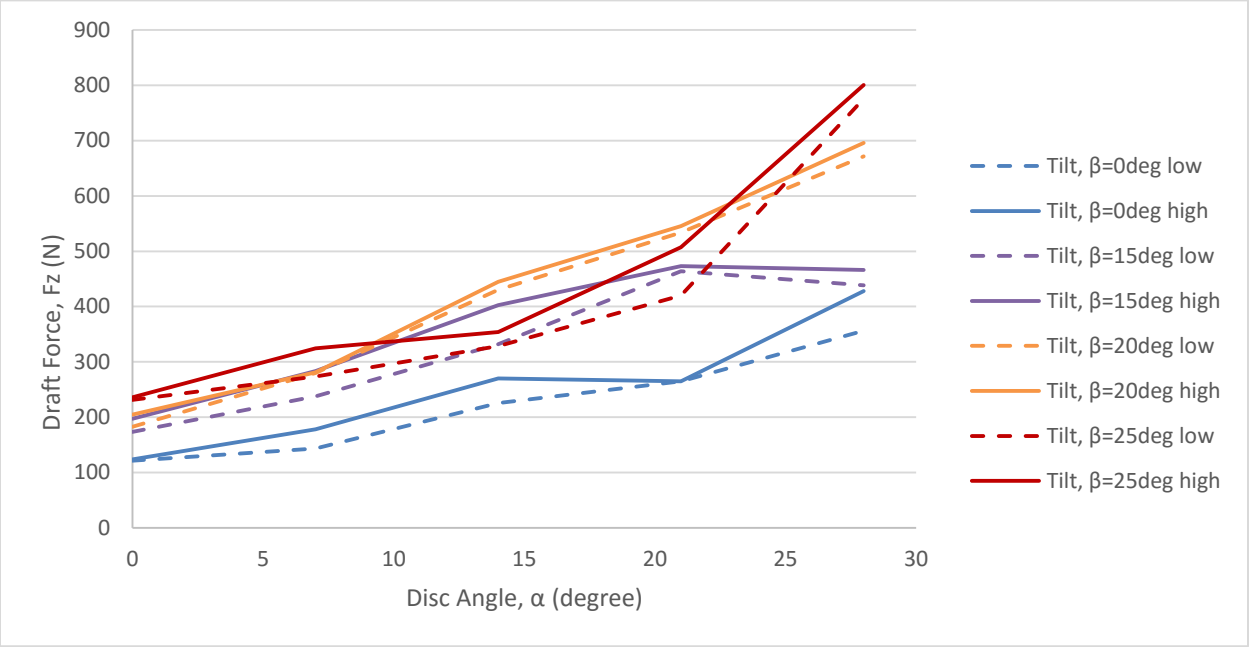

Figure B- 1: Draft Force, Fz, for the Disc with Depth=3in Speed=3mph

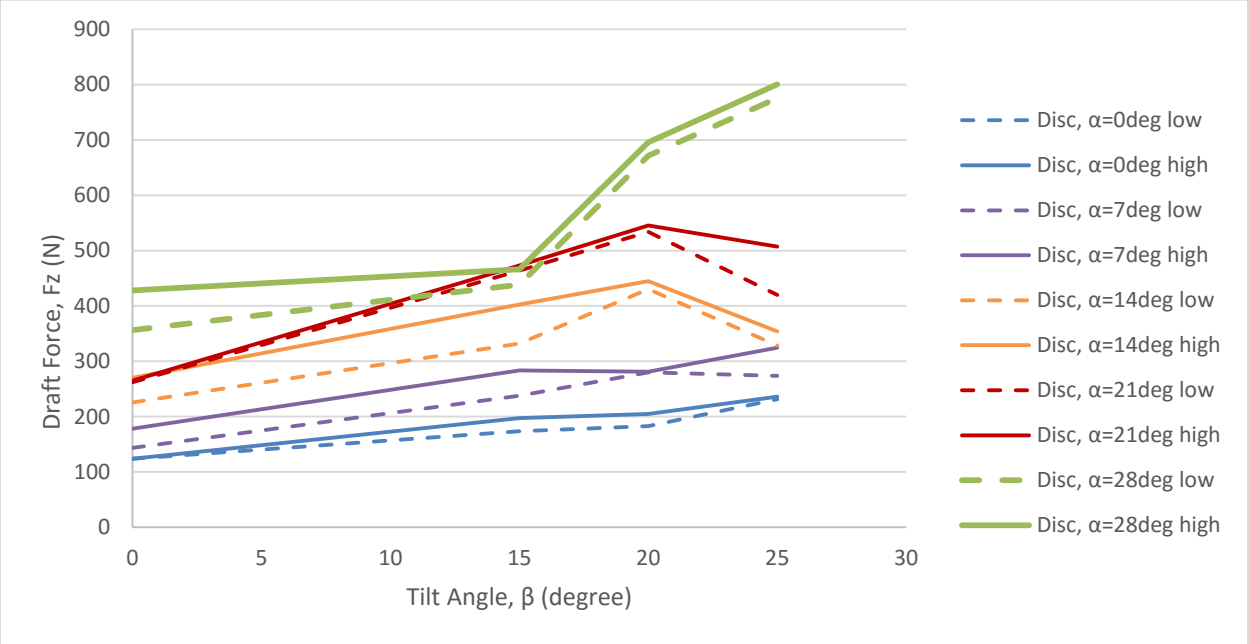

Figure B- 2: Draft Force, Fz, for the Disc with Depth=3in Speed=3mph

The amount of the force we need to keep the disc into the soil when pushing the disc forward is called the vertical force. The weight of the disc does not affect the vertical load, since the zero of the load cells was set when the disc is attached to the carriage and not in touch with soil. Figure B-3 and Figure B-4 showed the vertical force for different disc angles (0°, 7°, 14°, 21°, 28°) with different tilt angles (0°, 15°, 20°, 25°) respectively. Figure B-3 showed the vertical force, Fy, increased negatively with increased disc angle for the disc with depth of 3in and speed of 3mph. Figure B-4 showed the vertical force, Fy, increased with increased tilt angle for the disc with depth of 3in and speed of 3mph. The most suitable disc and tilt compound angle is mainly chosen by the lowest draft force. The vertical force is not a criterion for further study and analysis of the experimental tests. As the experimental results showed, the corresponding average vertical force for the minimum draft force with a compound angle of 7° disc angle and 25° tilt angle is -503N.

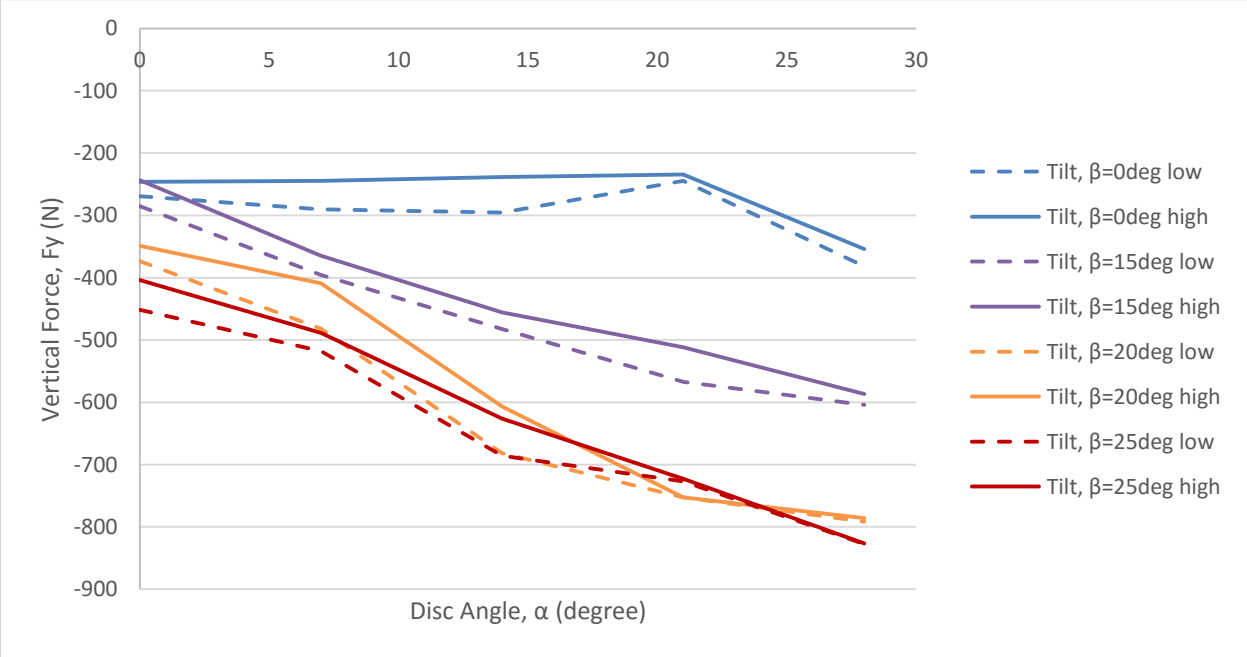

Figure B- 3: Vertical Force, Fy, for the Disc with Depth=3in Speed=3mph

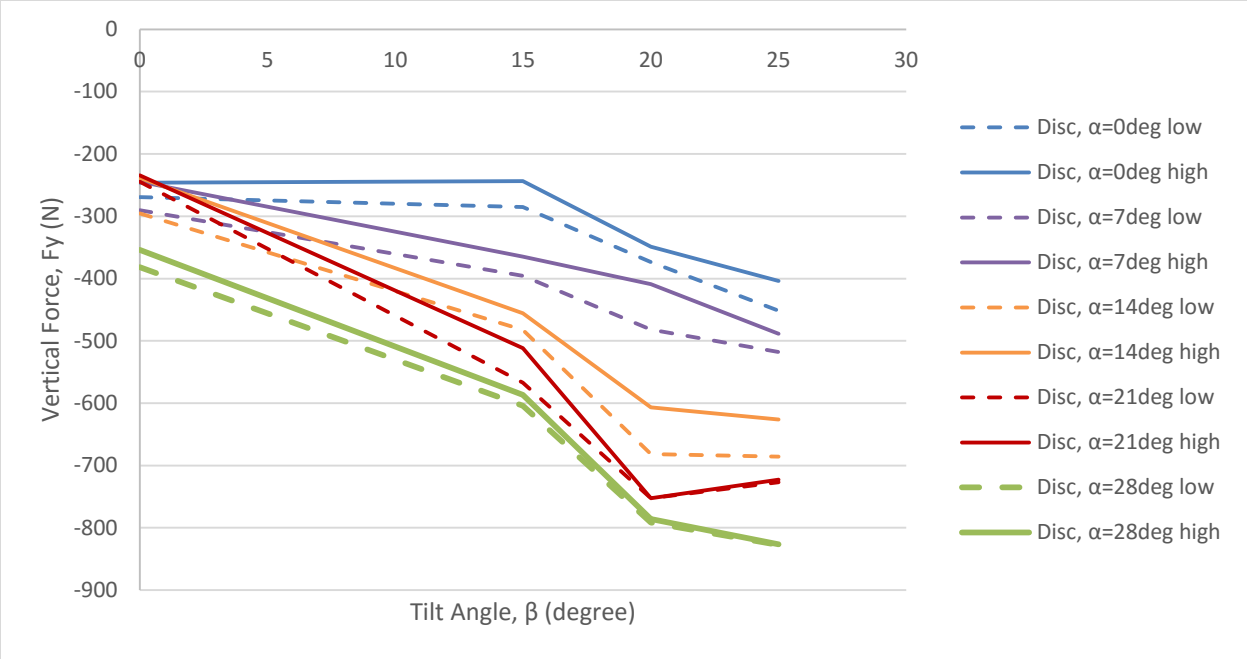

Figure B- 4: Vertical Force, Fy, for the Disc with Depth=3in Speed=3mph

From the results of the side (lateral) forces, it showed that increased the disc angle will increase the side force. Due to the non-zero disc angle and non-symmetrical system, some of the higher side forces results are high in some angles. However, the combination of disc and tilt angle reduced the side force. The compound angle disc lifted up the soil and displaced it to the side instead of pushing and pressing the soil to the side. Figure B-5 showed the side force, Fx, increased with increased disc angle for the disc with depth of 3in and speed of 3mph. Figure B-6 showed the side force, Fx, increased with increased tilt angle for the disc with depth of 3in and speed of 3mph. The chosen disc and tilt angle for the lowest draft force has the average side force of 366N.

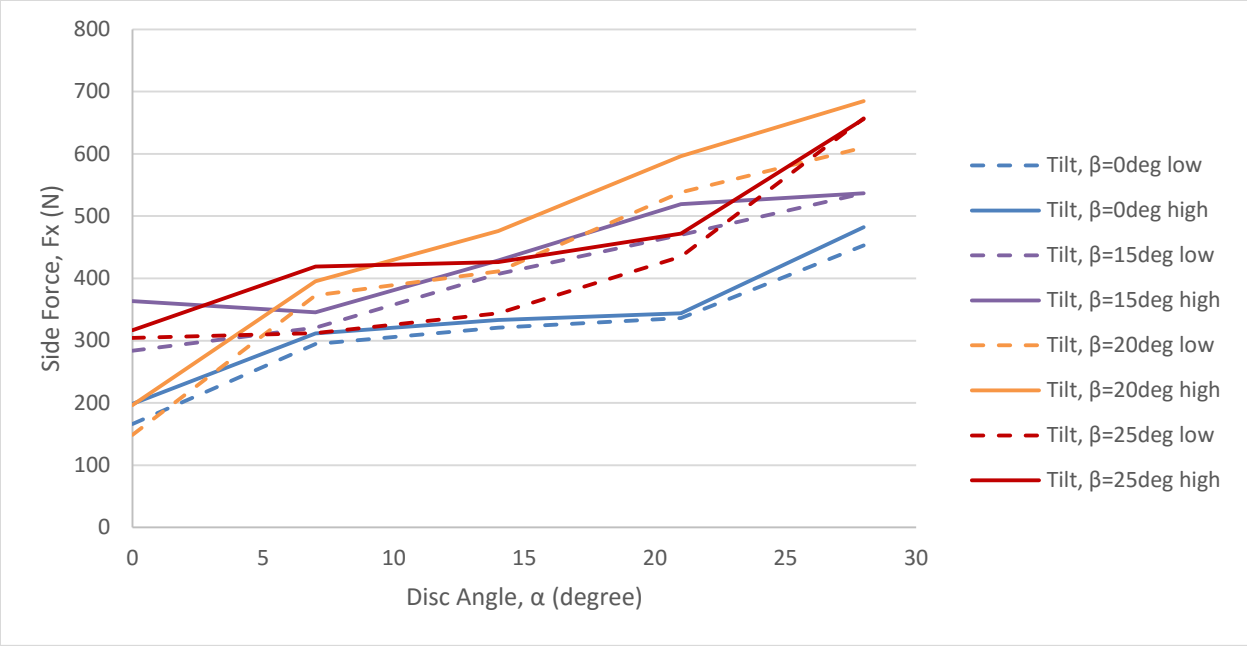

Figure B- 5: Side Force, Fx, for the Disc with Depth=3in Speed=3mph

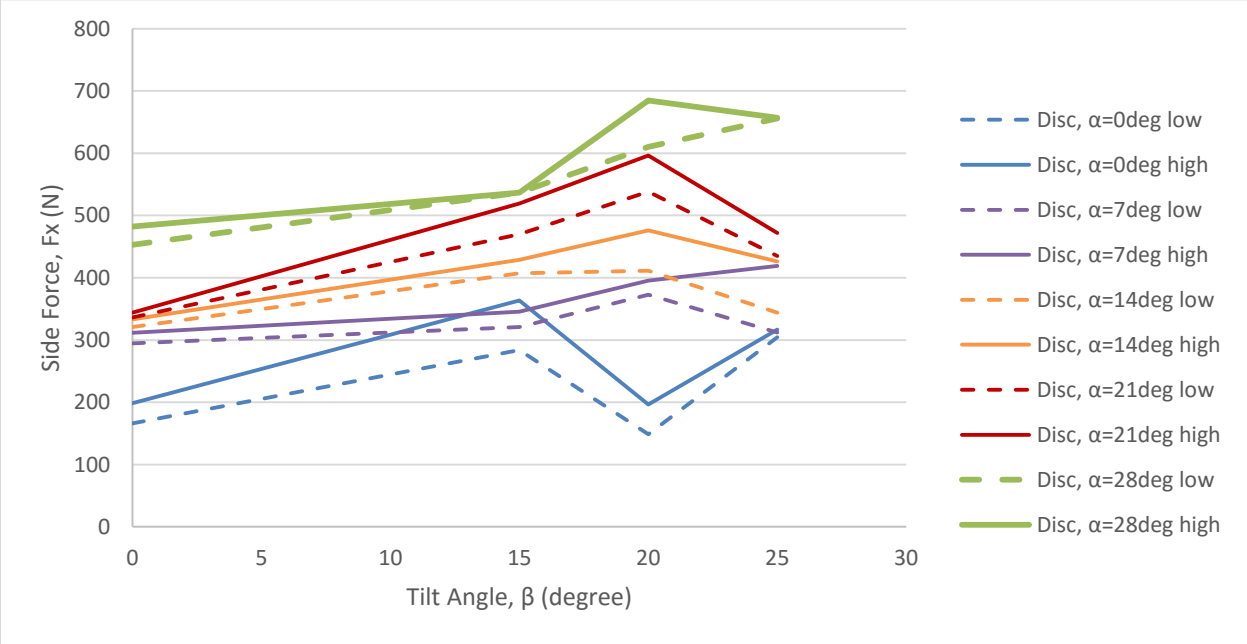

Figure B- 6: Side Force, Fx, for the Disc with Depth=3in Speed=3mph

The goal of these tests was to find the best combination of disc angle and tilt angle which leads to minimum draft force for depth is 3in speed is 3mph. Force in 3 direction of draft,

vertical and side are measured by load cells. The results of the experiments showed that the compound angle of 7° disc angle and 25° tilt angle gives the lowest draft force.

B.2 - Depth=2in and Speed=5mph

Another set of experimental test is has depth of 2in and speed of 5mph. The two data after using the filter of 2Hz of the average of the vertical, draft, and side force for the disc experimental tests is analyzed. The average of the vertical, draft, and side forces is modified and plotted, which were shown in the following figures.

The effect of disc and tilt angles on the draft force shown in Figure B-7 and Figure B-8. When tilt angle is zero, draft force increased when increased the disc angle. Figure B-7 showed the draft force, Fz, increased with increased disc angle for the disc with depth of 2in and speed of 5mph. When disc angle is zero, draft force increased when increased the tilt angle. Figure B.8 showed the draft force, Fz, increased with increased tilt angle for the disc with depth of 2in and speed of 5mph. With the depth of 2in and speed of 5mph, the most reasonable compound angle (non-zero disc angle) for the lowest draft force is 7° disc angle and 25° tilt angle. The average of the minimum draft force is 334N.

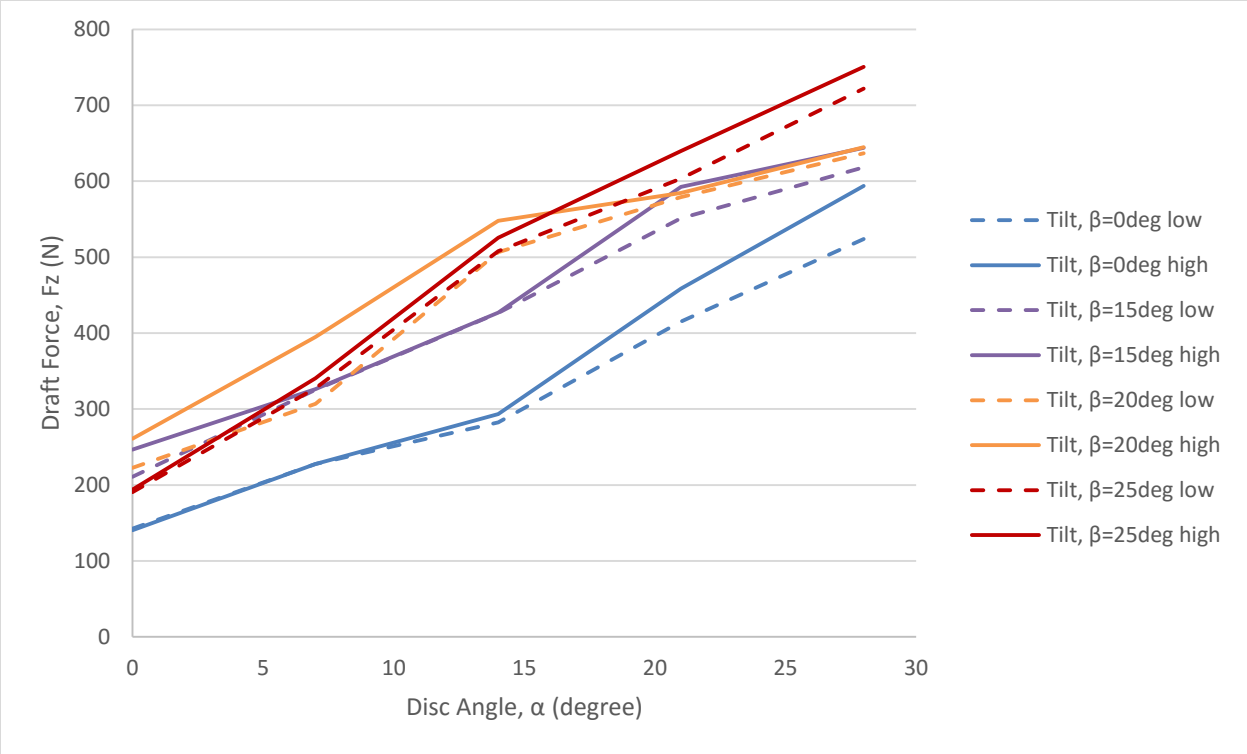

Figure B- 7: Draft Force, Fz, for the Disc with Depth=2in Speed=5mph

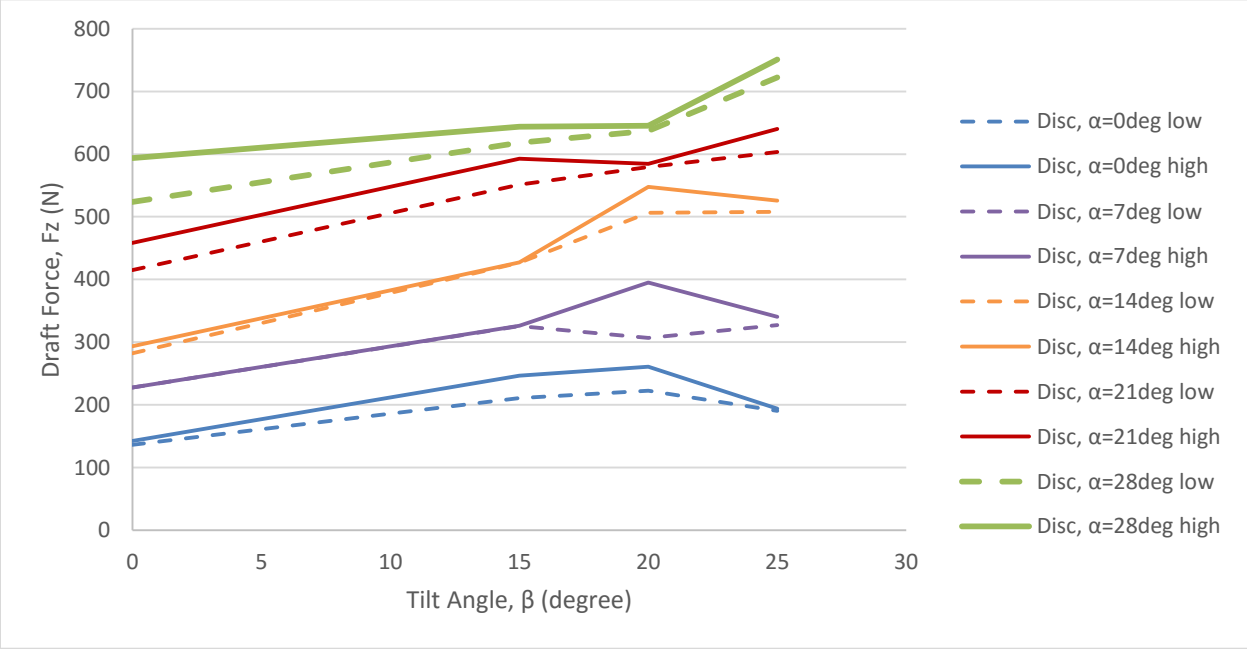

Figure B- 8: Draft Force, Fz, for the Disc with Depth=2in Speed=5mph

Figure B-9 and Figure B-10 showed the vertical force for different disc angles (0°, 7°, 14°, 21°, 28°) with different tilt angles (0°, 15°, 20°, 25°) respectively. Figure B-9 showed the vertical force, Fy, increased negatively with increased disc angle for the disc with depth of 2in and speed of 5mph. Figure B-10 showed the vertical force, Fy, increased with increased tilt angle for the disc with depth of 2in and speed of 5mph. Since the most suitable disc and tilt compound angle is mainly chosen by the lowest draft force, the corresponding average vertical force for the minimum draft force with a compound angle of 7° disc angle and 25° tilt angle is -502N.

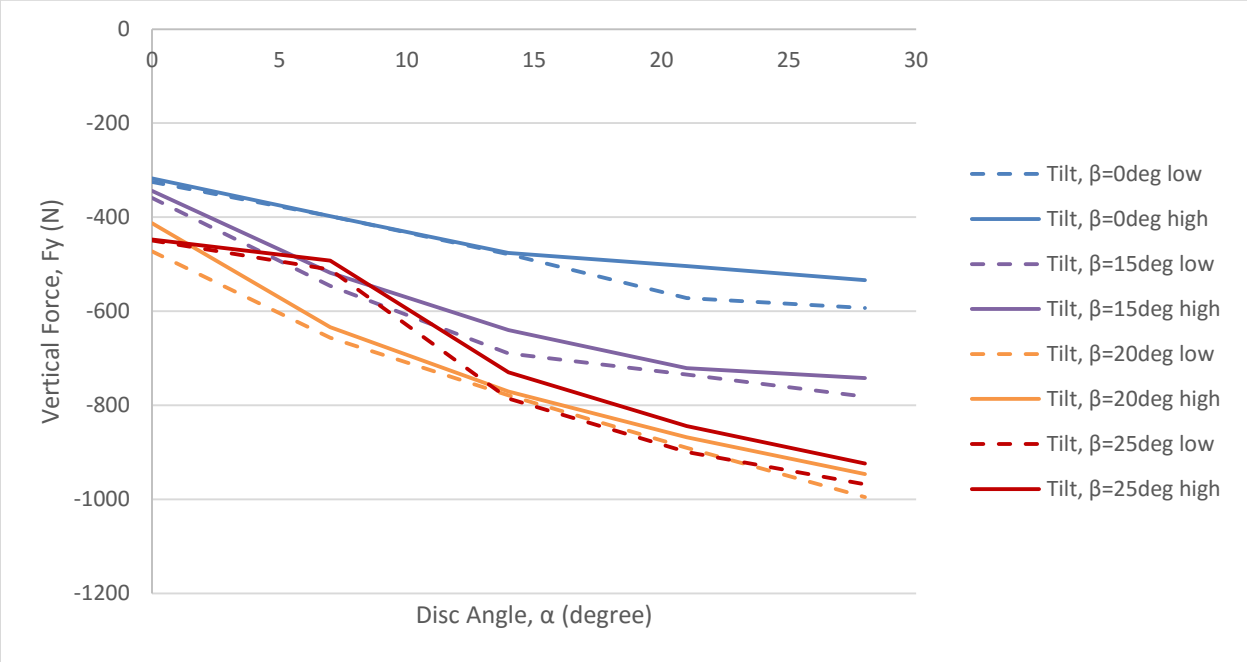

Figure B- 9: Vertical Force, Fy, for the Disc with Depth=2in Speed=5mph

Figure B- 10: Vertical Force, Fy, for the Disc with Depth=2in Speed=5mph

Similarly, it showed that increased the disc angle will increase the side force, from the results of the side (lateral) forces. Figure B-11 showed the side force, Fx, increased with increased disc angle for the disc with depth of 2in and speed of 5mph. Figure B-12 showed the side force, Fx, increased with increased tilt angle for the disc with depth of 2in and speed of 5mph. The chosen disc and tilt angle for the lowest draft force has the average side force of 424N.

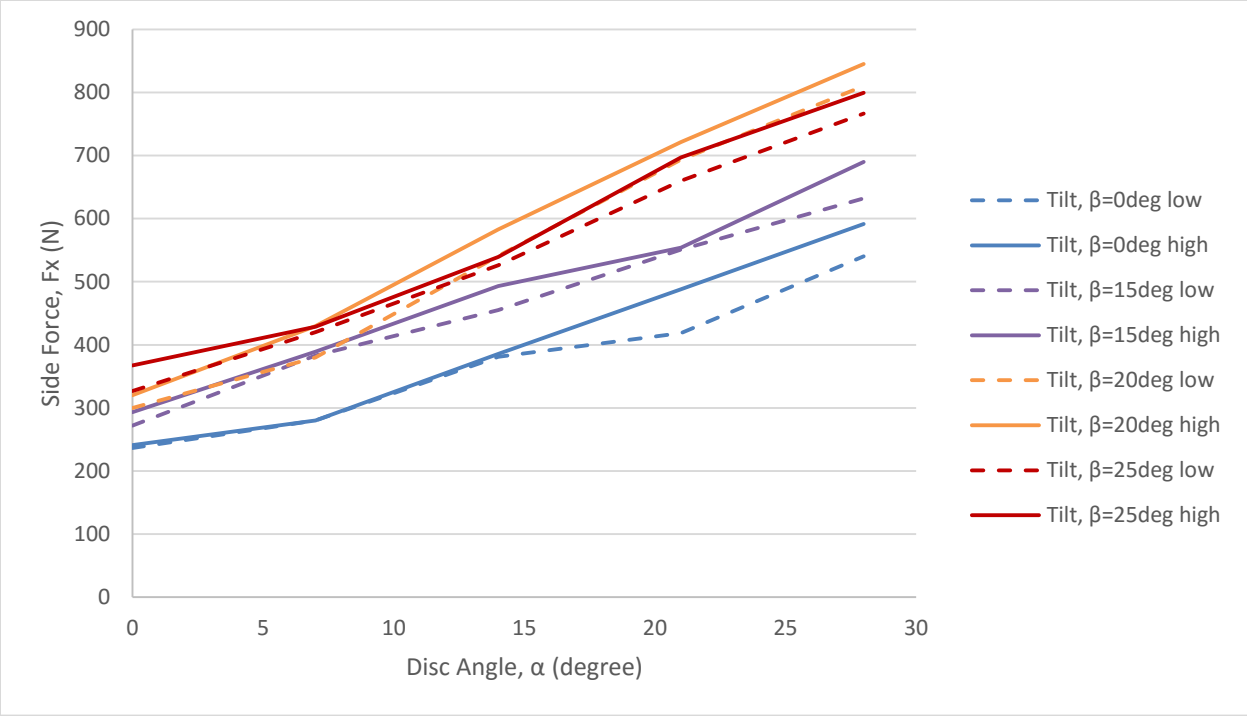

Figure B- 11: Side Force, Fx, for the Disc with Depth=2in Speed=5mph

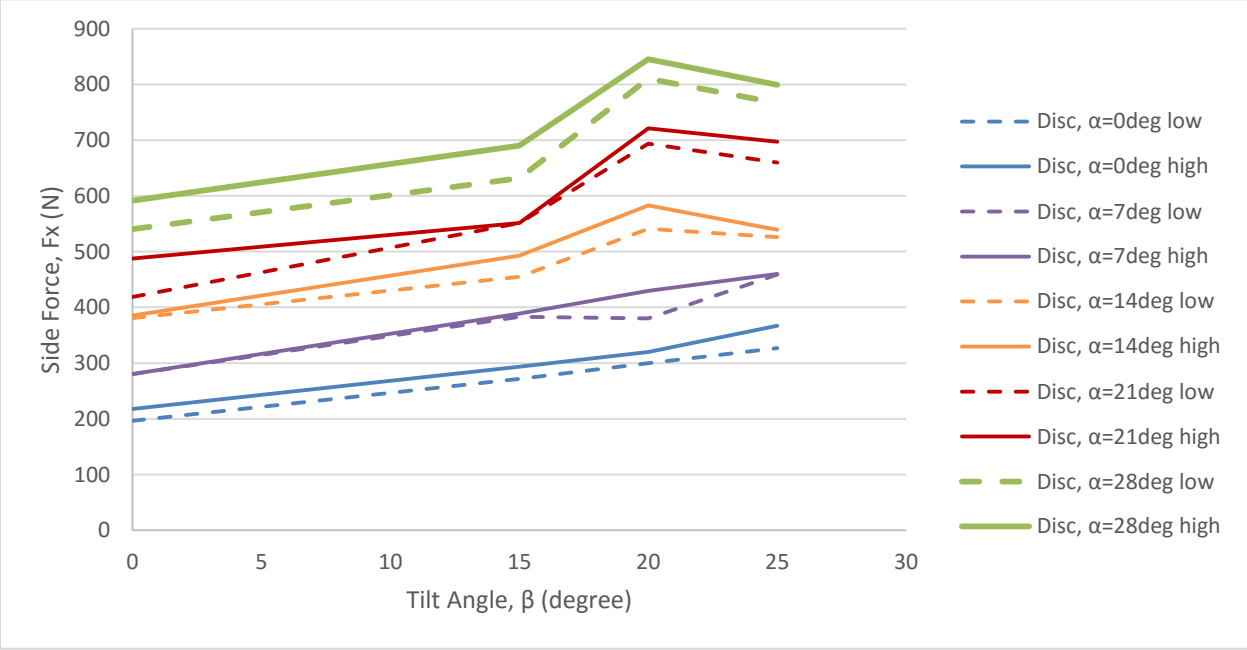

Figure B- 12: Side Force, Fx, for the Disc with Depth=2in Speed=5mph

The goal of these tests was to find the best combination of disc angle and tilt angle which leads to minimum draft force for depth is 2in speed is 5mph. The results of the experiments showed that the lowest draft force has the compound angle of 7° disc angle and 25° tilt angle.

B.3 - Depth=3in and Speed=5mph

Another set of experimental test has depth of 3in and speed of 5mph. The average of the vertical, draft, and side forces of the two data after using the filter of 2Hz for the disc experimental tests is analyzed. The modified average of the vertical, draft, and side forces can be plotted, which were shown in the following figures.

Figure B-13 and Figure B-14 showed the effect of disc and tilt angles on the draft force. When tilt angle is zero, draft force increased when increased the disc angle. Figure B-13 showed the draft force, Fz, increased with increased disc angle for the disc with depth of 3in and speed of 5mph. When disc angle is zero, draft force increased when increased the tilt angle. Figure B-14 showed the draft force, Fz, increased with increased tilt angle for the disc with depth of 3in and speed of 5mph. With the depth of 3in and speed of 5mph, the most reasonable compound angle (non-zero disc angle) for the lowest draft force is 7° disc angle and 25° tilt angle. The average of the minimum draft force is 343N.

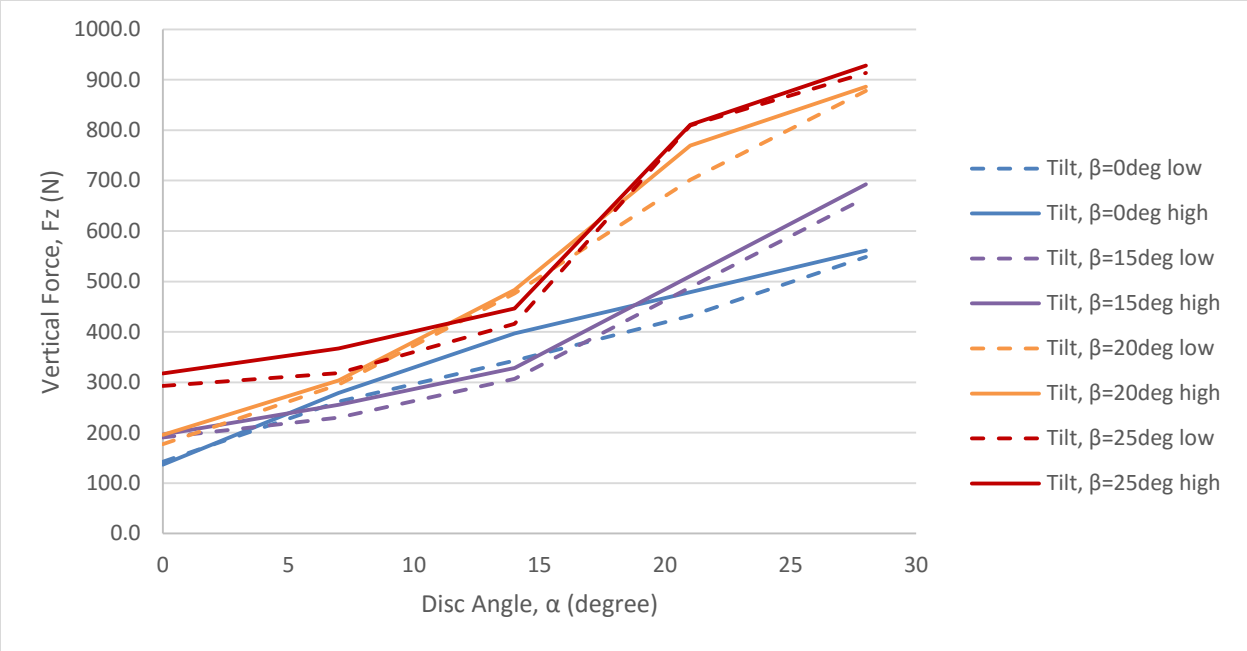

Figure B- 13: Draft Force, Fz, for the Disc with Depth=3in Speed=5mph

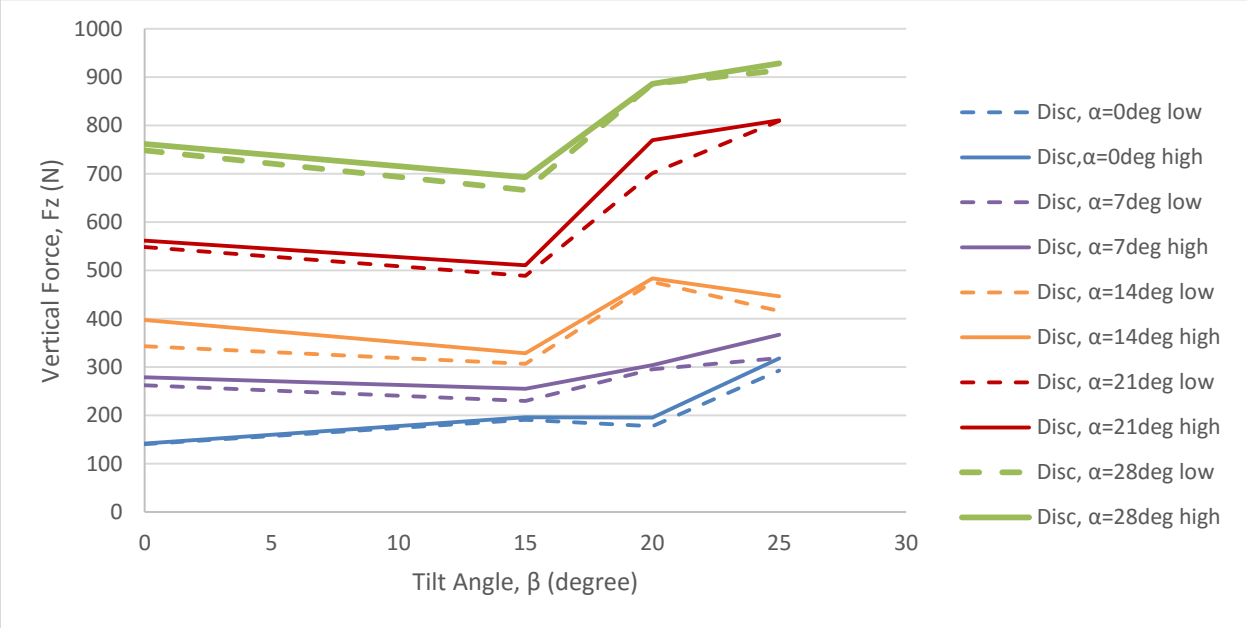

Figure B- 14: Draft Force, Fz, for the Disc with Depth=3in Speed=5mph

Figure B-15 and Figure B-16 showed the vertical force for different disc angles (0°, 7°, 14°, 21°, 28°) with different tilt angles (0°, 15°, 20°, 25°) respectively. Figure B-15 showed the

vertical force, Fy, increased negatively with increased disc angle for the disc with depth of 3in and speed of 5mph. Figure B-16 showed the vertical force, Fy, increased with increased tilt angle for the disc with depth of 3in and speed of 5mph.The most suitable disc and tilt compound angle is mainly chosen by the lowest draft force. As the experimental results showed, the corresponding average vertical force for the minimum draft force with a compound angle of 7° disc angle and 25° tilt angle is -525N.

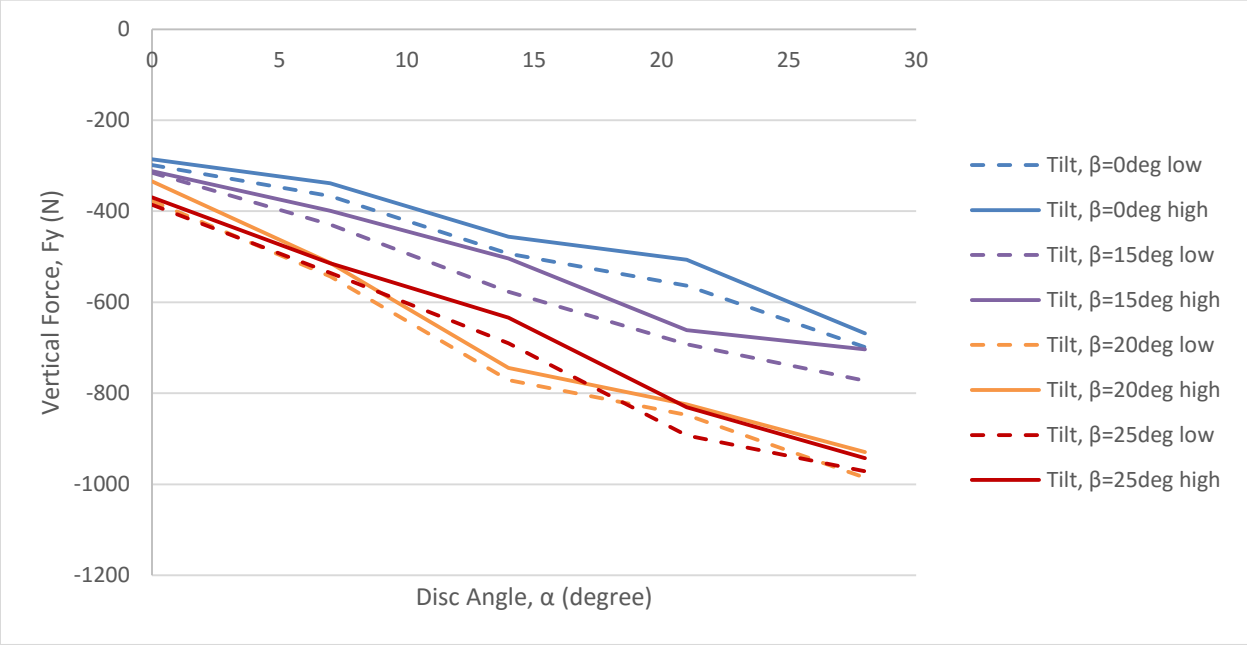

Figure B- 15: Vertical Force, Fy, for the Disc with Depth=3in Speed=5mph

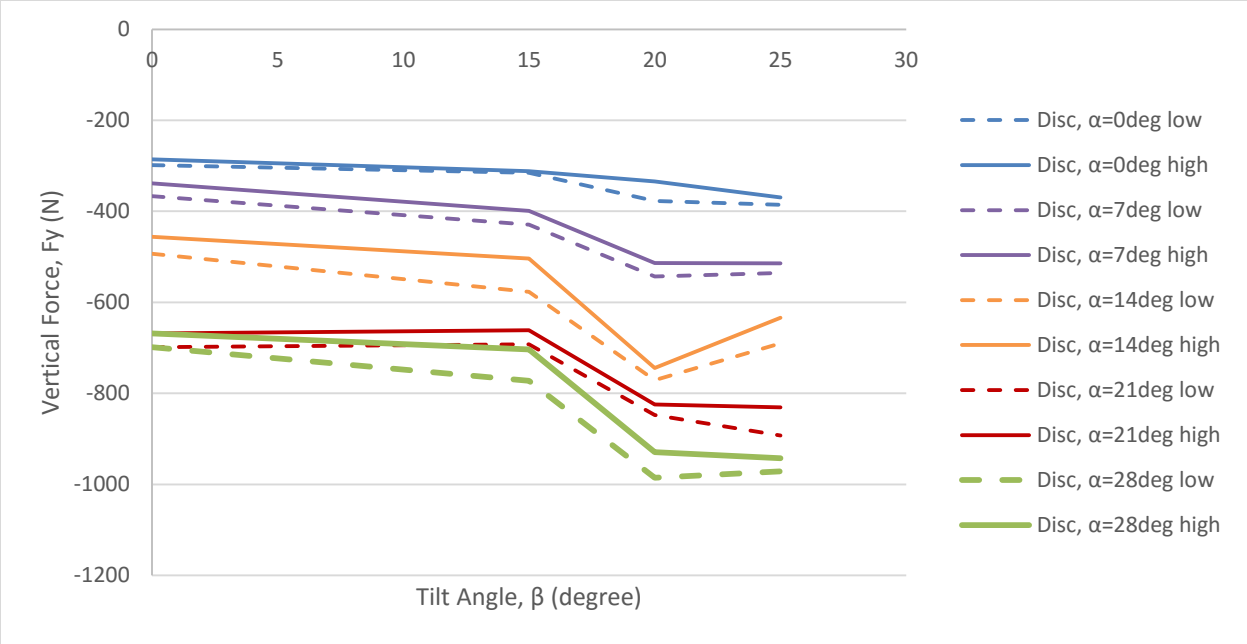

Figure B- 16: Vertical Force, Fy, for the Disc with Depth=3in Speed=5mph

The increased the disc angle will increase the side force is shown from the results of the side (lateral) forces. Figure B-17 showed the side force, Fx, increased with increased disc angle for the disc with depth of 3in and speed of 5mph. Figure B-18 showed the side force, Fx, increased with increased tilt angle for the disc with depth of 3in and speed of 5mph. The chosen disc and tilt angle for the lowest draft force has the average side force of 430N.

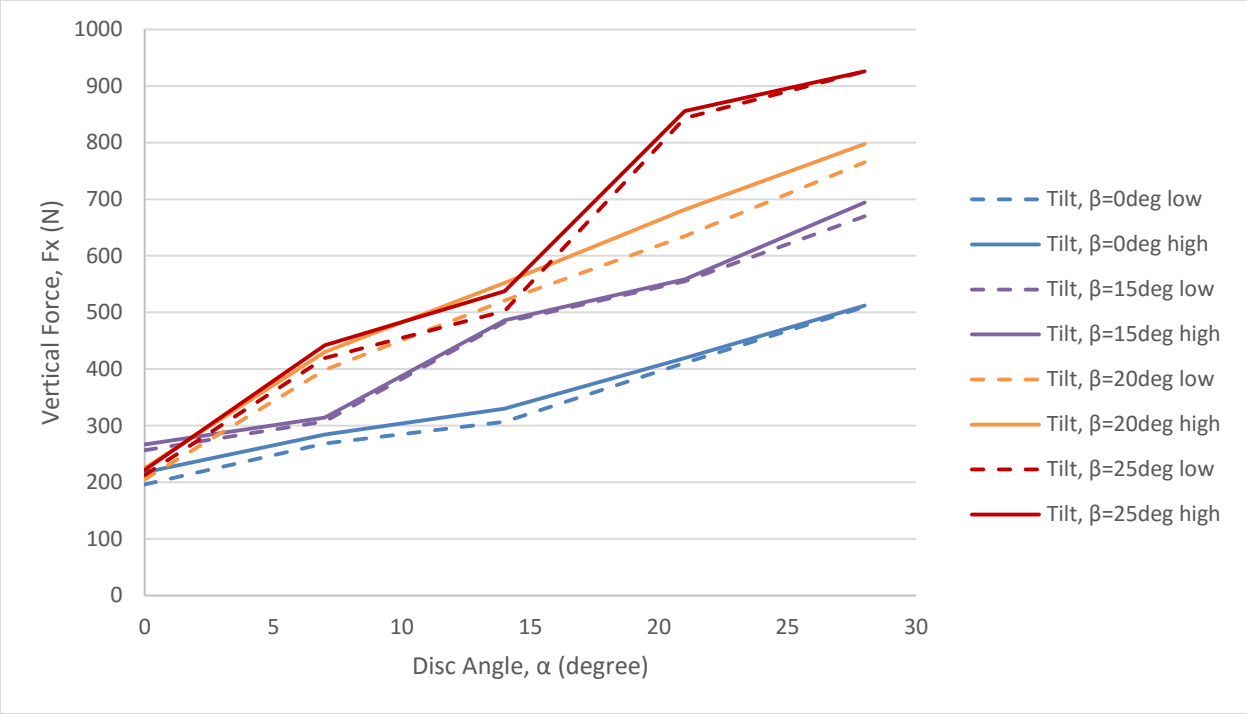

Figure B- 17: Side Force, Fx, for the Disc with Depth=3in Speed=5mph

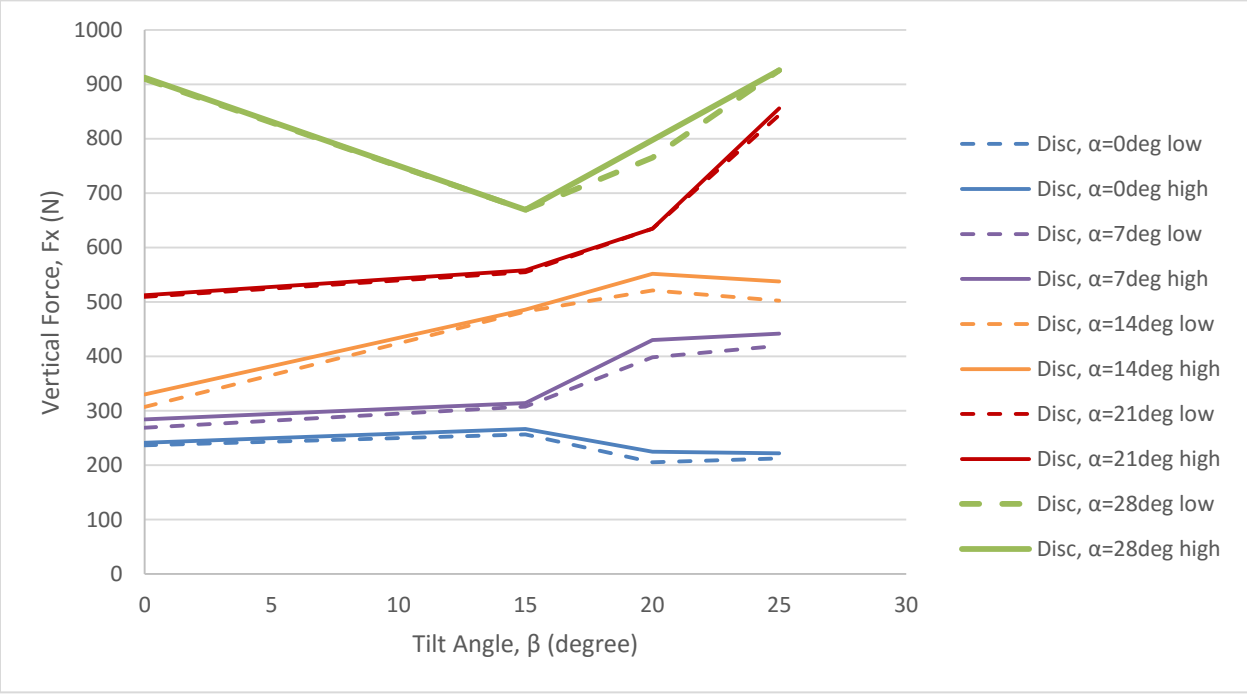

Figure B- 18: Side Force, Fx, for the Disc with Depth=3in Speed=5mph

The goal of these tests was to find the best combination of disc angle and tilt angle which leads to minimum draft force for depth is 3in speed is 5mph. The results of the experiments showed that the compound angle of 7° disc angle and 25° tilt angle gives the lowest draft force.

Appendix C – Compare with Re-test

Part of the experimental test data has been retested in order to verify the previous data. The rest data are shown in Appendix C.

Table C-1 is the retest experimental test data for disc angle at 14degree and tilt angle at 0degree. The data included different depths (2in or 3in) and different speeds (3mph or 5mph). The moisture content is at 11% and cone index at 1.22-1.24 for the retested data. The average of the two retested trials is compared to the average of the two original trials. The percent errors are mostly within 20%, which is a reasonable range.

Table C- 1: Disc=14 and Tilt=0 Comparison

				26-May			after 22%		
		Tilt	Disc	Vertical	Draft	Side	Vertical	Draft	Side
Depth=2 in Speed=5 mph	a	0	14	-473	320	311	-476	282	385
	b	0	14	-454	286	346	-479	293	381
Original difference				4%	11%	-11%	-1%	-4%	1%
Depth=2 in Speed=5 mph	Re a	0	14	-421	303	335	-434	300	380
	Re b	0	14	-431	295	313	-443	291	342
Re-rest difference				-2%	3%	7%	-2%	3%	11%
Difference with original				-8%	-1%	-1%	-8%	3%	-6%
				Moisture	11%		**Cone Index**		1.22
Depth=3 in Speed=5 mph	a	0	14	-470	316	382	-493	397	307
	b	0	14	-434	353	313	-456	343	330
Original difference				8%	-11%	20%	8%	15%	-7%
Depth=3 in Speed=5 mph	Re a	0	14	-506	339	344	-437	356	326
	Re b	0	14	-496	342	332	-419	377	366
Re-rest difference				2%	-1%	4%	4%	-6%	-11%
Difference with				10%	2%	-3%	-10%	-1%	8%

original									
				Moisture	11%		**Cone Index**		1.22
Depth=2 in Speed=3 mph	a	0	14	-300	225	331	-324	243	355
	b	0	14	-335	206	311	-345	212	322
Original difference				-11%	9%	6%	-6%	14%	10%
Depth=2 in Speed=3 mph	Re a	0	14	-305	238	309	-329	257	342
	Re b	0	14	-277	207	360	-292	212	397
Re-test difference				10%	14%	-15%	12%	19%	-15%
Difference with original				-9%	3%	4%	-8%	3%	9%
				Moisture	11%		**Cone Index**		1.24
Depth=3 in Speed=3 mph	a	0	14	-290	267	323	-295	270	333
	b	0	14	-235	226	321	-239	225	321
Original difference				21%	17%	1%	20%	18%	4%
Depth=3 in Speed=3 mph	Re a	0	14	-245	264	322	-290	303	294
	Re b	0	14	-275	244	268	-292	256	302
Re-test difference				-12%	8%	18%	-1%	17%	-3%
Difference with original				-1%	3%	-9%	9%	12%	-9%
				Moisture	11%		**Cone Index**		1.24

Table C-2 is the retest experimental test data for disc angle at 0degree and tilt angle at 25degree with different depths (2in or 3in) and different speeds (3mph or 5mph). The moisture content is at 10% and cone index at 1.14 for the retested data. The average of the two retested trials is compared to the average of the two original trials. The percent errors are mostly within a reasonable range.

Table C- 2: Disc=0 and Tilt=25 Comparison

				26-May			after 22%		
		Tilt	Disc	Vertical	Draft	Side	Vertical	Draft	Side
Depth=2 in Speed=5 mph	a	25	0	-515	181	323	-447	191	367
	b	25	0	-478	183	361	-450	194	327
Original difference				7%	-1%	-11%	-1%	-2%	12%
Depth=2 in Speed=5 mph	Re a	25	0	-504	192	335	-521	209	356
	Re b	25	0	-539	224	377	-571	242	398
Re-rest difference				-7%	-16%	-12%	-9%	-15%	-11%
Difference with original				5%	13%	4%	20%	16%	8%
				Moisture	10%		**Cone Index**		1.14
Depth=3 in Speed=5 mph	a	25	0	-388	314	228	-386	293	222
	b	25	0	-403	346	209	-370	318	212
Original difference				-4%	-10%	9%	4%	-8%	4%
Depth=3 in Speed=5 mph	Re a	25	0	-456	317	247	-481	315	266
	Re b	25	0	-484	337	269	-435	333	229
Re-rest difference				-6%	-6%	-8%	10%	-5%	15%
Difference with original				17%	-1%	17%	19%	6%	13%
				Moisture	10%		**Cone Index**		1.14
Depth=2 in Speed=3 mph	a	25	0	-258	101	172	-271	110	168
	b	25	0	-305	118	186	-325	120	187
Original difference				-17%	-16%	-8 %	-18%	-9%	-11%
Depth=2 in Speed=3 mph	Re a	25	0	-313	122	213	-341	114	215
	Re b	25	0	-345	141	211	-384	127	215
Re-test difference				-10%	-14%	1%	-12%	-11%	0%
Difference with original				16%	18%	17%	19%	5%	19%

				Moisture	10%		**Cone Index**		1.14
Depth=3 in Speed=3 mph	a	25	0	-434	233	297	-452	236	317
	b	25	0	-385	231	346	-404	231	305
Original difference				12%	1%	-15%	11%	2. %	4%
Depth=3 in Speed=3 mph	Re a	25	0	-424	207	316	-450	193	289
	Re b	25	0	-382	246	270	-412	225	301
Re-test difference				11%	-17%	16%	9%	-15%	-4%
Difference with original				-2%	-3%	-9%	1%	-11%	-5%
				Moisture	10%		**Cone Index**		1.14

Table C-3 is the retest experimental test data for disc angle at 14degree and tilt angle at 25degree with different depths (2in or 3in) and different speeds (3mph or 5mph). The moisture content is at 10% and cone index is between 1.11 and 1.29 for the retested data. The average of the two retested trials is compared to the average of the two original trials. The percent error is mostly within a reasonable range.

Table C- 3: Disc=14 and Tilt=25 Comparison

				26-May			after 22%		
		Tilt	Disc	Vertical	Draft	Side	Vertical	Draft	Side
Depth=2 in Speed=5 mph	a	25	14	-731	510	553	-730	526	539
	b	25	14	-812	466	562	-786	508	526
Original difference				-11%	9%	-2%	-7%	3%	3%
Depth=2 in Speed=5 mph	Re a	25	14	-846	442	577	-953	462	626
	Re b	25	14	-850	438	591	-918	451	629
Re-rest difference				-1%	1%	-2%	4%	2%	0%
Difference with original				9%	-10%	5%	21%	-12%	16%
				Moisture	10%		**Cone Index**		1.29

Depth=3 in Speed=5 mph	a	25	14	-627	394	486	-634	416	538
	b	25	14	-634	405	464	-690	446	503
Original difference				-1%	-3%	5%	-9%	-7%	7%
Depth=3 in Speed=5 mph	Re a	25	14	-695	390	546	-669	403	509
	Re b	25	14	-626	422	590	-673	436	547
Re-rest difference				10%	-8%	-8%	-1%	-8%	-7%
Difference with original				5%	2%	18%	1%	-3%	2%
				Moisture	10%		**Cone Index**		1.29
Depth=2 in Speed=3 mph	a	25	14	-444	307	359	-479	339	314
	b	25	14	-487	287	349	-423	299	362
Original difference				-9%	7%	3%	13%	13%	-14%
Depth=2 in Speed=3 mph	Re a	25	14	-375	349	361	-442	373	427
	Re b	25	14	-403	333	374	-423	346	389
Re-test difference				-7%	5%	-4%	5%	7%	9%
Difference with original				-18%	14%	4%	-4%	12%	19%
				Moisture	10%		**Cone Index**		1.11
Depth=3 in Speed=3 mph	a	25	14	-593	357	425	-686	354	426
	b	25	14	-528	323	344	-626	329	344
Original difference				12%	10%	20%	9.0%	7%	21%
Depth=3 in Speed=3 mph	Re a	25	14	-509	347	463	-621	351	472
	Re b	25	14	-560	310	386	-589	335	390
Re-test difference				-9%	11%	18%	5%	4%	19%
Difference with original				-5%	-3%	10%	-8%	0%	11%
				Moisture	10%		**Cone Index**		1.11

Table C-4 is the retest experimental test data for disc angle at 28degree and tilt angle at 0degree with different depths (2in or 3in) and different speeds (3mph or 5mph). For the retested data, the moisture content is in between 9% and 11%. The cone index is in between 1.12 and 1.19. The average of the two retested trials is compared to the average of the two original trials. The percent error is mostly within a reasonable range.

Table C- 4: Disc=28 and Tilt=0 Comparison

				26-May			after 22%		
		Tilt	Disc	Vertical	Draft	Side	Vertical	Draft	Side
Depth=2 in Speed=5 mph	a	0	28	-550	558	516	-593	594	540
	b	0	28	-526	507	565	-534	524	591
Original difference				4%	10%	-9%	11%	13%	-9 %
Depth=2 in Speed=5 mph	Re a	0	28	-496	570	477	-566	602	508
	Re b	0	28	-510	581	490	-517	565	545
Re-rest difference				-3%	-2%	-3%	9%	6%	-7%
Difference with original				-7%	8%	-11%	-4%	4%	-7%
				Moisture	11%		**Cone Index**		1.12
Depth=3 in Speed=5 mph	a	0	28	-651	516	475	-669	562	510
	b	0	28	-680	560	490	-699	549	512
Original difference				-5%	-8%	-3%	-4%	2%	-1%
Depth=3 in Speed=5 mph	Re a	0	28	-585	607	469	-666	600	481
	Re b	0	28	-584	535	499	-640	587	486
Re-rest difference				0%	13%	-6%	4%	2%	-1%
Difference with original				-13%	6%	0%	-5%	7%	-5%
				Moisture	11%		**Cone Index**		1.18
Depth=2 in	a	0	28	-396	357	475	-420	366	523

Speed=3 mph	b	0	28	-351	330	433	-477	352	565
Original difference				12%	8%	9%	-13%	4%	-8%
Depth=2 in Speed=3 mph	Re a	0	28	-339	348	496	-361	370	525
	Re b	0	28	-347	348	411	-383	362	528
Re-test difference				-2%	0%	19%	-6%	2%	-1%
Difference with original				-9%	1%	0%	-19%	2%	-3%
				Moisture	9%		**Cone Index**		1.19
Depth=3 in Speed=3 mph	a	0	28	-339	418	473	-354	428	482
	b	0	28	-368	439	430	-382	357	453
Original difference				-8%	-5%	9%	-8%	18%	6%
Depth=3 in Speed=3 mph	Re a	0	28	-450	432	420	-405	487	486
	Re b	0	28	-406	472	472	-373	457	465
Re-test difference				10%	-9%	-12%	8%	6%	4%
Difference with original				19%	5%	-1%	5%	18%	2%
				Moisture	9%		**Cone Index**		1.19

Table C-5 is the retest experimental test data for disc angle at 25degree and tilt angle at 28degree with different depths (2in or 3in) and different speeds (3mph or 5mph). The moisture content is at 9% and cone index is in between 1.08 and 1.14 for the retested data. The average of the two retested trials is compared to the average of the two original trials. The percent error is mostly within a reasonable range.

Table C- 5: Disc=28 and Tilt=25 Comparison

				26-May			after 22%		
		Tilt	Disc	Vertical	Draft	Side	Vertical	Draft	Side
Depth=2 in Speed=5 mph	a	25	28	-882	668	772	-969	722	767
	b	25	28	-848	603	733	-924	751	799
Original difference				4%	10%	5%	5%	-4%	-4 %
Depth=2 in Speed=5 mph	Re a	25	28	-777	625	720	-839	668	775
	Re b	25	28	-723	591	660	-776	632	708
Re-rest difference				7%	6%	9%	8%	6%	9%
Difference with original				-14%	-4%	-9%	-16%	-12%	-5%
				Moisture	9%		**Cone Index**		1.16
Depth=2 in Speed=3 mph	a	25	28	-701	537	536	-693	523	618
	b	25	28	-731	584	575	-642	584	681
Original difference				-4%	-8%	-7%	8%	-11%	-10%
Depth=2 in Speed=3 mph	Re a	25	28	-622	449	525	-661	477	558
	Re b	25	28	-596	490	513	-669	511	601
Re-rest difference				4%	-9%	2%	-1%	-7%	-7%
Difference with original				-16%	-18%	-7%	0%	-11%	-11%
				Moisture	9%		**Cone Index**		1.08

Appendix D – Cutting Force

Cutting force is the force required to cut the soil. Cutting force cannot be measured directly. The cutting force can be evaluated by using the equation (2.11) Cutting forces are a combination of the draft, vertical, and side forces. During all the cutting force calculation, the assumption for δ angle is required, such that $\delta = \delta_{avg} = 24°$. The following plots showed the cutting force for different depths and different speeds (Table 3-1).

The compound angle (non-zero disc angle) for the lowest draft force is 7° disc angle and 25° tilt angle. For depth of 3in and speed of 3mph, the average of the minimum cutting force at 7° disc angle and 25° tilt angle is 684N. The disc cutting force,F_c, with disc angle of 0°, 7°, 14°, 21°, 28° for depth of 3in and speed of 3mph is shown in Figure D-1. Figure D-1 shows the cutting force, Fc, increased with increased disc angle for the disc with depth of 3in and speed of 3mph.

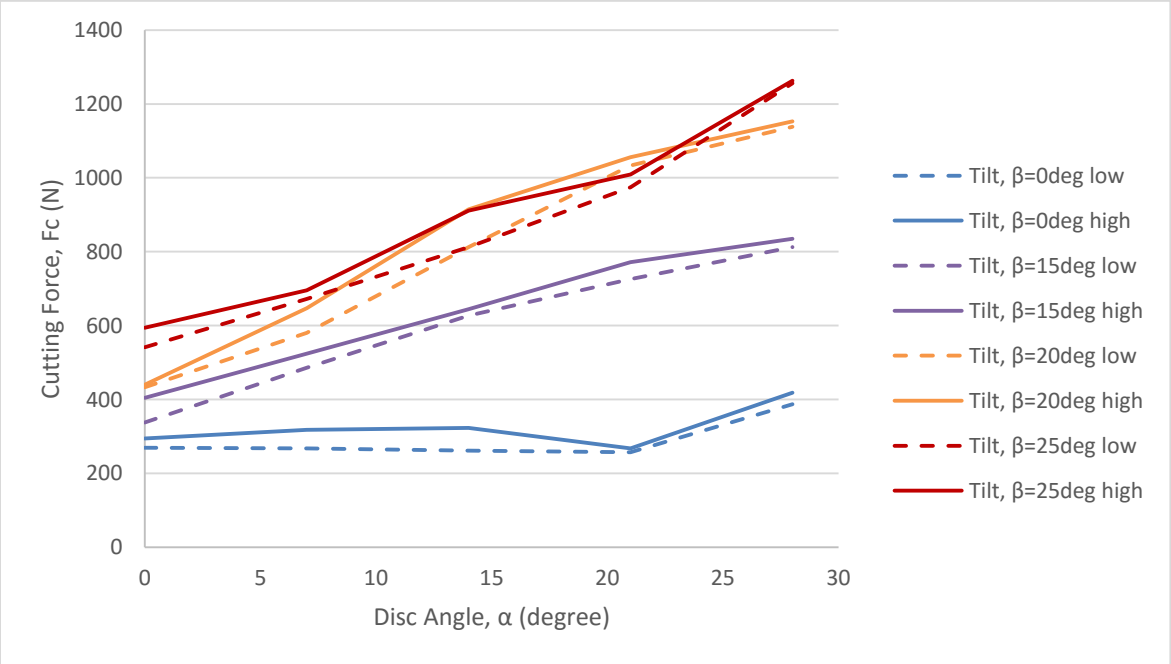

Figure D- 1: Cutting Force, Fc, for the Disc (Disc Angle, α) with Depth=3in Speed=3mph

The cutting force,F_c, of the disc with tilt angles of 0°, 15°, 20°, 25° for depth of 3in and speed of 3mph is shown in Figure D-2. Figure D-2 shows the cutting force, Fc, increased with increased tilt angle for the disc with depth of 3in and speed of 3mph

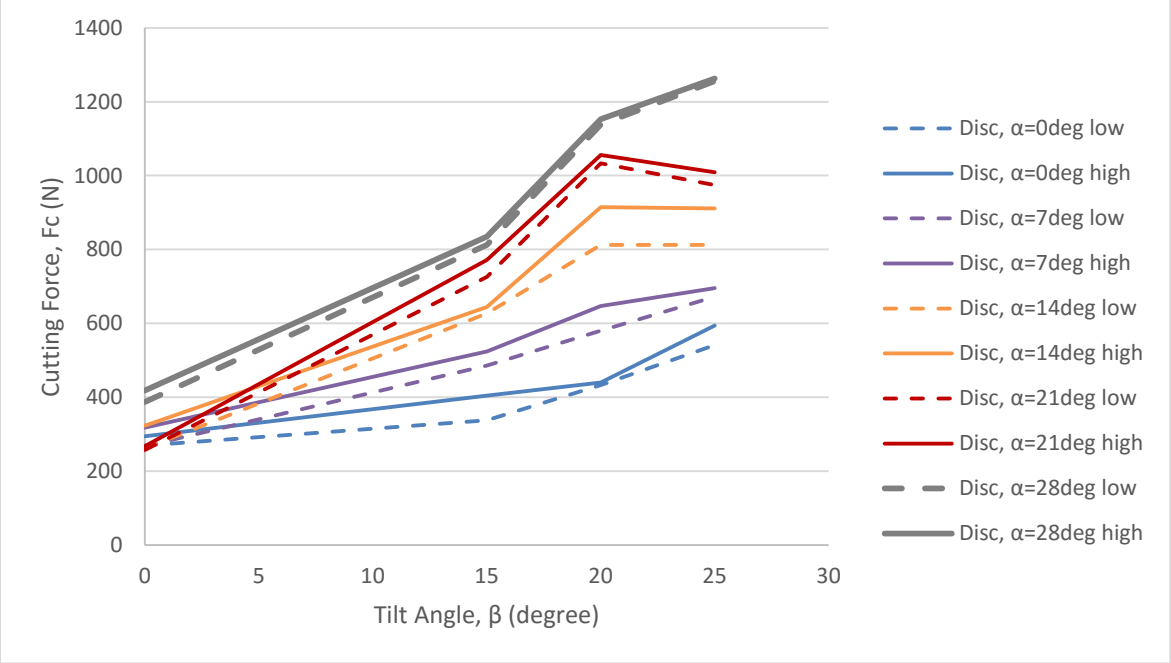

Figure D- 2: Cutting Force, Fc, for the Disc (Tilt Angle, β) with Depth=3in Speed=3mph

The cutting force,F_c, of the disc for disc angles of 0°, 7°, 14°, 21°, 28° for depth of 2in and speed of 5mph is shown in Figure D-3. The compound angle (non-zero disc angle) for the lowest draft force is 7° disc angle and 25° tilt angle. For depth of 2in and speed of 5mph, the average of the minimum cutting force at 7° disc angle and 25° tilt angle is 711N. Figure D-3 shows the cutting force, Fc, increased with increased disc angle for the disc with depth of 2in and speed of 5mph.

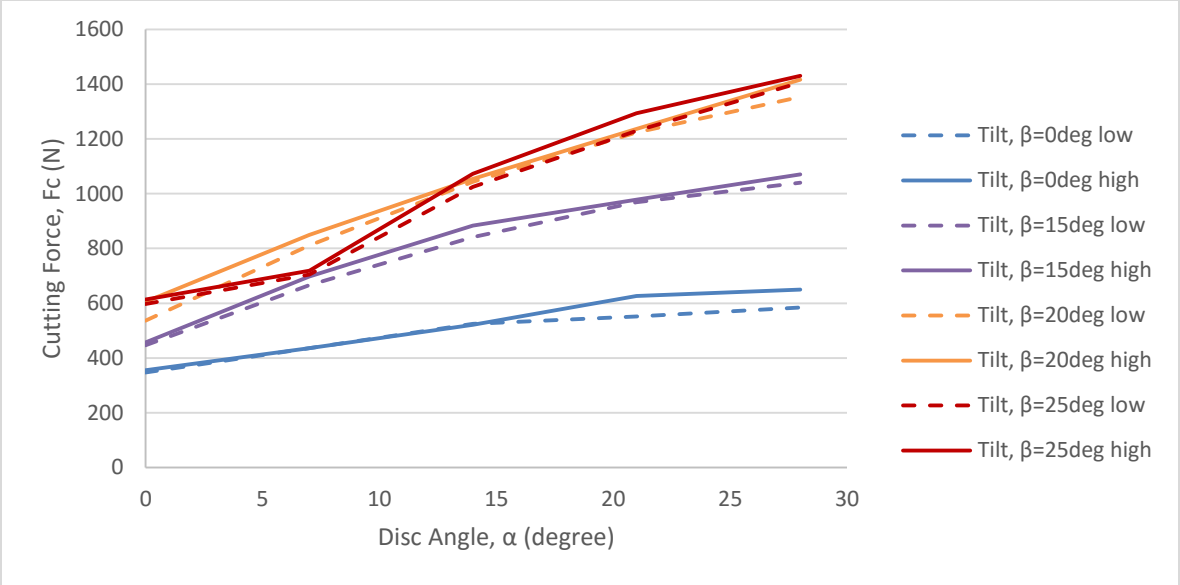

Figure D- 3: Cutting Force, Fc, for the Disc (Disc Angle, α) with Depth=2in Speed=5mph

The cutting force,F_c, of the disc for tilt angles of 0°, 15°, 20°, 25° for a depth of 2in and speed of 5mph is shown in Figure D-4. Figure D-4 shows the cutting force, Fc, increased with increased tilt angle for the disc with depth of 2in and speed of 5mph

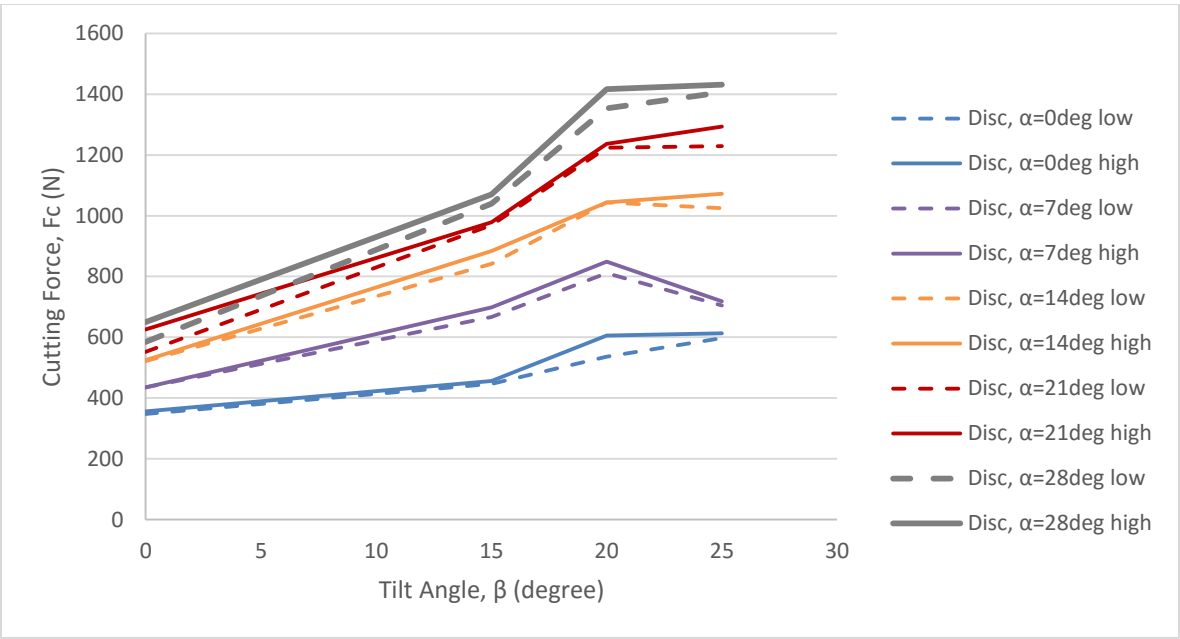

Figure D- 4: Cutting Force, Fc, for the Disc (Tilt Angle, β) with Depth=2in Speed=5mph

The cutting force,F_c, of the disc for disc angles of 0°, 7°, 14°, 21°, 28° for a depth of 3in and speed of 5mph is shown in Figure D-5. The compound angle (non-zero disc angle) for the lowest draft force is 7° disc angle and 25° tilt angle. For depth of 3in and speed of 5mph, the average of the minimum cutting force at 7° disc angle and 25° tilt angle is 738N. Figure D.5 shows the cutting force, Fc, increased with increased disc angle for the disc with depth of 3in and speed of 5mph.

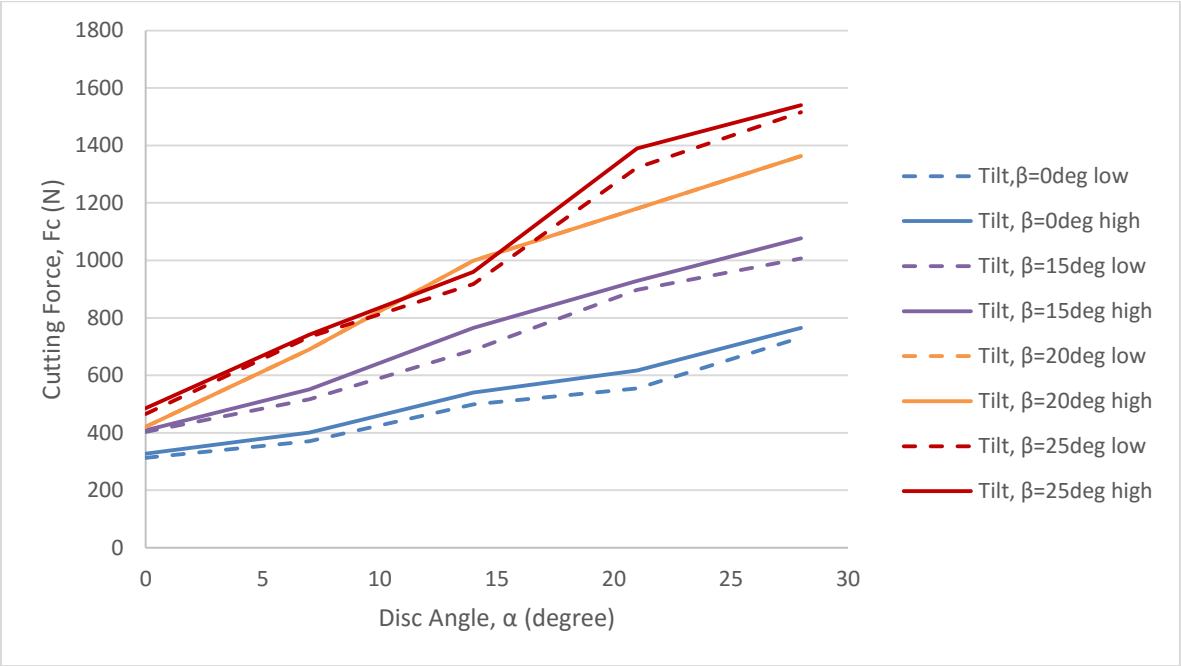

Figure D- 5: Cutting Force, Fc, for the Disc (Disc Angle, α) with Depth=3in Speed=5mph

The cutting force,F_c, of the disc with tilt angles of 0°, 15°, 20°, 25° for a depth of 3in and speed of 5mph is shown in Figure D-6. Figure D-6 showed the cutting force, Fc, increased with increased tilt angle for the disc with depth of 3in and speed of 5mph.

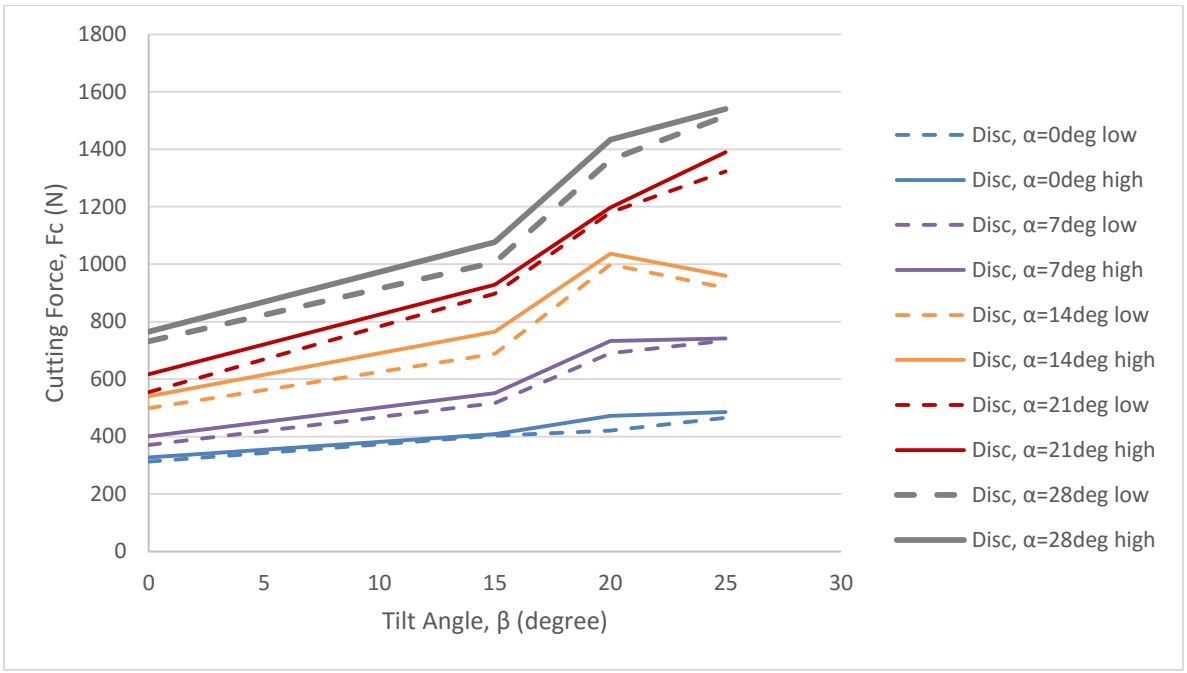

Figure D- 6: Cutting Force, Fc, for the Disc (Tilt Angle, β) with Depth=3in Speed=5mph

Appendix E – Normal Force

Normal force is the force from the soil that acts on the disc. The normal force also cannot be measured easily. The normal force can be evaluated by using the above equation(2.11). The assumption for δ angle is required to be, such that $\delta = \delta_{avg} = 24°$ for all the cutting force calculation. The following plots only show the cutting force for different depths with different speeds (Table 3-1).

For a depth of 3in and speed of 3mph, the compound angle 7° disc angle and 25° tilt angle has the lowest draft force (non-zero disc angle). The average of the minimum normal force with 7° disc angle and 25° tilt angle is 149N. The Normal force,N, of the disc with increased disc angle (0°, 7°, 14°, 21°, 28°) at depth of 3in and speed of 3mph is shown in Figure E-1. Figure E-1 shows the Normal force, N, increased with increased disc angle for the disc with depth of 3in and speed of 3mph.

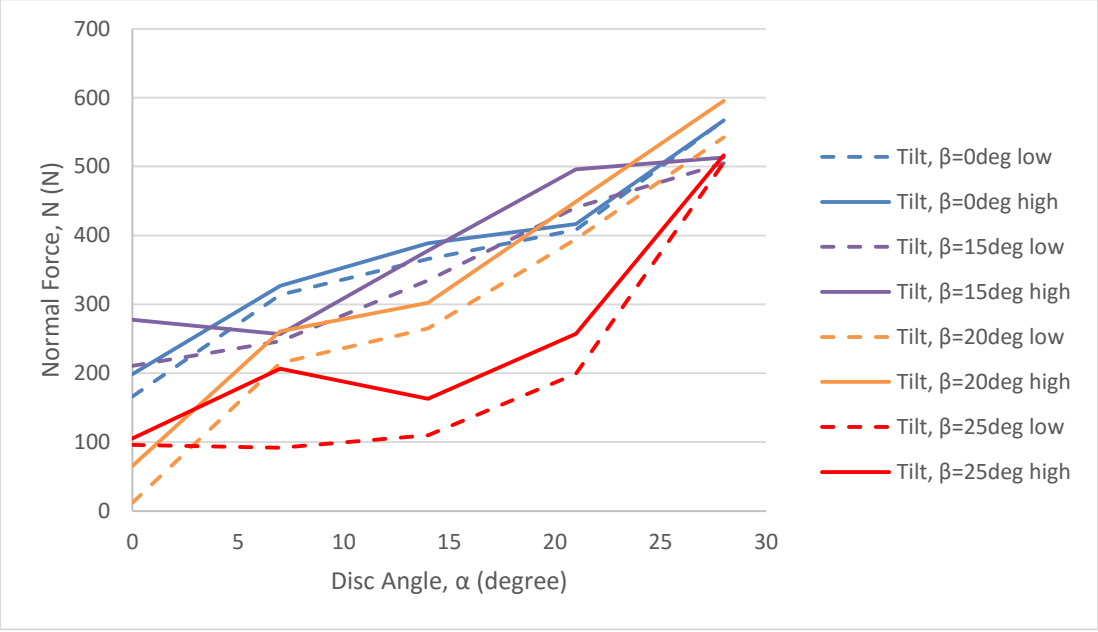

Figure E- 1: Normal Force, N, for the Disc (Disc Angle, α) with Depth=3in Speed=3mph

The normal force,N, of the disc with increased tilt angle (0°, 15°, 20°, 25°) at depth of 3in and speed of 3mph is shown in Figure E-2. Figure E-2 shows the Normal force, N, increased with decreased tilt angle for the disc with depth of 3in and speed of 3mph.

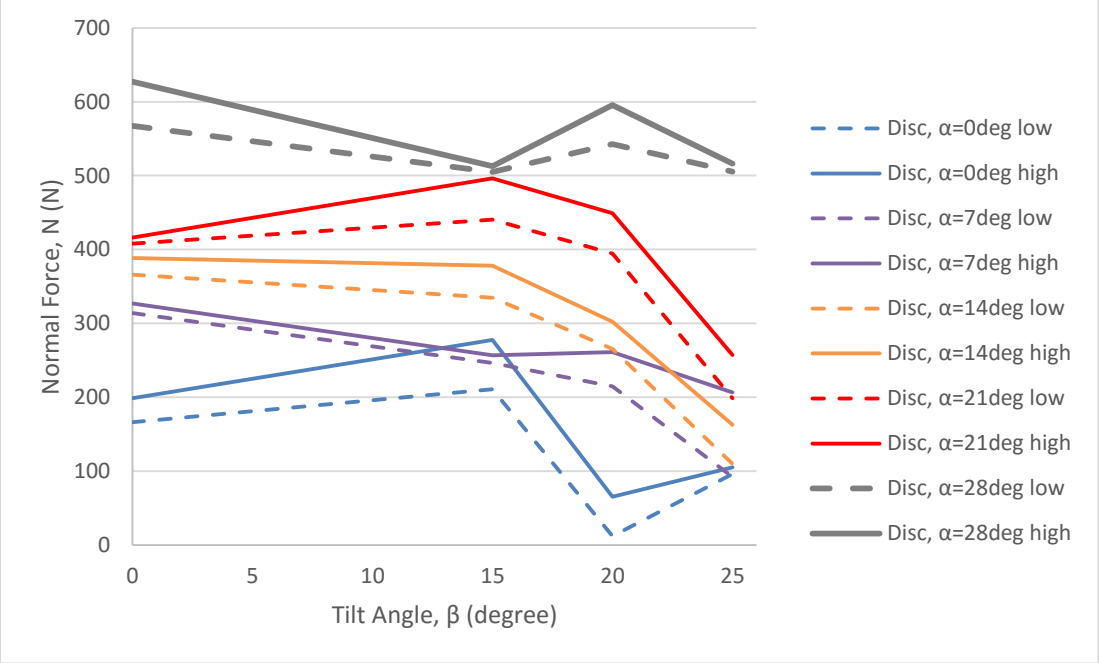

Figure E- 2: Normal Force, N, for the Disc (Tilt Angle, β) with Depth=3in Speed=3mph

For depth of 2in and speed of 5mph, the compound angle 7° disc angle and 25° tilt angle has the lowest draft force (non-zero disc angle). The average of the minimum normal force with 7° disc angle and 25° tilt angle is 207N. The Normal force,N, of the disc with increased disc angle (0°, 7°, 14°, 21°, 28°) at depth of 2in and speed of 5mph is shown in Figure E-3. This Figure shows the Normal force, N, increased with increased disc angle for the disc with depth of 2in and speed of 5mph.

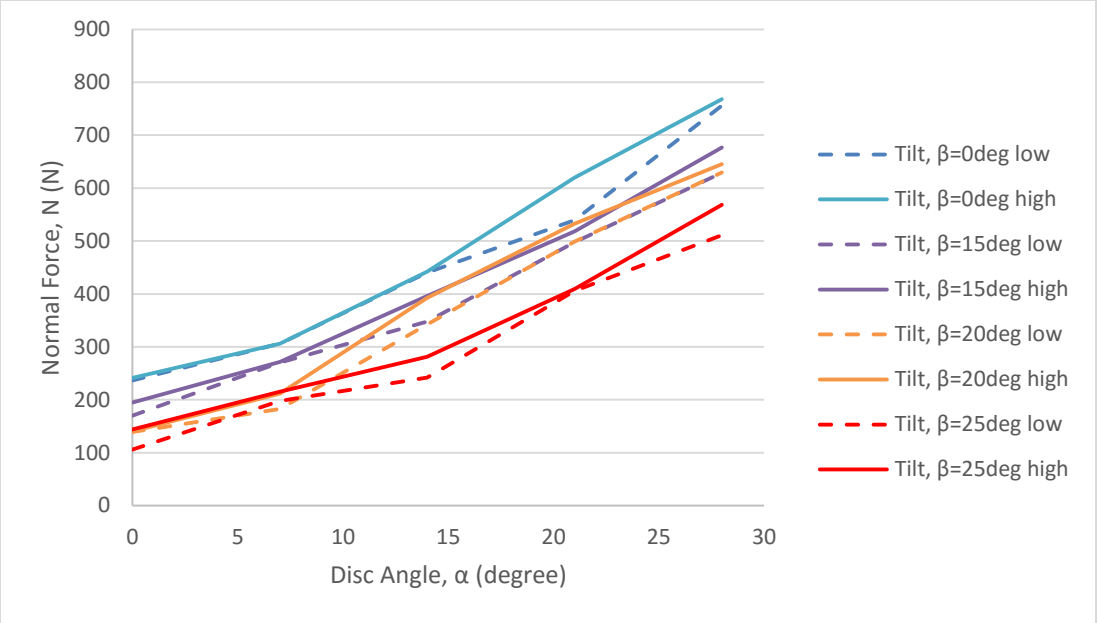

Figure E- 3: Normal Force, N, for the Disc (Disc Angle, α) with Depth=2in Speed=5mph

The normal force,*N*, of the disc with increased tilt angle (0°, 15°, 20°, 25°) at depth of 2in and speed of 5mph is shown in Figure E.4. Figure E.4 shows the Normal force, N, increased with decreased tilt angle for the disc with depth of 2in and speed of 5mph.

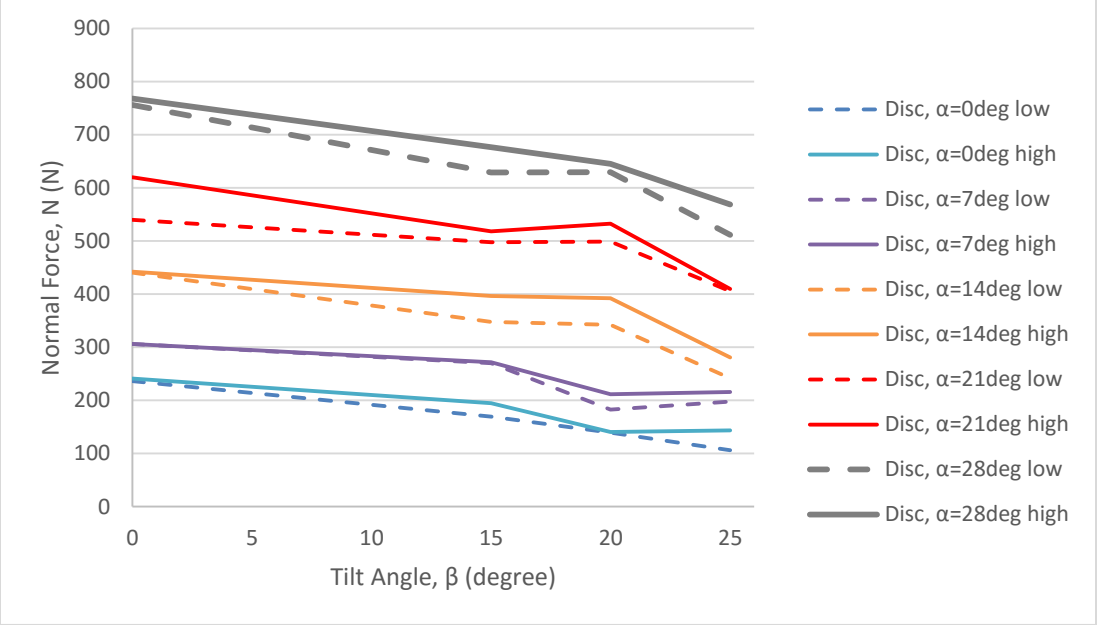

Figure E- 4: Normal Force, N, for the Disc (Tilt Angle, β) with Depth=2in Speed=5mph

For depth of 3in and speed of 5mph, the compound angle 7° disc angle and 25° tilt angle has the lowest draft force (non-zero disc angle). The average of the minimum normal force with 7° disc angle and 25° tilt angle is 203N. The Normal force,N, of the disc with increased disc angle (0°, 7°, 14°, 21°, 28°) at depth of 3in and speed of 5mph is shown in Figure E-5. It showed the Normal force, N, increased with increased disc angle for the disc with depth of 3in and speed of 5mph.

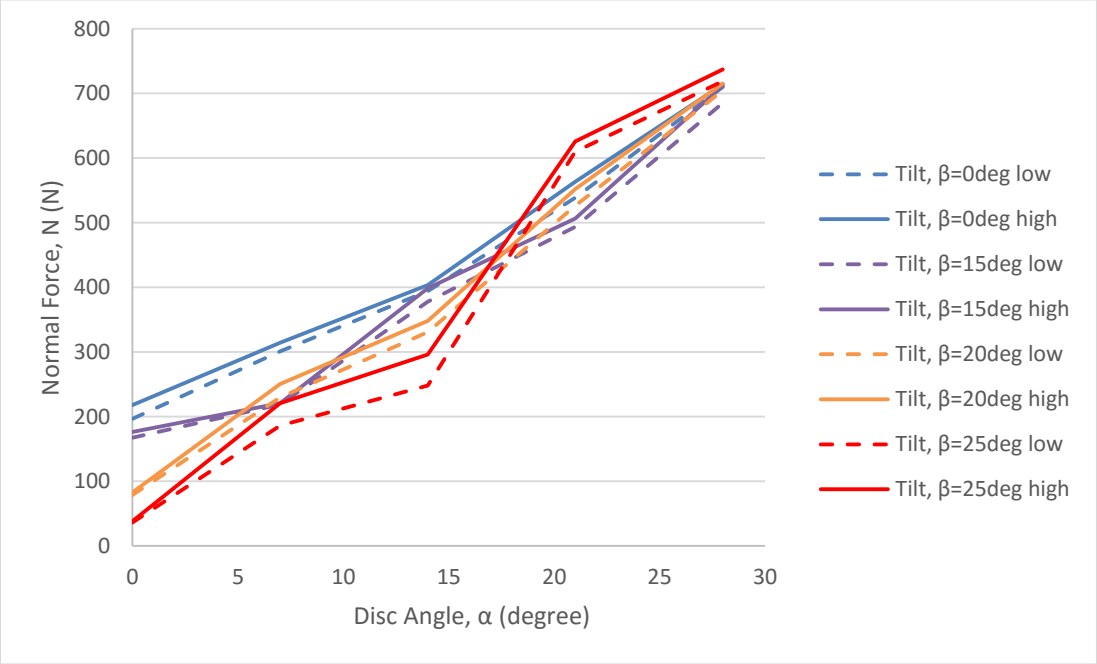

Figure E- 5: Normal Force, N, for the Disc (Disc Angle, α) with Depth=3in Speed=5mph

The normal force,N, of the disc with increased tilt angle (0°, 15°, 20°, 25°) at depth of 3in and speed of 5mph is shown in Figure E-6. Figure E-6 showed the Normal force, N, increased with decreased tilt angle for the disc with depth of 3in and speed of 5mph.

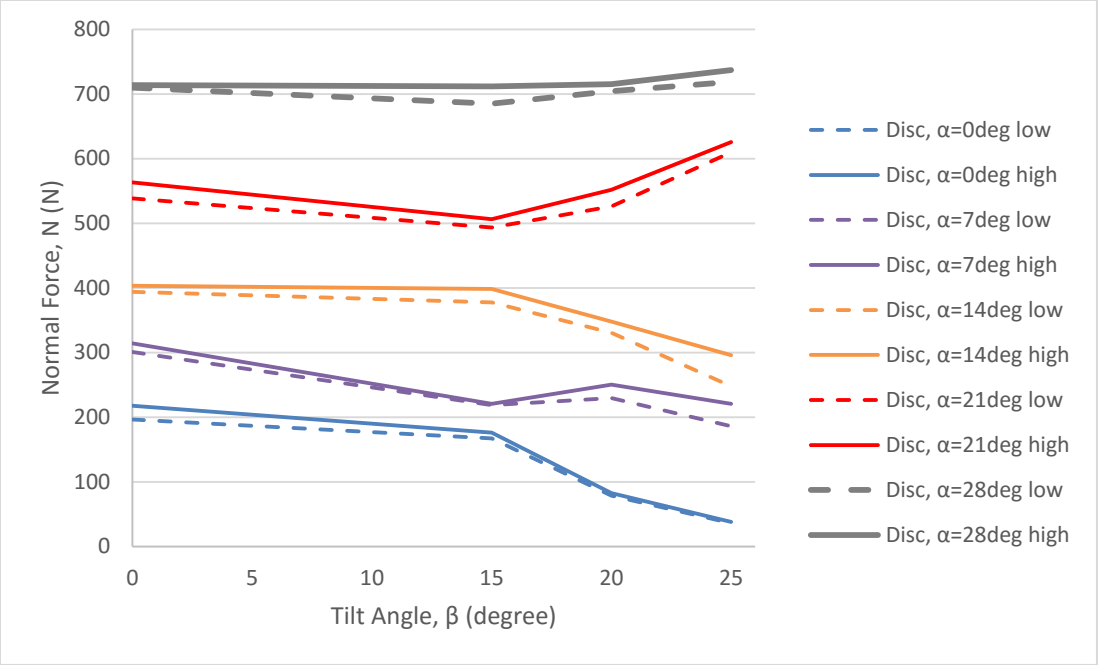

Figure E- 6: Normal Force, N, for the Disc (Tilt Angle, β) with Depth=3in Speed=5mph

Appendix F – Cutting Width

F.1 – Cutting Width Data

In the global coordinate system X-Y (see Figure 2-1), the furrow's width is represented by a line of the length P1-P2 as shown in Figure F-1. This Figure also shows the disc in the configuration specified by the angles α and β as well as seen from the direction Z. In such a configuration the disc is represented by the ellipsis of axes a and b where $a = \rho sin\alpha$, $b = \rho sin\beta''$ for $\rho = 0.23m$, where $sin\beta' = sin\beta cos\alpha$ and $sin\beta'' = sin\beta sin\alpha$. For the range of α and β considered one can assume $cos\beta'' \approx 1$ and $\beta' \approx \beta$.

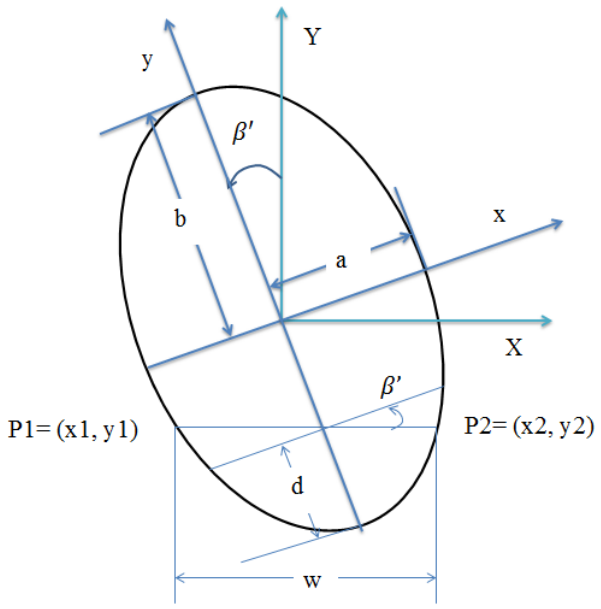

Figure F- 1: Disc Parameters

By combining the equation of an ellipse and the equation of a line, the location of P1 and P2 is found. Then the distance between P1 and P2, which is the cutting width, is determined. The following equations showed how the coordinates x1, y1 and x2, y2 are calculated.

$$\frac{x^2}{a^2}+\frac{y^2}{b^2}=1 \qquad (F.1)$$

$$y=-(tan\beta)x-(b-d) \qquad (F.2)$$

Substitute (5.6) into (5.7)

$$x1,x2=\frac{-f\pm\sqrt{f^2-4eg}}{2e} \qquad where \begin{cases} e=\dfrac{1}{a^2}+\dfrac{(tan\beta)^2}{b^2} \\ f=\dfrac{2(tan\beta)(b-d)}{b^2} \\ g=\dfrac{(b-d)^2}{b^2}-1 \end{cases} \qquad (F.3)$$

$$y=-(tan\beta)x-(b-d) \qquad (F.4)$$

Then, the cutting width will be

$$w(\alpha,\beta,d)=\sqrt{(x1-x2)^2+(y1-y2)^2} \qquad (F.5)$$

Table F-1 showed the analyzed data for cutting width with depth of 2in (0.0508m).

Table F- 1: Cutting width data for depth of 2in (0.0508m)

α	β										Width
deg	deg	a(m)	b(m)	e(m)	f(m)	g(m)	X1(m)	X2(m)	Y1(m)	Y2(m)	W(m)
0	0	0.000	0.230	0	0.00	-0.393	0.000	0.000	0.000	0.000	0.000
7	0	0.028	0.230	1273	0.00	-0.393	0.018	-0.018	-0.179	-0.179	0.035
14	0	0.056	0.230	323	0.00	-0.393	0.035	-0.035	-0.179	-0.179	0.070
21	0	0.082	0.230	147	0.00	-0.393	0.052	-0.052	-0.179	-0.179	0.103
28	0	0.108	0.230	86	0.00	-0.393	0.068	-0.068	-0.179	-0.179	0.135

0	15	0.000	0.230	0	1.82	-0.393	0.000	0.000	0.000	0.000	0.000
7	15	0.028	0.230	1274	1.82	-0.393	0.017	-0.018	-0.184	-0.174	0.036
14	15	0.056	0.230	324	1.82	-0.393	0.032	-0.038	-0.188	-0.169	0.072
21	15	0.082	0.230	149	1.82	-0.393	0.046	-0.058	-0.191	-0.164	0.107
28	15	0.108	0.230	87	1.82	-0.393	0.058	-0.078	-0.195	-0.158	0.141
0	20	0.000	0.230	0	2.47	-0.393	0.000	0.000	0.000	0.000	0.000
7	20	0.028	0.230	1275	2.47	-0.393	0.017	-0.019	-0.185	-0.172	0.037
14	20	0.056	0.230	325	2.47	-0.393	0.031	-0.039	-0.191	-0.165	0.074
21	20	0.082	0.230	150	2.47	-0.393	0.044	-0.060	-0.195	-0.157	0.110
28	20	0.108	0.230	88	2.47	-0.393	0.054	-0.082	-0.199	-0.149	0.145
0	25	0.000	0.230	0	3.16	-0.393	0.000	0.000	0.000	0.000	0.000
7	25	0.028	0.230	1277	3.16	-0.393	0.016	-0.019	-0.187	-0.170	0.039
14	25	0.056	0.230	327	3.16	-0.393	0.030	-0.040	-0.193	-0.161	0.077
21	25	0.082	0.230	151	3.16	-0.393	0.042	-0.062	-0.199	-0.150	0.115
28	25	0.108	0.230	90	3.16	-0.393	0.051	-0.086	-0.203	-0.139	0.151

Table F-2 showed the analyzed data for cutting width with depth of 3in (0.0762m).

Table F- 2: Cutting width data for depth of 3in (0.0762m)

α	β										Width
deg	deg	a(m)	b(m)	e(m)	f(m)	g(m)	X1(m)	X2(m)	Y1(m)	Y2(m)	W(m)
0	0	0.000	0.230	0	0.00	-0.553	0.000	0.000	0.000	0.000	0.000
7	0	0.028	0.230	1273	0.00	-0.553	0.021	-0.021	-0.154	-0.154	0.042

14	0	0.056	0.230	323	0.00	-0.553	0.041	-0.041	-0.154	-0.154	0.083
21	0	0.082	0.230	147	0.00	-0.553	0.061	-0.061	-0.154	-0.154	0.123
28	0	0.108	0.230	86	0.00	-0.553	0.080	-0.080	-0.154	-0.154	0.161
0	15	0.000	0.230	0	1.56	-0.553	0.000	0.000	0.000	0.000	0.000
7	15	0.028	0.230	1274	1.56	-0.553	0.020	-0.021	-0.159	-0.148	0.043
14	15	0.056	0.230	324	1.56	-0.553	0.039	-0.044	-0.164	-0.142	0.086
21	15	0.082	0.230	149	1.56	-0.553	0.056	-0.066	-0.169	-0.136	0.127
28	15	0.108	0.230	87	1.56	-0.553	0.071	-0.089	-0.173	-0.130	0.166
0	20	0.000	0.230	0	2.12	-0.553	0.000	0.000	0.000	0.000	0.000
7	20	0.028	0.230	1275	2.12	-0.553	0.020	-0.022	-0.161	-0.146	0.044
14	20	0.056	0.230	325	2.12	-0.553	0.038	-0.045	-0.168	-0.138	0.088
21	20	0.082	0.230	150	2.12	-0.553	0.054	-0.068	-0.173	-0.129	0.130
28	20	0.108	0.230	88	2.12	-0.553	0.068	-0.092	-0.179	-0.120	0.170
0	25	0.000	0.230	0	2.71	-0.553	0.000	0.000	0.000	0.000	0.000
7	25	0.028	0.230	1277	2.71	-0.553	0.020	-0.022	-0.163	-0.144	0.046
14	25	0.056	0.230	327	2.71	-0.553	0.037	-0.045	-0.171	-0.133	0.091
21	25	0.082	0.230	151	2.71	-0.553	0.052	-0.070	-0.178	-0.121	0.135
28	25	0.108	0.230	90	2.71	-0.553	0.065	-0.095	-0.184	-0.110	0.176

F.2 - Define Cutting Width

In order to analyze the combination angle for the furrow width, both Table F-1 and Table F-2 are used. The combination disc and tilt angle can be generated as follow

$$w(\alpha,\beta) = (A + B\alpha) + (C + D\alpha)\left(\frac{\beta}{25}\right)^2 \qquad (F.6)$$

For d=3in, substitute $\alpha = 0$ and $\beta = 0$ in equation $(F.6)$, then

$$w(0,0) = A = 0 \qquad (F.7)$$

For d=3in, substitute $\alpha = 0$ and $\beta = 25$ in equation $(F.6)$, then

$$w(0,25) = A + C = 0 \qquad (F.8)$$

For d=3in, substitute $\alpha = 28$ and $\beta = 0$ in equation $(F.6)$, then

$$w(28,0) = A + 28B = 0.161 \qquad (F.9)$$

For d=3in, substitute $\alpha = 28$ and $\beta = 25$ in equation $(F.6)$, then

$$w(28,25) = A + 28B + C + 28D = 0.176 \qquad (F.10)$$

Combined equation $(F.7)$, $(F.8)$, $(F.9)$, and $(F.10)$, then

$$\begin{cases} A = 0 \\ B = 0.00573 \\ C = 0 \\ D = 0.000560 \end{cases} \qquad (F.11)$$

Then, the combination of disc and tilt angle with depth of 3in (0.0762m) of the furrow width equation is

$$w(\alpha,\beta) = 0.00573\alpha + 0.000560\alpha\left(\frac{\beta}{25}\right)^2 \qquad (F.12)$$

The equation for interpret the depth in term of the furrow width while using $\alpha = 0$ and $\beta = 0$ is showing as follow

$$w(\alpha, \beta, d) = a + bd \qquad (F.13)$$

For d=2in=0.0508m

$$w(28, 25, 0.0508) = a + b(0.0508) = 0.151 \qquad (F.14)$$

For d=3in=0.0762m

$$w(28, 25, 0.0762) = a + b(0.0762) = 0.176 \qquad (F.15)$$

Combined equation $(F.14)$ and $(F.15)$, then

$$\begin{cases} a = 0.100 \\ b = 0.995 \end{cases} \qquad (F.16)$$

Substitute equation $(F.16)$ to equation $(F.13)$, we get

$$w(\alpha, \beta, d) = 0.100 + 0.995d \qquad (F.17)$$

The combination of disc and tilt angle for the furrow width is as follow

$$w(\alpha, \beta, d) = \left(0.00573 + 0.000560\left(\frac{\beta}{25}\right)^2\right)\alpha\left(\frac{0.100 + 0.995d}{0.176}\right) \qquad (F.18)$$

Moreover, the tilt angle is showing as follow

$$\alpha = \frac{w}{\left(0.00573 + 0.000560\left(\frac{\beta}{25}\right)^2\right)\left(\frac{0.100 + 0.995d}{0.176}\right)} \qquad (F.19)$$

Check the furrow with by using equation $(F.18)$

Angles: $\alpha = 28°, \beta = 25°$

Depth: $d = 3in = 0.0762m$

Recall equation $(F.18)$ showing as follow

$$w(\alpha, \beta, d) = \left(0.00573 + 0.000560\left(\frac{25}{25}\right)^2\right)(28)\left(\frac{0.100 + 0.995(0.0762)}{0.176}\right) \qquad (F.19)$$

By using equation $(F.19)$ we get

$$w(\alpha, \beta, d) = 0.176m \qquad (F.20)$$

The defined furrow width is compared with the original furrow width

$$\%error = \frac{Original - Defining}{Original} = \frac{0.176 - 0.176}{0.176} = 0\% \qquad (F.21)$$

Since the error is within a reasonable range, the furrow width w is verified with the experimental data.

Appendix G–Cutting Force

G.1 - Plot the Cutting Force

The formula for cutting force in terms of disc angle can be generated by using the average of the maximum and minimum cutting force for each disc angle. Figure G-1 showed the increased cutting force increased disc angle with depth at 3in (0.0762m) and speed at 3mph. It also showed increased cutting force increased tilt angle with depth at 3in (0.0762m) and speed at 3mph.

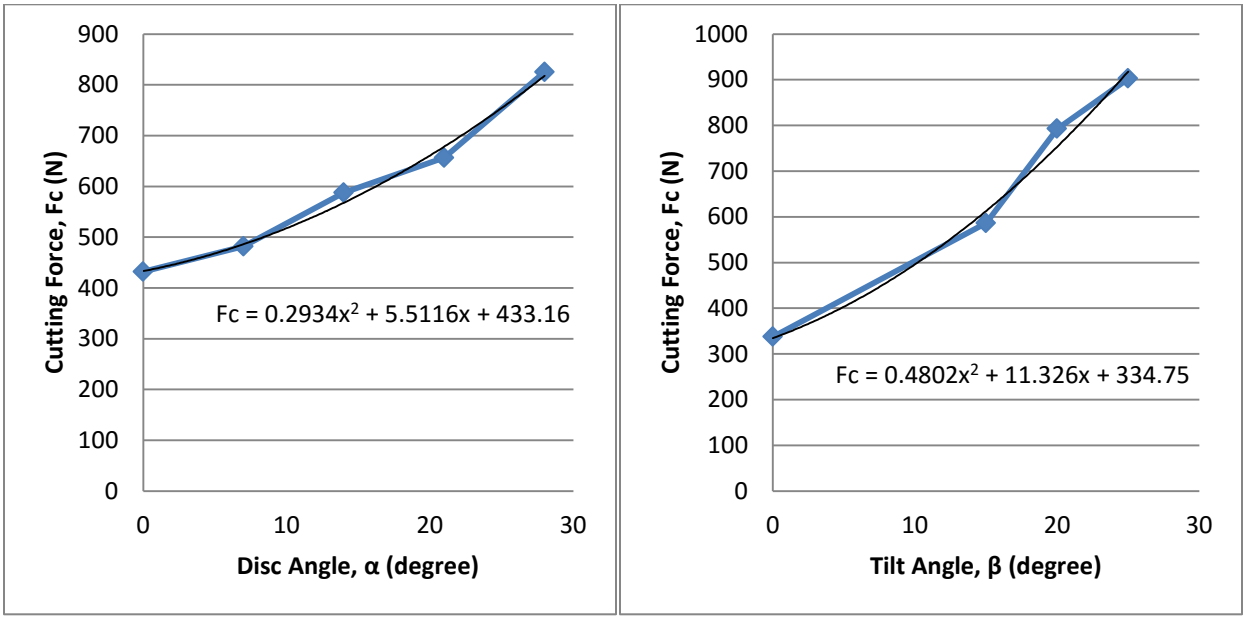

Figure G- 1: Cutting Force, Fc, with Depth=3in (0.762m) Speed=3mph

$$F_c(\alpha) = 0.293\alpha^2 + 5.51\alpha + 433 \qquad (G.1)$$

$$F_c(\beta) = 0.480\beta^2 + 11.3\beta + 335 \qquad (G.2)$$

The formula for cutting force in terms of disc angle can be generated by using the average of the maximum and minimum cutting force for each disc angle. Figure G-2 showed the

increased cutting force increased disc angle with depth at 2in (0.0508m) and speed at 5mph. It also showed increased cutting force increased tilt angle with depth at 2in (0.0508m) and speed at 5mph.

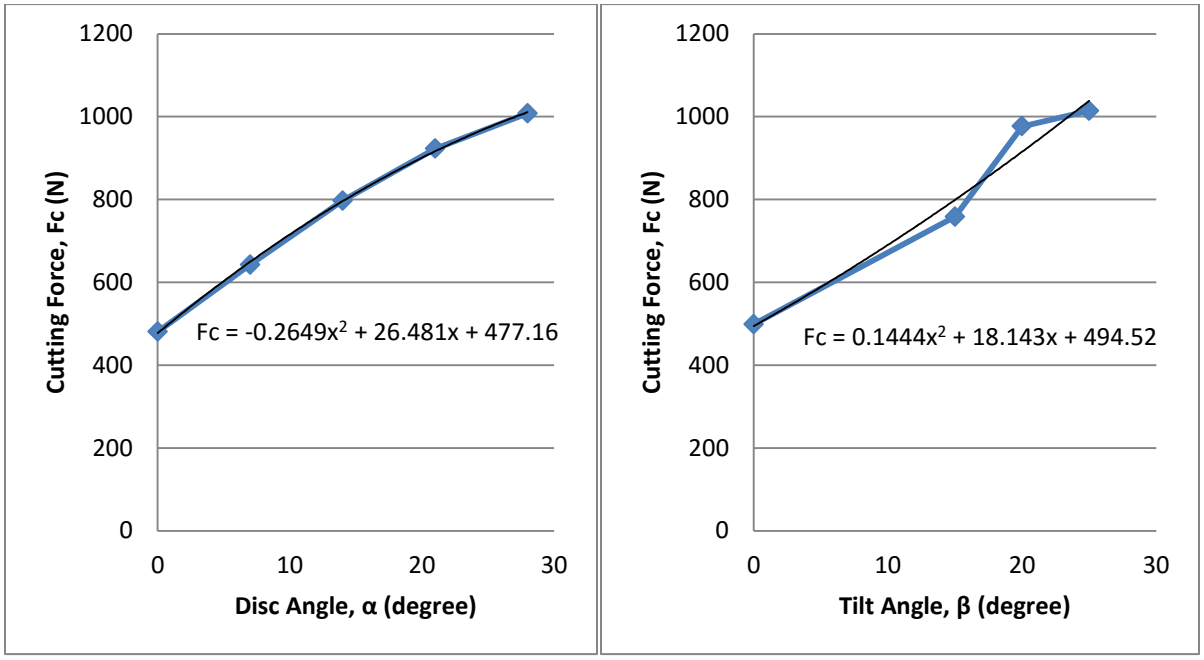

Figure G- 2: Cutting Force, Fc, with Depth=2in (0.0508m) Speed=5mph

$$F_c(\alpha) = -0.265\alpha^2 + 26.5\alpha + 477 \qquad (G.3)$$

$$F_c(\beta) = 0.144\beta^2 + 18.1\beta + 495 \qquad (G.4)$$

The formula for cutting force in terms of disc angle can be generated by using the average of the maximum and minimum cutting force for each disc angle. Figure G-3 showed the increased cutting force increased disc angle with depth at 3in (0.0762m) and speed at 5mph. It also showed increased cutting force increased tilt angle with depth at 3in (0.0762m) and speed at 5mph.

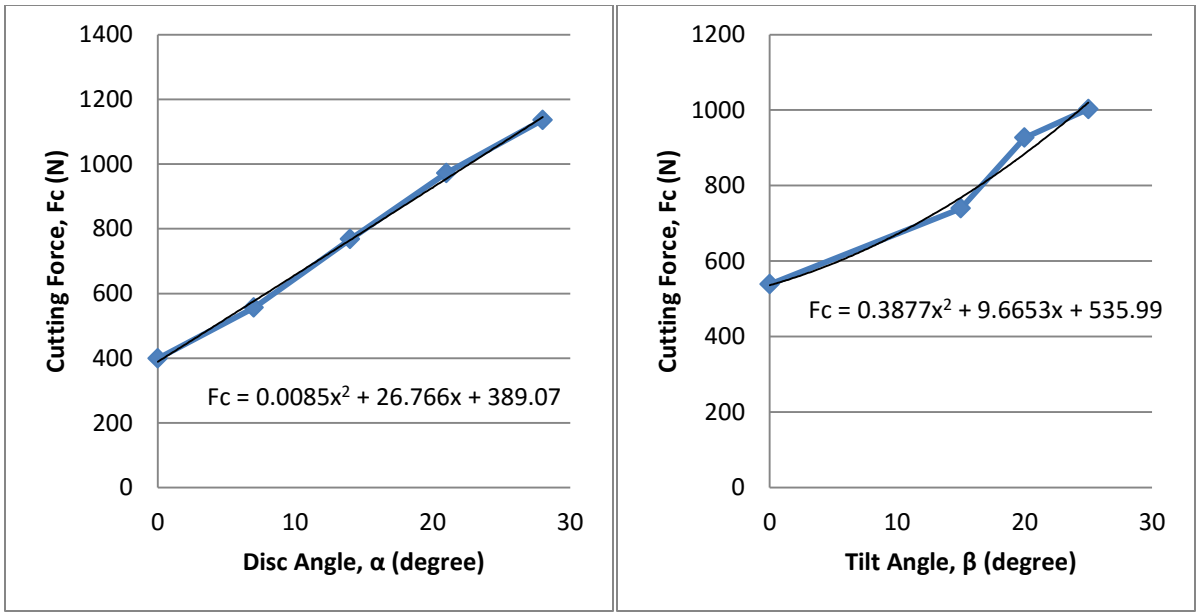

Figure G- 3: Cutting Force, Fc, with Depth=3in (0.0762m) Speed=5mph

$$F_c(\alpha) = 0.00850\alpha^2 + 26.8\alpha + 389 \qquad (G.5)$$

$$F_c(\beta) = 0.388\beta^2 + 9.67\beta + 536 \qquad (G.6)$$

G.2 - Defining Cutting Force

In order to analyze the combination angle for the cutting force, both Figure 5.7 and Figure 4.17 are used. The cutting force chosen for the certain combination disc and tilt angle from Figure 4.17 is the average of the cutting force at that particular combination disc and tilt angle. The combination disc and tilt angle can be generated as follows

$$F_c(\alpha,\beta) = \left(A + B\beta + C\beta^2\right) + \left(D + E\beta + F\beta^2\right)\left(\frac{\alpha}{28}\right) + \left(G + H\beta + I\beta^2\right)\left(\frac{\alpha}{28}\right)^2 \qquad (G.7)$$

The calculation for the combination disc and tilt angle with depth of 3in (0.0762m) and speed of 3mph is showing as follows

Substitute $\alpha = 0$ and $\beta = 0$ in equation $(G.7)$

$$F_c(0,0) = A = 282 \qquad (G.8)$$

Substitute $\alpha = 0$ and $\beta = 15$ in equation $(G.7)$

$$F_c(0,15) = A + 15B + 225C = 371 \qquad (G.9)$$

Substitute $\alpha = 0$ and $\beta = 25$ in equation $(G.7)$

$$F_c(0,25) = A + 25B + 625C = 568 \qquad (G.10)$$

Substitute $\alpha = 14$ and $\beta = 0$ in equation $(G.7)$

$$F_c(14,0) = A + \frac{1}{2}D + \frac{1}{4}G = 292 \qquad (G.11)$$

Substitute $\alpha = 28$ and $\beta = 0$ in equation $(G.7)$

$$F_c(28,0) = A + D + G = 403 \qquad (G.12)$$

Substitute $\alpha = 14$ and $\beta = 15$ in equation $(G.7)$

$$F_c(14,15) = (A + 15B + 225C) + \frac{1}{2}(D + 15E + 225F) + \frac{1}{4}(G + 15H + 225I)$$

$$= 636 \qquad (G.13)$$

Substitute $\alpha = 14$ and $\beta = 25$ in equation $(G.7)$

$$F_c(14,15) = (A + 25B + 625C) + \frac{1}{2}(D + 25E + 625F) + \frac{1}{4}(G + 25H + 625I)$$

$$= 862 \qquad (G.14)$$

Substitute $\alpha = 28$ and $\beta = 15$ in equation $(G.7)$

$$F_c(28,15) = (A + 15B + 225C) + (D + 15E + 225F) + (G + 15H + 225I)$$

$$= 824 \qquad (G.15)$$

Substitute $\alpha = 28$ and $\beta = 25$ in equation $(G.7)$

$$F_c(28,25) = (A + 25B + 625C) + (D + 25E + 625F) + (G + 25H + 625I)$$
$$= 1260 \qquad (G.16)$$

The equation $(G.7)$ is solved as follows

$$\begin{cases} A = 282 \\ B = -2.29 \\ C = 0.549 \\ D = -80.2 \\ E = 80.6 \\ F = -2.32 \\ G = 201 \\ H = -59.5 \\ I = 2.39 \end{cases} \qquad (G.17)$$

Then, the combination of disc and tilt angle with depth of 3in (0.0762m) and speed of 3mph of the cutting force equation is

$$F_c(\alpha,\beta) = \left(282 - 2.29\beta + 0.549\beta^2\right) + \left(-80.2 + 80.6\beta - 2.32\beta^2\right)\left(\frac{\alpha}{28}\right)$$
$$+ \left(201 - 59.5\beta + 2.39\beta^2\right)\left(\frac{\alpha}{28}\right)^2 \qquad (G.18)$$

The equation for interpret the depth in term of the cutting force while using $\alpha = 25$ and $\beta = 28$ is showing as follows

$$F_c(\alpha,\beta,d) = a + bd \qquad (G.19)$$

For d=2in=0.0508m

$$F_c(25,28,0.0508) = a + b(0.0508) = 1050 \qquad (G.20)$$

For d=3in=0.0762m

$$F_c(25, 28, 0.0762) = a + b(0.0762) = 1260 \qquad (G.21)$$

Combined equation $(G.20)$and $(G.21)$, then

$$\begin{cases} a = 626 \\ b = 8340 \end{cases} \qquad (G.22)$$

Then,

$$F_c(\alpha, \beta, d) = 626 + 8340d \qquad (G.23)$$

Then, the combination of disc and tilt angle with speed of 3mph for the cutting force equation is

$$F_c(\alpha, \beta, d) = \left(\left(282 - 2.29\beta + 0.549\beta^2\right) + \left(-80.2 + 80.6\beta - 2.32\beta^2\right)\left(\frac{\alpha}{28}\right) + \left(201 - 59.5\beta + 2.39\beta^2\right)\left(\frac{\alpha}{28}\right)^2 \right)\left(\frac{626 + 8340d}{1260}\right) \qquad (G.24)$$

Check the cutting force with speed of 3mph by using equation $(G.24)$

Angles: $\alpha = 28°, \beta = 25°$

Depth: $d = 3in = 0.0762m$

Recall equation $(G.24)$ showing as follow

$$F_c(\alpha, \beta, d) = \left(\left(282 - 2.29(25) + 0.549(25)^2\right) + \left(-80.2 + 80.6(25) - 2.32(25)^2\right)\left(\frac{28}{28}\right) + \left(201 - 59.5(25) + 2.39(25)^2\right)\left(\frac{28}{28}\right)^2 \right)\left(\frac{626 + 8340(0.0762)}{1260}\right) \qquad (G.25)$$

By using equation $(G.25)$we get

$$F_c(\alpha, \beta, d) = 1260N \qquad (G.26)$$

The defined cutting force is compared with the original cutting force

$$\%error = \frac{Original - Defining}{Original} = \frac{1260 - 1260}{1260} = 0\% \qquad (G.27)$$

Since the error is within a reasonable range, the cutting force F_c with speed of 3mph is verified with the experimental data.

Similarly, the calculation for the combination disc and tilt angle with depth of 3in (0.0762m) and speed of 5mph is showing as follows

$$\begin{cases} A = 320 \\ B = 5.02 \\ C = 0.0476 \\ D = 370 \\ E = 20.1 \\ F = -0.114 \\ G = 58.5 \\ H = -23.0 \\ I = 1.23 \end{cases} \qquad (G.28)$$

The combination of disc and tilt angle with depth of 3in (0.0762m) and speed of 5mph of the cutting force equation is showing as follows

$$F_c(\alpha, \beta) = \left(320 + 5.02\beta + 0.0476\beta^2\right) + \left(370 + 20.1\beta - 0.114\beta^2\right)\left(\frac{\alpha}{28}\right) + \left(58.5 - 23.0\beta + 1.23\beta^2\right)\left(\frac{\alpha}{28}\right)^2 \qquad (G.29)$$

The equation for interpret the depth in term of the cutting force while using $\alpha = 25$ and $\beta = 28$ is showing as follows

$$F_c(\alpha, \beta, d) = a + bd \qquad (G.30)$$

For d=2in=0.0508m

$$F_c(28, 25, 0.0508) = a + b(0.0508) = 1420 \qquad (G.31)$$

For d=3in=0.0762m

$$F_c(28, 25, 0.0762) = a + b(0.0762) = 1530 \qquad (G.32)$$

Combined equation $(G.31)$ and $(G.32)$, then

$$\begin{cases} a = 1200 \\ b = 4310 \end{cases} \qquad (G.33)$$

Then,

$$F_c(\alpha, \beta, d) = 1200 + 4310d \qquad (G.34)$$

Then, the combination of disc and tilt angle with speed of 5mph of the cutting force equation is

$$F_c(\alpha, \beta, d) = \left(\left(320 + 5.02\beta + 0.0476\beta^2\right) + \left(370 + 20.1\beta - 0.114\beta^2\right)\left(\frac{\alpha}{28}\right) + \left(58.5 - 23.0\beta + 1.23\beta^2\right)\left(\frac{\alpha}{28}\right)^2 \right)\left(\frac{1200 + 4310d}{1530}\right) \qquad (G.35)$$

Check the cutting force with speed of 5mph by using equation $(G.35)$

Angles: $\alpha = 28°, \beta = 25°$

Depth: $d = 3in = 0.0762m$

Recall equation $(G.35)$ showing as follow

$$F_c(\alpha,\beta,d) = \Bigg(\left(320 + 5.02(25) + 0.0476(25)^2\right) + \left(370 + 20.1(25) - 0.114(25)^2\right)\left(\frac{28}{28}\right) + \left(58.5 - 23.0(25) + 1.23(25)^2\right)\left(\frac{28}{28}\right)^2 \Bigg)\left(\frac{1200 + 4310(0.0762)}{1530}\right) \quad (G.36)$$

By using equation $(G.36)$ we get

$$F_c(\alpha,\beta,d) = 1530N \quad (G.37)$$

The defined cutting force is compared with the original cutting force

$$\%error = \frac{Original - Defining}{Defining} = \frac{1530 - 1530}{1530} = 0\% \quad (G.38)$$

Since the error is within a reasonable range, the cutting force F_c with speed of 5mph is verified with the experimental data.

Appendix H–Normal Force

H.1 - Plot the Normal Force

The formula for normal force in terms of disc angle can be generated from the experimental data by using the average of the normal force for each disc angle. The data in Figure H-1 shows the normal force increases as disc angle increases for depth of 3in (0.0763m) and speed of 3mph. It also showed a trend of decreasing normal force for increasing tilt angle for depth of 3in (0.0762m) and speed of 3mph.

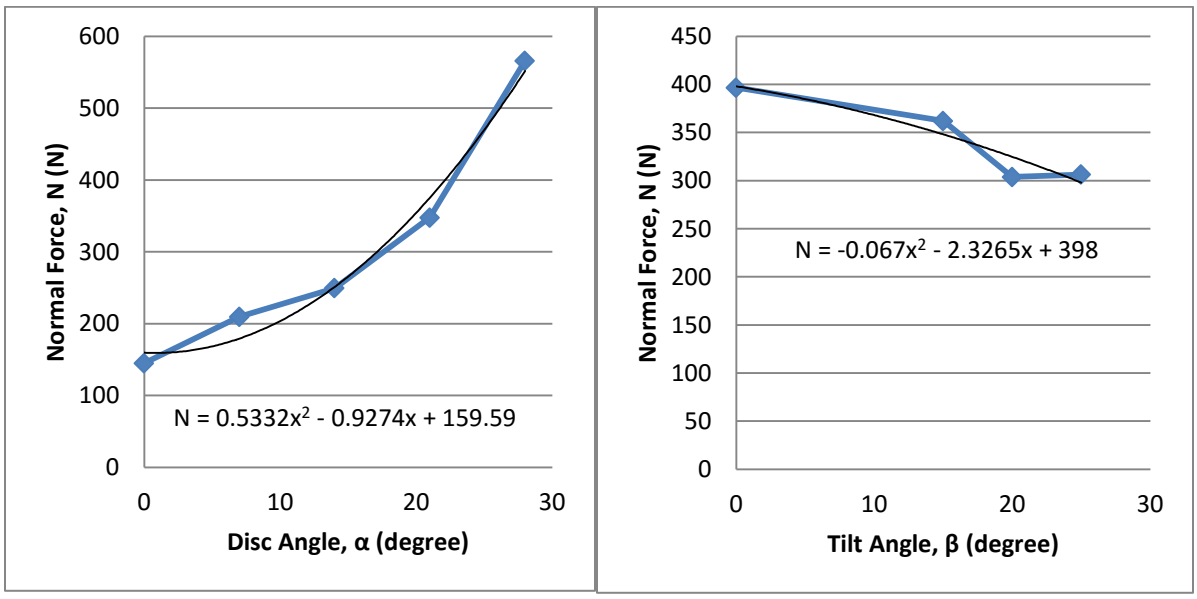

Figure H- 1: Normal Force, Fc, with Depth=3in (0.0762m) Speed=3mph

$$N(\alpha) = 0.533\alpha^2 - 0.927\alpha + 160 \qquad (H.1)$$

$$N(\beta) = -0.0670\beta^2 - 2.33\beta + 398 \qquad (H.2)$$

The empirical formula for normal force in terms of disc angle is generated the same way. Figure H-2 shows the normal force increases as disc angle increases for depth of 2in (0.0508m) and speed of 5mph. The formula for normal force in terms of tilt angle is also generated the same

way. It showed normal force decreases as tilt angle increases for depth of 2in (0.0508m) and speed of 5mph.

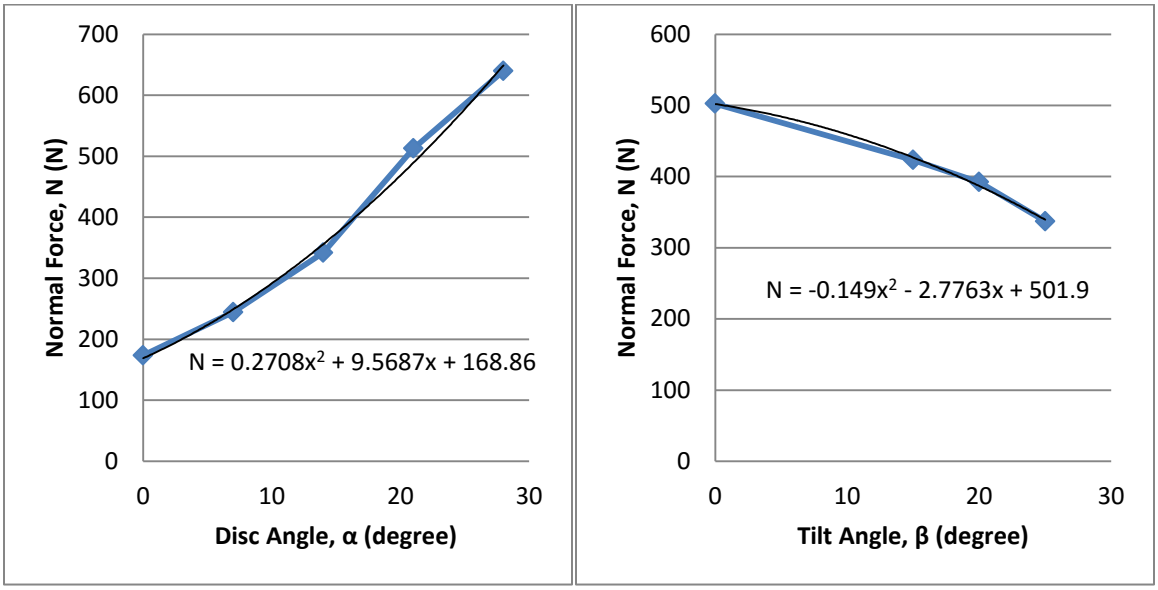

Figure H- 2: Normal Force, Fc, with Depth=2in (0.0508m) Speed=5mph

$$N(\alpha) = 0.271\alpha^2 + 9.57\alpha + 169 \qquad (H.3)$$

$$N(\beta) = -0.149\beta^2 - 2.78\beta + 502 \qquad (H.4)$$

The empirical formula for normal force is generated in the same manner as previous formulas. Figure H-3 shows the normal force increases with increased disc angle for depth of 3in (0.0762m) and speed of 5mph. It also showed that decreased normal force for increasing tilt angle for depth of 3in (0.0762m) and speed of 5mph.

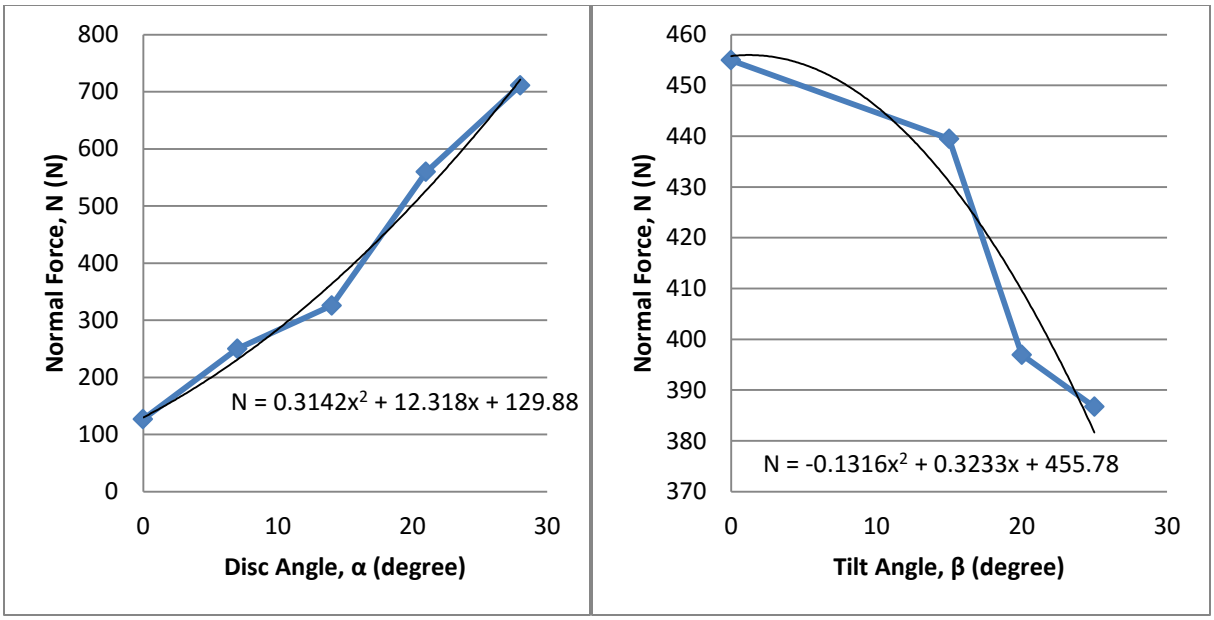

Figure H- 3: Normal Force, Fc, with Depth=3in (0.0762m) Speed=3mph

$$N(\alpha) = 0.314\alpha^2 + 12.3\alpha + 130 \qquad (H.5)$$

$$N(\beta) = -0.132\beta^2 + 0.323\beta + 456 \qquad (H.6)$$

H.2 - Defining Normal Force

In order to analyze the combination of disc and tilt angle for normal force (Figure 5.9 and Figure 4.19), the combination of disc and tilt angle can be generated by using equation (H.7). The normal force chosen for the certain combination of disc and tilt angles from Figure 4.19 is the average of the normal force at that particular combination disc and tilt angle.

$$N(\alpha,\beta) = \left(A + B\beta + C\beta^2\right) + \left(D + E\beta + F\beta^2\right)\left(\frac{\alpha}{28}\right) + \left(G + H\beta + I\beta^2\right)\left(\frac{\alpha}{28}\right)^2 \qquad (H.7)$$

The combination of disc and tilt angle with depth of 3in (0.0762m) and speed of 3mph for the normal force equation is showing as follows

Substitute $\alpha = 0$ and $\beta = 0$ in equation $(H.7)$

$$N(0,0) = A = 182 \qquad (H.8)$$

Substitute $\alpha = 0$ and $\beta = 15$ in equation $(H.7)$

$$N(0,15) = A + 15B + 225C = 244 \qquad (H.9)$$

Substitute $\alpha = 0$ and $\beta = 25$ in equation $(H.7)$

$$N(0,25) = A + 25B + 625C = 101 \qquad (H.10)$$

Substitute $\alpha = 14$ and $\beta = 0$ in equation $(H.7)$

$$N(14,0) = A + \frac{1}{2}D + \frac{1}{4}G = 377 \qquad (H.11)$$

Substitute $\alpha = 28$ and $\beta = 0$ in equation $(H.7)$

$$N(28,0) = A + D + G = 597 \qquad (H.12)$$

Substitute $\alpha = 14$ and $\beta = 15$ in equation $(H.7)$

$$N(14,15) = (A + 15B + 225C) + \frac{1}{2}(D + 15E + 225F) + \frac{1}{4}(G + 15H + 225I)$$

$$= 356 \qquad (H.13)$$

Substitute $\alpha = 14$ and $\beta = 25$ in equation $(H.7)$

$$N(14,15) = (A + 25B + 625C) + \frac{1}{2}(D + 25E + 625F) + \frac{1}{4}(G + 25H + 625I)$$

$$= 136 \qquad (H.14)$$

Substitute $\alpha = 28$ and $\beta = 15$ in equation $(H.7)$

$$N(28,15) = (A + 15B + 225C) + (D + 15E + 225F) + (G + 15H + 225I)$$

$$= 509 \qquad (H.15)$$

Substitute $\alpha = 28$ and $\beta = 25$ in equation $(H.7)$

$$N(28,25) = (A + 25B + 625C) + (D + 25E + 625F) + (G + 25H + 625I)$$
$$= 511 \qquad (H.16)$$

The equation $(H.7)$ is solved as follows

$$\begin{cases} A = 182 \\ B = 15.2 \\ C = -0.738 \\ D = 365 \\ E = 7.76 \\ F = -1.32 \\ G = 49.5 \\ H = -32.5 \\ I = 2.30 \end{cases} \qquad (H.17)$$

Then, the combination disc and tilt angle depth of 3in (0.0762m) and speed of 3mph of the normal force equation is

$$N(\alpha,\beta) = \left(182 + 15.2\beta - 0.738\beta^2\right) + \left(365 + 7.76\beta - 1.32\beta^2\right)\left(\frac{\alpha}{28}\right)$$
$$+ \left(49.5 - 32.5\beta + 2.30\beta^2\right)\left(\frac{\alpha}{28}\right)^2 \qquad (H.18)$$

The equation for interpret the depth in term of the normal force while using $\alpha = 25$ and $\beta = 28$ is showing as follows

$$N(28,25,d) = a + bd \qquad (H.19)$$

For d=2in=0.0508m

$$N(28,25,0.0508) = a + b(0.0508) = 473 \qquad (H.20)$$

For d=3in=0.0762m

$$N(28, 25, 0.0762) = a + b(0.0762) = 511 \qquad (H.21)$$

Combined equation $(H.20)$ and $(H.21)$, then

$$\begin{cases} a = 398 \\ b = 1480 \end{cases} \qquad (H.22)$$

Then,

$$N(\alpha, \beta, d) = 398 + 1480d \qquad (H.23)$$

Then, the combination of disc and tilt angle with speed of 3mph of the normal force equation is

$$N(\alpha, \beta, d) = \left(\left(182 + 15.2\beta - 0.738\beta^2\right) + \left(365 + 7.76\beta - 1.32\beta^2\right)\left(\frac{\alpha}{28}\right) + \left(49.5 - 32.5\beta + 2.30\beta^2\right)\left(\frac{\alpha}{28}\right)^2 \right)\left(\frac{398 + 1480d}{511}\right) \qquad (H.24)$$

Check the cutting force with speed of 3mph by using equation $(H.24)$

Angles: $\alpha = 28°, \beta = 25°$

Depth: $d = 3in = 0.0762m$

Recall equation $(H.24)$ showing as follow

$$N(\alpha, \beta, d) = \left(\left(182 + 15.2(25) - 0.738(25)^2\right) + \left(365 + 7.76(25) - 1.32(25)^2\right)\left(\frac{28}{28}\right) + \left(49.5 - 32.5(25) + 2.30(25)^2\right)\left(\frac{28}{28}\right)^2 \right)\left(\frac{398 + 1480(0.0762)}{511}\right) \qquad (H.25)$$

By using equation $(H.25)$ we get

$$N(\alpha, \beta, d) = 509N \qquad (H.26)$$

The defined normal force is compared with the original normal force

$$\%error = \frac{Original - Defining}{Original} = \frac{511 - 509}{511} = 0.391\% \qquad (H.27)$$

Since the error is within a reasonable range, the Normal force N with speed of 3mph is verified with the experimental data.

Similarly, the combination of disc and tilt angle with depth of 3in (0.0762m) and speed of 5mph for the normal force equation is showing as follows

$$\begin{cases} A = 207 \\ B = 4.31 \\ C = -0.444 \\ D = 262 \\ E = 13.7 \\ F = -0.567 \\ G = 243 \\ H = -21.2 \\ I = 1.16 \end{cases} \qquad (H.28)$$

Then, the combination disc and tilt angle with depth of 3in (0.0762m) and speed of 5mph of the normal force equation is

$$N(\alpha, \beta) = \left(207 + 4.31\beta - 0.444\beta^2\right) + \left(262 + 13.7\beta - 0.567\beta^2\right)\left(\frac{\alpha}{28}\right) + \left(243 - 21.2\beta + 1.16\beta^2\right)\left(\frac{\alpha}{28}\right)^2 \qquad (H.29)$$

The equation for interpret the depth in term of the cutting force while using $\alpha = 25$ and $\beta = 28$ is showing as follows

$$N(\alpha, \beta, d) = a + bd \qquad (H.30)$$

For d=2in=0.0508m

$$N(28, 25, 0.0508) = a + b(0.0508) = 540 \qquad (H.31)$$

For d=3in=0.0762m

$$N(28, 25, 0.0762) = a + b(0.0762) = 728 \qquad (H.32)$$

Combined equation $(H.31)$and $(H.32)$, then

$$\begin{cases} a = 164 \\ b = 7410 \end{cases} \qquad (H.33)$$

Then,

$$N(\alpha, \beta, d) = 164 + 7410d \qquad (H.34)$$

Then, the combination of disc and tilt angle with speed of 5mph of the normal force equation is

$$N(\alpha, \beta, d) = \left(\left(207 + 4.31\beta - 0.444\beta^2\right) + \left(262 + 13.7\beta - 0.567\beta^2\right)\left(\frac{\alpha}{28}\right) + \left(243 - 21.2\beta + 1.16\beta^2\right)\left(\frac{\alpha}{28}\right)^2 \right)\left(\frac{164 + 7410d}{728}\right) \qquad (H.35)$$

Check the cutting force with speed of 5mph by using equation $(H.35)$

Angles: $\alpha = 28°, \beta = 25°$

Depth: $d = 3in = 0.0762m$

Recall equation $(H.35)$ showing as follow

$$N(\alpha,\beta,d)=\left(\left(207+4.31\beta-0.444\beta^2\right)+\left(262+13.7\beta-0.567\beta^2\right)\left(\frac{\alpha}{28}\right)\right.$$

$$\left.+\left(243-21.2\beta+1.16\beta^2\right)\left(\frac{\alpha}{28}\right)^2\right)\left(\frac{164+7410d}{728}\right) \qquad (H.36)$$

By using equation $(H.36)$ we get

$$N(\alpha,\beta,d)=726N \qquad (H.37)$$

The defined normal force is compared with the original normal force

$$\%error=\frac{Original-Defining}{Original}=\frac{728-726}{728}=0.275\% \qquad (H.38)$$

Since the error is within a reasonable range, the Normal force N with speed of 5mph is verified with the experimental data.

Appendix I - Frequency Test

The natural frequency of the disc is validated by a vibration test performed using a sensor on the disc shown in Figure I-1. An accelerometer (Figure I-1) is used to test the natural frequency for the disc in the air and also when the disc is in the soil. The accelerometer and equipment was selected to be in the correct range for proper measurement and calibrated. From the experimental test data, the natural frequency was determined for the disc coulter. The natural frequency was calculated in two ways. The natural frequency was calculated by using the code developed using a Matlab frequency analysis program. For the other method, the data from the accelerometer was plotted using a Matlab program which measured peak to peak response in order to double check the natural frequency calculation of the data analyzer. They were selected to insure the frequency response was correct for the application.

After recording the natural frequency data, the data was evaluated by using those two methods.

Figure I- 1: Accelerometer for the natural frequency test

I.1 - Method 1: Matlab code

The first method uses the Matlab code which invokes the Fast Fourier Transform (FFT) code to evaluate the natural frequency. The Fast Fourier Transform is a mathematical method for transforming a function in the time domain into a function in the frequency domain [45]. An example of the Matlab code evaluating the natural frequency is shown in Figure I-2.

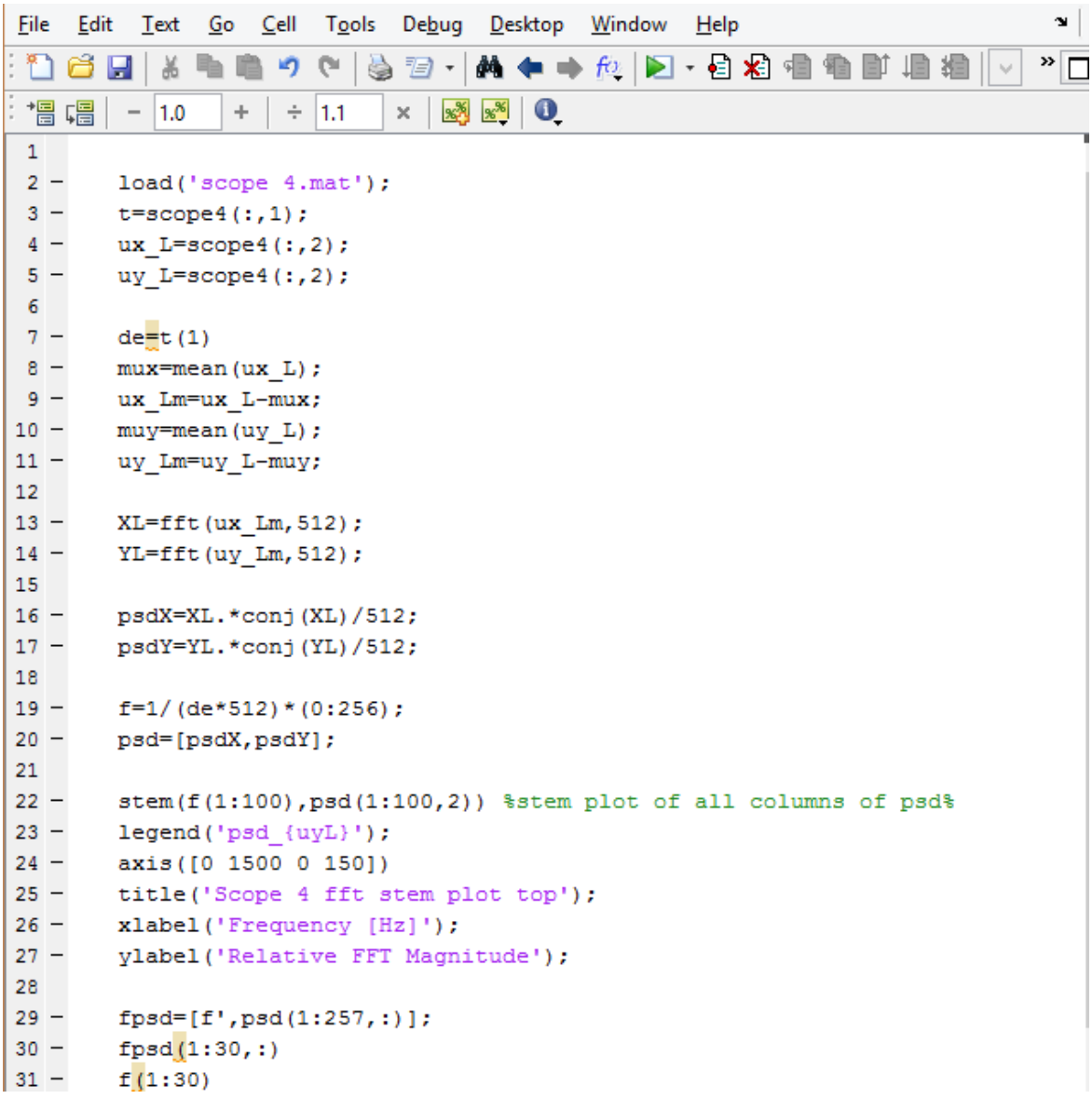


```
1
2 -     load('scope 4.mat');
3 -     t=scope4(:,1);
4 -     ux_L=scope4(:,2);
5 -     uy_L=scope4(:,2);
6
7 -     de=t(1)
8 -     mux=mean(ux_L);
9 -     ux_Lm=ux_L-mux;
10 -    muy=mean(uy_L);
11 -    uy_Lm=uy_L-muy;
12
13 -    XL=fft(ux_Lm,512);
14 -    YL=fft(uy_Lm,512);
15
16 -    psdX=XL.*conj(XL)/512;
17 -    psdY=YL.*conj(YL)/512;
18
19 -    f=1/(de*512)*(0:256);
20 -    psd=[psdX,psdY];
21
22 -    stem(f(1:100),psd(1:100,2)) %stem plot of all columns of psd%
23 -    legend('psd_{uyL}');
24 -    axis([0 1500 0 150])
25 -    title('Scope 4 fft stem plot top');
26 -    xlabel('Frequency [Hz]');
27 -    ylabel('Relative FFT Magnitude');
28
29 -    fpsd=[f',psd(1:257,:)];
30 -    fpsd(1:30,:)
31 -    f(1:30)
```

Figure I- 2: Matlab code for Scope 4

The plotted data from the Matlab code (Figure I-2) is shown in Figure I-3. For this particular example, the natural frequency for this plot is 78.1Hz.

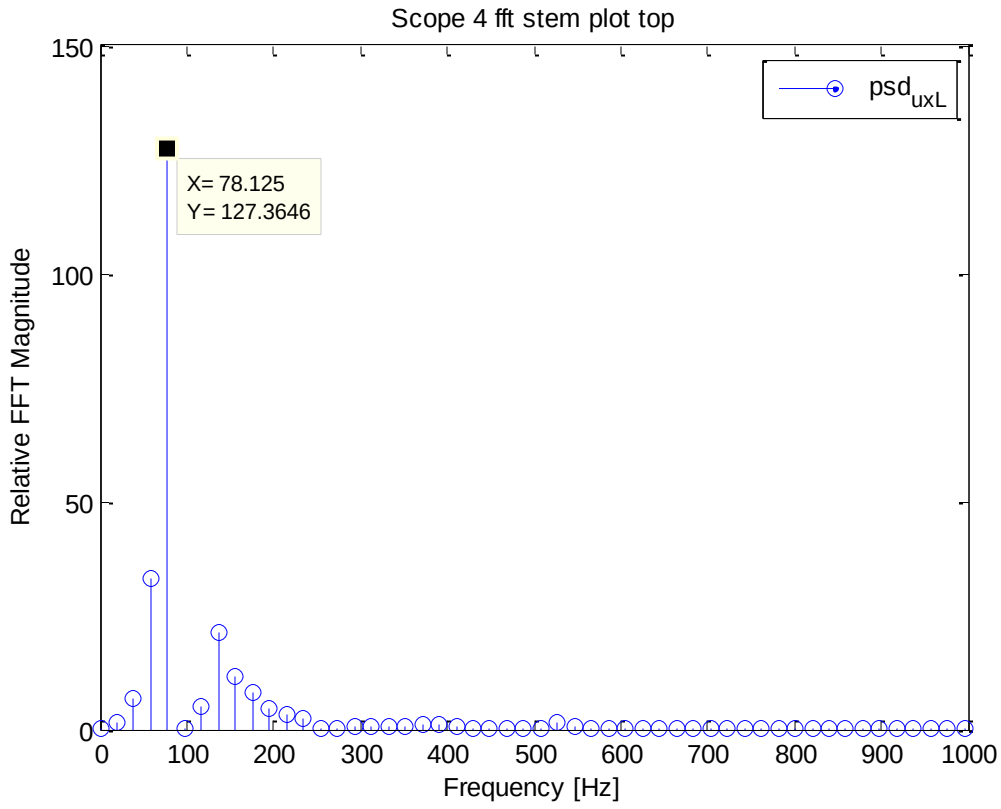

Figure I- 3: Plot of natural frequency for Scope 4

I.2 - Method 2: Matlab plot

The second method used incorporates the original data plotted in Matlab. The data from the accelerometer was plotted using a Matlab program which displays peak to peak response information. This can be used to double check the first Matlab program results. The natural frequency is the inverse of the period shown in equation (I.1). An example of the code is shown in Figure I-4.

$$natural\ frequency = \frac{1}{Period} = \frac{1}{X_1 - X_2} \qquad (I.1)$$

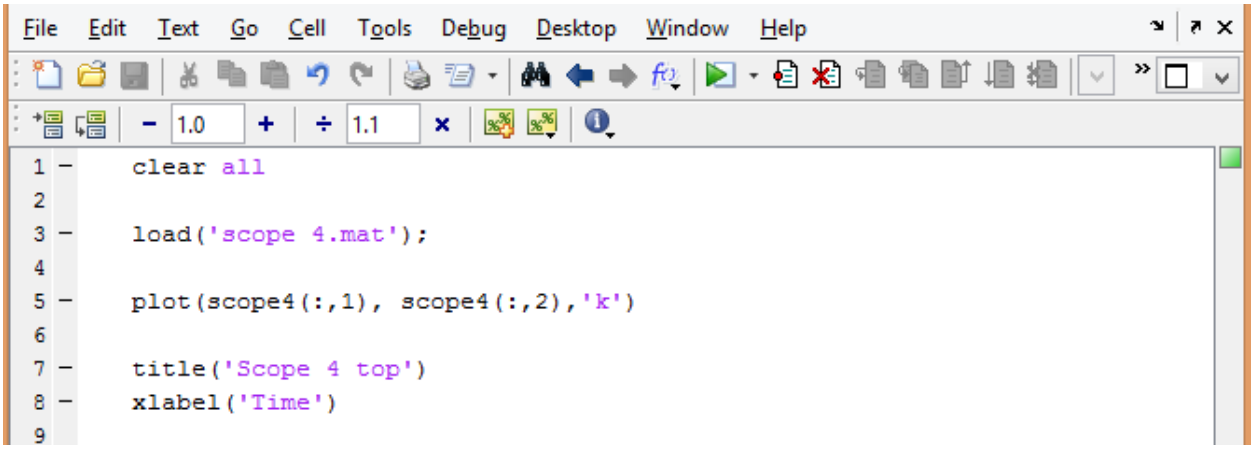

Figure I- 4: Matlab code for Scope 4 using the data

The Period is the horizontal distance between peak 1 and peak 2. The example for the plotted data is shown in Figure I-5. The natural frequency calculated by using equation (I.1) for this particular example is 78.7Hz.

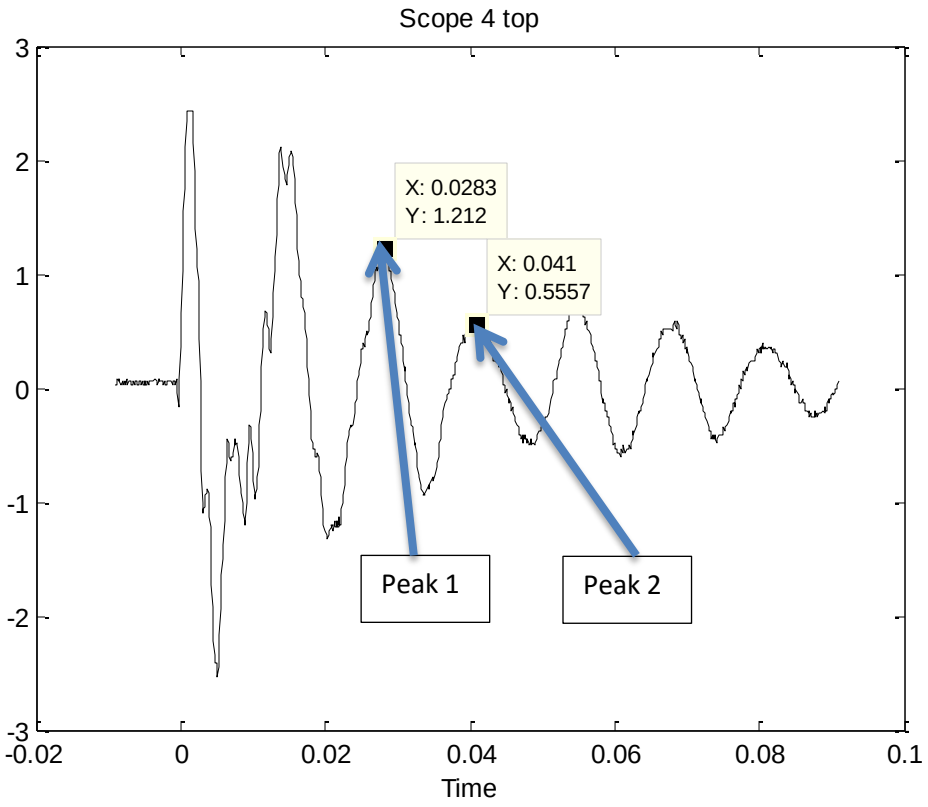

Figure I- 5: Plot for Scope 4 using the data

Table I-1 shows the result of the natural frequency of the disc. The natural frequency from the analyzer is 195Hz to 234Hz in the air and 78Hz to 98Hz in the soil. The Matlab program natural frequency result is 218Hz to 270Hz in the air and 77Hz to 79Hz in the soil. The values are within 20% of each other, which means the value for the natural frequency is within the reasonable range. With a natural frequency above 75Hz it is safe to assume that all effects of the disc vibration will be excluded from the data if the low pass filter is set to 2Hz. My fellow graduated PhD student Ahad Armin in his thesis (Page 93-98), Mechanics of soil-blade interaction, has proved that 2Hz filter is the most reasonable amount for soil-blade interaction [43]. With a similar analogy it can be shown that for the disc coulter, a 2-Hz filter is reasonable to exclude the noisy signals for soil-disc interactions.

Table I- 1: Results for natural frequency test

		Matlab						Accelerometer	% diff
Top		Peak 1		Peak 2		Period	Freq	Freq	
		x	y	x	y	T(s)	1/T(Hz)	1/T(Hz)	
scope	location	Second	Volt	Second	Volt			x	
0	air	0.008	0.135	0.012	0.160	0.004	270	234	14%
1	air	0.000	0.155	0.005	0.180	0.005	218	195	11%
2	air	0.008	0.193	0.013	0.180	0.004	233	234	-1%
3	air	0.005	0.993	0.009	1.087	0.004	237	195	19%
4	soil	0.028	1.212	0.041	0.556	0.013	79	78	1%
5	soil	0.002	0.637	0.015	0.497	0.013	77	98	-23%

Appendix J – Optimization

The simplest method to achieve optimization of the combination disc and tilt angle is to use the 1-D optimization Method. The best combination angle would provide the minimized draft force, F_z, with a reasonable furrow width, w. For 1-D Optimization, the equations are showing as follow

$$F_z = N cos\beta_r sin\alpha_r + F_c(cos\alpha_r sin\delta_r + sin\alpha_r sin\beta_r cos\delta_r) \quad (J.1)$$

The disc and tilt angle can be transferred from degree in radius

$$\beta_r = \frac{\pi}{180}\beta \ \ for\ 0 \le \beta \le 25° \quad (J.2)$$

$$\alpha_r = \frac{\pi}{180}\alpha \ \ for\ 0 \le \alpha \le 28° \quad (J.3)$$

Part of the equation (5.75) can be rearranged as follow

$$sin\alpha = \alpha_r\left(1 - \frac{{\alpha_r}^2}{6}\right) \quad (J.4)$$

$$sin\beta = \beta_r\left(1 - \frac{{\beta_r}^2}{6}\right) \quad (J.5)$$

$$cos\alpha = \left(1 - \frac{{\alpha_r}^2}{2}\right) \quad (J.6)$$

$$cos\beta = \left(1 - \frac{{\beta_r}^2}{2}\right) \quad (J.7)$$

Substitute equation (5.78), (5.79), (5.80), and (5.81) into equation (5.75), then

$$F_z = \left(1 - \frac{{\beta_r}^2}{2}\right)\alpha_r\left(1 - \frac{{\alpha_r}^2}{6}\right)N$$

$$+\left(\left(1 - \frac{{\alpha_r}^2}{2}\right)sin\delta_r + \alpha_r\left(1 - \frac{{\alpha_r}^2}{6}\right)\beta_r\left(1 - \frac{{\beta_r}^2}{6}\right)cos\delta_r\right)F_c \qquad (J.8)$$

J.1 - Result for Width=0.12m (Speed=3mph)

The code for speed of 3mph is shown in Figure J-1.

File Edit Text Go Cell Tools Debug Desktop Window Help

```
1
2 -   clear
3 -   clc
4 -   format short
5
6     % solve for draft force Fz
7 -   syms N Fc a b d w
8
9 -    d=3*0.0254;
10 -   w=0.12;
11
12 -  b = 25
13 -  b25 = b/25;
14
15    % a = 7
16 -  a = w/((0.00573+0.000560*(b25^2))*((0.100+0.995*d)/0.176))
17 -  a28 = a/28;
18
19 -  ar = a*pi()/180;
20 -  br = b*pi()/180;
21 -  delta = 24*pi()/180;
22
23    % speed = 3mph
24 -  Fc = ((282-2.29*b+0.549*b^2)+(-80.2+80.6*b-2.32*b^2)*a28+(201-59.5*b+2.39*b^2)*(a28^2))*((626+8340*d)/1260)
25
26 -  N = ((182+15.2*b-0.738*b^2)+(365+7.76*b-1.32*b^2)*a28+(49.5-32.5*b+2.30*b^2)*(a28^2))*((398+1480*d)/511)
27
28 -  Fz = N*cos(br)*sin(ar)+Fc*(cos(ar)*sin(delta)+sin(ar)*sin(br)*cos(delta))
29
```

Figure J- 1: Matlab Code for 1-D Optimization (Speed of 3mph)

For speed of 3mph, the draft force can be optimized as follow

$$\delta_r = \frac{24\pi}{180} \qquad (J.9)$$

$$\alpha = \frac{w}{\left(0.00573 + 0.000560\left(\frac{\beta}{25}\right)^2\right)\left(\frac{0.100 + 0.995d}{0.176}\right)} \qquad (J.10)$$

$$F_c(\alpha,\beta,d) = \left((282 - 2.29\beta + 0.549\beta^2) + (-80.2 + 80.6\beta - 2.32\beta^2)\left(\frac{\alpha}{28}\right) + (201 - 59.5\beta + 2.39\beta^2)\left(\frac{\alpha}{28}\right)^2\right)\left(\frac{626 + 8340d}{1260}\right) \qquad (J.11)$$

$$N(\alpha,\beta,d) = \left((182 + 15.2\beta - 0.738\beta^2) + (365 + 7.76\beta - 1.32\beta^2)\left(\frac{\alpha}{28}\right) + (49.5 - 32.5\beta + 2.30\beta^2)\left(\frac{\alpha}{28}\right)^2\right)\left(\frac{398 + 1480d}{511}\right) \qquad (J.12)$$

The δ angle is assumed constant ($\delta_{avg} = 24°$, detail is showing in Chapter 2) and the furrow width is assumed to be 0.12 m for defining the cutting force, normal force, and draft force with depth of 2in (0.0508m) and speed of 3mph. Table J-1 showed the disc angle α, cutting force F_c, normal force N, and the draft force F_z in term of tilt angle β.

Table J- 1: Combination of Disc and Tilt Angle for Depth=2in (0.0508m)

β	α	Fc	N	Fz
(deg)	(deg)	(N)	(N)	(N)
0	24	305	499	320
5	24	406	482	362
10	24	520	457	411
15	24	645	423	465
20	23	775	371	521
25	22	904	293	574
25	7	585	71	271

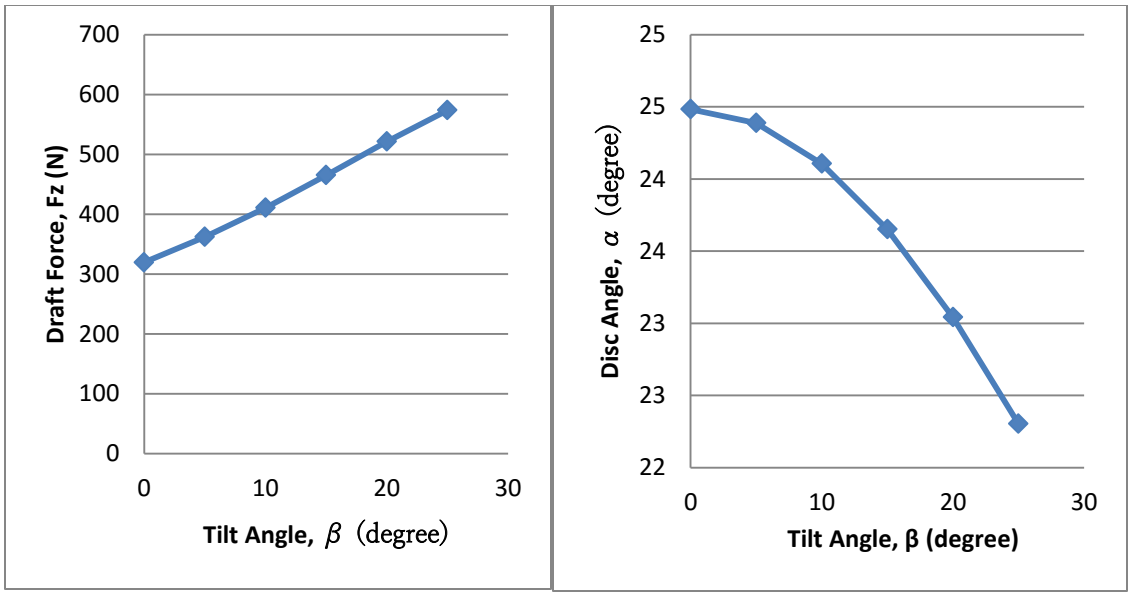

Figure J- 2: Draft Force, Fz, and Disc Angle, α, with Depth=2in (0.0508m) Speed=3mph

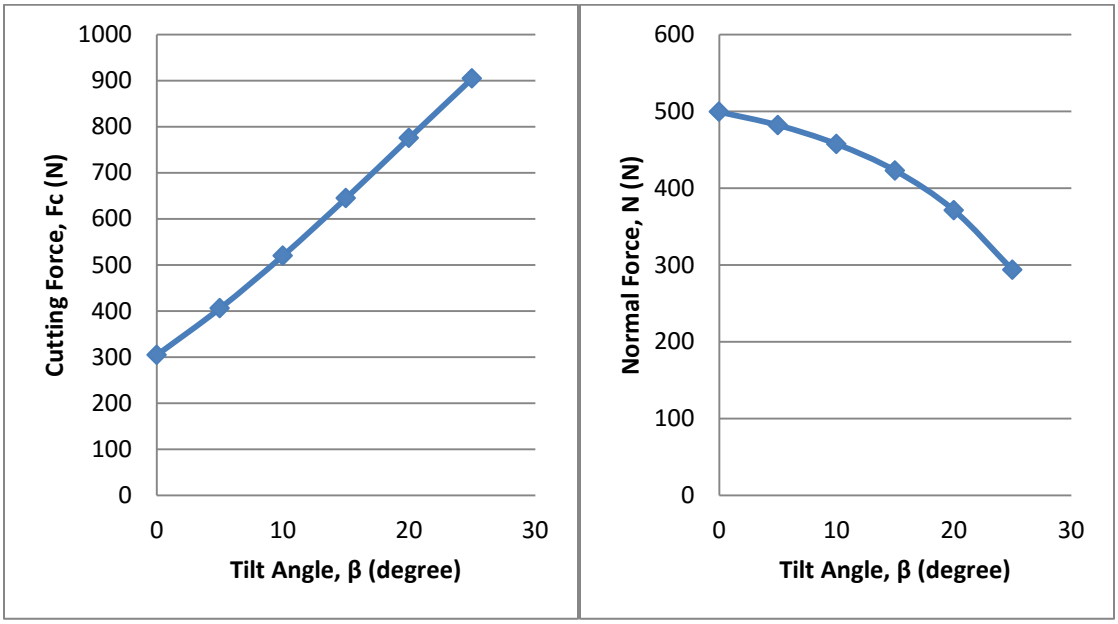

Figure J- 3: Cutting Force, Fc, and Normal Force, N, with Depth=2in (0.0508m) Speed=3mph

In Figure J-2, it showed that with a constant furrow width of 0.12m, increased of tilt angle would decrease the disc angle. Moreover, with the increased tilt angle the draft force

increased. In Figure J-3, it showed that the higher the tilt angle the higher the cutting force, the higher the tilt angle the lower the normal force. This also verified the experimental test data.

Similarly, the δ angle is assumed constant ($\delta_{avg} = 24°$) and furrow width is assumed to be 0.12 m for defining cutting force, normal force, and draft force with depth of 3in (0.0762m) and speed of 3mph. The disc angle α, cutting force F_c, normal force N, and the draft force F_z in term tilt angle β is showing in Table J-2.

Table J- 2: Combination of Disc and Tilt Angle for Depth=3in (0.0762m)

β	α	Fc	N	Fz
(deg)	(deg)	(N)	(N)	(N)
0	21	335	483	300
5	21	462	485	361
10	21	594	464	421
15	20	730	419	479
20	20	866	344	532
25	19	996	233	578
25	7	703	76	325

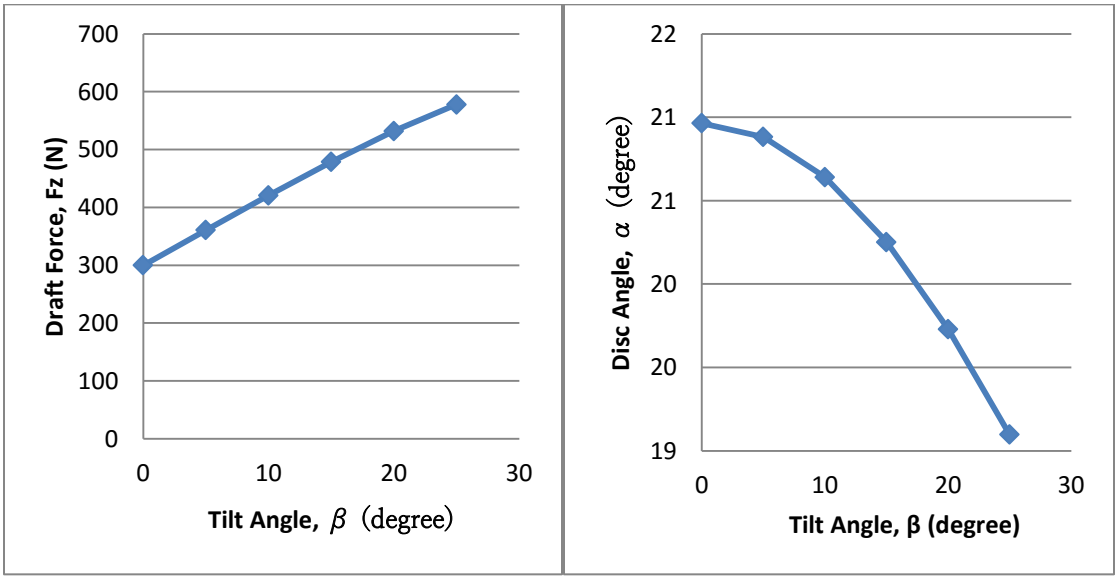

Figure J- 4: Draft Force, Fz, and Disc Angle, α, with Depth=3in (0.0762m) Speed=3mph

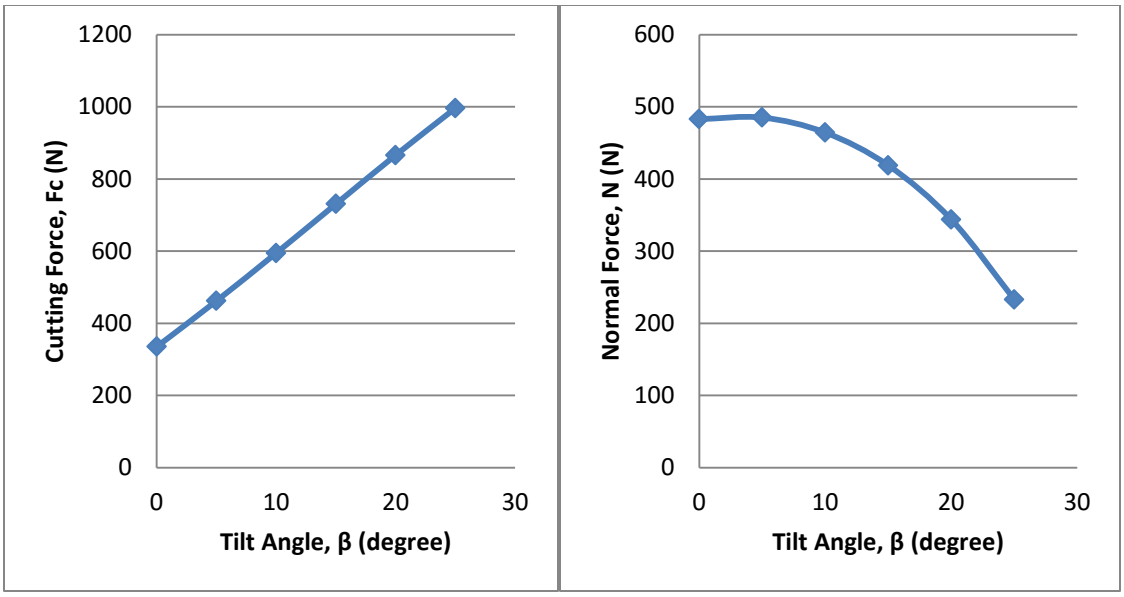

Figure J- 5: Cutting Force, Fc, and Normal Force, N, with Depth=3in (0.0762m) Speed=3mph

Figure J-4 showed that with a constant furrow width of 0.12m, increased of tilt angle would decrease the disc angle, while with the increased tilt angle the draft force increased. Figure J-5 showed that with a constant furrow width of 0.12m, increased of tilt angle would decrease the disc angle, while with the increased tilt angle the draft force increased.

Since the furrow width cannot be zero, that means both disc and tilt angle cannot be zero. Also, the disc angle, α, has to be within the range of $0 \leq \alpha \leq 28°$ and the tilt angle, β, has to be within the range of $0 \leq \beta \leq 25°$. Therefore, the best combination of the disc and tilt angle with speed of 3mph is

$$\alpha = 7° \qquad (J.13)$$

$$\beta = 28° \qquad (J.14)$$

J.2 - Result for Width=0.12m (Speed=5mph)

The code for speed of 5mph is shown in Figure J-6.

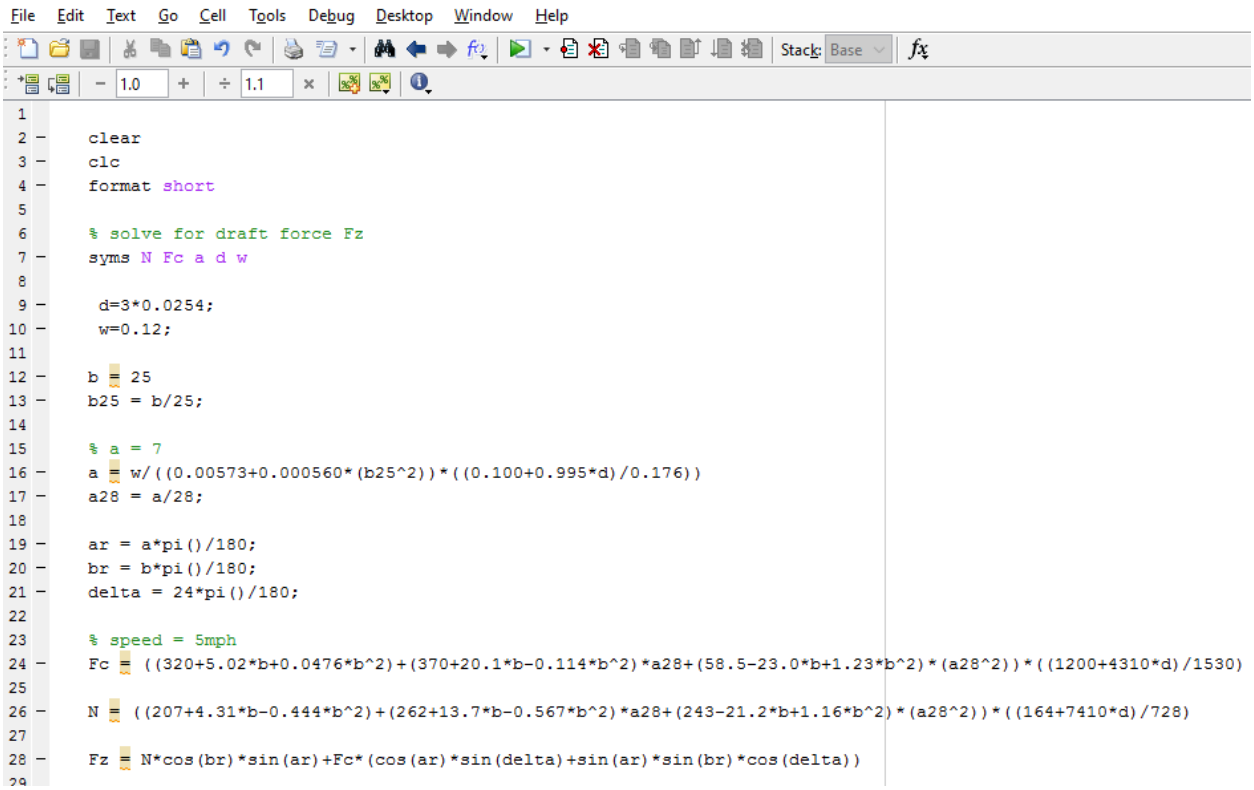

```
clear
clc
format short

% solve for draft force Fz
syms N Fc a d w

 d=3*0.0254;
 w=0.12;

b = 25
b25 = b/25;

% a = 7
a = w/((0.00573+0.000560*(b25^2))*((0.100+0.995*d)/0.176))
a28 = a/28;

ar = a*pi()/180;
br = b*pi()/180;
delta = 24*pi()/180;

% speed = 5mph
Fc = ((320+5.02*b+0.0476*b^2)+(370+20.1*b-0.114*b^2)*a28+(58.5-23.0*b+1.23*b^2)*(a28^2))*((1200+4310*d)/1530)

N = ((207+4.31*b-0.444*b^2)+(262+13.7*b-0.567*b^2)*a28+(243-21.2*b+1.16*b^2)*(a28^2))*((164+7410*d)/728)

Fz = N*cos(br)*sin(ar)+Fc*(cos(ar)*sin(delta)+sin(ar)*sin(br)*cos(delta))
```

Figure J- 6: Matlab Code for 1-D Optimization (Speed of 5mph)

For Speed is 5mph, the draft force can be optimized as follow

$$\delta_r = \frac{24\pi}{180} \qquad (J.15)$$

$$\alpha = \frac{w}{\left(0.00573 + 0.000560\left(\frac{\beta}{25}\right)^2\right)\left(\frac{0.100 + 0.995d}{0.176}\right)} \qquad (J.16)$$

$$F_c(\alpha,\beta,d) = \left((320 + 5.02\beta + 0.0476\beta^2) + (370 + 20.1\beta - 0.114\beta^2)\left(\frac{\alpha}{28}\right) + (58.5 - 23.0\beta + 1.23\beta^2)\left(\frac{\alpha}{28}\right)^2\right)\left(\frac{1200 + 4310d}{1530}\right) \quad (J.17)$$

$$N(\alpha,\beta,d) = \left((207 + 4.31\beta - 0.444\beta^2) + (262 + 13.7\beta - 0.567\beta^2)\left(\frac{\alpha}{28}\right) + (243 - 21.2\beta + 1.16\beta^2)\left(\frac{\alpha}{28}\right)^2\right)\left(\frac{164 + 7410d}{728}\right) \quad (J.18)$$

Table J-3 shows the tilt angle β, cutting force F_c, normal force N, and the draft force F_z in term of disc angle α with depth of 2in and speed of 5mph. The δ angle is assumed constant ($\delta_{avg} = 24°$, detail is showing in Chapter 2) and the furrow width is assumed to be 0.12 m for defining all forces.

Table J- 3: combination of disc and tilt angle for depth of 2in (0.0508m) and speed of 5mph

width	0.12m	delta	24deg	
depth	2in (0.0508m)	speed	5mph	
β	α	Fc	N	Fz
0	24	638	462	428
5	24	681	459	464
10	24	761	452	514
15	24	876	439	580
20	23	1019	417	659
25	22	1181	382	749
25	7	641	94	299

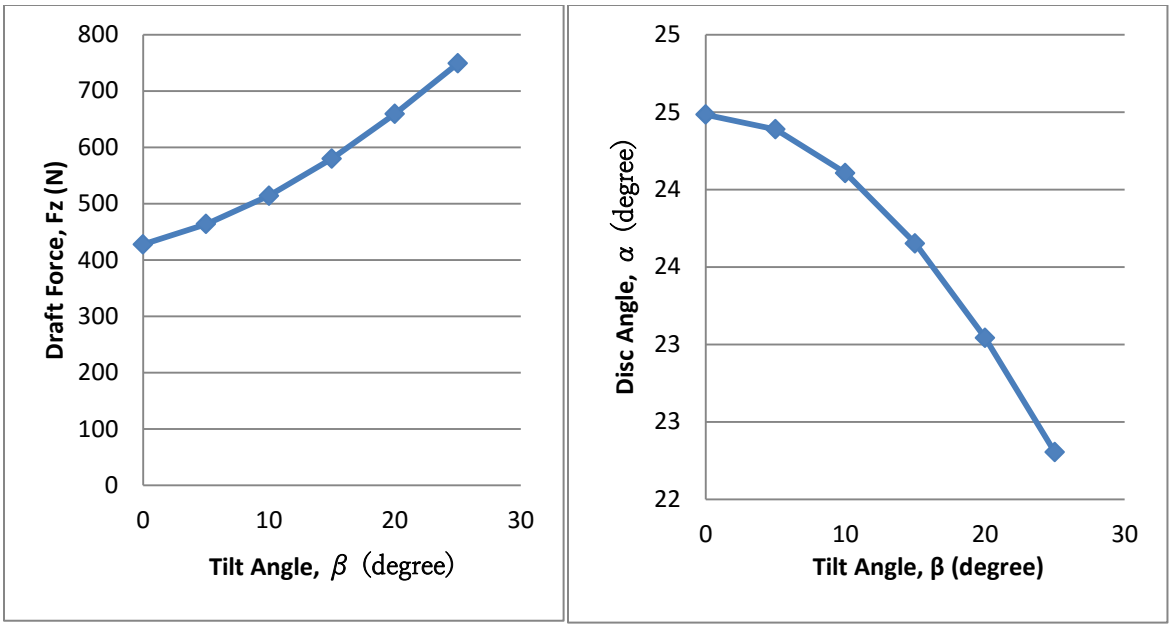

Figure J- 7: Draft Force, Fz, and Disc Angle, α, with Depth=2in (0.0508m) Speed=5mph

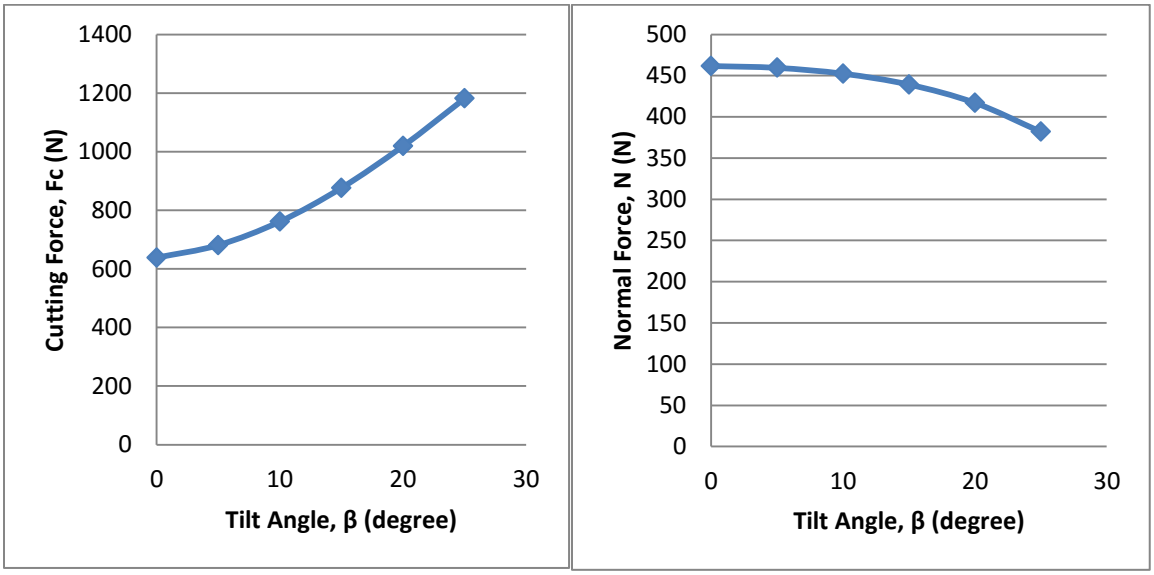

Figure J- 8: Cutting Force, Fc, and Normal Force, N, with Depth=2in (0.0508m) Speed=5mph

Figure J-7 also showed that the higher the tilt angle the higher the draft force. While the cutting width is a constant of 0.12m, the higher the tilt angle the lower the disc angle. In Figure

J-8, it showed that the higher the tilt angle the higher the cutting force; the higher the tilt angle the lower the normal force. This also verified the experimental test data.

The tilt angle β, cutting force F_c, normal force N, and the draft force F_z in term of disc angle α with depth of 2in and speed of 3mph showing in Table J-4. Similarly, the δ angle is assumed constant ($\delta_{avg} = 24°$) and furrow width is assumed to be 0.12 m for defining all the forces.

Table J- 4: combination of disc and tilt angle for depth of 3in (0.0762m) and speed of 5mph

width	0.12m	delta	24deg	
depth	3in (0.0762m)	speed	3mph	
β	α	Fc	N	Fz
0	21	629	540	432
5	21	680	546	472
10	21	760	538	519
15	20	867	515	574
20	20	995	474	636
25	19	1138	412	703
25	7	691	127	325

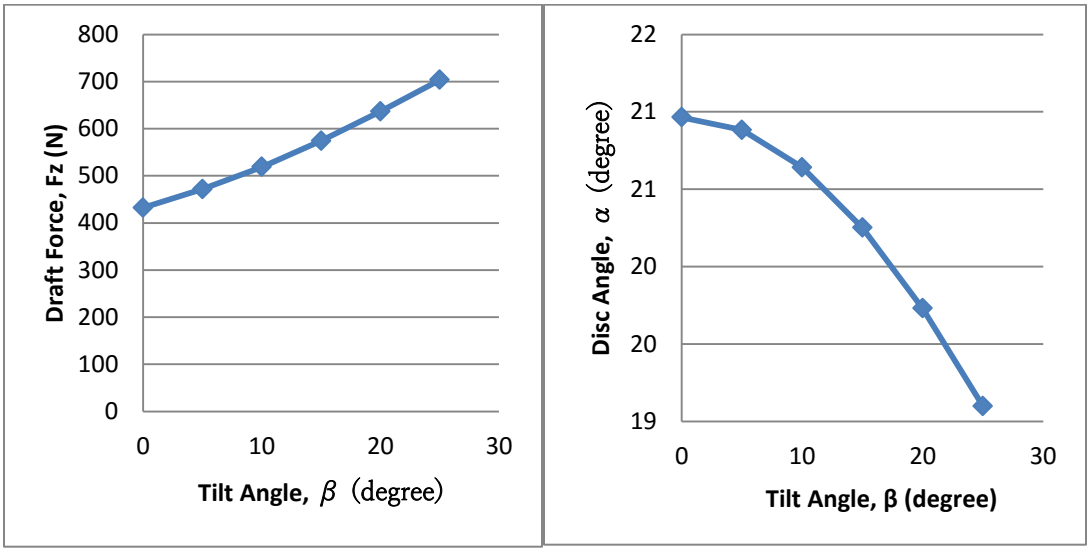

Figure J- 9: Draft Force, Fz, and Disc Angle, α, with Depth=3in (0.0762m) Speed=5mph

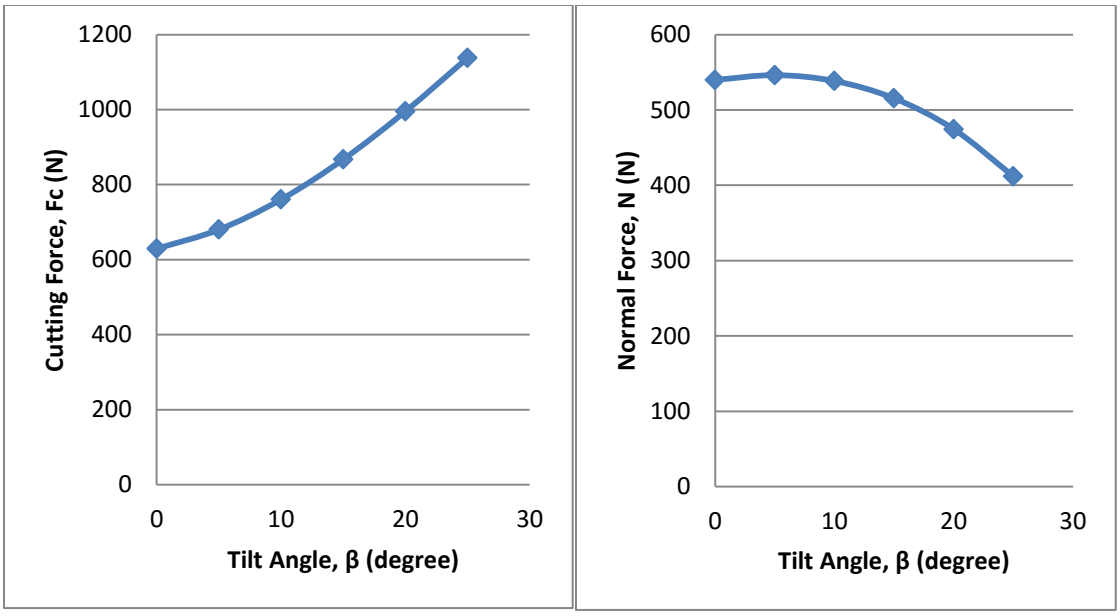

Figure J- 10: Cutting Force, Fc, and Normal Force, N, with Depth=3in (0.0762m) Speed=5mph

Figure J-9 also showed that the higher the tilt angle the higher the draft force. While the cutting width is a constant of 0.12m, the higher the tilt angle the lower the disc angle. In Figure J-10, it showed that the higher the tilt angle the higher the cutting force; the higher the tilt angle the lower the normal force. This also verified the experimental test data.

Since the furrow width cannot be zero, that means both disc and tilt angle cannot be zero. Also, the disc angle, α, has to be within the range of $0 \leq \alpha \leq 28°$ and the tilt angle, β, has to be within the range of $0 \leq \beta \leq 25°$. Therefore, the best combination of the disc and tilt angle with speed of 5mph is

$$\alpha = 7° \qquad (J.19)$$

$$\beta = 28° \qquad (J.20)$$

J.2 2-D optimization

For 2-D Optimization, the equations are showing as follow (disc and tilt angles are in term of radius)

$$F_z = Ncos\beta sin\alpha + F_c(cos\alpha sin\delta + sin\alpha sin\beta cos\delta) \quad (J.21)$$

Another method to achieve optimization of the combination disc and tilt angle is to use the Lagrange Multiplier Method. The best combination angle would provide the minimized draft force, F_z, with a reasonable furrow width, w. The equations for Lagrange Multiplier Method are shown as follow.

$$J = F_z + \lambda w \rightarrow min \quad (J.22)$$

$$\frac{\partial J}{\partial \alpha} = \frac{\partial F_z}{\partial \alpha} + \lambda \frac{\partial w}{\partial \alpha} = 0 \quad (J.23)$$

$$\frac{\partial J}{\partial \beta} = \frac{\partial F_z}{\partial \beta} + \lambda \frac{\partial w}{\partial \beta} = 0 \quad (J.24)$$

$$w = w(\alpha, \beta) = constant \quad (J.25)$$

The equations above can be solved by using the Matlab program. The code is shown in Figure J-11.

```
% solve for draft force, Fz
syms N Fc a b
delta = 24*pi()/180;                          % 0<a<28 and 0<b<25
Fz = N*cos(b)*sin(a)+Fc*(cos(a)*sin(delta)+sin(a)*sin(b)*cos(delta));

% solve for width, W
syms x y p d
% S = solve('x^2/(aa^2)+y^2/(bb^2)=1', 'y=tan(a)*x-(bb-d)');
S = solve('x^2/((p*cos(b))^2)+y^2/((p*sin(b))^2)=1', 'y=tan(a)*x-((p*sin(b))-d)');
X1 = S.x(1);
Y1 = S.y(1);
X2 = S.x(2);
Y2 = S.y(2);
W = ((X1-X2)^2+(Y1-Y2)^2)^0.5

% J=Fz+L*W  --> min
% dJ/da = dFz/da + L*dW/da
% dJ/db = dFz/db + L*dW/db
% W = ((X1-X2)^2+(Y1-Y2)^2)^0.5

% syms L
Fza = diff(Fz,a)
Fzb = diff(Fz,b)
Wa = diff(W,a)
Wb = diff(W,b)

% J = solve('Fza+L*Wa=0', 'Fzb+L*Wb=0', 'W=((X1-X2)^2+(Y1-Y2)^2)^0.5');
```

Figure J- 11: Matlab Code for 2D Optimization

As the result solve by using the Matlab Program, we get the width, w, is shown as follow

```
W=(((p*sin(b)^3 - d*sin(b)^2 + sin(a)*tan(a)*sin(b)*(2*d*p*sin(b) - d^2 +
p^2*sin(a)^2*tan(a)^2)^(1/2))/(sin(a)^2*tan(a)^2 + sin(b)^2) + (d*sin(b)^2 -
p*sin(b)^3 + sin(a)*tan(a)*sin(b)*(2*d*p*sin(b) - d^2 +
p^2*sin(a)^2*tan(a)^2)^(1/2))/(sin(a)^2*tan(a)^2 + sin(b)^2))^2 + ((p*sin(b)
- d + (d*sin(b)^2 - p*sin(b)^3 + sin(a)*tan(a)*sin(b)*(2*d*p*sin(b) - d^2 +
p^2*sin(a)^2*tan(a)^2)^(1/2))/(sin(a)^2*tan(a)^2 + sin(b)^2))/tan(a) + (d -
p*sin(b) + (p*sin(b)^3 - d*sin(b)^2 + sin(a)*tan(a)*sin(b)*(2*d*p*sin(b) -
d^2 + p^2*sin(a)^2*tan(a)^2)^(1/2))/(sin(a)^2*tan(a)^2 +
sin(b)^2))/tan(a))^2)^(1/2)                                    (J.26)
```

We have $\frac{\partial F_z}{\partial \alpha}$ is shown as follow

```
Fza = N*cos(a)*cos(b) - Fc*((457944748548525*sin(a))/1125899906842624 -
(8228485965250453*cos(a)*sin(b))/9007199254740992)
```

$(J.27)$

We have $\frac{\partial F_z}{\partial \beta}$ is shown as follow

```
Fzb = (8228485965250453*Fc*cos(b)*sin(a))/9007199254740992 - N*sin(a)*sin(b)
```

$(J.28)$

We have $\frac{\partial w}{\partial \alpha}$ is shown as follow

```
Wa = -(2*((p*sin(b)^3 - d*sin(b)^2 + sin(a)*tan(a)*sin(b)*(2*d*p*sin(b) - d^2
+ p^2*sin(a)^2*tan(a)^2)^(1/2))/(sin(b)^2 + sin(a)^2*tan(a)^2) + (d*sin(b)^2
- p*sin(b)^3 + sin(a)*tan(a)*sin(b)*(2*d*p*sin(b) - d^2 +
p^2*sin(a)^2*tan(a)^2)^(1/2))/(sin(b)^2 +
sin(a)^2*tan(a)^2))*(((2*cos(a)*sin(a)*tan(a)^2 + 2*sin(a)^2*tan(a)*(tan(a)^2
+ 1))*(p*sin(b)^3 - d*sin(b)^2 + sin(a)*tan(a)*sin(b)*(2*d*p*sin(b) - d^2 +
p^2*sin(a)^2*tan(a)^2)^(1/2)))/(sin(b)^2 + sin(a)^2*tan(a)^2)^2 -
(2*(sin(a)*sin(b)*(tan(a)^2 + 1)*(2*d*p*sin(b) - d^2 +
p^2*sin(a)^2*tan(a)^2)^(1/2) + cos(a)*tan(a)*sin(b)*(2*d*p*sin(b) - d^2 +
p^2*sin(a)^2*tan(a)^2)^(1/2) +
(sin(a)*tan(a)*sin(b)*(2*p^2*sin(a)^2*tan(a)*(tan(a)^2 + 1) +
2*p^2*cos(a)*sin(a)*tan(a)^2))/(2*(2*d*p*sin(b) - d^2 +
p^2*sin(a)^2*tan(a)^2)^(1/2))))/(sin(b)^2 + sin(a)^2*tan(a)^2) +
((2*cos(a)*sin(a)*tan(a)^2 + 2*sin(a)^2*tan(a)*(tan(a)^2 + 1))*(d*sin(b)^2 -
p*sin(b)^3 + sin(a)*tan(a)*sin(b)*(2*d*p*sin(b) - d^2 +
p^2*sin(a)^2*tan(a)^2)^(1/2)))/(sin(b)^2 + sin(a)^2*tan(a)^2)^2) -
2*((p*sin(b) - d + (d*sin(b)^2 - p*sin(b)^3 +
```

```
sin(a)*tan(a)*sin(b)*(2*d*p*sin(b) - d^2 +
p^2*sin(a)^2*tan(a)^2)^(1/2))/(sin(b)^2 + sin(a)^2*tan(a)^2))/tan(a) + (d -
p*sin(b) + (p*sin(b)^3 - d*sin(b)^2 + sin(a)*tan(a)*sin(b)*(2*d*p*sin(b) -
d^2 + p^2*sin(a)^2*tan(a)^2)^(1/2))/(sin(b)^2 +
sin(a)^2*tan(a)^2))/tan(a))*(((sin(a)*sin(b)*(tan(a)^2 + 1)*(2*d*p*sin(b) -
d^2 + p^2*sin(a)^2*tan(a)^2)^(1/2) + cos(a)*tan(a)*sin(b)*(2*d*p*sin(b) - d^2
+ p^2*sin(a)^2*tan(a)^2)^(1/2) +
(sin(a)*tan(a)*sin(b)*(2*p^2*sin(a)^2*tan(a)*(tan(a)^2 + 1) +
2*p^2*cos(a)*sin(a)*tan(a)^2))/(2*(2*d*p*sin(b) - d^2 +
p^2*sin(a)^2*tan(a)^2)^(1/2)))/(sin(b)^2 + sin(a)^2*tan(a)^2) -
((2*cos(a)*sin(a)*tan(a)^2 + 2*sin(a)^2*tan(a)*(tan(a)^2 + 1))*(p*sin(b)^3 -
d*sin(b)^2 + sin(a)*tan(a)*sin(b)*(2*d*p*sin(b) - d^2 +
p^2*sin(a)^2*tan(a)^2)^(1/2)))/(sin(b)^2 + sin(a)^2*tan(a)^2)^2)/tan(a) +
((sin(a)*sin(b)*(tan(a)^2 + 1)*(2*d*p*sin(b) - d^2 +
p^2*sin(a)^2*tan(a)^2)^(1/2) + cos(a)*tan(a)*sin(b)*(2*d*p*sin(b) - d^2 +
p^2*sin(a)^2*tan(a)^2)^(1/2) +
(sin(a)*tan(a)*sin(b)*(2*p^2*sin(a)^2*tan(a)*(tan(a)^2 + 1) +
2*p^2*cos(a)*sin(a)*tan(a)^2))/(2*(2*d*p*sin(b) - d^2 +
p^2*sin(a)^2*tan(a)^2)^(1/2)))/(sin(b)^2 + sin(a)^2*tan(a)^2) -
((2*cos(a)*sin(a)*tan(a)^2 + 2*sin(a)^2*tan(a)*(tan(a)^2 + 1))*(d*sin(b)^2 -
p*sin(b)^3 + sin(a)*tan(a)*sin(b)*(2*d*p*sin(b) - d^2 +
p^2*sin(a)^2*tan(a)^2)^(1/2)))/(sin(b)^2 + sin(a)^2*tan(a)^2)^2)/tan(a) -
((tan(a)^2 + 1)*(d - p*sin(b) + (p*sin(b)^3 - d*sin(b)^2 +
sin(a)*tan(a)*sin(b)*(2*d*p*sin(b) - d^2 +
p^2*sin(a)^2*tan(a)^2)^(1/2))/(sin(b)^2 + sin(a)^2*tan(a)^2)))/tan(a)^2 -
((tan(a)^2 + 1)*(p*sin(b) - d + (d*sin(b)^2 - p*sin(b)^3 +
sin(a)*tan(a)*sin(b)*(2*d*p*sin(b) - d^2 +
p^2*sin(a)^2*tan(a)^2)^(1/2))/(sin(b)^2 +
sin(a)^2*tan(a)^2)))/tan(a)^2))/(2*(((p*sin(b)^3 - d*sin(b)^2 +
```

```
sin(a)*tan(a)*sin(b)*(2*d*p*sin(b) - d^2 +
p^2*sin(a)^2*tan(a)^2)^(1/2))/(sin(b)^2 + sin(a)^2*tan(a)^2) + (d*sin(b)^2 -
p*sin(b)^3 + sin(a)*tan(a)*sin(b)*(2*d*p*sin(b) - d^2 +
p^2*sin(a)^2*tan(a)^2)^(1/2))/(sin(b)^2 + sin(a)^2*tan(a)^2))^2 + ((p*sin(b)
- d + (d*sin(b)^2 - p*sin(b)^3 + sin(a)*tan(a)*sin(b)*(2*d*p*sin(b) - d^2 +
p^2*sin(a)^2*tan(a)^2)^(1/2))/(sin(b)^2 + sin(a)^2*tan(a)^2))/tan(a) + (d -
p*sin(b) + (p*sin(b)^3 - d*sin(b)^2 + sin(a)*tan(a)*sin(b)*(2*d*p*sin(b) -
d^2 + p^2*sin(a)^2*tan(a)^2)^(1/2))/(sin(b)^2 +
sin(a)^2*tan(a)^2))/tan(a))^2)^(1/2))
```

$(J.29)$

We have $\frac{\partial w}{\partial \beta}$ is shown as follow

```
Wb = (2*((p*sin(b)^3 - d*sin(b)^2 + sin(a)*tan(a)*sin(b)*(2*d*p*sin(b) - d^2
+ p^2*sin(a)^2*tan(a)^2)^(1/2))/(sin(b)^2 + sin(a)^2*tan(a)^2) + (d*sin(b)^2
- p*sin(b)^3 + sin(a)*tan(a)*sin(b)*(2*d*p*sin(b) - d^2 +
p^2*sin(a)^2*tan(a)^2)^(1/2))/(sin(b)^2 +
sin(a)^2*tan(a)^2))*((3*p*cos(b)*sin(b)^2 - 2*d*cos(b)*sin(b) +
cos(b)*sin(a)*tan(a)*(2*d*p*sin(b) - d^2 + p^2*sin(a)^2*tan(a)^2)^(1/2) +
(d*p*cos(b)*sin(a)*tan(a)*sin(b))/(2*d*p*sin(b) - d^2 +
p^2*sin(a)^2*tan(a)^2)^(1/2))/(sin(b)^2 + sin(a)^2*tan(a)^2) +
(2*d*cos(b)*sin(b) - 3*p*cos(b)*sin(b)^2 + cos(b)*sin(a)*tan(a)*(2*d*p*sin(b)
- d^2 + p^2*sin(a)^2*tan(a)^2)^(1/2) +
(d*p*cos(b)*sin(a)*tan(a)*sin(b))/(2*d*p*sin(b) - d^2 +
p^2*sin(a)^2*tan(a)^2)^(1/2))/(sin(b)^2 + sin(a)^2*tan(a)^2) -
(2*cos(b)*sin(b)*(p*sin(b)^3 - d*sin(b)^2 + sin(a)*tan(a)*sin(b)*(2*d*p*sin(b)
- d^2 + p^2*sin(a)^2*tan(a)^2)^(1/2)))/(sin(b)^2 + sin(a)^2*tan(a)^2)^2 -
(2*cos(b)*sin(b)*(d*sin(b)^2 - p*sin(b)^3 + sin(a)*tan(a)*sin(b)*(2*d*p*sin(b)
- d^2 + p^2*sin(a)^2*tan(a)^2)^(1/2)))/(sin(b)^2 + sin(a)^2*tan(a)^2)^2) +
2*((p*cos(b) + (2*d*cos(b)*sin(b) - 3*p*cos(b)*sin(b)^2 +
```

```
cos(b)*sin(a)*tan(a)*(2*d*p*sin(b) - d^2 + p^2*sin(a)^2*tan(a)^2)^(1/2) +
(d*p*cos(b)*sin(a)*tan(a)*sin(b))/(2*d*p*sin(b) - d^2 +
p^2*sin(a)^2*tan(a)^2)^(1/2))/(sin(b)^2 + sin(a)^2*tan(a)^2) -
(2*cos(b)*sin(b)*(d*sin(b)^2 - p*sin(b)^3 + sin(a)*tan(a)*sin(b)*(2*d*p*sin(b)
- d^2 + p^2*sin(a)^2*tan(a)^2)^(1/2)))/(sin(b)^2 +
sin(a)^2*tan(a)^2)^2)/tan(a) - (p*cos(b) - (3*p*cos(b)*sin(b)^2 -
2*d*cos(b)*sin(b) + cos(b)*sin(a)*tan(a)*(2*d*p*sin(b) - d^2 +
p^2*sin(a)^2*tan(a)^2)^(1/2) + (d*p*cos(b)*sin(a)*tan(a)*sin(b))/(2*d*p*sin(b)
- d^2 + p^2*sin(a)^2*tan(a)^2)^(1/2))/(sin(b)^2 + sin(a)^2*tan(a)^2) +
(2*cos(b)*sin(b)*(p*sin(b)^3 - d*sin(b)^2 + sin(a)*tan(a)*sin(b)*(2*d*p*sin(b)
- d^2 + p^2*sin(a)^2*tan(a)^2)^(1/2)))/(sin(b)^2 +
sin(a)^2*tan(a)^2)^2)/tan(a))*((p*sin(b) - d + (d*sin(b)^2 - p*sin(b)^3 +
sin(a)*tan(a)*sin(b)*(2*d*p*sin(b) - d^2 +
p^2*sin(a)^2*tan(a)^2)^(1/2))/(sin(b)^2 + sin(a)^2*tan(a)^2))/tan(a) + (d -
p*sin(b) + (p*sin(b)^3 - d*sin(b)^2 + sin(a)*tan(a)*sin(b)*(2*d*p*sin(b) -
d^2 + p^2*sin(a)^2*tan(a)^2)^(1/2))/(sin(b)^2 +
sin(a)^2*tan(a)^2))/tan(a)))/(2*(((p*sin(b)^3 - d*sin(b)^2 +
sin(a)*tan(a)*sin(b)*(2*d*p*sin(b) - d^2 +
p^2*sin(a)^2*tan(a)^2)^(1/2))/(sin(b)^2 + sin(a)^2*tan(a)^2) + (d*sin(b)^2 -
p*sin(b)^3 + sin(a)*tan(a)*sin(b)*(2*d*p*sin(b) - d^2 +
p^2*sin(a)^2*tan(a)^2)^(1/2))/(sin(b)^2 + sin(a)^2*tan(a)^2))^2 + ((p*sin(b)
- d + (d*sin(b)^2 - p*sin(b)^3 + sin(a)*tan(a)*sin(b)*(2*d*p*sin(b) - d^2 +
p^2*sin(a)^2*tan(a)^2)^(1/2))/(sin(b)^2 + sin(a)^2*tan(a)^2))/tan(a) + (d -
p*sin(b) + (p*sin(b)^3 - d*sin(b)^2 + sin(a)*tan(a)*sin(b)*(2*d*p*sin(b) -
d^2 + p^2*sin(a)^2*tan(a)^2)^(1/2))/(sin(b)^2 +
sin(a)^2*tan(a)^2))/tan(a))^2)^(1/2))
```

$(J.30)$

By substitute the experimental combination disc and tilt angle (shown in Table 3-1) in equation (J.21) (using the Matlab Program), we are able to determine that

$$\frac{\partial w}{\partial \alpha} \approx 0 \qquad (J.31)$$

$$\frac{\partial w}{\partial \beta} \approx 0 \qquad (J.32)$$

By substitute the above equations in (J.31) and (J.32) we are able to find the exact value for $\frac{\partial F_z}{\partial \alpha}$ and $\frac{\partial F_z}{\partial \beta}$ shown in Table J-5.

Table J- 5: Optimization for Combination of Disc and Tilt Angle

				Depth	2in	Depth	3in	Depth	2in	Depth	3in
		d=2in	d=3in	Speed	3mph	Speed	3mph	Speed	5mph	Speed	5mph
α	β	w	w	Fza	Fzb	Fza	Fzb	Fza	Fzb	Fza	Fzb
(deg)	(deg)	(m)	(m)	(N)	(N)	(N)	(N)	(N)	(N)	(N)	(N)
0	0	0.000	0.000	122	0	199	0	241	0	218	0
0	0	0.000	0.000	146	0	166	0	236	0	196	0
7	0	0.000	0.000	247	34	298	30	282	48	279	45
7	0	0.000	0.000	237	30	309	35	282	48	293	41
14	0	0.000	0.000	356	78	345	71	378	115	329	119
14	0	0.000	0.000	315	83	330	58	376	116	342	110
21	0	0.000	0.000	406	141	343	84	423	181	436	202
21	0	0.000	0.000	455	134	350	88	487	205	422	181
28	0	0.000	0.000	471	197	480	166	543	279	490	314
28	0	0.000	0.000	487	224	421	179	567	251	481	328

0	15	0.076	0.090	180	0	284	0	272	0	257	0
0	15	0.076	0.090	167	0	364	0	294	0	267	0
7	15	0.076	0.090	291	42	326	44	384	63	305	49
7	15	0.076	0.090	249	39	343	48	388	67	313	52
14	15	0.078	0.092	350	93	436	110	482	155	454	140
14	15	0.078	0.092	350	100	398	117	442	167	464	122
21	15	0.081	0.096	400	153	455	203	522	263	515	248
21	15	0.081	0.096	371	158	502	183	540	258	524	237
28	15	0.086	0.101	423	237	452	284	555	367	625	330
28	15	0.086	0.101	405	238	445	275	596	349	604	363
0	20	0.101	0.120	152	0	196	0	320	0	225	0
0	20	0.101	0.120	112	0	149	0	300	0	205	0
7	20	0.102	0.121	232	41	395	50	382	77	424	66
7	20	0.102	0.121	232	41	369	59	418	80	394	63
14	20	0.105	0.123	348	103	463	165	526	188	529	187
14	20	0.105	0.123	337	120	408	147	574	187	506	180
21	20	0.109	0.128	370	209	548	270	646	311	636	304
21	20	0.109	0.128	388	212	497	270	618	319	657	295
28	20	0.116	0.135	484	315	547	372	656	467	715	463
28	20	0.116	0.135	480	324	592	369	637	444	700	436
0	25	0.127	0.150	168	0	317	0	367	0	222	0
0	25	0.127	0.150	187	0	305	0	327	0	212	0
7	25	0.128	0.151	243	47	307	63	418	62	443	63
7	25	0.128	0.151	240	40	418	60	429	60	415	65
14	25	0.131	0.155	311	116	395	166	530	177	514	153

14	25	0.131	0.155	350	102	321	152	509	190	483	167
21	25	0.137	0.160	458	205	434	260	610	303	814	320
21	25	0.137	0.160	484	183	378	259	621	322	814	298
28	25	0.145	0.168	497	325	593	388	624	455	806	456
28	25	0.145	0.168	574	301	603	389	666	434	817	443

The width of the furrow is assumed to be in between of 0.15m to 0.18m. Either disc angle or tilt angle cannot be zero due to a minimal amount of furrow width being required for seeding, as a result, the 7° disc angle with 25° tilt angle would provide the minimum draft force.